

BIOLOGY

**THE IMPACT OF NITROGEN DEPRIVATION ON  
GENOME EVOLUTION IN *Escherichia coli***

DOCTORAL THESIS  
FOR SUBMISSION TO A DOCTORAL DEGREE  
AT THE FACULTY OF NATURAL SCIENCE  
OF THE WESTFÄLISCHE WILHELMS-UNIVERSITÄT MÜNSTER

SUBMITTED BY

**DIPL.-BIOLOGIN STEFANIE HENZE**  
FROM PLETTENBERG

-2016-

submitted on: 17.05.2016

Dean: Prof. Dr. Michael Weber  
Primary Supervisor: Prof. Dr. Claudia Acquisti  
Second Supervisor: Prof. Dr. Ulrich Dobrindt

Date of Public Defense: 30.06.2016  
Date of Receipt of Certificates: 08.07.2016

BIOLOGIE

DIE AUSWIRKUNGEN VON STICKSTOFFMANGEL  
AUF DIE GENOMEVOLUTION IN *Escherichia coli*

INAUGURAL-DISSERTATION  
ZUR ERLANGUNG DES DOKTORGRADES  
DER NATURWISSENSCHAFTEN IM FACHBEREICH BIOLOGIE  
DER MATHEMATISCH-NATURWISSENSCHAFTLICHEN FAKULTÄT  
DER WESTFÄLISCHEN WILHELMS-UNIVERSITÄT MÜNSTER

VORGELEGT VON

**DIPL.-BIOLOGIN STEFANIE HENZE**  
AUS PLETTENBERG

-2016-

Eingereicht am: 17.05.2016

Dekan: Prof. Dr. Michael Weber  
Erste Gutachterin: Prof. Dr. Claudia Acquisti  
Zweiter Gutachter: Prof. Dr. Ulrich Dobrindt

Tag der mündlichen Prüfung: 30.06.2016

Tag der Promotion: 08.07.2016

FÜR MARCO

FÜR NOCH VIELE TAGE WIE DIESEN

## Acknowledgements

First of all, I offer my gratitude to my supervisor Prof. Dr. Claudia Acquisti for the continuous support of my PhD study whilst allowing me the room to work in my own way. Thanks for your academic advice and for numerous fruitful discussions.

My sincere thanks goes to Prof. Dr. Ulrich Dobrindt for offering me the opportunity to work in his lab. Thanks for sharing your knowledge and for your guidance at any stage of my project. Lastly, I'd like to thank you for being part of my thesis committee.

I want to thank Prof. Dr. Joachim Kurtz for being part of my thesis committee and for the assistance he provided to me.

Robert Fürst, many thanks for your patient and professional work and help in all matters concerning bioinformatics.

Thanks to Lukas Stroot for being a great trainee and for his tirelessly help in the lab.

I want to thank the whole ICB group for the great working atmosphere. Special thanks to Olena Mantel and Gabriele Trinczek for their help and support at any time. Many thanks to Dr. Michael Berger for his numerous ideas concerning my project and his guidance in the molecular work.

Further, I would like to thank Prof. Dr. Sebastian Leidl for sequencing a part of my RNA samples and for sharing his expertise on filter cultures. In this context I also want to thank Dr. Danny Nedialkova for her practical advice in this matter.

Many thanks to Barbara Hasert for always answering my questions and to Jörn Schar-sack for his advice on aquarium equipment.

Apart from the scientific interaction a big thank is dedicated to Dr. Birgit Ewert for numerous conversations and laughs during the writing phase. Special thanks goes to the women I got to know in Frankfurt who accompanied me on my scientific and private way.

My family, especially my parents, my sister Andrea and my brother-in-law Markus for your love, your insight and your support at every stage of my life.

Thank you Marco for being what matters most. Half of all is yours.

---

# Contents

<b>List of Figures</b>	<b>V</b>
<b>List of Tables</b>	<b>VII</b>
<b>List of Abbreviations</b>	<b>VIII</b>
<b>Summary</b>	<b>1</b>
<b>Zusammenfassung</b>	<b>3</b>
<b>1 Introduction</b>	<b>5</b>
1.1 The way of elements from the environment to biomolecules . . . . .	5
1.1.1 How essential elements enter ecosystems . . . . .	5
1.1.2 Maintenance of elemental composition . . . . .	6
1.1.3 Nitrogen and carbon assimilation in <i>Escherichia coli</i> . . . . .	7
1.2 The role of nutrient availability for genome evolution . . . . .	10
1.2.1 Why nutrient deprivation might shape the element composition of macromolecules . . . . .	10
1.2.2 Evidence for element based monomer usage bias . . . . .	11
1.3 Two Experiments - Two Timescales . . . . .	15
1.3.1 Transient nutrient starvation of filter cultures . . . . .	15
1.3.2 Persistent nitrogen limitation in continuous culture . . . . .	17
<b>2 Material</b>	<b>18</b>
2.1 Devices . . . . .	18
2.2 Consumables . . . . .	19
2.3 Kits . . . . .	20
2.4 Chemicals, enzymes and media . . . . .	21
2.4.1 Chemicals . . . . .	21
2.4.2 Enzymes and corresponding buffers . . . . .	22
2.4.3 Culture media and buffer . . . . .	23
2.5 Software . . . . .	24
2.6 Databases . . . . .	25
2.7 Oligonucleotides . . . . .	26
2.8 Strains and plasmids . . . . .	27
2.8.1 <i>Escherichia coli</i> Nissle 1917 $\Delta$ <i>fliC</i> . . . . .	28
<b>3 Methods</b>	<b>30</b>
3.1 Microbiological Methods . . . . .	30

---

3.1.1	Storage and incubation of bacterial cultures . . . . .	30
3.1.2	Determination of cell density and cell number . . . . .	30
3.1.3	Congored assay . . . . .	31
3.1.4	Motility assay . . . . .	31
3.2	Molecular biological Methods . . . . .	32
3.2.1	Isolation of genomic DNA . . . . .	32
3.2.2	Polymerase chain reaction . . . . .	32
3.2.2.1	<i>E. coli</i> Nissle 1917-specific multiplex PCR . . . . .	32
3.2.2.2	Amplification of the <i>kanR</i> gene from pACY177 . . . . .	33
3.2.2.3	Amplification of the <i>kanR</i> gene from pUC-kanR . . . . .	34
3.2.3	Gel electrophoresis and DNA purification . . . . .	35
3.2.4	Isolation of plasmid DNA . . . . .	35
3.2.5	Restriction digest . . . . .	35
3.2.6	Ligation . . . . .	35
3.2.7	Ethanol precipitation of DNA . . . . .	36
3.2.8	Concentration and purity of nucleic acids . . . . .	36
3.2.9	Transformation of <i>E. coli</i> cells . . . . .	37
3.2.9.1	Preparation of electrocompetent cells . . . . .	37
3.2.9.2	Electroporation . . . . .	37
3.2.10	Insertion of the kanamycin resistance gene into the chromosome of <i>E. coli</i> Nissle 1917 . . . . .	38
3.3	Preparation of a defined culture medium . . . . .	39
3.3.1	Composition and preparation . . . . .	39
3.3.2	Testing the full minimal medium . . . . .	41
3.3.3	Minimal media for the short-term starvation experiment . . . . .	42
3.3.4	Nitrogen limited medium for the long-term continuous culture experiment . . . . .	43
3.4	Transient nutrient starvation of filter cultures . . . . .	46
3.4.1	General overview of the experimental design . . . . .	46
3.4.1.1	Filter loading with liquid culture . . . . .	47
3.4.1.2	Incubation on solid full minimal medium . . . . .	49
3.4.1.3	Starvation on deficient minimal medium . . . . .	50
3.4.2	Sampling scheme . . . . .	52
3.5	Persistent nitrogen limitation in continuous culture . . . . .	53
3.5.1	General overview of the experimental design . . . . .	53
3.5.1.1	Dilution rate, generation time and ammonium availability . . . . .	56
3.5.1.2	Construction and Cleaning . . . . .	59
3.5.1.3	Housekeeping and backups . . . . .	60



---

3.5.2	Sampling scheme . . . . .	62
3.6	Chromatographic analyses . . . . .	63
3.6.1	Detection of free cellular metabolites of filter cultures . . . . .	63
3.6.2	Determination of the carbon to nitrogen ratio of continuous cultures . . . . .	64
3.6.3	Detection of cations in the effluent of continuous cultures . . . . .	64
3.7	Transcriptomics . . . . .	65
3.7.1	Cell harvest for RNA isolation from filter cultures . . . . .	65
3.7.2	Cell harvest for RNA isolation from continuous cultures . . . . .	65
3.7.3	RNA isolation . . . . .	66
3.7.4	RNA quality . . . . .	67
3.7.5	cDNA library preparation . . . . .	67
3.7.6	RNA sequencing . . . . .	68
3.8	Bioinformatics . . . . .	69
3.8.1	Annotation . . . . .	69
3.8.2	Assesment of differential levels of expression . . . . .	70
3.8.3	Mapping to metabolic pathways . . . . .	71
3.9	Statistics . . . . .	72
<b>4</b>	<b>Results</b>	<b>73</b>
4.1	Transient nutrient starvation of filter cultures . . . . .	73
4.1.1	Basic cellular starvation-survival response . . . . .	73
4.1.1.1	Ribosomal gene expression . . . . .	74
4.1.1.2	Dynamics of nutrient key metabolites . . . . .	77
4.1.1.3	Expression of genes . . . . .	82
4.1.2	Intracellular mobilization of deprived nutrients . . . . .	89
4.1.2.1	Mobilization of nitrogen rich amino acids during nitro- gen starvation . . . . .	89
4.1.2.2	Mobilization of lipids during carbon starvation . . . . .	94
4.1.2.3	Mobilization of carbohydrates during carbon starvation . . . . .	100
4.1.2.4	Mobilization of amino acids during carbon starvation . . . . .	102
4.1.3	Nitrogen conservation in proteins and utilization of internal ni- trogen reserves . . . . .	105
4.1.3.1	Protein nitrogen content . . . . .	105
4.1.3.2	Nitrogen rich amino acids: avoided in proteins and uti- lized as nitrogen source . . . . .	108
4.2	Persistent nitrogen limitation in continuous culture . . . . .	114
4.2.1	Basic cellular response to nitrogen limitation . . . . .	114
4.2.1.1	Expression of key genes . . . . .	115
4.2.1.2	Enhancement of ammonium uptake . . . . .	116

---

4.2.1.3	Morphological changes . . . . .	118
4.2.2	Signals of nitrogen conservation . . . . .	121
4.2.2.1	Cellular carbon and nitrogen content . . . . .	121
4.2.2.2	Protein nitrogen content . . . . .	125
4.2.3	Did adaptation to prolonged nitrogen limitation lead to growth advantages? . . . . .	131
4.2.3.1	Fitness during comparative growth of evolved continuous cultures . . . . .	131
4.2.3.2	Fitness during competitive growth of evolved continuous cultures . . . . .	135
<b>5</b>	<b>Discussion</b>	<b>143</b>
5.1	Transient nutrient starvation of filter cultures . . . . .	143
5.1.1	Basic cellular starvation-survival response . . . . .	145
5.1.1.1	Decrease of protein synthesis . . . . .	145
5.1.1.2	Metabolic cascades . . . . .	145
5.1.1.3	Improved nutrient scavenging . . . . .	148
5.1.2	Intracellular mobilization of deprived nutrients . . . . .	150
5.1.2.1	Mobilization of carbon and energy reserves during carbon starvation . . . . .	150
5.1.2.2	Mobilization of nitrogen reserves during nitrogen starvation . . . . .	153
5.1.3	Nitrogen conservation in proteins is linked to a biased free amino acid pool . . . . .	154
5.2	Persistent nitrogen limitation in continuous culture . . . . .	159
5.2.1	Basic cellular response to nitrogen limitation . . . . .	161
5.2.1.1	Improved nitrogen acquisition . . . . .	161
5.2.1.2	Enhancement of ammonium uptake . . . . .	161
5.2.1.3	Morphological changes . . . . .	163
5.2.2	Signals of nitrogen conservation . . . . .	164
5.2.2.1	Increase of the carbon to nitrogen ratio . . . . .	164
5.2.2.2	Nitrogen conservation in upregulated proteins . . . . .	165
5.2.3	Improved fitness under nitrogen limited conditions . . . . .	167
<b>6</b>	<b>Conclusion &amp; Outlook</b>	<b>170</b>
	<b>Appendix</b>	<b>i</b>

---

---

## List of Figures

1.1	Ammonium assimilation in <i>E. coli</i> . . . . .	8
1.2	Nitrogen allocation of biomolecules . . . . .	11
2.1	Motility of <i>E. coli</i> Nissle 1917 $\Delta$ <i>fliC</i> on swarming agar . . . . .	28
2.2	Motility of <i>E. coli</i> Nissle 1917 on swarming agar . . . . .	28
2.3	Congo red agar with colonies of <i>E. coli</i> Nissle 1917 . . . . .	29
2.4	rdar morphotype of <i>E. coli</i> Nissle 1917 . . . . .	29
3.1	Testing the composition of the full minimal medium . . . . .	42
3.2	Defining a growth limiting nitrogen concentration . . . . .	43
3.3	Verifying the growth limiting nitrogen concentration . . . . .	45
3.4	Starvation of filter cultures . . . . .	47
3.5	Growth of filter cultures on full MM . . . . .	49
3.6	Growth of filter cultures with and without washing step . . . . .	51
3.7	Picture of a bioreactor . . . . .	53
3.8	Drawing of a bioreactor . . . . .	53
3.9	Picture of the continuous culture: Part A . . . . .	55
3.10	Picture of the continuous culture: Part B . . . . .	55
4.1	Ribosomal gene expression in nutrient starved cultures . . . . .	76
4.2	Cellular abundance of nitrogen key metabolites during nutrient starvation	78
4.3	Cellular abundance of carbon key metabolites during nutrient starvation	81
4.4	Expression of nitrogen key genes during nutrient starvation . . . . .	84
4.5	Expression of carbon (glucose) key genes during nutrient starvation . .	88
4.6	Cellular abundance of nitrogen rich amino acids during nutrient starvation	93
4.7	Lipid degradation related gene expression in nutrient deficient cultures	95
4.8	Cellular abundance of fatty acids during nutrient starvation . . . . .	99
4.9	Carbohydrate degradation related gene expression in nutrient deficient cultures . . . . .	101
4.10	Cellular abundance of amino acids during carbon starvation . . . . .	104
4.11	Nitrogen content of proteins upregulated in response to nutrient starvation	107
4.12	Relation of protein amino acid composition and the availability of free amino acids during nutrient starvation . . . . .	112
4.13	Expression of nitrogen key genes during nitrogen limitation . . . . .	116
4.14	Ammonium uptake during nitrogen limitation . . . . .	117
4.15	Morphotypes after 1600 generations under nitrogen limitation . . . . .	118
4.16	Morphotypes after 1600 generations under control conditions . . . . .	118
4.17	rdar morphotype . . . . .	119
4.18	new morphotype 1 . . . . .	119
4.19	new morphotype 2 . . . . .	119

---

4.20	new morphotype 3 . . . . .	119
4.21	Multiplex PCR assay of colonies from the nitrogen limited cultures . . .	120
4.22	Carbon to nitrogen ratio of the continuous cultures and their ancestor over time . . . . .	122
4.23	Nitrogen and carbon content of continuous cultures and their ancestor over time . . . . .	124
4.24	Protein nitrogen content in response to nitrogen limitation . . . . .	127
4.25	Protein nitrogen content in nitrogen rich control cultures . . . . .	129
4.26	Comparative growth of the evolved continuous lines and their ancestor	134
4.27	Insertion of a kanamycin resistance into the ancestor and the evolved nitrogen limited line . . . . .	136
4.28	Competitive growth of the evolved continuous lines and their ancestor I	139
4.29	Competitive growth of the evolved continuous lines and their ancestor I	142
5.1	Impact of nutrient starvation on <i>E. coli</i> . . . . .	144
5.2	Impact of nitrogen limitation on <i>E. coli</i> . . . . .	160
6.1	Testing neutrality of the kanamycin resistance marker . . . . .	xvi

---

## List of Tables

2.1	List of devices . . . . .	18
2.2	List of consumables, continuous culture . . . . .	19
2.3	List of consumables, filter culture . . . . .	19
2.4	List of chemicals . . . . .	21
2.5	List of antibiotics . . . . .	23
2.6	List of oligonucleotides for detection of <i>E. coli</i> Nissle 1917 . . . . .	26
2.7	List of oligonucleotides for the amplification of the <i>kanR</i> gene from pACY177 . . . . .	26
2.8	List of oligonucleotides for the amplification of the <i>kanR</i> gene from pUC-kanR . . . . .	26
2.9	List of bacterial strains . . . . .	27
2.10	List of vectors and plasmids . . . . .	27
3.1	Composition of the complete minimal medium . . . . .	39
3.2	Growth of filter cultures with and without washing step . . . . .	51
3.3	Sampling schema of filter cultures . . . . .	52
3.4	Backup scheme of nitrogen limited cultures . . . . .	61
3.5	Backup scheme of nitrogen rich control cultures . . . . .	61
3.6	Sampling scheme of the continuous cultures . . . . .	62
4.1	Nitrogen allocation of amino acids . . . . .	90
4.2	Nitrogen content of upregulated proteins in continuous cultures . . . . .	130

---

## List of Abbreviations

ampR	ampicillin resistance
ATP	adenosine triphosphate
bp	base pairs
C	carbon
cAMP	cyclic adenosine monophosphate
C-def MM	carbon deficient minimal medium
CFU	colony forming units
C/N	carbon to nitrogen
CoA	coenzyme A
CRP	catabolite regulation protein
CsrA	Carbon storage regulator A
CO <sub>2</sub>	carbon dioxide
D	dilution rate
DA	dalton
DEPC	diethylpyrocarbonate
dH <sub>2</sub> O	deionized water
DNA	deoxyribonucleic acid
cDNA	complementary DNA
<i>E. coli</i>	<i>Escherichia coli</i>
EDTA	ethylenediaminetetraacetic acid
EMP	Embden-Meyerhof-Parnas
EtOH	ethanol
F	flow rate
FAD	flavin adenine dinucleotide
full MM	complete minimal medium
G	generation
gt	generation time
x g	gravitational force (9.81 ms <sup>-2</sup> )
GC-MS	gas chromatography-mass spectrometry
GDH	glutamate dehydrogenase
GOGAT	glutamine oxoglutarate aminotransferase
GS	glutamine synthetase
kanR	kanamycin resistance
kb	kilobase
kV	kilo volt
LB	lysogeny broth
LC-QTOF MS	liquid chromatography quadrupole time of light mass spectrometry

ln	natural logarithm
Mb	megabase
Mio	million
MM	minimal medium
NAD	nicotinamide adenine dinucleotide
NADP	nicotinamide adenine dinucleotide phosphate
N	nitrogen
-NH <sub>2</sub>	gaseous form of nitrogen
NH <sub>4</sub> <sup>+</sup>	ammonium
NO <sub>2</sub> <sup>-</sup>	nitrite
NO <sub>3</sub> <sup>-</sup>	nitrate
NC	negative control
N-def MM	nitrogen deficient minimal medium
N-lim MM	nitrogen limited minimal medium
nt	nucleotides
Ntr	nitrogen regulatory system
OD	optical density
P	phosphorus
PBS	phosphate-buffered saline
PBT	polybutylenterephthalate
PC	positive control
PCR	polymerase chain reaction
PEP	phosphoenolpyruvate
PES	polyethersulfon
PP	polypropylen
PTFE	polytetrafluorethylen
PTS	phosphotransferase system
r	radius
RIN	RNA integrity number
rdar	red dry and rough
RNA	ribonucleic acid
mRNA	messenger RNA
rRNA	ribosomal RNA
RNAseq	RNA sequencing
RPKM	reads per kilobase of gene per Mio reads mapped
rpm	revolutions per minute
sd	standard deviation
TAE	TRIS-Acetate-EDTA
TCA	Tricarboxylic acid cycle

TE	TRIS-EDTA
TRIS	Tris(hydroxymethyl)-aminomethan
U	units
UV	ultraviolet
V	volume
v/v	volume per volume
vs	versus
$\mu$	growth rate

**Units**

$^{\circ}\text{C}$	degree Celsius
g	gram
h	hour
ht	height
l	liter
M	molar
m	meter
min	minutes
sec	seconds

**Prefixes**

$\mu$	micro
c	centi
m	milli
n	nano
p	pico



**IUPAC amino acid code****DNA**

<u>Nucleotide code</u>	<u>Base</u>
A	adenine
C	cytosine
T (U)	thymine (uracil)
G	guanine

**Protein**

<u>Amino acid code</u>	<u>Three letter code</u>	<u>amino acid</u>
A	Ala	alanine
C	Cys	cysteine
D	Asp	aspartate
E	Glu	glutamic acid
F	Phe	phenylalanine
G	Gly	glycine
H	His	histidine
I	Ile	isoleucine
K	Lys	lysine
L	Leu	leucine
M	Met	methionine
N	Asn	asparagine
P	Pro	proline
Q	Gln	glutamine
R	Arg	arginine
S	Ser	serine
T	Thr	threonine
V	Val	valine
W	Trp	tryptophan
Y	Tyr	tyrosine

## Summary

Nutrients are taken up by bacterial cells and used for the de novo synthesis of biomolecules, such as amino acids and other monomers. Nitrogen, a key component of biomolecules is often a factor limiting growth in natural environments. Since the different amino acids vary in their number of nitrogen atoms, selection could in principle play a role in shaping the amino acid composition of proteins. For efficient nitrogen allocation, especially proteins upregulated in response to nitrogen deprivation are expected to be primary targets of this type of selection. Different studies have suggested that recurring periods of nutrient deprivation in the evolutionary history of microorganisms are reflected in a reduced element demand but laboratory evidence for the existence of nutrient conservation is still missing. Further, nothing is known on the cellular processes that enable selection to shape the composition of biomolecules for parsimonious nutrient allocation.

The present study aimed at quantifying the impact of nitrogen deprivation on bacterial genome evolution and to identify the cellular processes involved. In this context, we hypothesized that proteins upregulated in response to nitrogen deprivation have a lowered nitrogen demand and that the environmental availability of nitrogen drives the efficiency of translation via biased abundance of free amino acids. These aspects were analyzed by combining experimental approaches to study the response to nitrogen deprivation and evolutionary comparative genomics. First, a short-term carbon and nitrogen starvation experiment in *Escherichia coli* cultures was performed. Combining transcriptomics and metabolomics we examined the distribution of nitrogen in the free amino acid pool and their incorporation in the proteins upregulated in response to nitrogen starvation. Here, we observed a reduction of nitrogen rich amino acids in the upregulated proteins. This study indeed confirmed that selection owing to recurring nitrogen deprivation in the evolutionary history of *E. coli* had shaped the architecture of proteins involved in the nitrogen stress response. Further, we observed that the abundance of the different free cellular amino acids varied, depending on their nitrogen composition, between carbon and nitrogen starved cultures. These findings support the idea that transcriptional efficiency plays a role in shaping the evolution of the stress response.

To extend our understanding of the dynamics of nitrogen allocation in response to nitrogen availability, we established a continuous culture in which *E. coli* evolved for 1600 generations under nitrogen limiting conditions. We expected to see evolution in action, further reducing the nitrogen demand of the nitrogen limited cultures. To test this hypothesis, transcriptomics data were produced at regular intervals of time. This enabled a direct comparison of the nitrogen budget of proteins over time. We could show that proteins highly upregulated in nitrogen limited cultures had a reduced

nitrogen demand. Especially in the later generations, the mean nitrogen content of upregulated proteins was markedly lower than that of downregulated proteins. These findings confirm that natural selection owing to nitrogen deprivation acts primarily on proteins involved in the nitrogen stress response.

The present data are of paramount importance in quantify the strength of the selection pressure exerted by environmental nitrogen deprivation on molecular evolution of *E. coli*. Further work connecting the transcriptional response to the cellular metabolic status will be important in shedding further light on the role of nitrogen deprivation in shaping molecular evolution.

## Zusammenfassung

Bakterien nehmen Nährstoffe aus Ihrer Umgebung auf und nutzen diese für die de-novo Synthese von Aminosäuren, Nukleotiden und anderen Biomolekülen. Stickstoff, ein wesentlicher Bestandteil von Biomolekülen, ist oft ein limitierender Faktor für das Wachstum in Ökosystemen. Da die verschiedenen Aminosäuren in ihrer Anzahl an Stickstoffatomen variieren, ist es möglich, dass Selektionsprozesse die Aminosäurezusammensetzung von Proteinen zugunsten einer effizienten Stickstoffverteilung verändern. Besonders die Proteine, die unter Stickstoffmangel besonders hochreguliert sind, stellen an dieser Stelle ein primäres Ziel dar. Verschiedene Studien deuten bereits darauf hin, dass sich wiederholender Stickstoffmangel in der Evolutionsgeschichte von Mikroorganismen in einem reduzierten Verbrauch dieses Elements spiegelt. Experimentelle Daten zu diesem Thema waren bisher aber nicht verfügbar. Zudem ist nicht bekannt, welche zellularen Prozesse es ermöglichen, dass die Zusammensetzung von Biomolekülen hinsichtlich einer sparsamen Stickstoffzuordnung durch Selektion verändert wird.

Die vorliegende Studie dient dazu, den Einfluss von Stickstoffmangel auf die Genomevolution von Bakterien zu quantifizieren und die zellulären Prozesse, die in die Mechanismen der Stickstoffeinsparung involviert sind, zu identifizieren. In diesem Zusammenhang nahmen wir an, dass während Stickstoffmangels hochregulierte Proteine einen verringerten Stickstoffanteil besitzen und dass die Verfügbarkeit von Stickstoff die Effizienz der Translation durch eine Verzerrung der Konzentration von frei in der Zelle vorliegenden Aminosäuren beeinflusst. Diese Aspekte wurden mit Hilfe von experimentellen Versuchen bezüglich Stickstoffverfügbarkeit, kombiniert mit evolutionärer vergleichender Genomik, untersucht. Zunächst wurde ein Kurzzeitversuch durchgeführt, bei dem *E. coli* Kulturen unter komplettem Stickstoff- oder Kohlenstoffentzug inkubiert wurden. Durch die Kombination von Analysen des Metaboloms und des Transkriptomts konnten wir die Verteilung von Stickstoff in den in der Zelle frei vorliegenden Aminosäuren und deren Einbau in die unter Nährstoffmangel hochregulierten Proteine untersuchen. Wir beobachteten eine reduzierte Häufigkeit von stickstoffreichen Aminosäuren in den Proteinen, die unter Stickstoffmangel hochreguliert waren. Diese Beobachtung in den nicht proliferierenden Stickstoffmangelkulturen bestätigt, dass Selektion infolge von wiederkehrendem Stickstoffmangel während der Evolutionsgeschichte von *E. coli* die Architektur der Proteine, die in die Stickstoffstress-Antwort involviert sind, verändert hat. Zudem konnten wir zeigen, dass die Häufigkeit der verschiedenen frei vorliegenden Aminosäuren zwischen Stickstoff- und Kohlenstoffmangelkulturen unterschiedlich war und dass diese Unterschiede im Stickstoffanteil der Aminosäuren begründet waren. Diese Beobachtung unterstützt die Theorie, dass die Effizienz der Translation eine wichtige Rolle bei evolutionsbedingten Änderungen der Stickstoffstress-Antwort spielt.

Um unser Verständnis über die Dynamiken der Stickstoffzuordnung im Zusammenhang mit der Stickstoffverfügbarkeit zu erweitern, wurde eine kontinuierliche *E. coli* Kultur etabliert. Diese evolvierte für 1600 Generationen unter Stickstofflimitation. Unsere Erwartung war, Evolution in Aktion und damit eine weitere Reduktion des Stickstoffanteils von hochregulierten Proteinen zu sehen. Um diese Hypothese zu testen, wurden in regelmässigen Abständen transkriptomische Daten von den kontinuierlichen Kulturen erhoben. Dies ermöglichte einen direkten Vergleich des Stickstoffanteils von Proteinen über die Versuchsdauer. Hier konnten wir zeigen, dass unter Stickstofflimitation hochregulierte Proteine einen reduzierten Anteil an Stickstoff aufwiesen. Besonders in den späteren Generationen des Evolutionsexperiments war der durchschnittliche Stickstoffgehalt von hochregulierten Proteinen deutlich geringer als der von herunterregulierten Proteinen. Die vorliegenden Ergebnisse bestätigen, dass durch Stickstoffmangel ausgelöste Selektionsprozesse tatsächlich primär auf die Proteine einwirken, die in die Stickstoffstress-Antwort involviert sind.

Die vorliegenden Daten sind von grosser Bedeutung für die Quantifizierung der Stärke des durch Stickstoffmangel ausgelösten Selektionsdruckes auf die molekulare Evolution von *E. coli*. In diesem Zusammenhang sind weiterführende Studien, die die Transkriptionsprozesse im Rahmen der Stickstoffmangel-Stressantwort mit dem zellulären metabolischen Status in Verbindung bringen, von grosser Bedeutung.

# 1 Introduction

## 1.1 The way of elements from the environment to biomolecules

### 1.1.1 How essential elements enter ecosystems

In nature there are eighty-one stable elements and a portion of those is found in every living organism [J. Koolman, 2003]. The so called macroelements hydrogen, oxygen, carbon, nitrogen, phosphorus, sulphur, potassium and calcium make up more than 99 % of living matter [Campbell and Reece, 2003]. In addition to these macroelements, organisms require minor amounts of different trace elements [Campbell and Reece, 2003] like metals. Iron and copper ions serve, for example, as cofactors of many enzymes [Nelson and Cox, 2000]. All these essential elements are taken up by organisms as organic or inorganic compounds. Some elements, like phosphorus, carbon and nitrogen become available to the majority of organisms only through biogeochemical nutrient cycling [Campbell and Reece, 2003; Purves *et al.*, 2006]:

The gaseous form of nitrogen,  $N_2$ , is highly abundant in the atmosphere but only a limited group of prokaryotes is able to access this compound directly by nitrogen fixation. In all known nitrogen-fixing bacteria and archaea the energetically expensive reduction of  $N_2$  to ammonium ( $NH_4^+$ ) is catalyzed by an enzyme complex called nitrogenase. Inorganic ammonium can be taken up by plants and many bacteria directly from the environment. On the contrary, animals utilize organic nitrogen (e.g. in form of amino acids or proteins) which they ingest with their diet (plants or other animals). When organisms die, their nitrogenous wastes are returned to the environment and decomposed to ammonium. This process is called ammonification. Environmental ammonium can also be oxidized to nitrite ( $NO_2^-$ ) and then further to nitrate ( $NO_3^-$ ) by a process called nitrification which is performed by prokaryotes under aerobic conditions. The initial conversion of ammonium to nitrite is carried out by a special group of archaea and bacteria known as ammonia-oxidizers. The final oxidation of nitrite to nitrate is performed by a second group of microbes, namely nitrite-oxidizing bacteria. Plants are able to utilize nitrate, however, in environments with little or no oxygen, nitrate is reduced to the gaseous  $N_2$  by anaerobic bacteria. This process is called denitrification and important since it removes bioavailable nitrogen from an ecosystem by returning  $N_2$  to the atmosphere [Campbell and Reece, 2003; Canfield *et al.*, 2010].

Another example is the carbon cycle. In the atmosphere, carbon and oxygen form the gaseous carbon dioxide ( $CO_2$ ) which is taken up and converted to usable carbohydrates by plants and phytoplankton during photosynthesis. Those organisms that build their own organic carbonous compounds from the inorganic carbon source of their surrounding are called autotrophs. Heterotrophic consumers cannot fix and assimilate atmospheric carbon on their own, they depend on the uptake of organic carbon com-

pounds build by autotrophs. Due to cellular respiration by organisms, decomposition of organic material and the burning of fossil fuels, CO<sub>2</sub> enters the atmosphere again [Campbell and Reece, 2003; Purves *et al.*, 2006].

### 1.1.2 Maintenance of elemental composition

Within biogeochemical cycles, elements are rearranged by and between organisms and their environments. During this cycling, elements and also energy are transformed but conserved. In chemical reactions, the conservation of mass between the involved reactants and products is known as stoichiometry. The patterns of matter and energy in the mentioned ecological interactions is studied within the research field ‘ecological stoichiometry’. A fundamental focus is on the differences between the chemical composition of organisms and their environments. Hence, one of the key questions of the framework ecological stoichiometry is how organisms deal with imbalances between their element demands and the element composition of their environment, including the food they eat [Sturner and Elser, 2002]. Some organisms, mainly heterotrophs, are able to maintain a constant element composition (within some biological limits) independent of their surrounding [Kooijman, 1995; Sturner and Elser, 2002]. The ability of keeping the internal element contents constant is called ‘stoichiometric homeostasis’ [Sturner and Elser, 2002] and is controlled by different physiological processes that deal with the uptake, incorporation and release of the elements [Frost *et al.*, 2005]. Animals for example are able to balance the uptake of different nutrients by modifying their ingestion rate, food selectivity and food sources. This behavior allows them to maintain their internal element composition [Frost *et al.*, 2005]. In contrast, many autotrophs are not capable of maintaining their inner element composition against varying environmental conditions. A study by Rhee [1978] shows for example, that the cellular nitrogen (N) : phosphorus (P) composition of the algae *Scenedesmus* matched the element composition of its environment when grown under different N:P ratios. Also for several species of marsh plants it was shown that their inner N:P ratios varies according to their N:P supplements [Shaver and Melillo, 1984]. Furthermore, some bacteria and fungi seem to be heavily affected by the element composition of their environment. Aquatic hyphomycetes for examples show highly variable element compositions when grown in culture media with different nitrogen and phosphorus concentrations [Danger and Chauvet, 2013]. Bacteria isolated from freshwater showed weak stoichiometric homeostasis as well, however this depended on resource availability [Scott *et al.*, 2012]. Also Danger *et al.* [2008] observed non-homeostatic behavior in some bacterial communities. One of the reasons for lacking element homeostasis in all of these organisms might be the direct dependence on the element composition of their surrounding envi-

ronment from which they take up individual elements. This is contrary to the ingestion of bounded nutrient constituents by animals [Frost *et al.*, 2005].

### 1.1.3 Nitrogen and carbon assimilation in *Escherichia coli*

Organisms do not simply consist of different elements, the key elements carbon, nitrogen, oxygen, sulphur and phosphorus are integrated in cellular monomers, like amino acids and nucleotides. The monomers themselves are further incorporated in the building blocks of life, as proteins and nucleic acids (DNA and RNA). Nucleotides consist of pentose (a sugar with five carbon atoms), one or more phosphate groups and a nitrogenous base (adenine or guanine (purine bases) or cytosine, thymine or uracil (pyrimidine bases)). The twenty different proteinogenic (protein building) amino acids are composed of at least one carboxyl (-COOH) and one amino (-NH<sub>2</sub>) group. Further, sulphur groups are implemented in the side chains of the amino acids cysteine and methionine [Nelson and Cox, 2000]. While heterotrophic organisms take up many of these biomolecules premade with their diet, most microorganisms are able to synthesize their cellular components themselves. Therefore, they need an organic carbon source and further inorganic element compounds which they take up from their surrounding environment [Gottschalk, 1979]. Glucose for example, which is the preferred carbon source of *E. coli* [Deutscher *et al.*, 2006; Martínez-Gómez *et al.*, 2012], is taken up via the phosphoenolpyruvate (PEP) : carbohydrate phospho-transferase system (PTS) [Postma *et al.*, 1993]. The glucose specific PEP:PTS is a group translocation system that transports glucose through the cell membrane and in parallel phosphorylates it via a phosphorylation cascade. Here, PEP serves as the donor of the phosphate group. The chemically modified glucose is then released as glucose-6-phosphate in the cytoplasm [Deutscher *et al.*, 2006] and, under aerobic conditions, a part of it is oxidized to CO<sub>2</sub>. This is mainly done by the Embden-Meyerhof-Parnas (EMP) pathway, the pyruvate dehydrogenase complex, the Tricarboxylic Acid Cycle (TCA) and the pentose phosphate pathway. The hydrogen atoms that become available during this oxidation process are transferred to the coenzymes nicotinamide adenine dinucleotide (NAD), nicotinamide adenine dinucleotide phosphate (NADP) and flavin adenine dinucleotide (FAD). The oxidized forms of these coenzymes are regenerated in the respiratory chain, resulting in the formation of various molecules of adenosine triphosphate (ATP). ATP is an energy carrier, transporting energy for metabolism throughout the cells. Additionally to the formation of ATP, the degradation of glucose yields precursors for the biosynthesis of cellular components [Gottschalk, 1979].





pathway which is used for ammonium assimilation, the synthesized glutamate represents the strongest nitrogen reservoir of *E. coli*. About 80% of the cellular nitrogen passes through it [Reitzer, 2004]. Glutamate serves as major intracellular nitrogen donor in transamination reactions [Gottschalk, 1979]. Here, its amino group is transferred to intermediates in the synthesis of the amino acids alanine, aspartate, valine, phenylalanine, tyrosine, isoleucine, leucine, lysine, and serine [Keseler *et al.*, 2013]. Glutamine is also an intracellular nitrogen reservoir of *E. coli* which serves as nitrogen donor in the synthesis of the amino acids tryptophan, histidine and asparagine as well as in the synthesis of purines and pyrimidines and other cellular compounds [Gottschalk, 1979; Reitzer, 2003]. As a third amino acid, aspartate serves as nitrogen donor, namely in the synthesis of arginine and purines [Reitzer, 2004]. Moreover, the amino acids arginine and lysine that contain respectively 4 and 2 nitrogen atoms act as nitrogen reservoirs in *E. coli* [Reitzer, 2003].

## 1.2 The role of nutrient availability for genome evolution

### 1.2.1 Why nutrient deprivation might shape the element composition of macromolecules

Even though different amino acids and nucleotides consist mainly of the same compounds, their element composition differs quantitatively from each other. This becomes obvious, when regarding the nitrogen (N) allocation of the nucleobases and the proteinogenic amino acids. While guanine (G) and cytosine (C) own eight nitrogen atoms when paired in the DNA double helix, adenine (A) and thymine (T) possess one nitrogen atom less (figure 1.2). These differences in nitrogen content are even higher in single stranded RNA since variation between the different bases is not buffered any longer by complementary rules of the double helix [Elser *et al.*, 2011]. Here, adenine and guanine possess five nitrogen atoms, cytosine three and thymine and uracil (U) possess only two each (figure 1.2). Further, the backbone of each amino acid consists of one nitrogen atom. However, the amino acids arginine (Arg), asparagine (Asn), histidine (His), lysine (Lys), glutamine (Gln) and tryptophan (Trp) carry one to three additional nitrogen atoms in their side chain (figure 1.2).

Despite its pivotal role for biomolecules, nitrogen is often a limiting growth factor in natural environments [Sternner and Elser, 2002]. The availability of nitrogen has been shown to affect the element composition of organisms that are not capable of stoichiometric homeostasis (see chapter 1.1.2). However, the nitrogen budget of an organism is not dictated by the number of its independent nitrogen atoms but rather by the biochemical composition of its biomolecules [Sternner and Elser, 2002]. The question is whether persistent or reoccurring nitrogen deprivation is able to affect the architecture of cellular macromolecules as DNA, RNA and proteins. The research field ‘Stoichiogenomics’ suggests that natural selection owing to nutrient deprivation might bias the usage of cellular monomers (amino acids and nucleotides) in macromolecules to reduce element cost. Even if this selective pressure is rather low, its cumulative effects during reoccurring nitrogen limitation over evolutionary relevant time scales might have favored monomers with a lower demand on nitrogen and thus conserving this element in the genome and in transcripts and proteins [Elser *et al.*, 2011]. Most likely, selection acts on some molecules more pronounced than on others. Proteins that contribute a high fraction to cellular biomass (up to 50 % in prokaryotes [Giese, 1979]) but also RNA (12-30 % of cellular biomass of *E. coli* [Maaloe and Kjeldgaard, 1966]) play a major role in the total element composition of an organism [Sternner and Elser, 2002]. In contrast, DNA contributes only 3-4% to the cellular biomass of *E. coli* [Maaloe and Kjeldgaard, 1966]. Additionally, complementary rules of the double helix buffer among-nucleotide variation. In the case of nitrogen, only one nitrogen atom could be saved when changing from a G-C to an A-T pairing (figure 1.2). Therefore,

selection owing to nitrogen deprivation most likely targets primarily proteins and transcripts since in these molecules the potential for nitrogen conservation is higher than in DNA.

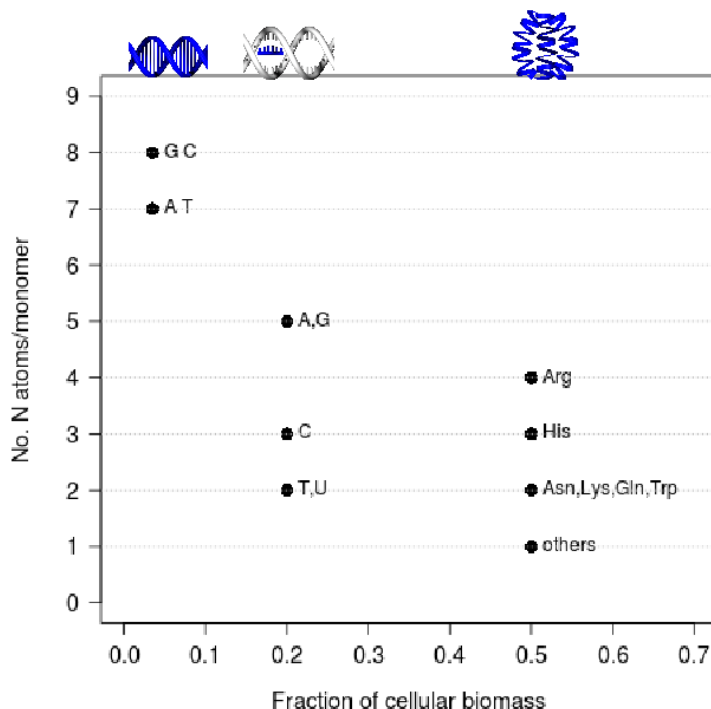


**Figure 1.2: Nitrogen allocation of biomolecules**

The number (No) of nitrogen (N) atoms in the different nucleobases and amino acids and the fraction of cellular biomass of the macromolecules DNA, RNA and proteins (from left to right)

### 1.2.2 Evidence for element based monomer usage bias

Some analyses have already shown that proteins that are involved in the assimilation of a given element have a lower demand on this specific element compared to the overall proteome. For example proteins of *Saccharomyces cerevisiae* and *E. coli* that are involved in the assimilation of carbon or sulphur show a decreased incorporation of sulphur containing amino acids and a depleted amount of carbon atoms in their side chains respectively, when compared to all other proteins [Baudouin-Cornu *et al.*, 2001]. The same study revealed that proteins of *S. cerevisiae* that are involved in nitrogen assimilation have a reduced nitrogen allocation compared to sulphur assimilatory proteins. It was further shown that element conservation is not restricted to proteins that are involved in nutrient assimilation. Analyses of the proteomes of *E. coli*, *S. cerevisiae* and *Schizosaccharomyces pombe* revealed that upregulated proteins have a lower demand on sulphur atoms than downregulated proteins. After excluding ribosomal proteins from the analysis, element conservation could also be shown for nitrogen. This is due to the fact that ribosomal proteins have a significantly higher nitrogen content

compared to the overall proteome due to specific structural constraints [Acquisti *et al.*, 2009b]. Further, Mazel and Marlière [1989] demonstrated that the cyanobacterium *Calothrix* possesses sulphur depleted versions of its light-harvesting proteins which are particularly upregulated during sulphur limitation.

Next to this general element conservation in highly abundant proteins and in those involved in nutrient assimilation, a number of recent studies has shown that environmental nitrogen limitation can directly affect the composition of proteomes and genomes in different eukaryotes. Acquisti *et al.* [2009b] proposed that the genome of plants, in contrast to that of animals, would be biased towards nitrogen poor nucleotides. This is due to the fact that plants are confronted with recurrent environmental nitrogen limitation due to insufficient supplies of inorganic nitrogen sources while animals are not likely to face nitrogen deprivation since they take up preformed, nitrogen containing biomolecules with their diet. When investigating the genome of *Arabidopsis thaliana*, it could indeed be shown that non coding parts of transcribed regions have a significantly lowered nitrogen content (5 %) compared to the whole genome. Contrary, genomes and transcriptomes of different animals do not show differences in their nitrogen content [Acquisti *et al.*, 2009b]. In a second study, the amino acid composition of the proteome of different animals and plants was compared, showing that the proteomes of the animal taxa contain significantly more nitrogen demanding amino acids than the plant proteomes [Elser *et al.*, 2006]. Further, Acquisti *et al.* [2009a] examined the nitrogen content of crop plant genomes and proteomes, expecting that natural selection would no longer bias the use of monomers towards nitrogen conservation since crops grow on soils that are massively fertilized and therefore nitrogen enriched. In fact, their study revealed that the nitrogen content of the genome and proteome of domesticated rice (*Oryza sativa*) is significantly higher compared to those of *A. thaliana* [Acquisti *et al.*, 2009a]. Nevertheless, for both plant species it could be shown that the nitrogen content of their proteins is negatively correlated to the expression levels of the encoding genes [Elser *et al.*, 2006].

These studies indeed suggest that persistent or sufficiently strong nutrient limitation is a factor that, in addition to structural and functional constraints, is able to shape the architecture of biological macromolecules. Here, selection owing to nutrient deprivation is predicted to lower the demand on the limiting elements as these hamper the production of crucial biomolecules [Elser *et al.*, 2011]. Whether the consequences of a mutation that affects the element cost of a biomolecule are actually pronounced enough to be detected by natural selection was investigated by Bragg and Wagner [2009]. They addressed this question in *S. cerevisiae* and calculated that natural selection owing to sulphur limitation would detect an additional sulphur atom in 66 % of yeast proteins. During nitrogen deprivation, the elevated cost of one nitrogen atom would be visible to

natural selection in only 3 % of all proteins. These differences between the two nutrients can be explained by their general allocation in proteins. Sulphur is a component of only two proteinogenic amino acids, namely cysteine and methionine, and its median content in yeast proteins is with 13 atoms much lower than the median nitrogen content (525 atoms). Therefore, the addition of only one sulphur atom to a protein has a larger effect on element cost than the addition of a single nitrogen atom [Bragg and Wagner, 2009]. However, nitrogen atoms are incorporated in the backbone of each amino acid as well as in the side chains of arginine, histidine, lysine, asparagine, tryptophan and glutamate [Nelson and Cox, 2000]. A possible substitution from glycine to arginine elevates the element cost of a protein directly by three nitrogen atoms [Bragg and Wagner, 2009]. For this case, Bragg and Wagner [2009] calculated that natural selection would detect 8.1 % of proteins carrying three additional nitrogen atoms during nitrogen limitation. The same calculations were performed on carbon atoms which are substantial components of all amino acids. In this context, even an addition of nine carbon atoms was found to be detected by natural selection owing to carbon limitation in only 4.4 % of all proteins [Bragg and Wagner, 2009].

Lastly, Acquisti *et al.* [2009a] compared the element composition of the anabolic machinery of four eukaryotic organisms to that of their catabolic machinery and found a substantially lowered nitrogen allocation in components of the catabolic apparatus. Since nutrient deprivation reduces anabolic processes as growth and contrary promotes components of the catabolic machinery, this observation shows that element conservation is associated with the catabolic apparatus [Acquisti *et al.*, 2009b]. Moreover, the study suggests that the driving force for enhanced nitrogen allocation in the anabolic machinery is due to structural constraints of ribosomes which are key components in anabolism. First, as already mentioned, ribosomal proteins contain more nitrogen demanding amino acids than other proteins which is due to binding capabilities to nucleic acids during protein translation. Second, nucleotides, which constitute the second component of ribosomes, are highly nutrient rich compared to other cellular compounds [Acquisti *et al.*, 2009b]. The authors propose further that the components of the anabolic apparatus, as ribosomes, are degraded during starvation which leads to a release of nucleotides and amino acids. Indeed, the degradation of ribosomes upon starvation seems to be functionally important. Kraft *et al.* [2008] discovered that in *S. cerevisiae* mature ribosomes are selectively degraded by autophagy upon nutrient starvation. Other publications show that also most bacterial species, including *E. coli*, degrade ribosomal RNA [Ben-Hamida and Schlessinger, 1966; Kaplan and Apirion, 1975a,b] and proteins [Mandelstam, 1963; Pine, 1965] in case their initial response towards nutrient deprivation (elevated expression of proteins that increases the nutrient uptake [Harder and Dijkhuizen, 1983; Magasanik and Neidhardt, 1987; Overbeeke and Lugtenberg,

1982]) is not sufficient. The released amino acids and nucleotides are thought to be recycled by the cell to construct the components of the catabolic apparatus which is induced upon nutrient deprivation [Acquisti *et al.*, 2009b; Reeve *et al.*, 1984b]. The mobilization of intracellular nutrient reservoirs contributes as well to the conservation of limiting nutrients and enables organisms to survive short periods of nutrient scarcity [Kraft *et al.*, 2008].

The mentioned studies show that natural selection owing to nutrient deprivation has the potential to shape the architecture of cellular macromolecules in different organisms, particularly plants, prokaryotes or single-celled eukaryotes. These organisms are directly dependent on the availability of key elements in their environment and face limitations of growth and reproduction by insufficient supplies of those. Reoccurring periods of nutrient deprivation in the evolutionary history of an organism were shown to be reflected in a reduced element demand as the use of limited available elements hampers a fast production of biomolecules. However, laboratory evidence for the existence of nutrient conservation is not yet available. Further, nothing is known on the cellular processes that enable selection to shape the composition of biomolecules for parsimonious nutrient allocation. Therefore, the central aspects of this study were to quantify the impact of nitrogen deprivation on bacterial biomolecules and to identify the cellular processes involved in nutrient conservation. These aspects were analyzed by combining experimental approaches on nitrogen deprivation and evolutionary comparative genomics.

## 1.3 Two Experiments - Two Timescales

### 1.3.1 Transient nutrient starvation of filter cultures

During their evolutionary history, microorganisms have faced reoccurring nutrient deprivation and thereby developed mechanisms to respond to limiting availability of key elements with specific transcriptional responses. In this context, it is hypothesized that the composition of proteins upregulated in response to nitrogen starvation has been shaped by selection, favoring amino acids with a low nitrogen allocation. The driving force that enables selection owing to nitrogen deprivation to shape amino acid composition for parsimonious nitrogen allocation might be a biased abundance of free cellular amino acids which affects the efficiency of protein translation. To test these hypotheses, we have designed a short-term starvation experiment in which filter cultures of *E. coli* were incubated on either nitrogen or carbon deficient minimal medium over four hours. Samples for transcriptome and metabolome analyses were taken repeatedly to follow the dynamics of free amino acids in the cell and further the kinetic of their incorporation into the newly synthesized proteins.

Carbon starvation was achieved by depriving glucose from the used minimal medium. This lead, additional to the starvation for the element carbon, to a starvation response towards energy. The analysis of protein regulation in nutrient starved cultures enabled us to distinguish proteins selectively upregulated in response to nitrogen starvation from proteins involved in a general stress response towards nutrient starvation. We expected to detect a decreased nitrogen content of proteins specifically upregulated under nitrogen starvation when compared to proteins that were specifically upregulated in response to carbon starvation. The decreased nitrogen allocation was further expected to be caused by a lowered incorporation of the six amino acids that carry additional nitrogen atoms in their side chains (arginine, asparagine, glutamine, histidine, lysine, tryptophan). To test this assumption, we compared the amino acid composition of the proteins upregulated in response to nitrogen starvation to that of the proteins upregulated in response to carbon starvation.

Due to the complete nutrient exhaustion, the nutrient starved cultures ceased growth and were expected to initiate the breakdown of cellular macromolecules as part of the known stress response. Amino acids released during the breakdown processes might have functioned as sources of nitrogen. Especially the nitrogen rich amino acids are known to be nitrogen storage molecules [Reitzer, 2003] and were supposed to be particularly degraded or at least transaminated to re-cycle their nitrogen atoms. If this were the case, the cellular abundance of nitrogen rich amino acids would be lower in nitrogen- than in carbon starved filter cultures. Lastly, the frequency of nitrogen rich amino acids in the free amino acid pool was linked to their incorporation into proteins that were upregulated in response to nitrogen starvation. A biased abundance of free



cellular amino acids has the potential to affect the efficiency of translation. When a particular amino acid needed for protein synthesis is not or hardly available in the cell, translation most likely decelerates which entails growth disadvantages to an organisms. Thus, we suggested that a reduced abundance of nitrogen rich amino acids in the free amino acid pool had been the driving force that enabled selection owing to nitrogen deprivation to shape the composition of proteins involved in the nitrogen stress response towards a lowered incorporation of nitrogen rich amino acids.

In contrast, amino acids are not the primary storage for carbon and energy, instead lipids, the most carbon rich macromolecules [Sterner and Elser, 2002] and also various internal carbohydrates serve as important carbon and also energy storage in bacteria [Wilkinson, 1963]. Therefore, carbon starved cultures were expected to particularly breakdown lipids and carbohydrates. The released metabolites were expected to be utilized as carbon and energy sources for cellular processes. The expression of genes involved in lipid and carbohydrate degradation and the dynamics of cellular fatty acids were analyzed in a side study.

The goals of these analyses were 1) to show that over millions of years of evolution, selection owing to nitrogen deprivation had shaped the architecture of proteins upregulated in response to nitrogen starvation towards a lower nitrogen demand. This was expected to be seen in a lowered incorporation of the six nitrogen rich amino acids (arginine, asparagine, glutamine, histidine, lysine, tryptophan) when compared to the amino acid composition of proteins upregulated in response to carbon starvation. 2) to reveal that during nitrogen starvation nitrogen rich amino acids are recycled so that their amino groups become available for the synthesis of other biomolecules. 3) to link the cellular abundance of amino acids to their frequency in proteins upregulated under nitrogen starvation and thus to show that parsimonious nitrogen allocation is driven by a biased abundance of free cellular amino acids.

### 1.3.2 Persistent nitrogen limitation in continuous culture

To extend our understanding of the dynamics of nitrogen conservation in response to nitrogen availability *E. coli*, cultures were grown in an environment where the availability of nitrogen was directly controlled over an evolutionary relevant timescale. Hence, a second experiment was designed in which *E. coli* was maintained in exponential growth phase for 1600 generations under nitrogen limitation. The advantage of such a continuous growing culture was a constant supply with fresh medium and thus preventing fluctuations in nutrient content. This created a stable environment in which the impact of a single limiting nutrient could be tested directly. Even though nitrogen limitation led to suboptimal growth rates, continuous cultures did not stop growing. Thus, the impact of nitrogen limitation was observed over much more generations than it would have been possible in the same amount of time with a regularly transferred shaking culture. This is due to the fact that shaking cultures reach stationary growth phase, in which growth is halted periodically due to unfavorable environmental conditions. Further, the continuous growing cultures were using their anabolic machinery permanently so that major processes of autophagy, resulting in a release of nitrogen storage molecules, were not expected to happen. A control culture was grown under identical conditions but it was supplied with nitrogen in excess.

By using this long-term cultivation experiment in which cultures were held in exponential growth phase continuously, it was expected to see evolution in action, further reducing the nitrogen demand of nitrogen limited cultures. To test this hypothesis, we observed the cellular carbon to nitrogen ratios of the continuous cultures over time to reveal overall nitrogen conservation in nitrogen limited cultures. Further, transcriptomics data were produced at regular intervals of time during the evolution experiment. This enabled us to compare the nitrogen budget of proteins significantly upregulated during nitrogen limitation over time.

Finally, evolved cultures were competed against each other and against their ancestor in nitrogen limited minimal medium to reveal whether the evolved nitrogen limited cultures had acquired growth advantages during their prolonged cultivation in a nitrogen limited environment.

The goals of these analyses were 1) to reveal that persistent nitrogen limitation over evolutionary relevant time scales further lowers the cellular nitrogen demand. This was expected to be seen in a decrease of the protein nitrogen budget, driven by evolutionary dynamics of gene expression levels. Further, protein nitrogen conservation was believed to increase over time. 2) to show that the adaptation to nitrogen limited conditions had an impact on the fitness of the evolved strains when grown in competition with their ancestor under nitrogen limiting conditions.

## 2 Material

### 2.1 Devices

All devices used in this study are listed in table 2.1.

**Table 2.1: List of devices used and device manufacturers**

<b>Device</b>	<b>Manufacturer</b>
Air pump (Air pump 3702-200)	Eheim, Deizisau
Benchtop centrifuges (5424 and 5424R)	Eppendorf, Hamburg
BioAnalyzer (TapeStation 2200)	Agilent Technologies, Santa Clara, USA
Centrifuge (Rotanta 460 RS)	Hettich Lab Technology, Tuttlingen
Centrifuge (5804R)	Eppendorf, Hamburg
Colony counter (ProtoCOL 2)	Synbiosis, Cambridge, England
Cycler (TPersonal48)	Biometra, Göttingen
Cycler (Mastercycler personal)	Eppendorf, Hamburg
Cycler (Applied Biosystems Gene Amp PCR Systems 9700)	Thermo Scientific, Waltham, USA
Electroporator & cuvettes (MicroPulser)	Bio-Rad Laboratories, München
Elemental Analyzer (EA3000)	EuroVector, Milan, Italy
Freezer (-20 °C, Premium No Frost)	Liebherr, Bulle, Switzerland
Freezer (-80 °C, VIP series ultra low)	Sanyo, Etten-Leur, Netherlands
Gel chambers	Bio-Rad Laboratories, München
Gel documentation (AlphaImager EP)	Alpha Innotech, San Leandro, USA
Incubator (Heratherm)	Thermo Scientific, Waltham, USA
Ion Chromatograph (792 Basic IC 1.0)	Methrom, Herisau, Switzerland
Magnetic stirrer (MR 30001 K)	Heidolph, Schwabach
Microplate Reader (Infinite 200)	Tecan, Männedorf, Switzerland
Mini centrifuge (Sprout)	Biozym, Hessisch Oldendorf
Mixing block (Thriller)	Peqlab, Erlangen
Peristaltic pumps (Ecoline VC-MS/CA8-6)	Ismatec, Wertheim
Pipettes (Research Plus)	Eppendorf, Hamburg
Power supply gel electrophoresis (E143)	Consort, Turnhout, Belgium
Refrigerator (Profiline)	Liebherr, Bulle, Switzerland
Shaker (Multitron Standrad)	Infors HT, Bottmingen, Switzerland
Ultrapure water system (Synergy UV)	Merck Millipore, Darmstadt
UV-Vis Spectrophotometer (Nano Drop 2000)	Thermo Scientific, Waltham, USA
Vacuum pump	Vacuubrand, Wertheim
Vortexer (Vortex Genie 2)	Scientific Industries, New York, USA
Water bath (WNB 29)	Memmert, Schwabach

## 2.2 Consumables

Standard consumables were obtained from the suppliers Carl Roth (Karlsruhe), Eppendorf (Hamburg), Greiner bio-one (Kremsmünster, Austria), Sarstedt (Nürnbrecht), Sigma-Aldrich (St. Louis, USA) and VWR (West Chester, USA). More specific consumables are listed in the tables 2.2 & 2.3.

**Table 2.2: List of consumables, corresponding trademarks and suppliers**

Items used for the persistent continuous cultures

Consumable	Trademark	Supplier
Air vent (5-way, metal)	Evolution	Kölle Zoo, Münster
Bioreactors	glass blown	Hans-Günther Schmidt & Sohn GbR
Bottle top filter (0.2 $\mu\text{m}$ PES membrane)	NALGENE <sup>®</sup>	Carl Roth, Karlsruhe
Caps bioreactors (PBT)	DURAN	Carl Roth, Karlsruhe
Filter sterile ventilation (PP, PTFE)	Millex <sup>®</sup> -FG	Carl Roth, Karlsruhe
Media bottle (glass screw neck, 10 l)		Carl Roth, Karlsruhe
Tubing (silicone)	Rotilabo <sup>®</sup>	Carl Roth, Karlsruhe
Tubing (tygone) for peristaltic pump		Ismatec, Wertheim
Tubing connectors (PP)	Rotilabo <sup>®</sup>	Carl Roth, Karlsruhe
Tubing reducers (PP)	Rotilabo <sup>®</sup>	Carl Roth, Karlsruhe
Tubing locking device (metal)	Rotilabo <sup>®</sup>	Carl Roth, Karlsruhe
Waste container (PP)		Carl Roth, Karlsruhe

**Table 2.3: List of consumables, corresponding trademarks and companies**

Items used for the short-term filter cultures

Consumable	Trademark	Company
Büchner funnel ( $\varnothing$ 90 mm,PP)	Rotilabo <sup>®</sup>	Carl Roth, Karlsruhe
Cuffs (rubber)	Rotilabo <sup>®</sup>	Carl Roth, Karlsruhe
Membrane filter (nitrocellulose, 0.45 $\mu\text{m}$ , $\varnothing$ 85 mm)	OXOID	Mibius, Düsseldorf
Suction flask (1 l)	Rotilabo <sup>®</sup>	Carl Roth, Karlsruhe

### 2.3 Kits

- Gel extraction Kit for extraction of DNA from agarose gels  
(Qiagen, Hilden)
- Nucleo Spin PCR clean-up for DNA concentration and removal of salts, enzymes, etc. from enzymatic reactions  
(Macherey and Nagel, Düren)
- Nucleo Spin Plasmid Kit for isolation of high and low copy plasmids  
(Macherey and Nagel, Düren)
- Ribo-Zero™ rRNA Removal Kit for gram-negative bacteria  
(epicentre, Madison, USA)
- RNA ScreenTape assay (including sample buffer) for quality check (RIN determination) of RNA samples  
(Agilent Technologies, Santa Clara, USA)
- RNeasy Mini Kit for isolation of bacterial RNA > 200 nt  
(Qiagen, Hilden)

All kits were used following the manuals strictly unless otherwise noted.

## 2.4 Chemicals, enzymes and media

### 2.4.1 Chemicals

Chemicals listed in table 2.4 were dissolved in sterile distilled water (dH<sub>2</sub>O) and obtained solutions were autoclaved at 121 °C for 20 minutes unless otherwise noted.

**Table 2.4: List of chemicals used and suppliers**

<b>Chemical</b>	<b>Supplier</b>
Acetanilide	Sigma Aldrich, St. Louis, USA
Agar-Agar	Carl Roth, Karlsruhe
Agarose (NEEO Ultra QualitÄdt)	Carl Roth, Karlsruhe
Ammonium sulphate	Carl Roth, Karlsruhe
Ampicillin sodiumsalt	Carl Roth, Karlsruhe
Calcium chloride	Carl Roth, Karlsruhe
Chelex <sup>®</sup> (100 Resin)	Biorad, Hercules, USA
Congored	Carl Roth, Karlsruhe
Coomassie (Brilliantblue R250)	Merck Millipore, Darmstadt
Coppersulphate-Pentahydrate	Carl Roth, Karlsruhe
D+-Glucose-Monohydrate	Applichem, Darmstadt
Diethylpyrocarbonate (DEPC)	Carl Roth, Karlsruhe
Difco Agar	BD Biosciences, San Jose, USA
Dipotassiumhydrogenphosphate	Applichem, Darmstadt
DNA ladder (100-10000 bp)	Peqlab, Erlangen
DNA ladder (100 bp)	Thermo Fisher Scientific, Waltham, USA
DNA loading dye (6 x)	Thermo Fisher Scientific, Waltham, USA
dNTP Mix (10 mM)	Thermo Fisher Scientific, Waltham, USA
EDTA-Dihydrate	AppliChem, Darmstedt
Ethanol (ultrapure)	Merck Millipore, Darmstadt
Ethanol (denaturated)	Carl Roth, Karlsruhe
Ethidium bromide	AppliChem, Darmstedt
Glacial acetic acid	AppliChem, Darmstedt
Glycerin (99%)	VWR, West Chester, USA
Go Taq <sup>®</sup> Master Mix	Promega, Madison, USA
Ironsulphate-Heptahydrate	Carl Roth, Karlsruhe
Kanamycinsulphate	Carl Roth, Karlsruhe
L-Arabinose	Carl Roth, Karlsruhe
Lysogeny broth medium	Carl Roth, Karlsruhe
Lysogeny broth agar	Carl Roth, Karlsruhe
Magnesiumsulphate-Heptahydrate	Carl Roth, Karlsruhe
Manganesesulphate-Hydrate	Carl Roth, Karlsruhe
Phenol (saturated, pH 4.3)	Sigma Aldrich, St. Louis, USA

Chemical	Supplier
Potassiumdihydrogenphosphate	Carl Roth, Karlsruhe
RNAProtect Bacteria Reagent	Qiagen, Hilden
Sodium acetate	Carl Roth, Karlsruhe
Sodium chloride	Applichem, Darmstadt
TRIS	Carl Roth, Karlsruhe
Tris-Chloride	Carl Roth, Karlsruhe
Tris-Sodiumcitrate-Dihydrate	Carl Roth, Karlsruhe
Tryptone	Carl Roth, Karlsruhe
Water Chromasolv <sup>®</sup>	Sigma Aldirch, St. Louis, USA
Yeast Extract	Carl Roth, Karlsruhe
Zincsulphate-Pentahydrate	Carl Roth, Karlsruhe
2-Mercaptoethanol	Carl Roth, Karlsruhe

#### 2.4.2 Enzymes and corresponding buffers

- DNaseI and 10X buffer  
(Roche, Basel, Switzerland)
- Vent R<sup>®</sup> DNA Polymerase and ThermoPol<sup>®</sup> buffer  
(New England Biolabs, Frankfurt)
- Phusion<sup>®</sup> DNA Polymerase and HF buffer  
(New England Biolabs, Frankfurt)
- Lysozyme  
(Applichem, Darmstadt)
- T4 DNA Ligase and corresponding buffer  
(New England Biolabs, Frankfurt)
- Restriction enzymes *KpnI*, *PstI* and *NdeI*, and buffers 1.1 and CutSmart  
(New England Biolabs, Frankfurt)
  - *KpnI*  
5'...GGTAC<sup>^</sup>C...3'  
3'...C<sup>^</sup>CATGG...5'
  - *PstI*  
5'...CTGCA<sup>^</sup>G...3'  
3'...G<sup>^</sup>ACGTC...5'
  - *NdeI*  
5'...CA<sup>^</sup>TATG...3'  
3'...GTAT<sup>^</sup>AC...5'

### 2.4.3 Culture media and buffer

Table 2.5 lists the antibiotics added to culture media and the concentration at which they were utilized. The antibiotics were dissolved in dH<sub>2</sub>O, sterile filtrated and stored at -20 °C.

**Table 2.5: List of antibiotics and their concentrations**

<b>Antibiotic</b>	<b>Stock concentration</b>	<b>End concentration</b>
Ampicillin	100 mg/ml	100 µg/ml
Kanamycin	10 mg/ml	50 µg/ml

### Culture media

double yeast tryptone  
(DYT) medium

5 g NaCl  
10g Yeast Extract  
16 g Tryptone

Congored agar

15 g Agar-Agar  
4 g Yeast Extract  
8 g Tryptone  
32 mg Congored  
16 mg Coomassie

Swarming agar

25 g LB medium  
3 g Difco Agar

lysogeny broth  
(LB) medium

25 g LB medium

lysogeny broth  
(LB) agar

40 g LB agar

Culture media were prepared with 1000 ml (Congored agar with 800 ml) dH<sub>2</sub>O and autoclaved for 20 minutes at 121 °C. Antibiotics were added aseptically to cooled (< 55 °C) dYT medium, LB medium and LB agar whenever needed.

### Buffer

TAE buffer (50 x)

2 M TRIS  
50 mM EDTA  
5.71 % (v/v) glacial  
acetic acid

TE buffer

10 mM Tris-Chloride  
1 mM EDTA  
set pH to 8.0  
autoclave

PBS buffer (10x)

1.37 M NaCl  
27 mM KCl  
100 mM Na<sub>2</sub>HPO<sub>4</sub>  
18 mM KH<sub>2</sub>PO<sub>4</sub>  
set pH to 7.2  
autoclave



## 2.5 Software

- Alpha Imager EP Software  
(Alpha Innotech, San Leandro, USA)
- BibTeX, Version 0.99c (TeX Live 2009/Debian)  
(<http://ctan.org/pkg/bibtex>)
- BioAnalyzer Software 2200  
(Agilent Technologies, Santa Clara, USA)
- Bowtie2  
[Langmead *et al.*, 2009]
- CLC main workbench  
(Qiagen, Hilden)
- DESeq  
[Wang *et al.*, 2010]
- Double digest finder  
(New England Biolabs, Frankfurt)
- EDGE-pro  
[Magoc *et al.*, 2013]
- Infinite 200 i-control Software  
(Tecan, Männedorf, Switzerland)
- Ion chromatograph 792 Basic IC Software  
(Methrom, Herisau, Switzerland)
- LaTeX, Version 3.1415926-1.40.10 (TeX Live 2009/Debian)  
(<http://latex-project.org>)
- Mendeley, Version 4.8.1  
(<https://www.mendeley.com/>)
- Nano Drop 2000 Software  
(Thermo Scientific, Waltham, USA)
- NEBioCalculator<sup>TM</sup>  
(New England Biolabs, Frankfurt)
- NEB cutter V2.0  
(New England Biolabs, Frankfurt)

- Perl, Version 14, subversion 2 (v5.14.2)  
(<https://www.perl.org/>)
- R, Version 2.14.1 (2011-12-22)  
(<http://www.r-project.org/>)

## 2.6 Databases

- BioCyc <http://biocyc.org/>
- EcoCyc <http://biocyc.org/organism-summary?object=ECOLI>
- KEGG <http://www.genome.jp/kegg/>
- NCBI <http://www.ncbi.nlm.nih.gov/>

## 2.7 Oligonucleotides

Oligonucleotides listed in the tables 2.6, 2.7 and 2.8 were obtained from Sigma Aldrich, St. Louis, USA. These were delivered desalinated and dry, their concentration was set to 100 pmol/ $\mu$ l by dissolving in Chromasolv<sup>®</sup> water.

**Table 2.6: List of oligonucleotides for the detection of *E. coli* Nissle 1917**

Name	Target	Sequence (5'→ 3')
Muta 5	plasmid pMUT1	AACTGTGAAGCGATGAACCC
Muta 6	plasmid pMUT1	GGACTGTTTCAGAGAGCTATC
Muta 7	plasmid pMUT2	GACCAAGCGATAACCGGATG
Muta 8	plasmid pMUT2	GTGAGATGATGGCCACGATT
Muta 9	plasmid pMUT2	GCGAGGTAACCTCGAACATG
Muta 10	plasmid pMUT2	CGGCGTATCGATAATTCACG

**Table 2.7: List of oligonucleotides for the amplification of the *kanR* gene from pACY177**

Name	Sequence (5'→ 3')
Kan.pACYCI	AACTGCAGTAAGCCAGTATACTC
Kan.pACYCII	GGGGTACCGTCCCGTCAAGTCAG

**Table 2.8: List of oligonucleotides for the amplification of the *kanR* gene from pUC-kanR**

Name	Sequence (5'→ 3')
Kan.pUCI	AAACACTATCTGCGTAAGCATGGCGCGAAGGCATATTACGGG CAGTAATGACGACGTTGTAAAACGACGG
Kan.pUCII	TCAAAAAACCAGGCTTGAGTATAGCCTGGTTTCGTTTGATTG GCTGTGGTAGGAAACAGCTATGACCATG

## 2.8 Strains and plasmids

Since *E. coli* Nissle 1917 harbors two plasmids and is genetically very stable, transformation and amplification of vectors used for cloning (table 2.10) were performed in the *E. coli* cloning strain DH5 $\alpha$  (table 2.9).

**Table 2.9: List of bacterial strains with references**

Name	Description	Reference
EcN	<i>E. coli</i> Nissle 1917 (DSM 6601), probiotic, O6:K5:H1	Mutaflor <sup>®</sup> , Ardeypharm (Herdecke)
EcN $\Delta$ <i>fliC</i>	EcN, deletion <i>fliC</i>	Troge [2012]
EcN $\Delta$ <i>fliC</i> , <i>kanR</i>	EcN, deletion <i>fliC</i> , kanamycin resistant	this study
DH5 $\alpha$	<i>E. coli</i> cloning strain	Invitrogen Sambrook and Russell [2001]

**Table 2.10: List of vectors and plasmids with references**

Name	Description	Reference
pKD46	helper plasmid, encodes $\lambda$ Red recombinase, temperature-sensitive replicon, ampR, 6.4 kb	Datsenko and Wanner [2000]
pACYC177	cloning vector, kanR, ampR, 3.9 kb	Chang and Cohen [1978]
pUC18	cloning vector, ampR, 2.7 kb	Yanisch-Perron <i>et al.</i> [1985]
pUC-kanR	ampR, kanR, 3.9 kb	this study

### 2.8.1 *Escherichia coli* Nissle 1917 $\Delta fliC$

The *E. coli* strain Nissle 1917 was used as model organism in the present study. The core genome of *E. coli* Nissle 1917 has a size of 5.1 Mb. Next to its core genome, *E. coli* Nissle 1917 has two small, stable and cryptic plasmids, namely pMUT1 (3173 bp) and pMUT2 (5526 bp) which can be detected via an *E. coli* Nissle 1917-specific PCR [Blum-Oehler *et al.*, 2003]. *E. coli* Nissle 1917 is closely related to the uropathogenic *E. coli* strain CFT073 and to the prophylactic *E. coli* strain ABU 83972 [Hancock *et al.*, 2010; Vejborg *et al.*, 2010]. Further, *E. coli* Nissle 1917 shows an encapsulated, fimbriated and motile phenotype [Vejborg *et al.*, 2010]. To reduce the motility of *E. coli* Nissle 1917 in the long-term continuous culture experiment performed for this study (see chapter 3.5.1), a mutant was used which lacked the *fliC* gene [Troge, 2012]. This gene is involved in the flagellar biosynthesis. *E. coli* Nissle 1917  $\Delta fliC$  showed a markedly decreased motility (figure 2.1) when compared to the wildtype *E. coli* Nissle 1917 (figure 2.2).

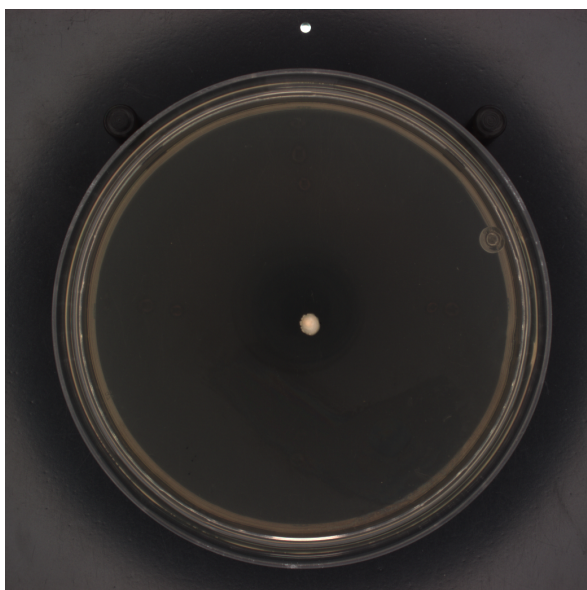


Figure 2.1: Motility of *E. coli* Nissle 1917  $\Delta fliC$  on swarming agar

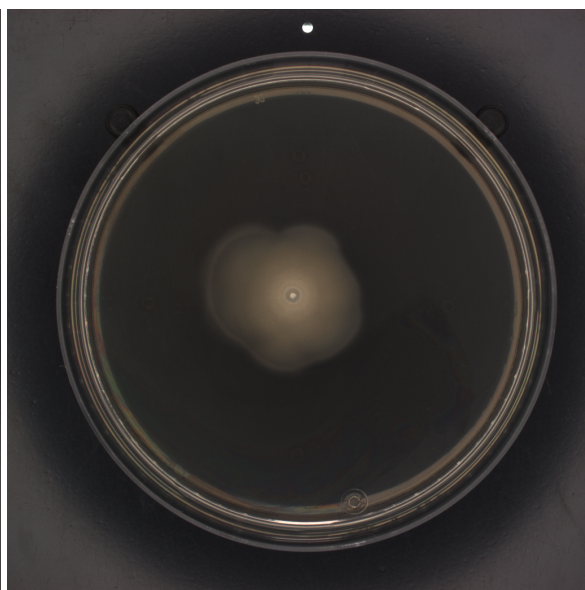
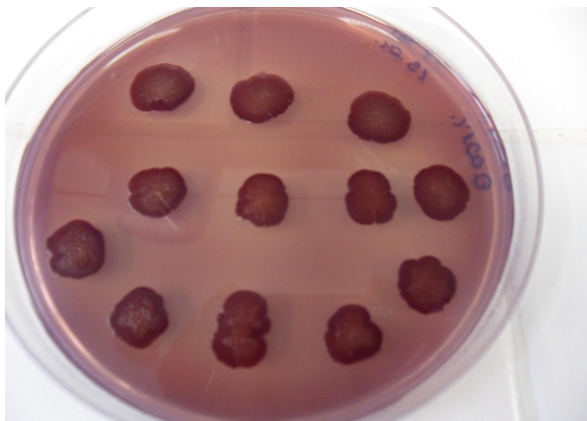


Figure 2.2: Motility of wild type *E. coli* Nissle 1917 on swarming agar

Furthermore, *E. coli* Nissle 1917 produces cellulose and curli as components of its extracellular matrix [Zogaj *et al.*, 2001]. Curli are thin, aggregative surface fibers [Gophna *et al.*, 2001] that are composed of the subunit curlin which is encoded by the *crl* gene. This gene is present and transcribed in most natural *E. coli* isolates [Olsen *et al.*, 1989]. While the assembling of the subunit protein into curli occurs below 37 °C in most strains [Olsen *et al.*, 1989], *E. coli* Nissle 1917 is able to assemble curli also at 37 °C. The binding of curli and cellulose to the dye congo red causes a specific morphotype which is called rdar, standing for red, dry and rough (figure 2.3 and figure

2.4) [Zogaj *et al.*, 2003]. Congored assays performed at 37 °C are reliable markers to test for the presence of pure cultures of *E. coli* Nissle 1917. They were performed with samples of the continuous cultures regularly to identify possible contaminations (see chapter 3.5.1.3). A contamination was recognizable by a morphotype deviating from the *E. coli* Nissle 1917-specific rdar one.



**Figure 2.3:** Congo red agar with colonies of *E. coli* Nissle 1917

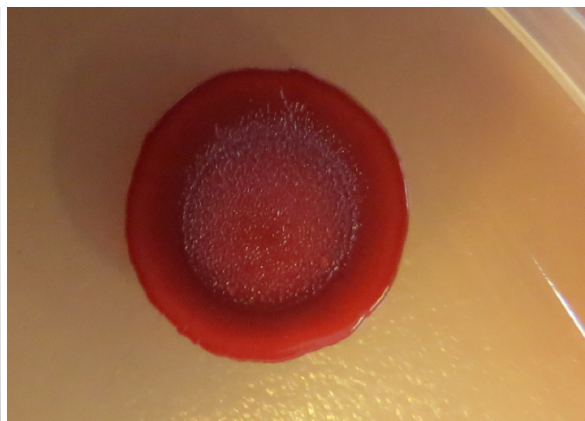


**Figure 2.4:** rdar morphotype of *E. coli* Nissle 1917  
On congo red agar, colonies of *E. coli* Nissle 1917 show a red, dry and rough (rdar) morphotype

---

## 3 Methods

### 3.1 Microbiological Methods

#### 3.1.1 Storage and incubation of bacterial cultures

Bacteria on solid media were stored at 4 °C for not more than one week.

Glycerol stocks were prepared for the long-term storage of bacteria . Therefore, 750 µl of a bacterial culture in exponential growth phase were transferred to a cryotube containing 250 µl of glycerin (100 %). The cryotube was vortexed thoroughly and stored at -80 °C. Glycerol stocks of bacteria were either used to inoculate liquid medium or streaked on solid medium.

Liquid cultures were cultivated in a shaking incubator at 180 rpm, solid cultures were incubated in an incubator. All cultures were cultivated under aeration at 37 °C, unless otherwise indicated. In general, bacterial cultures were grown in or on a self-made minimal medium and minimal agar, respectively (see chapter 3.3). For the different cloning procedures performed in this study, bacterial cultures were incubated in LB medium or on LB agar. Antibiotics were added in case of a present resistance.

#### 3.1.2 Determination of cell density and cell number

The concentration of bacteria in liquid cultures was determined by a measurement of the optical density (OD) at a wave length of 600 nm. A sample of the unconsumed growth medium served as reference. When the optical density was higher than 0.5, the corresponding culture was diluted to guarantee the linearity of the relationship between biomass concentration and optical density measured by the spectrophotometer.

The cell number of a liquid culture was estimated by counting the number of colony forming units (CFU). Here, a sample of the culture was diluted with PBS in a decimal serial dilution and 100 µl of each dilution were plated and incubated on LB agar overnight. Next day, the exact number of CFU on plates that contained 30 - 300 CFU was counted and the number of CFU per milliliter of the liquid culture was calculated (equation 1).

$$\text{CFU/ml} = \# \text{ CFU} \cdot 10 \cdot \text{dilution factor} \quad (1)$$

### 3.1.3 Congored assay

The presence of curli and cellulose in the extracellular matrix of bacteria was verified by the rdar morphotype expressed on congored agar. Samples taken from bacterial cultures were either spread on congored agar directly (10  $\mu$ l each) or transferred as single colonies from LB agar to congored agar. After incubation at 37 °C for 48 to 72 hours, congored assays were checked for the presence of the rdar morphotype.

### 3.1.4 Motility assay

To compare the swarming potential of *E. coli* Nissle 1917 and the deletion mutant *E. coli* Nissle 1917  $\Delta$ *fliC*, liquid cultures of these strains were adjusted to an optical density of 0.8. 1  $\mu$ l of the dilution was carefully transferred to a soft swarming agar. After incubation at 37 °C overnight, swarming assays were checked for motility of the strains. Motility was displayed by a circular movement of the cells originating from their initial insertion point.



## 3.2 Molecular biological Methods

### 3.2.1 Isolation of genomic DNA

For the isolation of genomic DNA from bacterial colonies grown on solid medium, a chelex based approach of DNA extraction was performed. 100 µl of a 5 % solution of Insta Gene Matrix were transferred to a sterile eppendorf tube while the solution was stirred on a magnetic stirrer. The colony from which genomic DNA needed to be isolated was picked up from the solid medium with an inoculation loop, transferred to the eppendorf tube and stirred in the Insta Gene Matrix solution. Next, this solution was vortexed, incubated at 100 °C for 10 minutes and then centrifuged at 12000 rpm for 3 minutes. After centrifugation, the supernatant which contained the genomic DNA was transferred to a new sterile eppendorf tube and stored at -20 °C.

### 3.2.2 Polymerase chain reaction

#### 3.2.2.1 *E. coli* Nissle 1917-specific multiplex PCR

The Nissle 1917-specific multiplex PCR after Blum-Oehler *et al.* [2003] was used to verify the plasmids pMUT1 (3173 bp) and pMUT2 (5526 bp) of *E. coli* Nissle 1917. The reaction mixture (total volume 20 µl) consisted of:

10 µl Go-Taq master mix (2x)  
 6 µl Primermix (5 pmol/µl each primer)  
 2 µl Template DNA  
 2 µl sterile Water Chromasolv®

Primermix: 1 µl of Muta 5 - Muta 10

PCR program:

Pre denaturation	95 °C	3 min
Denaturation	95 °C	45 sec
Annealing	60 °C	45 sec
Elongation	72 °C	45 sec
step 2 - 4:		35 cycles
End elongation	72 °C	5 min

The primers Muta 5 and Muta 6 amplified a 361 bp fragment of the plasmid pMUT1. The primers Muta 7 and Muta 8 amplified a 427 bp fragment and the primers Muta 9 and Muta 10 a 313 bp fragment, both originating from the plasmid pMUT2.

### 3.2.2.2 Amplification of the *kanR* gene from pACY177

With this PCR the *kanR* gene of the plasmid pACY177 was amplified. The reaction mixture consisted of:

0.5 µl	Vent Polymerase
2.5 µl	Thermopol buffer
1 µl	dNTPs (10 mM each)
2 µl	Primer Kan.pACYCI (10 pmol /µl)
2 µl	Primer Kan.pACYCII (10 pmol /µl)
x µl	Template DNA (→ 100 ng)

add sterile Water Chromasolv<sup>®</sup> to a total volume of 50 µl

PCR program:

Pre denaturation	95 °C	5 min
Denaturation	95 °C	30 sec
Annealing	58 °C	30 sec
Elongation	72 °C	1.5 min
<hr/>		
step 2 - 4:	30 cycles	
<hr/>		
End elongation	72 °C	5 min

The amplified *kanR* gene had a length of 1240 bp.

### 3.2.2.3 Amplification of the *kanR* gene from pUC-kanR

With this PCR the *kanR* gene of the generated plasmid pUC-kanR was amplified. The plasmid was linearized by inserting a single cut with the restriction enzyme NdeI before the PCR was started. The PCR reaction mixture consisted of:

0.5 µl	Phusion Polymerase
10 µl	HF buffer
1 µl	dNTPs (10 mM each)
1 µl	Primer Kan.pUCI (10 pmol /µl)
1 µl	Primer Kan.pUCII (10 pmol /µl)
x µl	Template DNA (→ 100 ng)

add sterile Water Chromasolv<sup>®</sup> to a total volume of 50 µl

PCR program:

Pre denaturation	98 °C	3 min
Denaturation	98 °C	10 sec
Annealing	60 °C	30 sec
Elongation	72 °C	60 sec
<hr/>		
step 2 - 4:	30 cycles	
<hr/>		
End elongation	72 °C	10 min

The amplified *kanR* gene had a length of 1515 bp and had overhangs that were homologue to the chromosomal region of *E. coli* that lies downstream of the arabinose operon.

### 3.2.3 Gel electrophoresis and DNA purification

DNA samples from restriction digests and PCR assays were mixed with 6 x DNA loading dye and applied on 1 - 2 % agarose gels (in TAE buffer). Applied markers were chosen according to the fragment length that was expected. The samples were separated electrophoretically at 80 - 120 Volt for 1 to 1.5 hours, 1 x TAE was used as running buffer. Afterwards, DNA was stained for 10 to 15 minutes in 1 µg/ml ethidiumbromide and DNA bands became visible by exposure of the gel to ultraviolet light. Bands of interest were cut out of the gel and purified with the Gel extraction kit.

### 3.2.4 Isolation of plasmid DNA

Plasmid DNA was isolated with the help of the Nucleo Spin Plasmid kit from 2 - 8 ml of an overnight culture grown in LB medium (10 g/l sodium chloride).

### 3.2.5 Restriction digest

1 µg of DNA was digested with 1 - 2 units of the restriction enzyme in a reaction volume of 30 µl. The reaction buffer was chosen according to the recommendation of New England Biolabs. The incubation time was 1 hour at 37 °C or, in case of a double digest, 2 hours at 37 °C. When possible, restriction enzymes were inactivated by an incubation at 65 °C for 10 minutes. In case the digestion mixture was not purified via gel extraction (see chapter 3.2.3), the Nucleo Spin PCR clean-up kit was used to remove remaining salts and enzymes.

### 3.2.6 Ligation

With the help of the NEBioCalculator, the ratio of insert : plasmid in ligation approaches was set to 3:1. Ligation mixtures consisted of 100 ng digested pUC18 and 140 ng of digested *kanR* gene. 1 µl T4 DNA ligase and 2 µl T4 ligase reaction buffer were added and the reaction mix was refilled with sterile Water Chromasolv<sup>®</sup> to a total volume of 20 µl. The ligation mixture was incubated at room temperature for 1 hour. Afterwards, the reaction was stopped by an incubation at 65 °C for 10 minutes, followed by a purification with the Nucleo Spin PCR clean-up kit.

### 3.2.7 Ethanol precipitation of DNA

Ethanol precipitation was used to concentrate DNA present in hydrous solution. First, 1 volume of DNA sample was mixed with 0.1 volume of ice cold 3 M sodium acetate (pH 5.2). Next, 2 volumes of 100 % ethanol were added and the mixture was stored at -80 °C for 15 minutes. Precipitated DNA was pelleted in a benchtop centrifuge at 4 °C and full speed for 20 minutes. The supernatant was discarded and the cell pellet was washed with 500 µl of 70 % ethanol. The sample was centrifuged again on the same conditions as before. Again, separated supernatant was discarded and the pellet was dried at 40 °C for about 3 minutes. The dry pellet was eluted in 30 µl of sterile Water Chromasolv®.

### 3.2.8 Concentration and purity of nucleic acids

The concentration and the purity of nucleic acids were determined with the Nano Drop method. DNA and RNA absorb light of a wavelength of 260 nm. An optical density of 1 at a wave length of 260 nm corresponds to a RNA concentration of 40 µg/ml and to a DNA concentration of 50 µg/ml, respectively.

The purity of RNA and DNA was determined by the ratio of absorbance at 260 nm and 280 nm. Here, a ratio of around 1.8 is accepted as pure for DNA and a ratio of about 2 is accepted as pure for RNA. Lower values report the presence of contaminants that absorb at 280 m, like proteins and phenol. Additionally, the ratio of absorbance at 260 nm and 230 nm was measured. Pure RNA and DNA samples have a 260/230 value between 2.0 and 2.2, lower values indicate the presence of contaminants like EDTA and carbohydrates that absorb at 230 nm.

### 3.2.9 Transformation of *E. coli* cells

Transformation is the transfer of free DNA into competent bacterial cells. In this study, plasmids and the *kanR* gene were transferred into electrocompetent cells of the *E. coli* strain DH5 $\alpha$  or of *E. coli* Nissle 1917  $\Delta$ *fliC* by electroporation.

#### 3.2.9.1 Preparation of electrocompetent cells

A single colony of an *E. coli* strain was incubated in DYT medium overnight and diluted 1:200 in 200 ml fresh DYT medium on the next day. The diluted culture was incubated again and harvested when an OD600 of 0.35 was reached. From this time point on, cells were kept on ice and all solutions and materials used were pre-cooled. Cultures were cooled on ice for 20 minutes and then centrifuged at 2000 x g for 15 minutes (4 °C). The supernatant was discarded and the cells were washed repeatedly with water and with a 10 % glycerol solution (1 x in 20 ml water, 1 x in 40 ml water, 1 x in 40 ml glycerol; 2000 x g for 15 min at 4 °C). After the last centrifugation step, the supernatant was discarded and the cell pellet was eluted in 0.5 ml 10 % glycerol. This suspension was diluted with 10 % glycerol in a way that a prepared 1:100 dilution had an OD600 of 0.4-0.6. The correctly diluted suspension was aliquoted (80  $\mu$ l each) and stored at -80 °C.

#### 3.2.9.2 Electroporation

Electrocompetent cells were thawed on ice and incubated with 100 - 200 ng plasmid DNA or 0.5  $\mu$ g of the amplified *kanR* gene on ice for 1 minute. The mixture was transferred to a cold electroporation cuvette and a short, electric pulse (1.8 kV, 6ms) was applied by the electroporator. Immediately, 1 ml of pre-warmed DYT medium was supplied and the cells were incubated at 30 °C (when the temperature-sensitive helper plasmid pKD46 was introduced) or at 37 °C (standard temperature for all other transformation) for 1 hour. Next, cells were pelleted by centrifugation (3000 rpm, 5 minutes). The supernatant was discarded and the cells were resuspended in the remainder. 100  $\mu$ l of this suspension were spread on a selective agar plate (LB agar containing ampicillin or kanamycin) and incubated overnight (30 °C or at 37 °C). On the next day, transformation efficiency was checked.

### **3.2.10 Insertion of the kanamycin resistance gene into the chromosome of *E. coli* Nissle 1917**

Colonies of *E. coli* Nissle 1917 in which the plasmid pKD46 was successfully transformed were made electrocompetent again. During this procedure, the expression of genes belonging to the plasmid's  $\lambda$  Red recombinase system was induced by the addition of 10 % arabinose. Next, the amplified *kanR* gene (see chapter 3.2.2.3) was inserted in the cells by electroporation and incorporated downstream of the arabinose operon. The incorporation of *kanR* into the bacterial chromosome was achieved with the help of the expressed recombination genes of plasmid pKD46. Clones identified to be kanamycin resistant after the transformation were incubated at 40 °C overnight to eliminate the temperature sensitive plasmid pKD46. Finally, glycerolstocks of *E. coli* Nissle 1917 *kanR* cultures were prepared.

### 3.3 Preparation of a defined culture medium

#### 3.3.1 Composition and preparation

Complex culture media like the lysogeny broth (LB) medium contain organic ingredients as yeast extracts and mixtures of different amino acids and peptides. Therefore, the exact content of the individual nutrients can not be quantified. Since the impact of nutrient availability on *Escherichia coli* was a key aspect of this study, nutrients had to be supplied in a well-defined way, most suitable as inorganic compounds. Hence, a minimal medium, referred to as full MM, that contained the minimal necessities for growth of *E. coli* was designed. Except for glucose, all mentioned nutrients were supplied in inorganic form as sulphate-, phosphate- or chloride salts (table 3.1).

**Table 3.1: Composition of the complete minimal medium (full MM)**

Nutrient	Supplied as	Molarity [mM]
Nitrogen	$(\text{NH}_4)_2\text{SO}_4$	30
Glucose	$\text{C}_6\text{H}_{12}\text{O}_6 \cdot \text{H}_2\text{O}$	28
Sodium	$\text{NaCl}$	8.6
Calcium	$\text{CaCl}_2 \cdot 2 \text{H}_2\text{O}$	0.2
Magnesium	$\text{MgSO}_4 \cdot 7 \text{H}_2\text{O}$	0.8
Manganese	$\text{MnSO}_4 \cdot \text{H}_2\text{O}$	0.3
Zinc	$\text{ZnSO}_4 \cdot 7 \text{H}_2\text{O}$	0.017
Copper	$\text{CuSO}_4 \cdot 5 \text{H}_2\text{O}$	0.02
Iron	$\text{FeSO}_4 \cdot 7 \text{H}_2\text{O}$	0.0018
Potassium	$\text{K}_2\text{HPO}_4$	50
Potassium	$\text{KH}_2\text{PO}_4$	50
	$\text{C}_6\text{H}_5\text{Na}_3\text{O}_7 \cdot 2 \text{H}_2\text{O}$	1.7

Glucose represented the carbon and energy source of this medium and nitrogen was added in the form of ammonium sulphate ( $(\text{NH}_4)_2\text{SO}_4$ ). Next to their use as potassium sources,  $\text{K}_2\text{HPO}_4$  and  $\text{KH}_2\text{PO}_4$  served also as a buffer solution with a strength of 50 mM that maintained the pH of the medium at 7.0.

Sodium citrate ( $\text{C}_6\text{H}_5\text{Na}_3\text{O}_7 \cdot 2 \text{H}_2\text{O}$ ) was used as a chelating agent for free cations to prevent precipitation of insoluble bounds between different ions (e.g., calciumphosphate). Complexed cations were still bio-available. Importantly, *E. coli* Nissle 1917 is unable to utilize sodium citrate as a carbon source (see figure 3.6, during incubation in glucose deficient minimal medium no growth was observed). Small amounts of metals (manganese, zinc, copper and iron) were added to the minimal medium since those, especially iron, are known to support growth of *E. coli* [Paliy and Gunasekera, 2007]. While the well known minimal medium DM25 (containing no iron) supports a maximal cell density of about  $5 \times 10^7$  cells per ml (for the *E. coli* strain B) [Lenski, 2015], the full minimal medium used in this study supported a maximal cell density which was about



eighteen times higher ( $\bar{O} 9 \times 10^8$  cells per ml). For this study, optimal growth in the full minimal medium was desired in order to create the best possible differences to cultures incubated in the different nutrient deficient minimal media (see chapter 3.3.3 and 3.3.4).

To prepare 1 liter of the full minimal medium the following recipe was used:

Glucose ( $C_6H_{12}O_6$ )	5 g
Magnesium sulphate ( $MgSO_4$ )	0.2 g
Sodium chloride ( $NaCl$ )	0.5 g
Sodium citrate ( $C_6H_5Na_3O_7$ )	0.5 g
add dH <sub>2</sub> O up to	888.9 ml

All the components were mixed thoroughly in a 1 l beaker and filtrated over a bottle top filter (pore size 0.22  $\mu m$ ) in a sterile 1 l glass bottle. Next, the following nutrients were added from sterile stock solutions:

Ammonium sulphate ( $(NH_4)_2SO_4$ , 40 %)	10 ml
Calcium chloride ( $CaCl_2$ , 2 M)	100 $\mu l$
Dipotassiumhydrogenphosphate ( $K_2HPO_4$ , 500 mM)	60 ml
Potassiumdihydrogenphosphate ( $KH_2PO_4$ , 500 mM)	40 ml
Metal solution	1 ml
(Iron sulphate ( $FeSO_4$ , 0.05%),	
Copper sulphate ( $CuSO_4$ , 0.5%),	
Manganese sulphate ( $MnSO_4$ , 5%),	
Zinc sulphate ( $ZnSO_4$ , 0.5%))	

For a detailed instruction of the medium preparation see chapter 6.

### 3.3.2 Testing the full minimal medium

To exclude the possibility that nutrients of the full minimal medium were supplied in a limited concentration, growth of *Escherichia coli* Nissle 1917  $\Delta fliC$  in full minimal medium was compared to its growth in full minimal media in which the concentration of one of the ingredients was doubled (figure 3.1). The testing was performed in shaking cultures and bacterial density was measured at OD600.

The tested doubled concentrations were:

- 17.2 mM NaCl ('Sodium')
- 0.4 mM CaCl<sub>2</sub> ('Calcium')
- 1.6 mM MgSO<sub>4</sub> ('Magnesium')
- 60 mM (NH<sub>4</sub>)<sub>2</sub>SO<sub>4</sub> ('Ammonium')
- 0.0036 mM FeSO<sub>4</sub>, 0.04 mM CuSO<sub>4</sub>, 0.6 mM MnSO<sub>4</sub>, 0.034 mM ZnSO<sub>4</sub> ('Metals')
- 56 mM C<sub>6</sub>H<sub>12</sub>O<sub>6</sub> ('Glucose')
- 100 mM K<sub>2</sub>HPO<sub>4</sub>, 100 mM KH<sub>2</sub>PO<sub>4</sub> ('Potassium')

Neither the maximal cell density nor the slope of the growth curves differed when *E. coli* Nissle 1917  $\Delta fliC$  was grown in the full minimal medium (full MM, figure 3.1) compared to the full minimal media in which the concentration of a certain ingredient was doubled (full MM + 2x X, figure 3.1). The generation time of *E. coli* Nissle 1917  $\Delta fliC$  was about 58 minutes in each medium tested. This clearly proved that the nutrient concentrations defined for the full minimal medium were high enough to support best possible growth of *E. coli* Nissle 1917  $\Delta fliC$  (at 37 °C).

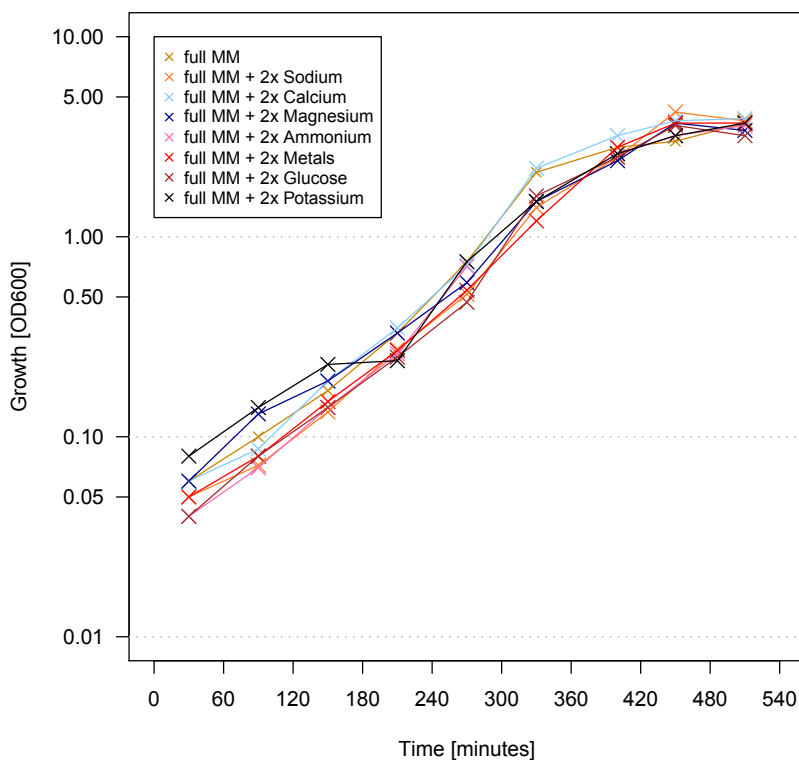


**Figure 3.1: Testing the composition of the full minimal medium**

Growth of *E. coli* Nissle 1917  $\Delta fliC$  in the defined full minimal medium (full MM) and in full minimal media with the double amount of a single ingredient (full MM + 2x X). Cell growth (optical density (OD) at 600 nm) is shown over 9 hours.

### 3.3.3 Minimal media for the short-term starvation experiment

For the short-term nutrient starvation experiment with filter cultures of *Escherichia coli* Nissle 1917 (see chapter 3.4), the full minimal medium could easily be adapted. The carbon deficient medium (referred to as C-def MM) lacked glucose and the nitrogen deficient medium (referred to as N-def MM) lacked ammonium sulphate while the concentrations of the residual nutrients were maintained unchanged. Solid media used in the nutrient starvation experiment were prepared by adding 15 g/l of sterile Agar-Agar to the different media (full MM, C-def MM and N-def MM).

### 3.3.4 Nitrogen limited medium for the long-term continuous culture experiment

For the long-term continuous culture experiment (see chapter 3.5), an adaptation of the full minimal medium to a nitrogen limited minimal medium was needed. To simplify this procedure, a growth limiting nitrogen concentration was first determined for a shaking culture of *Escherichia coli* Nissle 1917  $\Delta fliC$ . In a second step, this concentration was tested and verified in a continuously growing culture of *E. coli* Nissle 1917  $\Delta fliC$ .

Decreasing the amount of ammonium sulphate from 0.4 % (as it is set in the full MM) up to 0.05 % did not change the growth of shaking cultures of *E. coli* Nissle 1917  $\Delta fliC$  (figure 3.2). When decreasing the amount of ammonium sulphate below 0.05 %, the maximal cell density of *E. coli* Nissle 1917  $\Delta fliC$  decreased continuously until below 0.001 % ammonium sulphate no growth could be detected anymore (figure 3.2). According to these findings, a concentration of 0.001 % ammonium sulphate limited but not inhibited the growth of shaking cultures of *E. coli* Nissle 1917  $\Delta fliC$ .

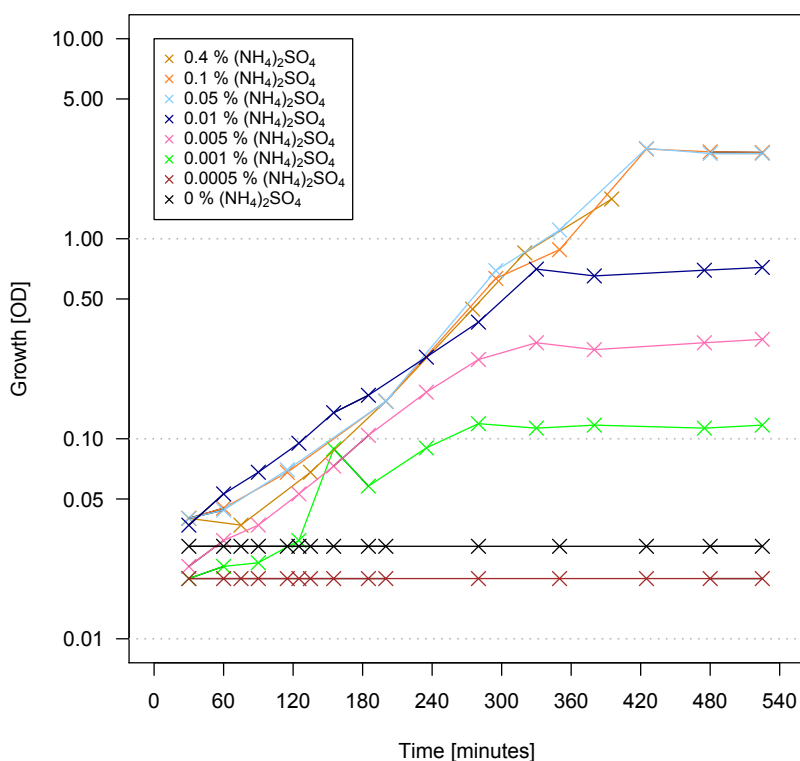


**Figure 3.2: Defining a growth limiting nitrogen concentration**

Growth of shaking cultures of *E. coli* Nissle 1917  $\Delta fliC$  in the defined minimal medium with different concentrations (0 to 0.4%) of ammonium sulphate ((NH<sub>4</sub>)<sub>2</sub>SO<sub>4</sub>). Cell growth (optical density (OD) at 600 nm) is shown over 9 hours.

Continuous cultures support constant cell growth via a consistent nutrient concentration. To test and verify that a concentration of 0.001 % ammonium sulphate also limits the growth of a continuous culture of *E. coli* Nissle 1917  $\Delta$ *fliC*, its cell density under these nutrient conditions was observed. A constant cell density of the corresponding continuous culture of about  $2.5 \times 10^7$  CFU/ml (figure 3.3) was measured over three days. After three days under these nutrient conditions, it was tested whether a lower ammonium sulphate concentration than 0.001 % would be sufficient to maintain a viable continuous culture of *E. coli* Nissle 1917  $\Delta$ *fliC*. For this purpose, the concentration of ammonium sulphate was halved to 0.0005 % which resulted in a constant decrease of culture density. On day seven, no cells were detected in the continuous culture anymore (figure 3.3). This verified that the concentration of ammonium sulphate should indeed be set to 0.001 % in the nitrogen limited minimal medium since a lower concentration failed to maintain a viable continuous culture.

It was further checked whether any other ingredient, besides nitrogen, turned out to be limiting in the continuous cultures. For this purpose, growth of the continuous culture of *E. coli* Nissle 1917  $\Delta$ *fliC* in a medium with 0.001 % ammonium sulphate and the double amount of all other ingredients (with respect to their defined amount in the full MM) was observed. Growth in this medium (2x MM with 0.001 %  $(\text{NH}_4)_2\text{SO}_4$ ) lead to an average cell density of  $2.5 \times 10^7$  CFU/ml (figure 3.3). The calculated cell density did not differ from the cell density of continuously growing cultures in MM with 0.001 %  $(\text{NH}_4)_2\text{SO}_4$  (figure 3.3). Contrary, when providing full minimal medium (with 0.4 %  $(\text{NH}_4)_2\text{SO}_4$ ) to the continuous culture, cell density of *E. coli* Nissle 1917  $\Delta$ *fliC* increased to about  $5 \times 10^8$  CFU/ml (figure 3.3). This analysis showed that nitrogen was the only limiting nutrient, thus the nitrogen limited minimal medium (referred to as N-lim MM in the following) was defined by a concentration of 0.001 % ammonium sulphate (0.076 mM) while the concentration of all other nutrients corresponded their concentration in the full minimal medium.

For a detailed instruction of the medium preparation see chapter 6.

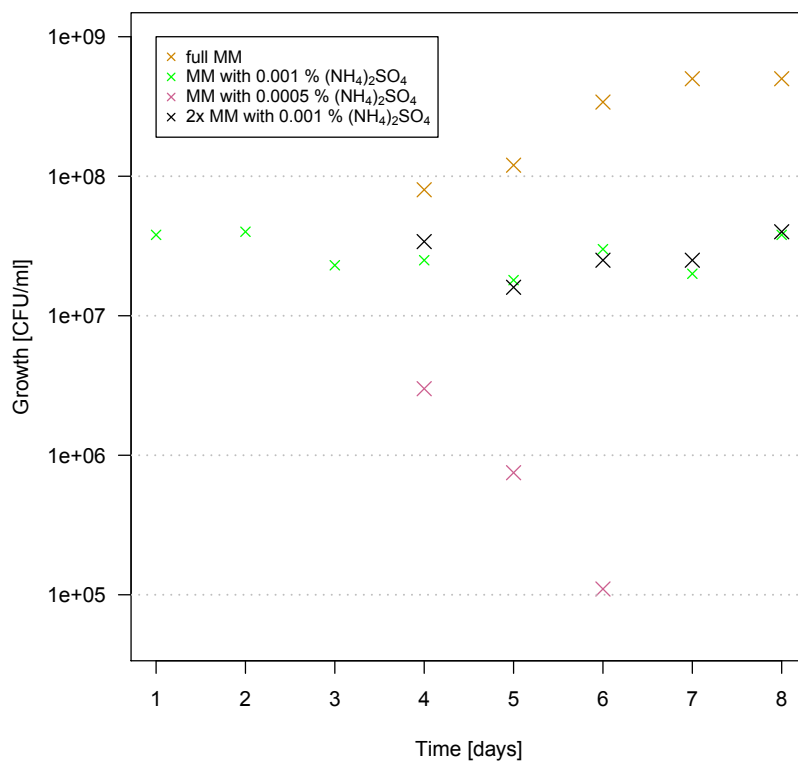


**Figure 3.3: Verifying the growth limiting nitrogen concentration**

Growth of continuous cultures of *E. coli* Nissle 1917  $\Delta flhC$  in full minimal medium (full MM), in minimal medium with 0.001%  $(\text{NH}_4)_2\text{SO}_4$  and the double amount of all other ingredients (2x MM with 0.001%  $(\text{NH}_4)_2\text{SO}_4$ ), in minimal medium with 0.001%  $(\text{NH}_4)_2\text{SO}_4$  and in minimal medium with 0.0005%  $(\text{NH}_4)_2\text{SO}_4$ . Cell growth (number of colony forming units per milliliter (CFU/ml) is shown over eight days.

---

## 3.4 Transient nutrient starvation of filter cultures

### 3.4.1 General overview of the experimental design

A single colony of *E. coli* Nissle 1917  $\Delta$ *fliC* was inoculated in 3 ml full MM and incubated for 6 hours. This culture was used to prepare an overnight culture in full MM. On the next day, 170 ml of the overnight culture were inoculated in 1530 ml full MM and cultivated in a shaker incubator. Once an optical density of about 1.0 was reached, the culture was placed on ice to cease growth. Nitrocellulose membrane filters were loaded with 20 ml of this culture each via vacuum pressure. The filters harboring bacterial cells on their surface were placed (side with bacteria up) in petri dishes containing solid full MM (figure 3.4). Filter cultures were incubated for 2.5 hours (figure 3.4, A). After this incubation step, the petri dishes were discarded while the filters were washed with pre-heated (37 °C) minimal medium. The washing step was performed with N-def MM (declaring nitrogen starved cultures, figure 3.4, B) or with C-def MM (declaring carbon starved cultures, figure 3.4, B). Next, the washed filter cultures were placed on pre-heated (37 °C) solid minimal medium (nitrogen starved cultures on solid N-def MM and carbon starved cultures on solid C-def MM). The starving cultures were incubated (figure 3.4, B) for different amounts of time until they were sampled for RNA and metabolites (see chapter 3.4.2). To grow the unstarved control cultures, some deviation from this procedure was needed. In this case, 20 ml of the liquid bacterial culture were loaded on membrane filters which were placed on solid full MM. The unstarved control filter cultures were incubated for 1.25 hours (figure 3.4, A). Next, filters were washed with pre-heated (37 °C) full MM, placed on fresh, pre-heated (37 °C) solid full MM and incubated again for 1.25 hours °C (figure 3.4, B). This division of incubation on solid full MM in two s allowed an identical treatment of the unstarved control and the nutrient starved filter cultures concerning the washing step and the transfer to a second fresh solid medium. The difference in incubation (1 x 2.5 hours for nutrient starved cultures and 2 x 1.25 hours for unstarved control cultures) did not bias the cell density of the different cultures. After in total 2.5 hours of incubation on solid full MM, the cell number of all filter cultures (unstarved control, nitrogen starved and carbon starved) was nearly identical ( $\bar{O}$  1 x 10<sup>10</sup> CFU/ml). The described approach was modified after Brauer *et al.* [2006]. The use of filter cultures allowed a fast and simple change of nutrient conditions as well as a fast quenching of metabolism during sampling (see chapter 3.6.1).

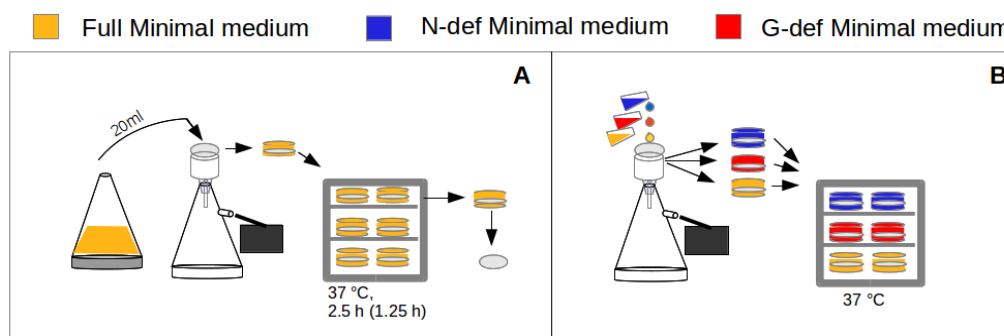


**Figure 3.4: Starvation of filter cultures**

A: Filter loading with exponentially growing cells of *E. coli* Nissle 1917  $\Delta fliC$  and incubation of filter cultures on solid full MM (yellow)

B: Washing of filter cultures and transfer to fresh solid full MM (unstarved control) or to solid deficient MM (blue: N-def MM for nitrogen starved cultures and red: C-def MM for carbon starved cultures)

### 3.4.1.1 Filter loading with liquid culture

Since the analysis of metabolites required a high amount of biomass, the cell density of the filter cultures had to be maximized without overloading and thereby clogging the filter pores. Several pre-testing was done, leading to the following decisions for the first part of the experiment (see figure 3.4, A).

The membrane filter's surface was chosen to be as big as possible, restricted by the size of the petri dishes that were used (filter:  $\varnothing$  85 mm, petri dish:  $\varnothing$  90 mm). The filter's pore size was 0.45  $\mu\text{m}$  since smaller sizes lead to clogged pores even with small amounts of liquid culture loaded.

The cell density of the liquid culture that was used to load the filter membranes was chosen to be as high as possible. The higher the cell density, the more biomass could remain attached to the filters. However, an excessive cell density would have led to an over-crowding and consequential to an insufficient nutrient supply, which was not desired at this stage of the experiment. To fit those requirements, the culture was grown until it had reached the exponential growth phase, and then, once a relatively high OD of 1.0 to 1.2 was reached (see figure 3.1), used for loading the filters. Further testing revealed that 20 ml of liquid bacterial culture with the given OD could be loaded per filter membrane without clogging the filter pores. Considering that an OD of 1.0 obtained under the given circumstances equals  $6 \times 10^8$  CFU/ml (own testing), it was assumed that about  $1.2 \times 10^{10}$  CFU/filter could be gained by loading 20 ml. However, when testing this, on average only  $4 \times 10^9$  CFU/filter could be detected. When using a liquid culture with an OD of 1.2 for loading no major differences in cell number were detected (on average  $4.5 \times 10^9$  CFU/filter). The difference between expected and real cell number was considered to be caused by a loss of cells during vacuum filtration when these were not able to attach to the filter surface quickly and properly enough. Nevertheless, it was decided to load 20 ml of a culture with an OD between 1.0 and 1.2 per filter. Therefore, 20 ml of the liquid culture were poured into a Büchner funnel



lined with a membrane filter. While the bacteria attached to the filter surface, the liquid was sucked into a 1000 ml suction flask using a vacuum pump.

Since the liquid culture had to be incubated for 6 to 7 hours to reach an OD of 1.0 when a 1:100 dilution was used, it was initially attempted to split the experiment in two consecutive days. On the first day, the liquid culture was incubated to an OD of 1.0, filters were loaded, placed onto the solid full MM and then stored in the refrigerator (4 °C) overnight. At this low temperature, no growth was possible. On the second day, the petri dishes were transferred to the incubator to start the actual experiment. However, this experiment resulted in weak growth during incubation on solid full MM at 37 °C, probably due to the overnight storage at low temperatures. Therefore it was decided to rather decrease the incubation time of the liquid culture to about 3.5 hours by diluting the overnight culture only 1:10. This enabled us to perform all parts of a nutrient starvation experiment on one day.

### 3.4.1.2 Incubation on solid full minimal medium

After loading, the filter cultures were first incubated on solid full minimal medium and not directly on a deficient minimal medium (see figure 3.4, part A). This was done since the vacuum filtration and the switch from liquid to solid medium might have triggered some kind of response in the bacteria which consequently would have interfered with the metabolic and/or the transcriptional response to nutrient starvation. This biased response would have been present in samples taken in the early phase after start of starvation (10 and 30 minutes, see chapter 3.4.2).

The incubation period on solid full minimal medium took 2.5 hours in which the bacteria doubled at least once (figure 3.5). All examined filter cultures increased their biomass even after those 2.5 hours (figure 3.5), showing that the nutrient supplementation during incubation on solid full minimal medium was sufficient.

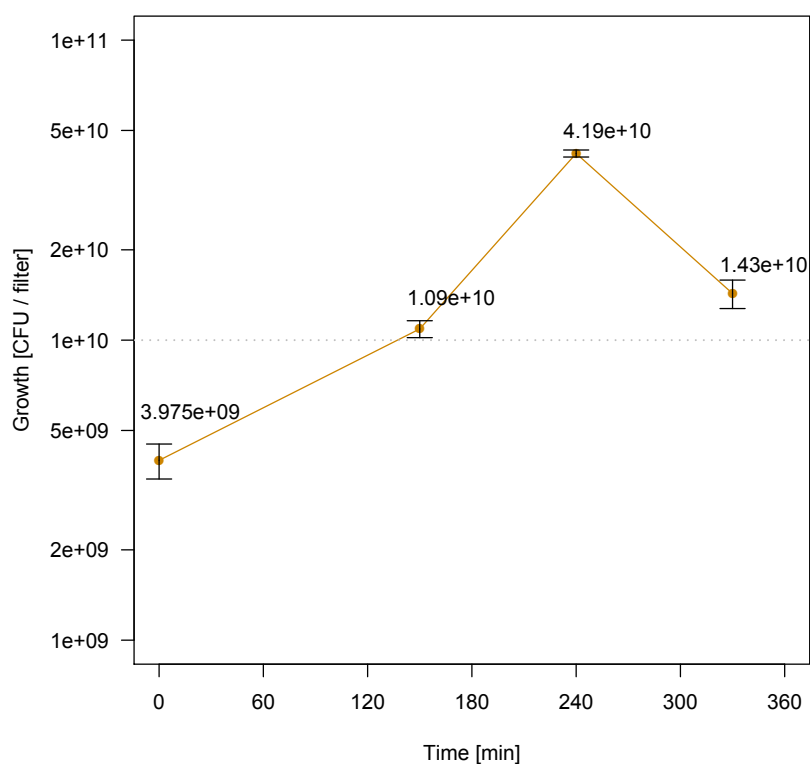


**Figure 3.5: Growth of filter cultures on full MM**

Growth of filter cultures of *E. coli* Nissle 1917  $\Delta fliC$  on full minimal medium. Mean cell growth  $\pm$  standard error (CFU/filter) of three biological replicates is shown over 5.5 hours.

### 3.4.1.3 Starvation on deficient minimal medium

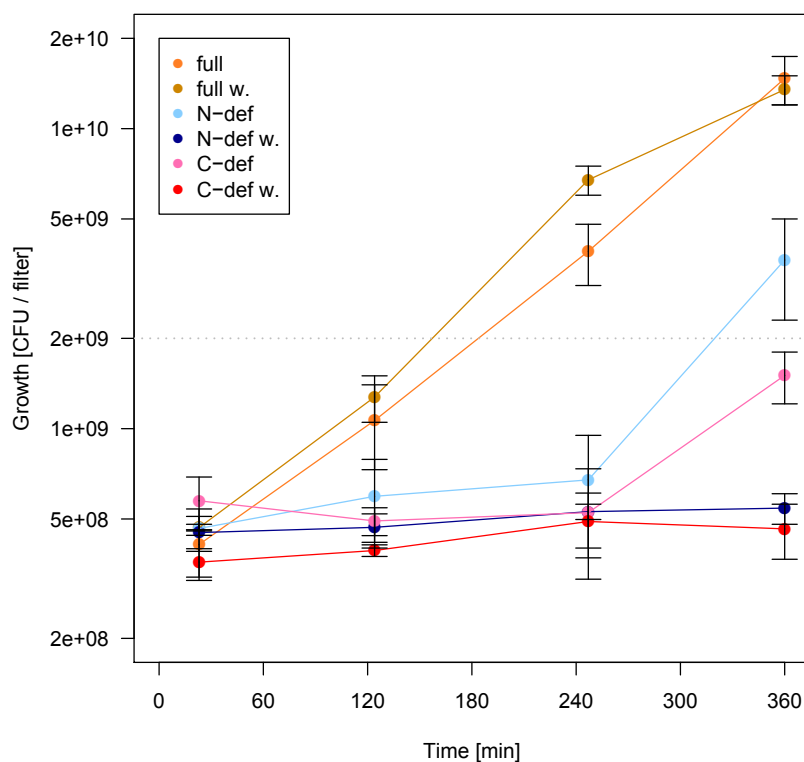
Parallel to the pre-testing described in the chapters 3.4.1.1 and 3.4.1.2, the starvation of filter cultures on the deficient minimal media was examined. It was observed that the filter cultures grew slightly when incubated on the deficient minimal media (figure 3.6 and table 3.2) which was not expected given the severe starvation applied. Considering that residues of nitrogen and carbon impurities in the media ingredients were too low to explain the observed pattern, it was assumed that the two nutrients had been transferred via the filter from the full to the deficient minimal media. To clarify this assumption and to avoid further nutrient transfer, a washing step was introduced (see figure 3.4, part B). Hereby, all nutrients sticking to the filter and to the bacteria should have been rinsed away. Washing was performed with the corresponding liquid deficient medium (N-def MM / C-def MM) thus providing the supplementation with all remaining nutrients during the washing procedure. Liquid media used for washing were pre-heated to 37 °C in order to avoid a confounding temperature stress response. As shown in figure 3.6 and in table 3.2, only minor growth of filter cultures on deficient medium was observed when filters were washed prior to their transfer to the deficient media. This implied that nitrogen and glucose indeed had been transferred from the full to the deficient media and therefore became available for the cultures.

As already described, the unstarved control cultures constantly grown on full minimal medium were washed and transferred to fresh medium as well (see figure 3.4), to guarantee that all cultures were exposed to the same treatment. When comparing the cell number of unstarved control cultures grown on solid full minimal medium with and without the washing step, no difference was observed (figure 3.6 and table 3.2), indicating that the washing procedure neither affected growth nor rinsed away cells from the filter.

**Table 3.2: Growth of filter cultures with and without washing step**

Mean number of colony forming units (CFU) and corresponding number of cell doublings of filter cultures of *E. coli* Nissle 1917  $\Delta fliC$  grown without washing step on: full MM (full), N-def MM (N-def), C-def MM (C-def) and grown with previous washing step on: full MM (full w.), N-def MM (N-def w.), C-def MM (C-def w.) after 20 and 360 minutes of incubation

filter culture	CFU 20 min	CFU 360 min	cell doublings
full	$4.00 \times 10^8$	$1.47 \times 10^{10}$	5
full w.	$4.68 \times 10^8$	$1.35 \times 10^{10}$	5
N-def	$4.65 \times 10^8$	$3.65 \times 10^9$	3
N-def w.	$4.50 \times 10^8$	$5.44 \times 10^8$	0
C-def	$5.75 \times 10^8$	$1.50 \times 10^9$	1
C-def w.	$3.59 \times 10^8$	$4.64 \times 10^8$	0

**Figure 3.6: Growth of filter cultures with and without washing step**











Growth of filter cultures of *E. coli* Nissle 1917  $\Delta fliC$  without washing step on: full MM (full), N-def medium (N-def), C-def medium (C-def) and with previous washing step on: full MM (full w.), N-def MM (N-def w.), C-def MM (C-def w.). Mean cell growth  $\pm$  standard error (CFU/filter) of three biological replicates for each conditions is shown over 6 hours.

### 3.4.2 Sampling scheme

The unstarved control cultures were sampled once, directly after the second incubation period on full MM which was referred to as time point T0 (table 3.3). The nutrient deficient cultures were sampled over time, following the time series T1-T5 (table 3.3), whereby time specifications refer to minutes after begin of starvation. At each time point, samples for RNA sequencing (see chapter 3.7.1) were taken while samples for metabolome analyses (see chapter 3.6.1) were only taken for T0, T1, T4 and T5 (table 3.3). The whole experiment was triplicated on three consecutive days and samples for a given time point were pooled in order to reach the minimum amount of biomass needed for the subsequent molecular work.

**Table 3.3: Sampling schema of filter cultures**

Sampling time point T0 for unstarved control cultures (yellow) and T1-T5 for nitrogen deficient cultures (blue) and carbon deficient cultures (red). Samples were taken for RNA sequencing ("RNA") and metabolite detection ("Metabolome"). Time refers to minutes after start of starvation

Sample point	T0	T1	T2	T3	T4	T5
Time [min]	0	10	30	60	120	240
RNA						
Metabolome			----	----		

### 3.5 Persistent nitrogen limitation in continuous culture

#### 3.5.1 General overview of the experimental design

In a continuous culture bacteria are constantly maintained in exponential growth phase. This is achieved via a steady supply of fresh growth medium to the culture vessel (referred to as ‘bioreactors’ in the following) while culture liquid is removed at the same flow rate. The flow rate of a continuous culture and its culture volume determine the dilution rate of the system (see chapter 3.5.1.1). When the dilution rate is constant, an equilibrium is established at which the growth rate of the bacteria equals the loss of bacteria due to removed culture liquid (see chapter 3.5.1.1). This equilibrium is called steady state and it causes a constant population size of a continuous culture [Drake and Brogden, 2002].

Figure 3.7 shows one of the bioreactors that were custom made for this study in a glass blowing factory. In the drawing of the bioreactor (figure 3.8) the positions of its four openings (reference 1 to 4) are shown. Fresh medium reaches the culture through opening 4 and the culture effluent passes opening 3. The openings 1 and 2 are needed for the aeration of the cultures. Incoming air is transported through opening 2 into the bioreactors. Through opening 1 expendable air is allowed to escape to prevent an increase of pressure inside the bioreactors.



**Figure 3.7: Picture of a bioreactor**  
The bioreactors used as culture vessels for the continuous cultures were custom made

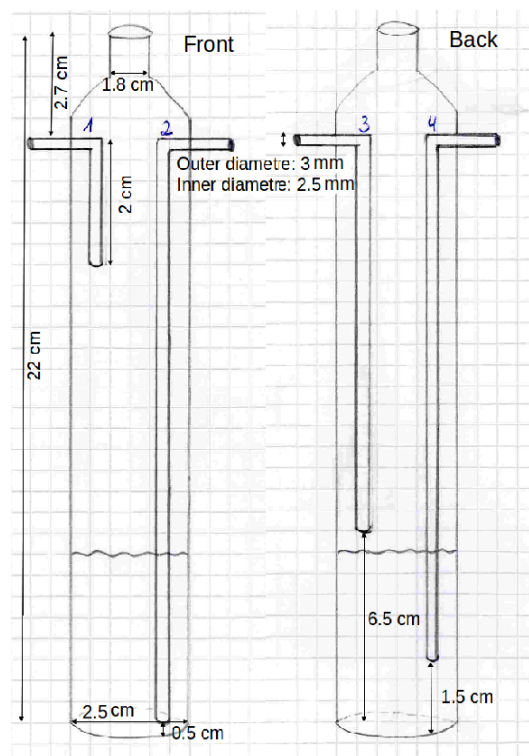


**Figure 3.8: Drawing of a bioreactor**  
The four openings (1-4) of the bioreactor and their positions: opening 1-2 on the front and opening 3-4 on the back of the bioreactor

The figures 3.9 and 3.10 show the experimental setup of the continuous cultures. The five bioreactors in the back row of the waterbath (figure 3.9) were the culture vessels of the control continuous cultures which were cultivated in full minimal medium. The five bioreactors in the front row contained the experimental cultures which were grown in nitrogen limited minimal medium. The five independent replicates per group (nitrogen rich control and nitrogen limited group) grew separately from each other. All continuous cultures originated from the same initial culture, referred to as ‘ancestor’. A sterile 10 liter medium vessel (figure 3.9 1) contained the growth medium which could leave the vessel by a tube leading through the screw cap. The medium was transported through this tube to a membrane pump (figure 3.9 2) and was distributed by a 5-way vent (figure 3.9 3) to the five bioreactors of a continuous group (figure 3.9 4). The five outlets of the 5-way vent could be adjusted individually to provide the same inflow of medium to each bioreactor. The bioreactors were placed in a water bath (figure 3.9 5) with a constant temperature of 37 °C. The water level was chosen to be high enough that the cultures were surrounded by water in their complete height. Fresh air was supplied constantly by aquarium air pumps (figure 3.9 8). The air stream that was leaving the pumps passed a sterile ventilation filter (pore size 0.22 µm) before it reached the bioreactors via a tube system. One air pump provided two individually adjustable outlets and the airflow could be further fine tuned via tube clamps placed in front of the bioreactors. This way the air pressure could be adjusted to be equal in each of the five bioreactors of a continuous group. The air stream generated air bubbles that aerated the cultures and provided a homogeneous distribution of the nutrients. Reference 9 in figure 3.9 shows the sterile ventilation filters that were attached to the opening 1 of the bioreactors (see figure 3.8) to guarantee that the whole culture system was closed against its surrounding. The medium effluent was collected in a waste container (figure 3.10 6) which was connected via a tube system to the bioreactors. Instead of flowing to the waste container, the effluent could be redirected to a clean short tube from which samples were taken (figure 3.9 7). This was achieved by implementing a T-shaped connector between the tube attached to the opening 3 of the bioreactor and the tube connected to the waste container. On the third opening of the T-shaped connector, the short tube for sampling was attached. The tube that was not in use (either waste container tube or sample tube) was clamped off from the system. Another sterile ventilation filter was connected to one of the openings of the waste container so that incoming air could escape. This prevented an increase of pressure within the waste container.

Since the openings of the bioreactors had a diameter of 3 mm (see figure 3.8), the tubes directly attached to the openings 1, 2 and 3 had the same diameter. The tube attached to the opening 4 only had a diameter of 2.54 mm since this was a special

tube (tygone tube) belonging to the media pump. Tubes that were directly attached to the waste container and the media vessel needed a bigger diameter (5 mm) to fit to the openings of these items. Therefore tube reducers were used when tubes of different diameters had to be connected. When tubes of the same diameter were connected, tube connectors were used.

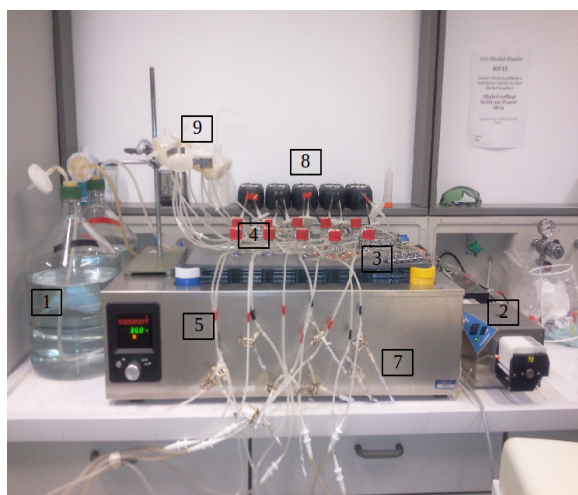


**Figure 3.9: Picture of the continuous culture: Part A**  
The picture shows the continuous culture with its media vessels (1), the membrane pumps (2), the 5-way vent for medium distribution (3), the bioreactors (4), the water bath (5), the tube for sampling and culture effluent (7), the air pumps (8) and the sterile filters (9)



**Figure 3.10: Picture of the continuous culture: Part B**  
The picture shows the waste container of the continuous cultures (6)

The system described was improved and adjusted in several pre-runs. The major challenge was to achieve an equal distribution of incoming air and medium to the five bioreactors. Unequal distribution of one or both of these components led to pressure imbalances between the reactors which resulted in an undirected effluent of medium and/or air belonging to the bioreactor(s) with the higher pressure. This problem was solved by using items that allowed a precise adjustment of air and medium inflow for each bioreactor separately (5-way vent for medium supply and adjustable air pumps). Herewith pressures in the reactors could be controlled completely.

Next to the pressure issue it was experienced that bacterial cells were able to some extent to move against the flow of the incoming medium and thereby reaching the tube system that transported the medium. Cells were able to attach to the inner layer of this tube and over time their biomass increased to an extent that the tube was massively clogged. The problem significantly decreased when using the deletion mutant of *E. coli* Nissle 1917 that lacked the *fliC* gene. This gene's product is the basic subunit of the flagellum of *E. coli*. The ability of *E. coli* Nissle 1917  $\Delta fliC$  to swarm was significantly decreased compared to the wildtype Nissle 1917 (see figures 2.1 & 2.2).

Prior to the start of the experiment, *E. coli* Nissle 1917  $\Delta fliC$  was kept in a shaking culture with daily transfer to fresh medium (full MM) for several days. In this time, *E. coli* Nissle 1917  $\Delta fliC$  could adapt its physiological and metabolic processes to the



minimal medium. A glycerolstock of this ancestor culture was stored. To start the continuous cultures, a sample of the ancestor culture was streaked on solid full minimal medium and incubated. After incubation, a part of a single colony was picked and inoculated in 3 ml full minimal medium and another part of the same colony was picked and inoculated in 3 ml N-lim minimal medium. Both cultures were incubated overnight. The next day, the cultures were inoculated 1:100 in 70 ml of the corresponding medium (full MM or N-lim MM) and incubated until the maximal cell densities were reached (culture in full MM: OD 1.3,  $1 \times 10^9$  CFU/ml; culture in N-lim MM: OD 0.2,  $3 \times 10^7$  CFU/ml). The shaking culture grown in N-lim minimal medium was distributed to five bioreactors to start the nitrogen limited cultures and the shaking culture grown in full MM was distributed to the second set of five bioreactors to start the nitrogen rich control cultures. The long-term continuous culture experiment was stopped after 1600 generations.

### 3.5.1.1 Dilution rate, generation time and ammonium availability

The dilution rate ( $D$ ) indicates the number of complete volume changes per hour of a continuous culture [Herbert *et al.*, 1956]. To calculate  $D$ , the flow rate of the system ( $F$ ) is divided by the culture volume ( $V$ ) (equation 2).

$$D = F \div V \quad (2)$$

The flow rate describes the speed of incoming fresh growth medium and of effluent culture broth. The culture volume is calculated by multiplying  $\Pi$  with the height ( $ht$ ) of the culture in the bioreactor and with the radius ( $r$ ) of the bioreactor (equation 3).

$$V = \Pi \cdot ht \cdot r^2 \quad (3)$$

The volume of each continuous culture was 25 ml. The culture volume was a constant in the present continuous culture system so that the dilution rate was solely adjustable via the flow rate. Generally, by adjusting the dilution rate, the number of cell divisions of a continuous culture can be varied by a factor of 10 without affecting the culture density [Dykhuizen and Hartl, 1983]. Within this range which is called ‘steady state’, the culture density is solely fixed by the proportion of the limiting nutrient in the growth medium [Dykhuizen and Hartl, 1983]. During the steady state, the dilution rate equals the growth rate of the culture [Herbert *et al.*, 1956]. Outside the steady state, the dilution rate can exceed the growth rate. When this happens, the culture will be washed out from the bioreactors since the increase of culture biomass is no

longer able to compensate the amount of cells lost with the culture effluent [Herbert *et al.*, 1956].

The maximal possible culture density of nitrogen limited cultures under the given nutrient supply ( $4.84 \times 10^8$  cells/bioreactor) was gained by choosing the lowest possible flow rate (10 ml/h/bioreactor). This was restricted by the sensitivity of the medium pump and its tubing size. With this flow rate and the given culture volume, the dilution rate for each nitrogen limited culture was  $0.4 \text{ h}^{-1}$  (see equation 2). In total, 1.2 liter N-lim minimal medium were depleted per day for the nitrogen limited cultures.

When the nitrogen rich control cultures were grown under the same flow rate as determined for the nitrogen limited cultures (10 ml/h/bioreactor), their culture density was on average  $7.25 \times 10^9$  cells/bioreactor. Enhancing the flow rate to 17 ml/h/bioreactor or to 25 ml/h/bioreactor decreased the generation time of the nitrogen rich control cultures but had no effect on their culture density. Hence, nitrogen rich control cultures could be maintained under steady state condition with all of the tested flow rates (10, 17 and 25 ml/h/bioreactor). Finally, it was chosen to run this cultures with a flow rate of 17 ml/h/bioreactor. The faster effluent (compared to 10 ml/h/bioreactor) decreased the amount of cellular biofilm which was build by the nitrogen rich control cultures especially in the tubing transporting the effluent (see chapter 3.5.1.2). With this flow rate and the given culture volume, the dilution rate per bioreactor was  $0.68 \text{ h}^{-1}$  (see equation 2). In total, about 2 liter full minimal medium were depleted per day for the nitrogen rich control cultures.

With the defined dilution rates and the fact that under steady state condition the dilution rate equals the growth rate ( $\mu$ ), it was possible to determine the generation time (gt) of the cultures. The generation time is calculated by dividing the natural logarithm of 2 ( $\ln 2$ ) by D or  $\mu$ , respectively (equation 4).

$$gt = \ln 2 \div D = \ln 2 \div \mu \quad (4)$$

Hence, the generation time of the nitrogen limited cultures was 104 minutes and the generation time of the nitrogen rich control cultures was 61 minutes. The given generation times resulted in about 14 doublings per day (nitrogen limited cultures) and about 23 doublings per day (nitrogen rich control cultures), respectively.

Since the biomass of the nitrogen rich control cultures was about ten times higher than the one of the nitrogen limited cultures, it was important to check whether the amount of ammonium available per bacterium was actually higher in the control cultures. Therefore, the concentration of ammonium in the culture effluents was measured by cation chromatography (see chapter 3.6.3) in a preliminary run.

The N-lim MM supplied the nitrogen limited cultures with 2.7 mg ammonium per liter. In the culture effluent, ammonium was detected at a level of 1.75 mg/l, showing that 0.95 mg/l were used up. Considering the given flow rate (10 ml/h/bioreactor), 240 ml of fresh medium were provided to a single culture in 24 hours, resulting in a daily ammonium consumption of 0.23 mg. With an average biomass of  $4.75 \times 10^8$  cells per culture, a single cell was estimated to consume about  $4.84 \times 10^{-10}$  mg ammonium each day and thus  $0.35 \times 10^{-10}$  mg ammonium per cell division (gt=104 minutes).

The full MM supplied the nitrogen rich control cultures with 1092 mg ammonium per liter. The cation chromatography of the culture effluent showed that 64 mg ammonium per liter were used up by the cultures. Considering the given flow rate (17 ml/h/bioreactor), 408 ml of fresh medium were provided to a single culture in 24 hours, resulting in a daily ammonium consumption of 26 mg. With an average biomass of  $7.25 \times 10^9$  cells per culture, a single cell was estimated to consume about  $3.56 \times 10^{-9}$  mg ammonium each day and therewith  $1.5 \times 10^{-10}$  mg ammonium per cell division (gt=61 minutes). These results showed that a bacterial cell of a nitrogen rich control culture consumed 4.3 times more ammonium than a bacterial cell of a nitrogen limited culture.

### 3.5.1.2 Construction and Cleaning

All the components of the continuous culture apparatus were sterilized. The openings of the tubes, the ventilation filters, the screw caps of the bioreactors and the media vessels and the different tube connectors and reducers were wrapped with aluminum foil, autoclaved (20 minutes at 121 °C) and dried. All glass vessels were capped with aluminum foil and sterilized by hot-air sterilization (2 hours, 180°C). As far as possible, given the size of the apparatus, the different items were connected under a sterile bench, else the aluminum foil was removed directly before setting the item in place and the connections were established as quickly as possible. Bioreactors were filled up with 10 ml of bacterial culture each and capped under the sterile bench. 10 l of the full minimal medium and of the N-lim minimal medium were prepared and filtrated through a bottle-top filter in sterile media vessels. When every system component was in its place, the media pump was switched on and each of the five bioreactors was filled to the same height (about 1 cm below the opening 3, see figure 3.8) with medium. The 5-way vent was adjusted in a way that the medium could reach each bioreactor at the same speed. During this refill phase, air bubbles in the media tube were removed by gently tapping the tube. When all reactors were filled, the air pumps were switched on and the aeration was adjusted for each culture until an effluent flow could be observed. Within the first 8 hours, the aeration of each culture possibly needed manual readjustment. All in all, the cultures typically reached a stable in- and outflow of air and medium within 30 minutes.

Media vessels were changed as soon as about 500 ml of medium were left within. Before this was done, all pumps were switched off. The tube connection proximal to the medium vessel was unplugged and connected to the tube of the new medium vessel. To minimize the risk of contamination during this switch, the exchange was performed as fast as possible and the tube was rinsed with ethanol before it was connected to the new medium vessel. The pumps were switched on directly after this exchange (which took about 30 seconds) and air and medium inflow and outflow were observed for a couple of minutes until they were stabilized again. The empty medium vessel was cleaned and sterilized again for further use.

The waste container was emptied once per week and gigasept (2%) was filled up to reduce growth of microorganisms and fungi. The liquid waste was autoclaved and then discarded.

Especially the nitrogen rich control cultures build biofilm which adhered to the pipes of the bioreactors and to the tubes transporting the effluent. Therefore, tubes were replaced regularly before the biofilm heavily clogged them. Furthermore, the nitrogen rich control cultures were stopped twice and the nitrogen limited cultures three times due to contaminations with different microbial strain. Even though the contaminations

affected mostly only single bioreactors, all five cultures were renewed to avoid spreading of the contaminant to other system components. Here, all pumps were switched off and the whole system was disconnected. All liquids were collected and autoclaved and all items of the system were pickled in Gigasept (2%) overnight. Next day, the tubes, tube connectors/reducers, the 5-way vent and the ventilation filters were rinsed with distilled water, hereby residues of biofilm were removed. All other items were cleaned in the dishwasher. After drying, everything was sterilized as described above and the system was started again (see chapter 3.5.1.3).

### 3.5.1.3 Housekeeping and backups

For a smooth performance of the continuous cultures, several testing and routine actions were performed on a regular basis. The day before the medium was exchanged, two small samples (5 ml each) of a freshly prepared medium were taken. One was used to measure the pH (always at  $7.0 \pm 0.1$ ), the second was incubated over night at  $37\text{ }^{\circ}\text{C}$  to check for contamination in the medium (which never occurred). Once per week, a sample of the culture effluent was taken and filtered through a syringe filter, then pH was measured (always at  $7.0 \pm 0.1$ ). The effluent and influent of medium and air were observed on a daily basis to assure that the pressures were balanced. Further, the tube system transporting the fresh medium was checked for air bubbles which sometimes occurred. In such case, these were removed by gently tapping against the tube. The amount of medium remaining in the media vessels was documented everyday to check the performance of the media pumps (depletion of  $\text{Ø } 1.2\text{ l N-lim MM/day}$  and of  $\text{Ø } 2\text{ l full MM/day}$ ). Also, the temperature and the water level of the water bath were controlled daily, water was refilled when necessary.

To assure that the cultures were maintained in steady state continuously, the optical density ( $\text{Ø } 0.03$  in the nitrogen limited cultures and  $\text{Ø } 0.6$  in the nitrogen rich control cultures) and the culture height ( $\text{Ø } 5\text{ cm}$ ) were checked daily. The culture densities were also controlled by determining the amount of colony forming units once per week ( $\text{Ø } 1.9 \times 10^7\text{ CFU/ml}$  in the nitrogen limited cultures and  $\text{Ø } 2.9 \times 10^8\text{ CFU/ml}$  in the nitrogen rich control cultures). Moreover, the dilution rate was checked weekly.

Due to the temporary disconnection of different tubes needed for the maintenance of the system, the system was vulnerable to contaminations of other microorganisms. In order to monitor the system, samples of each culture were streaked and incubated on congoled agar plates once per week and screened for the specific morphotype of *E. coli* Nissle 1917 (see chapter 2.8.1). Furthermore, a Nissle 1917-specific PCR (see chapter 3.2.2.1) was performed every 300 to 400 generations routinely and additionally, whenever the congoled screening assay revealed an *E. coli* Nissle 1917 unspecific morphotype.

Culture backups were prepared as glycerol stocks 24 hours after starting the continuous

cultures and then at regular intervals, at least once per week. Thus, backups of roughly about each 100th generation of the nitrogen limited cultures were prepared (table 3.4). Due to the shorter generation time of the nitrogen rich control cultures, more generations lie between two consecutive backups of this continuous group (table 3.5).

**Table 3.4: Backup scheme of nitrogen limited cultures**  
Number of generations at which backups of nitrogen limited cultures were prepared

Backup at generation
14
112
182
294
426
544
686
798
896
1008
1106
1204
1302
1400
1568

**Table 3.5: Backup scheme of nitrogen rich control cultures**  
Number of generations at which backups of nitrogen rich control cultures were prepared

Backup at generation
23
124
209
337
498
760
990
1105
1243
1427
1611

Backups were always prepared on the same day as a conged screening assay was performed to check whether the frozen back up contained a clean culture of *E. coli* Nissle 1917  $\Delta$ *ftiC*. The glycerolstocks were discarded when the conged assay revealed a culture contamination and the affected continuous cultures were unplugged and restarted with the latest respective clean culture backup. For that, the glycerol stock was used to inoculate 3 ml full minimal medium. This culture was incubated for 24 hours (37 °C, 180 rpm) and then diluted 1:100 in full minimal medium. Again, the culture was incubated for 24 hours (37 °C, 180 rpm). The next day, this culture was used to inoculate 70 ml of either full or N-lim minimal medium, depending on which continuous cultures had to be restarted. Unfortunately, no growth could be documented when the glycerol stocks were used to inoculate N-lim minimal medium directly. Therefore, the incubation of the backup cultures had to start in full MM as described above. Whenever the continuous cultures had to be restarted from a glycerol stock, no samples were taken for five days to allow the cultures to stabilize and adapt to their environment again.

### 3.5.2 Sampling scheme

Table 3.6 lists different molecular approaches performed with samples of the continuous cultures and timing at which they were performed. Generation (G) 100 to 1600 refer to the actual number of generations evolved in the continuous cultures and G14/23 refers to samples that were taken 24 h after the start of the continuous cultures and corresponds to 14 (nitrogen limited cultures) and 23 generations (nitrogen rich control), respectively. Samples for the C/N analysis (see chapter 3.6.2) and for the cation chromatography (see chapter 3.6.3) were taken for the generations 14/23, 100, 200, 300, 400, 500, 1000 and 1600 (table 3.6). To perform RNA sequencing (see chapter 3.7), samples from the generations 14/23, 100, 200, 500, 1000 and 1600 were analyzed (table 3.6). The competition experiment and the analysis of comparative growth were performed with shaking cultures of the frozen back ups from generation 1600 (table 3.6).

**Table 3.6: Sampling scheme of the continuous cultures**

Generation (G) 100 to 1600 refer to the actual number of generations evolved , G14/23 refers to samples taken 24 h after start of the continuous culture; an X indicates that a sample was taken

<b>Approach</b>	<b>G 14/23</b>	<b>G 100</b>	<b>G 200</b>	<b>G 300</b>	<b>G 400</b>	<b>G 500</b>	<b>G 1000</b>	<b>G 1600</b>
C/N	X	X	X	X	X	X	X	X
Cation chromatography	X	X	X	X	X	X	X	X
RNA	X	X	X			X	X	X
Comparative growth								X
Competition experiment								X

---

## 3.6 Chromatographic analyses

### 3.6.1 Detection of free cellular metabolites of filter cultures

The detection of free cellular metabolites was performed by the company Metabolomic Discoveries (Potsdam-Golm, Germany) on technical triplicates for each sampling time point of unstarved control- and nutrient deficient filter cultures. To harvest the filter cultures and to quench their metabolism as quickly as possible, cells were scratched from the filter surface with a clean metal spatula and immediately shock frozen in liquid nitrogen. The frozen cellular biomass was transferred to a sterile 1.5 ml cryotube. The weight of the obtained biomass was documented and the tubes were stored at -80 °C. Even though the biomass per filter was maximized (see chapter 3.4.1.1) and cells of multiple filters were pooled (see below), it was not possible to obtain the required amount of 100 mg wet biomass for each replicate on a single day. Therefore, the complete experiment was performed three times: At the first go, desired samples (unstarved control: T0, nitrogen- and carbon deficient: T1, T4, T5) were established in triplicates. Here, two filter cultures per replicate were sampled. The second and third time all replicates were restocked, whereby the number of filter cultures used depended on the amount of biomass already obtained. In total five to nine filter cultures were pooled per replicate.

For each sampling time point blanks were prepared by treating and sampling empty filters the same way as described above for the unstarved control- and nutrient deficient cultures. These blanks were analyzed by Metabolomic Discoveries to detect metabolite impurities originating from material and substances that were used during the experiment. Possible impurities were taken into account in the analysis of the samples. For the non-targeted detection of free cellular metabolites a combination of gas chromatography - mass spectrometry (GC-MS) and liquid chromatography - quadrupole time-of-flight mass spectrometry (LC-QTOF/MS) was used. These approaches allowed the detection of metabolites with masses between 50 and 1700 Da [Discoveries, 2013]. The quantity of the detected metabolites in a sample was normalized by the total cellular biomass. Metabolomic Discoveries identified successfully annotated metabolites by their name and not annotated ones by their mass and retention time. The intensities of all metabolites in the different samples were documented.

For the different analyses on amino acid abundance performed in this study, isoleucine and leucine were considered as a single amino acid. These two amino acid are too similar to be detected separately in the non-targeted detection of free cellular metabolites. Thus, only a common value on their abundance was provided by Metabolomic Discoveries.



### 3.6.2 Determination of the carbon to nitrogen ratio of continuous cultures

In the C/N analysis the ratio of the mass of overall carbon (C) to the mass of overall nitrogen (N) was determined for bacteria originating from the continuous cultures. For this analysis, culture effluent was collected in 50 ml Falcon Tubes which were cooled on ice. Full tubes were centrifuged at 5000 x g for 10 minutes and the supernatant was discarded. The biomass was resuspended in the remaining liquid, transferred to a sterile 1.5 ml tube and centrifuged for 1 minute at full speed in a benchtop centrifuge. Next, the complete supernatant was discarded and tubes were stored at -80 °C until further use. Samples were restocked until at least 25 mg of wet biomass were collected. The collected cell pellet was dried (72 hours at 37 °C) and 1 mg of the dried material was filled in tin capsules. Those were analyzed with an elemental analyzer which melted the sample and the capsule at 1020 °C. Due to an enriched atmosphere of oxygen within the analyzer, all substances were completely oxidized. The resulting substances CO<sub>2</sub>, N<sub>2</sub>, NO<sub>x</sub> and water passed a reduction reactor in which the nitrogen oxides were reduced to elemental nitrogen. The water was removed and the remaining carbon and nitrogen gases were detected and quantified. Acetanilide was analyzed in parallel and used as standard of known element composition. Empty tin capsules were used as blancs.

For each sampling time point two replicates of the nitrogen rich control cultures and two replicates of the nitrogen limited cultures were analyzed. The first replicate consisted of culture effluent from the bioreactors one to three of either nitrogen rich control- or nitrogen limited cultures and the second replicate consisted of culture effluent from the corresponding bioreactors four and five (numbers indicate position in the waterbath when counting from left to right, see figure 3.9).

### 3.6.3 Detection of cations in the effluent of continuous cultures

With a cation chromatography approach, the quantities of cations in the effluent of the continuous cultures were determined. The culture effluent was collected in 50 ml Falcon Tubes which were cooled on ice. The collected suspension was sterile filtrated and diluted (1:10) with dH<sub>2</sub>O. 10 µl of the diluted sample were injected in an ion chromatograph. An eluent (1.7 mmol/l nitric acid & 0.7 mmol/l dipicolinic acid) carried the sample through the system to a silicia column. Here, the different ions were separated. A detector measured the conductivity of the different cations. This enabled their identification and their quantification. The system was calibrated with the eluent before samples were measured.

For each sampling time point two replicates of the nitrogen rich control- and of the nitrogen limited cultures were analyzed. The replicates were pooled in the same way as described for the C/N analysis (sample 1: bioreactor 1 to 3, sample 2: bioreactor 4 and 5).

---

## 3.7 Transcriptomics

### 3.7.1 Cell harvest for RNA isolation from filter cultures

For RNA sequencing one sample of the unstarved control and of the nutrient deficient cultures were produced at each sampling time point. Although a single filter culture would have provided enough material for the one sample, RNA of multiple filter cultures was pooled to cover biological variation of a) different filter cultures of the same experimental day and b) filter cultures of the different experimental days.

Therefore, on each of the three experimental days two filter cultures per sampling point and condition (unstarved control, nitrogen- and carbon starved) were prepared as described in chapter 3.4.1. At each sampling time point the two filters were removed from the solid media and cut in two pieces. Each of the four filter-halves was placed in an empty petri dish and the bacterial cells were dissolved by pipetting 3 ml of bacteria stop solution quickly over the filter-halves. This solution consisted of 1 ml of the corresponding liquid culture medium (full MM, N-def or C-def MM) and of 2 ml of RNAProtect Bacteria Reagent (Qiagen). The bacteria stop solution immediately stabilized the RNA to ensure correct gene expression data. When all cells were eluted, the cell suspension was transferred to a 15 ml falcon tube, vortexed immediately and incubated at room temperature for 5 minutes. Next, the four tubes were centrifuged at 4 °C (5000 x g, 10 min). After centrifugation, the supernatants were discarded and cell pellets were stored at -80 °C. Hereby, the pellets of one filter-half were used as a back up while those of the second half were pooled together during RNA isolation.

### 3.7.2 Cell harvest for RNA isolation from continuous cultures

For RNA sequencing samples were taken from each bioreactor separately. Therefore, 50 ml Falcon tubes were prepared containing an ice-cold solution of 5 % (v/v) phenol, pH 4.3 and 95 % (v/v) ethanol. This RNA stabilizing solution constituted 2/5 of the sampled culture volume. 10 ml per nitrogen limited culture and 5 ml per nitrogen rich control culture were sampled. The tubes were chilled on ice while culture effluent was collected. The culture effluent/EtOH-Phenol mixture rested on ice for one hour, followed by centrifugation for 10 minutes (5000 x g, 4 °C). The supernatant was discarded, the cell pellet was resuspended in the remaining liquid and transferred to a sterile 1.5 ml tube. Another centrifugation step in the benchtop centrifuge (4 °C, full speed, 1 min) was performed. Next, complete supernatant was discarded and tubes were frozen at -80 °C until RNA was isolated (see chapter 3.7.3).

### 3.7.3 RNA isolation

RNA isolation from the cell pellets (see chapter 3.7.1 & 3.7.2) was performed using the RNeasy Mini kit. The TE-buffer was supplemented with 50 mg/ml lysozyme and the cells were incubated in this buffer for 15 minutes. Residual steps were performed strictly according to the manual of the RNeasy Mini Kit, whereby the optional second washing step with RPE-buffer was included. During this isolation process RNA molecules smaller than 200 nt were lost.

After RNA isolation, a DNA digestion step was performed to eliminate DNA traces that were not removed by the kit's spin-column technology. The DNA digestion reaction mixture consisted of:

x µl RNA (10 - 50 µg)  
5 µl 10 x DNaseI buffer  
2 µl DNaseI (20 U)

Sterile Water Chromasolv<sup>®</sup> was added to a total volume of 50 µl.

The reaction mixture was incubated at 37 °C for 30 minutes. The reaction was stopped by adding 2 µl of 0.2 M EDTA (pH 8.0) and incubating at 75 °C for 10 minutes. Afterwards, the RNA was purified according to the RNA cleanup protocol of the RNeasy Mini kit. After purification, the RNA was eluted in 25 µl of DEPC treated water.

In the nutrient starvation experiment, bacterial cells of two filter-halves were sampled at each sampling time point from the different filter cultures (unstarved control, nitrogen- or carbon starved) The obtained cell pellets were stored separately (see chapter 3.7.1). During RNA isolation, the two cell pellets that originated from the same nutrient condition and sampling time point were pooled after their incubation in TE-buffer. The whole filter culture experiment was performed three times and RNA of each experimental day was isolated separately. Isolated and digested RNA from equivalent samples of the three experimental days was pooled in a ratio 1:1:1 to establish one final RNA sample per sampling time point and nutrient condition.

All RNA samples derived from the continuous cultures and the filter cultures were stored at -80 °C.

### 3.7.4 RNA quality

The quality of the isolated RNA was determined by the measurement of its integrity number (RIN) via the Agilent Bioanalyzer. RIN is an objective measurement of RNA degradation with values ranging from 1 to 10. 1 is standing for totally degraded RNA and 10 for totally intact RNA. For the measurement, RNA samples were diluted to a concentration between 25 ng and 5000 ng and prepared according to the manual of the RNA ScreenTape assay. Next, sample tubes were placed in the Bioanalyzer which loaded the samples onto the screen tapes on which an electrophoresis was performed. Here, short RNA molecules as well as 16S and 23S rRNA were separated by length. The Bioanalyzer software generated a gel image and calculated the RIN of the samples. Samples with a RIN of at least 6 were further processed.

### 3.7.5 cDNA library preparation

Random-primed cDNA libraries of RNA samples originating from the short-term starvation experiment were prepared in a strand-specific manner by the company Vertis Biotechnology. In total, seven cDNA libraries were created (one for each of the sampling time points per nutrient condition, see chapter 3.4.2). The total RNA samples (10 µg each; RIN > 7) were first treated with a Terminator exonuclease to degrade ribosomal RNA (rRNA). Remaining messenger RNA (mRNA) was fragmented with ultrasound (4 pulses of 30 sec at 4 °C) and the fragments were poly(A)-tailed using poly(A) polymerase. Next, the 5' PPP and CAP structures were removed (using tobacco acid pyrophosphatase) and RNA adapters were ligated to the 5' monophosphate of the RNA fragments. First-strand cDNA synthesis was performed using an oligo(dT)-adapter primer and the M-MLV reverse transcriptase. The resulting cDNA was PCR amplified to about 30-50 ng/µl using a high fidelity DNA polymerase. During PCR amplification barcode sequences were added by the antisense primer to label the samples. The cDNA samples had a size range of 200 to 500 bp.

Due to the experimental setup, RNA samples of the long-term continuous culture experiment had a much lower quantity (1-6 µg; RIN > 6) than those of the short-term starvation experiment. Therefore, rRNA was removed from those RNA samples using the Ribo-Zero rRNA Removal Kit for gram-negative bacteria (Illumina). Here, only 1 µg of total RNA was needed as starting material. The rRNA depleted samples were further processed with the ScriptSeq RNA-Seq Library Preparation Kit (Illumina) to obtain strand-specific, indexed and random-primed cDNA libraries. The cDNA samples had a size range of 200 to 500 bp. The complete described preparation of cDNA libraries from RNA samples of the continuous cultures was performed in the laboratory of Professor Yutaka Suzuki (University of Tokyo, Japan). In total, 39 cDNA libraries were prepared, three from RNA samples of the ancestor and three for each sampling

time point of nitrogen limited cultures and nitrogen rich control cultures, respectively (3.5.2). The RNA samples of the continuous cultures always originated from the same three bioreactors of the corresponding continuous group (nitrogen limited or nitrogen rich control).

### **3.7.6 RNA sequencing**

The cDNA libraries of the short-term starvation experiment were sequenced on an Illumina highseq platform in the laboratory of Dr. Sebastian Leidel (Max-Planck-Institute, Münster). The cDNA libraries of the long-term continuous culture experiment were sequenced on an Illumina highseq platform in the laboratory of Professor Yutaka Suzuki (University of Tokyo, Japan). Multiplexed, single-end, 50 bp sequencing with 10 Mio reads/sample was performed.

---

## 3.8 Bioinformatics

### 3.8.1 Annotation

The program EDGE-Pro (Estimated degree of Gene Expression in Prokaryotes) [Magoc *et al.*, 2013] was specifically designed for quantifying the degree of gene expression in prokaryotes, typically showing high gene density and lack of alternative splicing. In a first step, EDGE-Pro performs an alignment of the short reads resulting from next generation sequencing to a reference genome using the program Bowtie2. Beforehand, Bowtie2 removes low quality positions and adapter sequences from the data. When aligning the reads to the reference genome, Bowtie2 allows up to ten alignments for each read as well as mismatches and small indels. In a second step, the reads with multiple alignments are filtered via an alignment score assigned by Bowtie2. Here, only the best-scoring alignments are assumed to be correct and all other alignments of the read are discarded. Next, the read coverage for each position in the genome is determined. By computing this per-base coverage for each gene, the EDGE-Pro pipeline overcomes the problem of assigning a read which maps in the overlapping part of two genes to one of these genes. In a last step, the coverage per base is converted into the RPKM (reads per kilo base per million mapped reads) value for each gene, which normalizes the expression level with respect to gene length and the total number of reads mapped. Finally, the EDGE-Pro pipeline outputs a report which contains the identity and coordinates of each gene and its average coverage, the number of reads mapped to the gene and the gene's RPKM value.

In the present study, the genome of the *E. coli* strain ABU 83972 (GenBank accession number: CP001671.1) was used as reference genome since the complete genome of *E. coli* Nissle 1917 has not been published until fall 2015. The strains ABU 83972 and Nissle 1917 are closely related to each other [Vejborg *et al.*, 2010] and the output of EDGE-Pro for sequence data of the short-term starvation experiment showed that more than 90 % of the reads originating from *E. coli* Nissle 1917 could be mapped to the genome of ABU 83972. This validated the use of the genome of *E. coli* ABU 83972 as reference genome.

The EDGE-Pro output for gene expression data of the short-term starvation experiment revealed that about 90 % of the mapped sequences of each sample belonged to rRNA, indicating that about 1 Million sequenced reads per sample originated from mRNA. The high number of rRNA sequences was due to an insufficient depletion of rRNA by the Terminator exonuclease (see chapter 3.7.5). In the RNA samples of the long-term continuous culture experiment rRNA was depleted with the Ribo-Zero rRNA Removal Kit for gram-negative bacteria (see chapter 3.7.5) which was much more effec-

---

tive. Almost all rRNA sequences (>99 % of the large cytoplasmic rRNA) were removed from the total RNA by this method, thus strongly enhancing the sequencing depth of mRNA sequences from this experiment (compared to that of the short-term starvation experiment).

### 3.8.2 Assessment of differential levels of expression

After processing of the sequencing reads with EDGE-Pro, the R package DESeq was used to test for differential expression of a given gene (based on the mRNA sequencing data) in two samples [Anders and Huber, 2010]. The EDGE-Pro output that provided information about the number of reads that had been mapped to a given gene in a specific sample was converted and adapted with a Perl script to a ‘read count table’ that could be used by DESeq. By declaring one set of samples as ‘case’ and the other one as ‘control’, DESeq compares the read counts of each gene between the ‘case’ and the ‘control’. Further, DESeq tests whether an observed difference in read counts is statistically significant using an algorithm based on the negative binomial distribution (referred to as nbinom-test in the present study). This method allows the analysis of experiments with no biological replicates as it was the case for the short-term starvation experiment. For the long-term continuous culture experiment, three biological replicates per continuous group (nitrogen limited and nitrogen rich control) and sampling time point and also three biological replicates of the ancestor were available for the analysis. In the end, one receives a table which lists the estimated mean expression level for each gene of a sample, the fold change of gene expression between the ‘case’ and the ‘control’ sample, the logarithm (to basis 2) of the fold change and the p-Value calculated for statistical significance of this change by testing on the negative binomial distribution. In the present study, the determined  $\log_2$  of the fold change (referred to as  $\log_2$  ratio in the following) is used when gene expression levels are analyzed. A gene that had a higher expression level in the ‘case’ sample than in the ‘control’ one had a  $\log_2$  ratio of  $> 0$  and a gene that had a lower expression level in the ‘case’ sample than in the ‘control’ one had a  $\log_2$  ratio of  $< 0$ . Before the analysis of gene expression levels for the different samples obtained from the long-term continuous culture experiment was performed with DESeq, transmembrane proteins were discarded from the data sets due to their biased nitrogen content exerted by structural constraints of the incorporated amino acids.

Gene expression levels calculated by DESeq were further used as reference for protein regulation in a given sample whenever we analyzed the nitrogen content and the amino acid composition of proteins. That means that in the framework of this study

a protein was considered to be ‘upregulated’ in a particular sample when the log<sub>2</sub> ratio of the expression of the encoding gene between this given sample (‘case’ sample) and the sample used as ‘control’ was positive. Consistently, a protein was declared as ‘downregulated’ in a particular sample when the log<sub>2</sub> ratio of the expression of the encoding gene between this given sample (‘case’ sample) and the sample used as ‘control’ was negative. Moreover, statistical significances of the change of gene expression between two samples were used as reference for statistical significances of the differences in protein regulation between these two samples. Thus, a protein that is assigned as ‘significantly upregulated’ or as ‘significantly downregulated’ in a specific sample is encoded by a gene for which a statistical significant difference in gene expression in this sample (with reference to the ‘control’) was validated by DESeq.

We are aware that mRNA levels have been found to not necessarily match the abundance of corresponding proteins [Maier *et al.*, 2009]. However, Ishihama *et al.* [2008] showed for *E. coli* a strong correlation between protein abundance and gene expression comparing protein levels obtained from LC-MS/MS approaches and computationally derived measures of gene expression levels. Further, we assumed that a protein which is encoded by a gene with a high expression level in response to nutrient depletion is crucial for cell viability under this circumstances and therefore gets translated accordingly. For the calculation of the protein nitrogen content and for the determination of the protein amino acid composition, protein sequences of *E. coli* ABU 83972 were obtained from NCBI.

### 3.8.3 Mapping to metabolic pathways

To investigate whether selected metabolic pathways were activated during the short-term nutrient starvation, genes that were associated to these pathways were identified and their expression level was analyzed. Therefore, an user account for the *E. coli* database EcoCyc was created and a ‘smart table’ for the strain ABU83972 was produced using the all pathways in the ‘add transform column’ field. The genes and enzymes of the pathways and citations, providing the codes for evidence, were added to the ‘smart table’. Given that every gene had to be mapped to its ABU83972 identifier, the corresponding html file was downloaded and parsed with a custom made perl script, thereby extracting relevant data such that each gene listed in the ‘smart table’ could be associated to its ECABU\_ID . Next, the ‘smart table’ was extended so each gene appeared as many times as it belongs to a different pathway and each line of the table contained the ECABU\_ID, the gene nickname, the number of pathways the gene belongs to, the chromosome and strand on which the gene is located, the gene’s start and end position on the chromosome, the name of the gene product, the metabolic pathway the gene is associated to and the correct citation. Next, a second table called



‘our\_superpathways’ was created in which a number of pathways was clustered together under a common broader metabolic function that was defined as superpathway (e.g. ‘Superpathway Carbohydrate degradation’ or ‘Superpathway Lipid degradation’). The superpathway information was added to the corresponding lines in the ‘smart table’. Finally, a perl script was produced which read the ‘our\_superpathways’ table and extracted all the genes belonging to each superpathway from the ‘smart table’. For each set of genes which was produced, a display of the log<sub>2</sub> ratios of gene expression in nitrogen deficient cultures versus the unstarved control and in carbon deficient cultures versus the unstarved control was created.

The described bioinformatic processing of the present data was performed by Robert Fürst, AG Acquisti, Münster.

### 3.9 Statistics

Whenever possible, data of independent technical and biological replicates were used for the different analyses performed within this study and either means with the corresponding standard deviation or standard error, else representative single data points were displayed.

The program R was used for generating the different diagrams as well as for the statistical analysis of the data. First, data were checked for normal distribution using the Shapiro-Wilk test and for variance homogeneity using the Bartlett’s test. Significant differences between data sets were validated by the Student’s-t test (when data were found to be normally distributed and homogeneity of variance was shown), the Welch’s test (when data were found to be normally distributed and heterogeneity of variance was shown) or the Wilcoxon’s test (when data were found to neglect normal distribution). Results were described as statistically significant if their error probability was less than 5 % ( $p < 0.05$ ) in either a one-sided test (when a certain expectation was tested) or a two-sided test otherwise. To test for differential expression of a given gene in two samples, the R package DESeq was used. DESeq uses an algorithm based on the negative binomial distribution (referred to as nbniom-test) to test for statistically significant differences in gene expression (see chapter 3.8).

---

## 4 Results

### 4.1 Transient nutrient starvation of filter cultures

This study aimed at investigating the starvation-survival response of filter cultures of *E. coli* Nissle 1917  $\Delta fliC$  towards the complete and short-term absence of an external nitrogen- or carbon source.

In response to nutrient starvation, many bacteria have developed strategies which allow them to overcome the starvation period until nutrient conditions change and become favorable for growth again [López-Maury *et al.*, 2008; Matin, 1991; Ropers *et al.*, 2006]. The basic cellular starvation-survival response includes a reduction of bulk protein synthesis [Reeve *et al.*, 1984a; Nyström *et al.*, 1990], pathways leading to the formation of key molecules that signal nutrient deprivation [Jozefczuk *et al.*, 2010; Postma *et al.*, 1993] and an increased expression level of genes involved in an improved scavenging of the nutrient concerned and in the acquisition of the desired nutrient from a variety of different substrates [Peterson *et al.*, 2005]. The different aspects of the described basic cellular starvation-survival response were analyzed in the nitrogen- and carbon starved cultures of the present study. Data of the unstarved control (see chapter 3.4.1) were used as reference for data obtained from nutrient starved cultures.

Additional to these basic cellular processes, nutrient starved cells mobilize internal reservoirs of the deprived nutrient by degradation of biomolecules, such as lipids [Singh and Cuervo, 2012], ribosomes [Zundel *et al.*, 2009] and proteins [Reeve *et al.*, 1984a]. These degradation processes are referred to as autophagy and their activation enables the starved cells to recycle the obtained nutrients in cellular components synthesized during nutrient starvation [Davis *et al.*, 1986; Hardie, 2011]. The mobilization of different nitrogen storage and carbon/energy storage in the nutrient starved cultures was analyzed, aiming to highlight the usage of nutrient specific internal reservoirs during the deprivation of a corresponding external source.

On the molecular level, we expected that the nitrogen stress response was reflected by a low nitrogen content of proteins upregulated in response to nitrogen starvation. Further, special emphasis was laid on the linkage between nitrogen conservation in proteins upregulated in response to nitrogen starvation, achieved through a lowered incorporation of the six nitrogen rich amino acids, and the mobilization of those amino acids as internal nitrogen reservoirs.

#### 4.1.1 Basic cellular starvation-survival response

The transfer of the filter cultures of *E. coli* Nissle 1917  $\Delta fliC$  to the media lacking either the carbon or the nitrogen source was expected to trigger a basic cellular starvation-survival response, including a reduction of protein synthesis, the dynamics of nutrient

deprivation specific key metabolites and an increased expression level of genes involved in nutrient acquisition. The investigation of these aspects of the starvation-survival response aimed to validate the starvation experiment.

As a measurement of protein synthesis, expression levels of ribosomal genes in nutrient deficient cultures were analyzed with respect to corresponding expression data of the unstarved control. Further, literature findings on specific genes and metabolites responding to nitrogen or carbon (prior glucose) starvation were retested with the available data of this study.

#### 4.1.1.1 Ribosomal gene expression

Figure 4.1 shows the distribution of the log<sub>2</sub> ratio of ribosomal gene expression in nutrient starved cultures to ribosomal gene expression in the unstarved control over time (for detailed information on gene expression analysis see chapter 3.8). Gene expression levels of the nutrient starved cultures were estimated for five sampling time points (see chapter 3.4.2). Log<sub>2</sub> ratios above zero indicate that ribosomal genes had a higher expression level in nutrient starved cultures, whereas a log<sub>2</sub> ratio below zero testifies a higher gene expression level in the unstarved control. The fifty ribosomal genes integrated in this analysis were obtained from GO:0003735 ('structural constituent of ribosome'), a complete list of these genes can be found in chapter 6.

All in all, the expression level of ribosomal genes declined in nitrogen and carbon starved cultures already 10 minutes after the onset of nutrient starvation and remained low for the remaining time course (figure 4.1).

The upper whiskers of the boxplots showing ribosomal gene expression in carbon starved cultures at the time points 10 to 60 minutes as well as the upper whiskers of the boxplots displaying ribosomal gene expression in nitrogen starved cultures at the time points 10 to 120 minutes ended below a log<sub>2</sub> ratio of zero (figure 4.1), showing that all ribosomal genes (except for those depicted as outliers) had a lower expression level in the nutrient starved cultures than in the unstarved control at these time points. After 240 minutes of nitrogen starvation, at least 75 % of all ribosomal genes had a lower expression level in nitrogen starved cultures than in the unstarved control, displayed by the the upper quantile of the concerned boxplot which was set at a log<sub>2</sub> ratio of -0.87 (figure 4.1). Similarly, at 120 and 240 minutes after the onset of carbon starvation at least 75 % of all ribosomal genes had a lower expression level in carbon starved and cultures than in the unstarved control, depicted by the the upper quantiles of the concerned boxplots which were set at log<sub>2</sub> ratios of -1.36 and -0.98, respectively (figure 4.1). The median log<sub>2</sub> ratios of expression data of nitrogen starved cultures declined from -1.07 at 10 minutes to -1.64 at 30 minutes and remained quiet constant for the residual time course (figure 4.1). Also the lower quantiles of these

---

boxplots remained stable at a log<sub>2</sub> ratio of around 2 between 30 and 240 minutes (figure 4.1). The lower whiskers of the boxplots showing ribosomal gene expression in nitrogen starved cultures decreased from a log<sub>2</sub> ratio of -2.28 at 10 minutes to -3.28 at 240 minutes, with a slight drop to -3.65 at 120 minutes (figure 4.1). In boxplots which display ribosomal gene expression in carbon starved cultures the median log<sub>2</sub> ratio declined from -1.21 at 10 minutes to about -2 (at 30, 120 and 240 minutes), interrupted by a slight increase to -1.61 at 60 minutes (figure 4.1). The lower quantile of these boxplots decreased from a log<sub>2</sub> ratio of -1.73 at 10 minutes to about -2.5 (at 30, 120 and 240 minutes), also interrupted by a slight increase to -2.15 at 60 minutes (figure 4.1). The lower whiskers of the concerned boxplots decreased from a log<sub>2</sub> ratio of -2.28 at 10 minutes to about -3 at 30 and 60 minutes and further to a log<sub>2</sub> ratio of about -4.65 at 120 and 240 minutes (figure 4.1). The general shifting of the boxplots towards more negative log<sub>2</sub> ratios between 30 and 240 minutes after start of nutrient starvation hinted on an increase in the difference of ribosomal gene expression between nutrient starved cultures and the unstarved control after the first 10 minutes of starvation. Outliers depicting extremely low log<sub>2</sub> ratios when comparing expression data of nitrogen starved cultures to the unstarved control were only detected at 10 and 30 minutes (figure 4.1). The genes whose data are represented by these outliers belong to the same operon: *rpsJ* showed a log<sub>2</sub> ratio of -2.42 at 10 minutes, *rplC* and *rplD* showed log<sub>2</sub> ratios of about -3.5 at 30 minutes (figure 4.1). The log<sub>2</sub> ratios of the same ribosomal genes and additionally of *rplW* were depicted as outliers in the comparison of gene expression between carbon starved cultures and the unstarved control at 30 minutes (figure 4.1). The log<sub>2</sub> ratios of those genes were quiet similar at 120 and 240 minutes after the onset of carbon starvation but slightly higher at 60 minutes (around -3.5) (figure 4.1). Outliers describing extremely high log<sub>2</sub> ratios in the comparison of gene expression in nitrogen starved cultures and the unstarved control represent data of the genes *rpsV* and *ykgM* whose log<sub>2</sub> ratios increased over time (10 to 120 minutes) as well as of the gene with the identifier ECABU\_c03820 for which a log<sub>2</sub> ratio of 0.35 was calculated at 30 minutes (figure 4.1). The log<sub>2</sub> ratios of the same genes were depicted as outliers in the comparison of gene expression between carbon starved cultures and the unstarved control: the gene *rpsV* had the highest log<sub>2</sub> ratios (2.09, 2.16, 1.80) within the first three sampling time points (10, 30 and 60 minutes) but its log<sub>2</sub> ratios were not defined as extreme values in the later time points (figure 4.1). The log<sub>2</sub> ratio of *ykgM* increased constantly from 1.01 at 30 minutes to 2.41 at 240 minutes (figure 4.1). Log<sub>2</sub> ratios of a third gene, *rplO*, were as well considered as outliers in carbon starved cultures (log<sub>2</sub> ratios increased from 0.40 to 1.13 between 30 and 120 minutes) (figure 4.1).

Ribosomal gene expression was analyzed as a measurement of protein synthesis. Hence, the present analysis shows that bulk protein synthesis was decreased comparably in response to carbon- or nitrogen starvation.

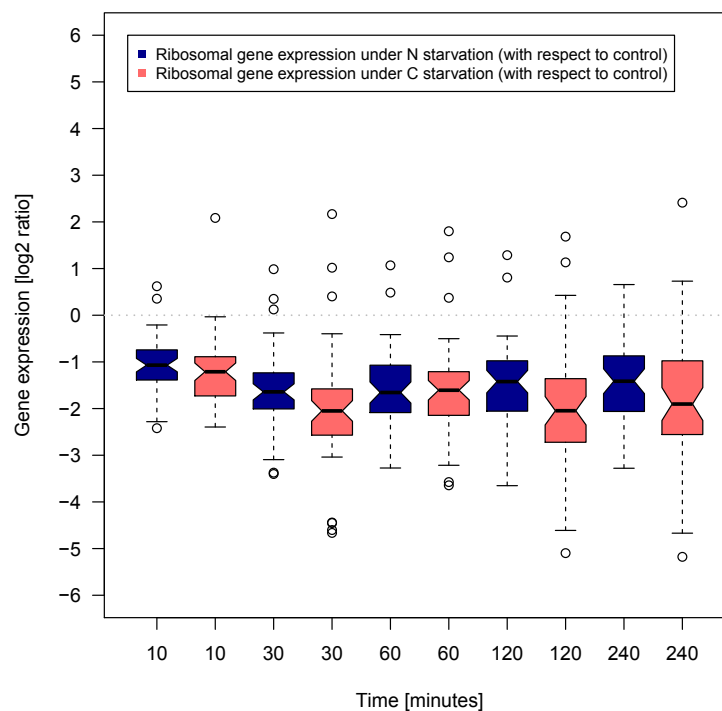


**Figure 4.1: Ribosomal gene expression in nutrient starved cultures**

Distribution of the log<sub>2</sub> ratio of ribosomal gene expression of nutrient starved cultures to ribosomal gene expression of the unstarved control at the sampling time points 10, 30, 60, 120 and 240 minutes after starvation onset. N = nitrogen, C= carbon

#### 4.1.1.2 Dynamics of nutrient key metabolites

##### Nitrogen starvation key metabolites

Figure 4.2 shows the mean ratio  $\pm$  the standard error of glutamine and 2-oxoglutarate abundance in nutrient starved cultures to their abundance in the unstarved control over time (for detailed information on the analysis of free metabolites see chapter 3.6.1). Hereby, the mean metabolite abundance (averaged over three biological replicates) in nutrient deficient cultures obtained at the three sampling time points was set each in relation to corresponding mean abundance levels in the unstarved control (averaged over three biological replicates) (see chapter 3.4.2). A ratio above one indicated that the metabolite was more abundant in nitrogen- or carbon starved cultures, whereas a ratio below one testified a higher metabolite abundance in the unstarved control.

In summary, the present data show that the cellular glutamine abundance was low in the nitrogen starved cultures and that the cellular 2-oxoglutarate level increased upon nitrogen starvation. The dynamics of these metabolites were different under carbon starvation, here glutamine accumulated and the 2-oxoglutarate level was low upon starvation.

Cellular glutamine levels were lowered during nitrogen starvation (ratio to unstarved control:  $0.86 \pm 0.39$  (10 minutes),  $0.93 \pm 0.17$  (120 minutes) and  $0.77 \pm 0.1$  (240 minutes)) (figure 4.2 A). In carbon starved cultures, cellular glutamine had accumulated already 10 minutes after the onset of starvation (ratio to unstarved control:  $2.48 \pm 0.2$ ) but its abundance decreased over time (ratio to unstarved control:  $1.74 \pm 0.09$  (120 minutes) and  $1.48 \pm 0.08$  (240 minutes)) (figure 4.2 A). The abundance of glutamine was significantly lower in nitrogen than in carbon starved cultures at each sampling time point (figure 4.2 A).

Already 10 minutes after the onset of starvation, 2-oxoglutarate levels had accumulated markedly in nitrogen starved cultures (ratio to unstarved control:  $8.17 \pm 0.77$ ) (figure 4.2 B). At the following time points, 2-oxoglutarate was still highly abundant in the nitrogen deficient cultures, even though its abundance decreased over time (ratio to unstarved control:  $5.23 \pm 0.6$  (120 minutes) and  $4.06 \pm 0.54$  (240 minutes)) (figure 4.2 B). In carbon starved cultures, the cellular 2-oxoglutarate level had dropped after 120 minutes of starvation (ratio to unstarved control:  $0.16 \pm 0.13$ ) and was found to be similarly low at 240 minutes after the onset of starvation (ratio to unstarved control:  $0.12 \pm 0.08$ ) (figure 4.2 B). 2-oxoglutarate was significantly more abundant in nitrogen than in carbon starved cultures at each of the three sampling time points (figure 4.2 B).

The observed dynamics of glutamine- and 2-oxoglutarate abundance in nitrogen starved cultures are consistent with literature findings (see chapter 5.1.1.2) and thereby con-

firm that nitrogen starvation was performed correctly in the filter cultures.

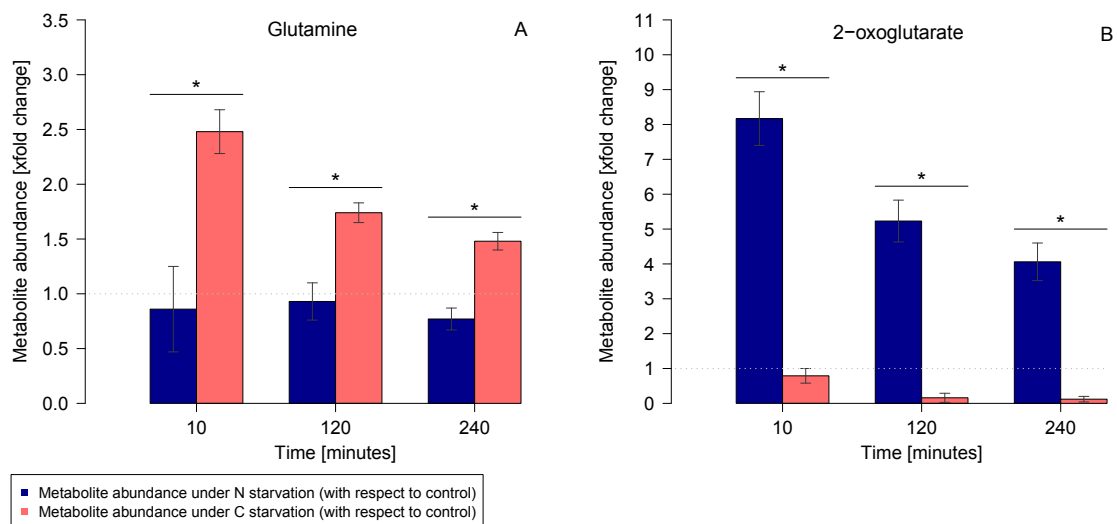


**Figure 4.2: Cellular abundance of nitrogen key metabolites during nutrient starvation**

Mean ratio  $\pm$  standard error of glutamine (A) and 2-oxoglutarate (B) abundance in nutrient starved cultures compared to the unstarved control at the sampling time points 10, 120 and 240 minutes after starvation onset. N = nitrogen, C = carbon; Statistical differences were computed for the comparison of metabolite abundance in nitrogen-compared to carbon starved cultures by the Welch's test or the Student's-t test (one-tailed), \*  $p < 0.05$

### Carbon starvation key metabolites

Figure 4.3 shows the mean ratio  $\pm$  the standard error of glucose, cAMP and PEP abundance in nutrient starved cultures compared to their abundance in the unstarved control over time (for detailed information on the analysis of free metabolites see chapter 3.6.1). Hereby, the mean metabolite abundance (averaged over three biological replicates) in nutrient deficient cultures obtained at three sampling time points was set each in relation to corresponding mean abundance levels in the unstarved control (averaged over three biological replicates) (see chapter 3.4.2).

Cellular glucose levels decreased quickly and stringently after the removal of glucose from the growth medium. Cellular cAMP and PEP levels increased markedly in response to carbon starvation. Under nitrogen starvation the cellular abundance of PEP did not change and glucose levels were about twice as high than in the unstarved control. The abundance of cAMP increased during nitrogen starvation but less than under carbon starvation.

Already 10 minutes after the start of carbon starvation, glucose levels had markedly decreased (ratio to unstarved control:  $0.14 \pm 0.05$ ) and at 120 minutes glucose was almost completely absent (ratio to unstarved control:  $0.02 \pm 0.07$  (120 minutes) and  $0.02 \pm 0.03$  (240 minutes) (figure 4.3 A). Contrary, in nitrogen starved cultures glucose accumulated and was about 1.7 to 2 times more present than in the unstarved control (ratio:  $1.76 \pm 0.12$  (10 minutes),  $2.07 \pm 0.22$  (120 minutes) and  $1.83 \pm 0.2$  (240 minutes) (figure 4.3 A). At each sampling time point glucose abundance was significantly lower in carbon starved cultures than in nitrogen starved cultures (figure 4.3 A).

After 10 minutes of carbon starvation, cAMP levels were about 80 times higher compared to the unstarved control (ratio:  $80.44 \pm 1.5$ ) (figure 4.3 B). Cellular cAMP levels dropped in the remaining time course of carbon starvation but were still markedly higher than in the unstarved control (ratio:  $39.03 \pm 0.63$  (120 minutes) and  $27.74 \pm 0.62$  (240 minutes)) (figure 4.3 B). In nitrogen starved cultures, cellular cAMP levels increased over time (ratio to unstarved control:  $0.85 \pm 0.63$  (10 minutes),  $12.27 \pm 2.65$  (120 minutes) and  $18.23 \pm 0.91$  (240 minutes) (figure 4.3 B). At 240 minutes, cAMP levels in nitrogen and carbon starved cultures were comparable (figure 4.3 B), statistically significant differences in the abundance of cAMP between nitrogen and carbon starved cultures could only be confirmed for the first sampling time point (figure 4.3 B).

PEP was about 16 times more frequent after 10 minutes of carbon starvation (ratio to unstarved control:  $16.3 \pm 0.85$ ) (figure 4.3 C). Afterwards, cellular PEP abundance decreased again in carbon starved cultures but was still higher concentrated than in the unstarved control at 120 minutes (ratio:  $7.9 \pm 0.46$ ) and 240 minutes (ratio: 4.01



$\pm 0.37$ ) (figure 4.3 C). In contrast, the abundance of PEP was highly similar in nitrogen starved cultures and the unstarved control at each sampling time point (ratio 10 minutes:  $1.29 \pm 0.18$ , ratio 120 minutes:  $0.87 \pm 0.2$ , ratio 240 minutes:  $0.69 \pm 0.15$ ) (figure 4.3 C). The abundance of PEP was significantly higher in carbon starved cultures than in nitrogen starved cultures at each sampling time point (figure 4.3 C).

The described results confirm literature findings on glucose, cAMP and PEP abundance under glucose deprivation (see chapter 5.1.1.2), thus validating the carbon starvation experiment.

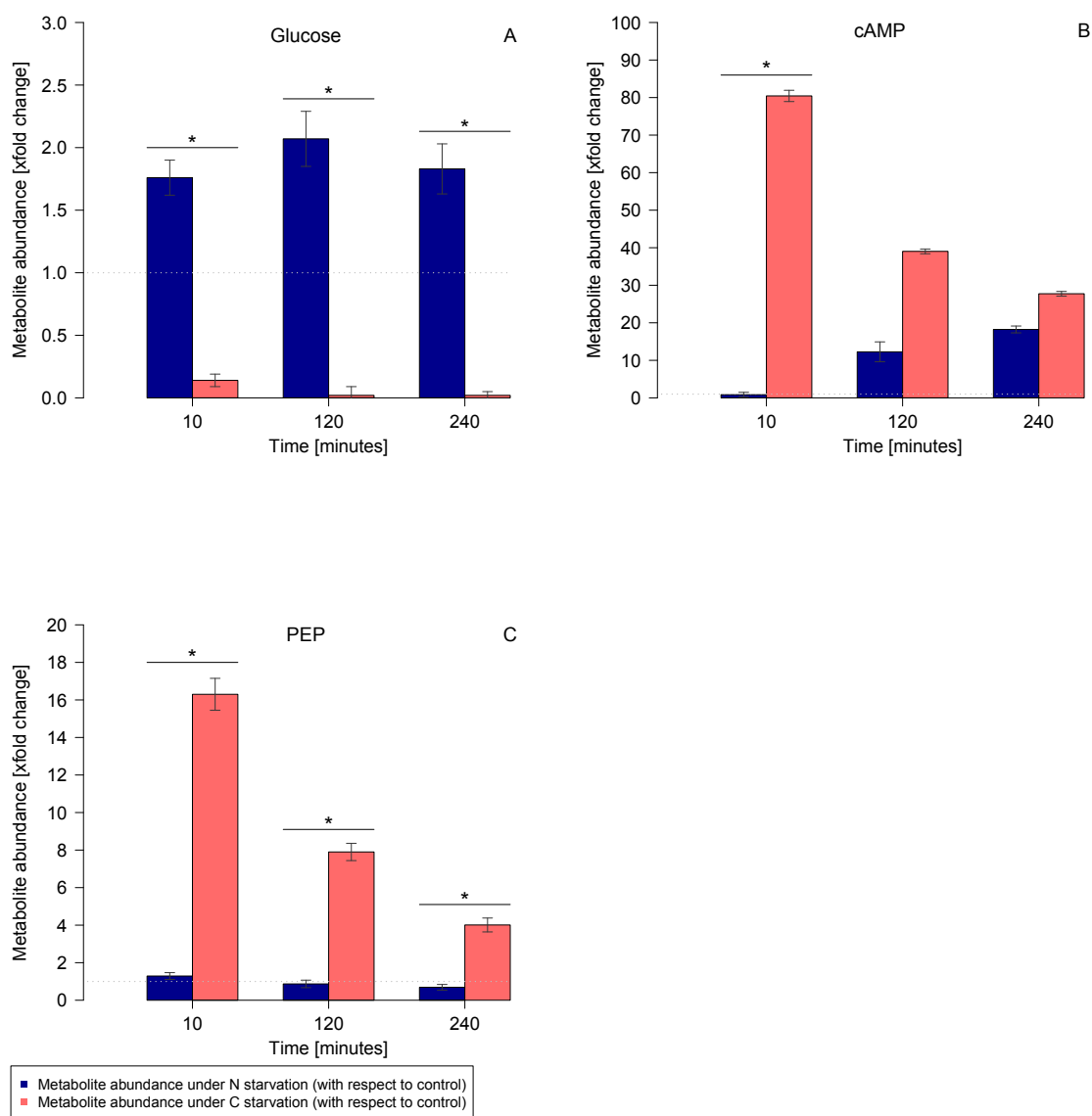


**Figure 4.3: Cellular abundance of carbon key metabolites during nutrient starvation**  
Mean ratio ± standard error of glucose (A), cyclic adenosine monophosphate (cAMP) (B) and phosphoenolpyruvate (PEP) (C) abundance in nutrient starved cultures compared to the unstarved control at the sampling time points 10, 120 and 240 minutes after starvation onset. N = nitrogen, C= carbon; Statistical differences were computed for the comparison of metabolite abundance in nitrogen- to carbon starved cultures by the Welch's test or the Student's-t test (one-tailed), \* p<0.05

### 4.1.1.3 Expression of genes

#### Nitrogen starvation related genes

Figure 4.4 shows the log<sub>2</sub> ratio of gene expression in nutrient starved cultures with respect to the unstarved control over time (for detailed information on gene expression analysis and statistical differences see chapter 3.8 & 3.9). Estimated gene expression levels of three sampling time points (see chapter 3.4.2) are shown.

All in all, the six genes described were found to have a high expression level under nitrogen starvation. During carbon starvation, the expression level of these genes was either lowered (*glnA*) or not significantly different compared to the unstarved control (figure 4.4).

The expression levels of the genes *glnA*, *glnG* and *glnL* were similarly enhanced under nitrogen starvation, the differences in expression compared to the unstarved control became smaller at the later sampling time points (average log<sub>2</sub> ratios: about 3.7 (10 minutes), about 2.4 (120 minutes) and about 1.9 (240 minutes) (figure 4.4 A, B & C). Under carbon starvation, the expression level of *glnA* was lowered (log<sub>2</sub> ratio to unstarved control: -1.67 (10 minutes), -3.29 (120 minutes) and -3.62 (240 minutes) (figure 4.4 A) and statistical differences in expression towards nitrogen starved cultures were confirmed for each sampling time point (figure 4.4 A). The expression level of the genes *glnG* and *glnL* did only change after 240 minutes of carbon starvation (log<sub>2</sub> ratios to unstarved control at 240 minutes: about -1.27) (figure 4.4 B & C). At 10 minutes, statistically significant differences in the expression level of both genes between carbon- and nitrogen starved cultures were confirmed (figure 4.4 B & C).

Out of all six genes tested in this analysis, the gene *glnK* had the highest expression level in response to nitrogen starvation (log<sub>2</sub> ratios to unstarved control: 8.57 (10 minutes), 7.61 (120 minutes) and 6.88 (240 minutes) (figure 4.4 D). Contrary, carbon starvation did hardly influence the expression of *glnK* (ratios to unstarved control: 0.29 (10 minutes), 0.78 (120 minutes), 0 (240 minutes) (figure 4.4 D). Thus, *glnK* was significantly different expressed under the two types of starvation at each sampling time point ((figure 4.4 D).

The expression level of the gene *nac* was markedly and consistently elevated over the complete time course of nitrogen starvation (log<sub>2</sub> ratio to unstarved control: >5) (figure 4.4 E). Lastly, also *amtB* had a higher expression level in response to nitrogen starvation (log<sub>2</sub> ratios to unstarved control: 5.12 (10 minutes), 4.19 (120 minutes) and -3.34 (240 minutes) (figure 4.4 F). Carbon starvation had almost no influence on the expression of the genes *nac* and *amtB* (log<sub>2</sub> ratios to unstarved control between -0.68 (*nac*, 240 minutes) and 0.4 (*nac*, 120 minutes) (figure 4.4 E & F). The differences in expression of both genes under carbon and nitrogen starvation were found to be sig-

nificant at all three time points (figure 4.4 E & F).

The present analysis confirms that nitrogen starvation caused a transcriptional response particularly towards nitrogen starvation, including an increased expression level of genes involved in nitrogen scavenging and metabolism.

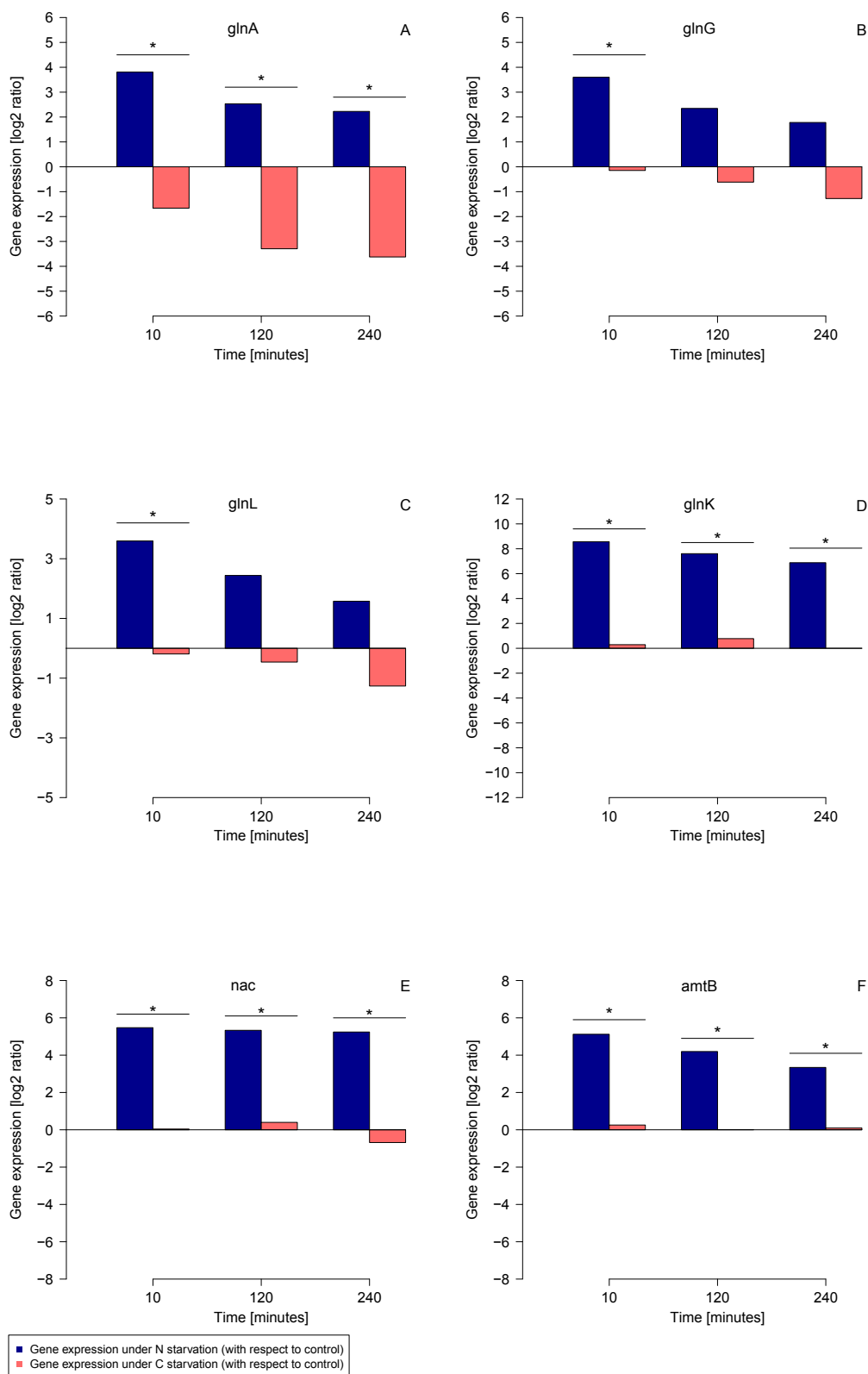


**Figure 4.4: Expression of nitrogen key genes during nutrient starvation**

Log<sub>2</sub> ratios of *glnA* (A), *glnG* (B), *glnL* (C), *glnK* (D), *nac* (E) and *amtB* (F) expression in response to nutrient starvation with respect to the unstarved control at the sampling time points 10, 120 and 240 minutes after starvation onset.

N = nitrogen, C= carbon; Statistical differences were estimated by the program DESeq (nbinom-test, \* p<0.05) for the comparison of gene expression levels in nitrogen and carbon starved cultures

### Carbon starvation related genes

Figure 4.5 shows the log<sub>2</sub> ratio of gene expression in nutrient starved cultures versus the unstarved control over time (for detailed information on gene expression analysis and statistical differences see chapter 3.8 & 3.9). Estimated gene expression levels of the nutrient starved cultures of three sampling time points (see chapter 3.4.2) are shown.

In summary, the gene *EIIBC* had a similar expression level under both types of nutrient starvation. The expression levels of the six remaining genes were elevated in response to carbon starvation at least at one sampling time point (figure 4.5). During nitrogen starvation, the expression level of these genes was either lowered or not significantly different compared to the unstarved control (figure 4.5).

After 10 and 120 minutes of nitrogen and carbon starvation, the expression level of the gene *EIIBC* was similarly lowered compared to its expression level in the unstarved control (log<sub>2</sub> ratios: about -0.8 (10 minutes) and about -0.9 (120 minutes)). After 240 minutes of starvation, *EIIBC* still had a lower expression level in the nutrient depleted cultures but the log<sub>2</sub> ratios differed more pronounced (-0.51 (carbon starvation) and -1.13 (nitrogen starvation)) (figure 4.5 A).

The gene *crr* was found to have an almost equal expression level in carbon deficient cultures and in the unstarved control at 10 minutes (log<sub>2</sub> ratio: -0.09) but showed a higher expression level in carbon deficient cultures after 120 and 240 minutes of starvation (log<sub>2</sub> ratios: 1.16 and 1.29) (figure 4.5 B). Nitrogen starvation did respectively not or only slightly affect the expression of *crr* (log<sub>2</sub> ratios to unstarved control: 0 (10 minutes), 0.07 (120 minutes) and -0.63 (240 minutes) (figure 4.5 B).

Carbon starvation lead to a continuous increase of the expression level of *csrA* over the time course (log<sub>2</sub> ratios to unstarved control: 1.29 (10 minutes), 2.09 (120 minutes) and 2.21 (240 minutes)) (figure 4.5 C). During nitrogen starvation, *csrA* was expressed at an almost equal level as in the unstarved control (log<sub>2</sub> ratios around 0.25) (figure 4.5 C).

Also the expression level of *cstA* was elevated under carbon starvation, the differences in expression towards the unstarved control decreased slightly over time (log<sub>2</sub> ratios: 4.07 (10 minutes), 3.65 (120 minutes) and 3.37 (240 minutes)) (figure 4.5 D). During nitrogen starvation, the expression level of *cstA* was consistently lowered (log<sub>2</sub> ratios to unstarved control: -0.75 (10 minutes), -0.59 (120 minutes) and -1.35 (240 minutes)) (figure 4.5 D). Differences in the expression level of *cstA* between nitrogen and carbon starved cultures were found to be statistically significant at each sampling time point (figure 4.5 D).

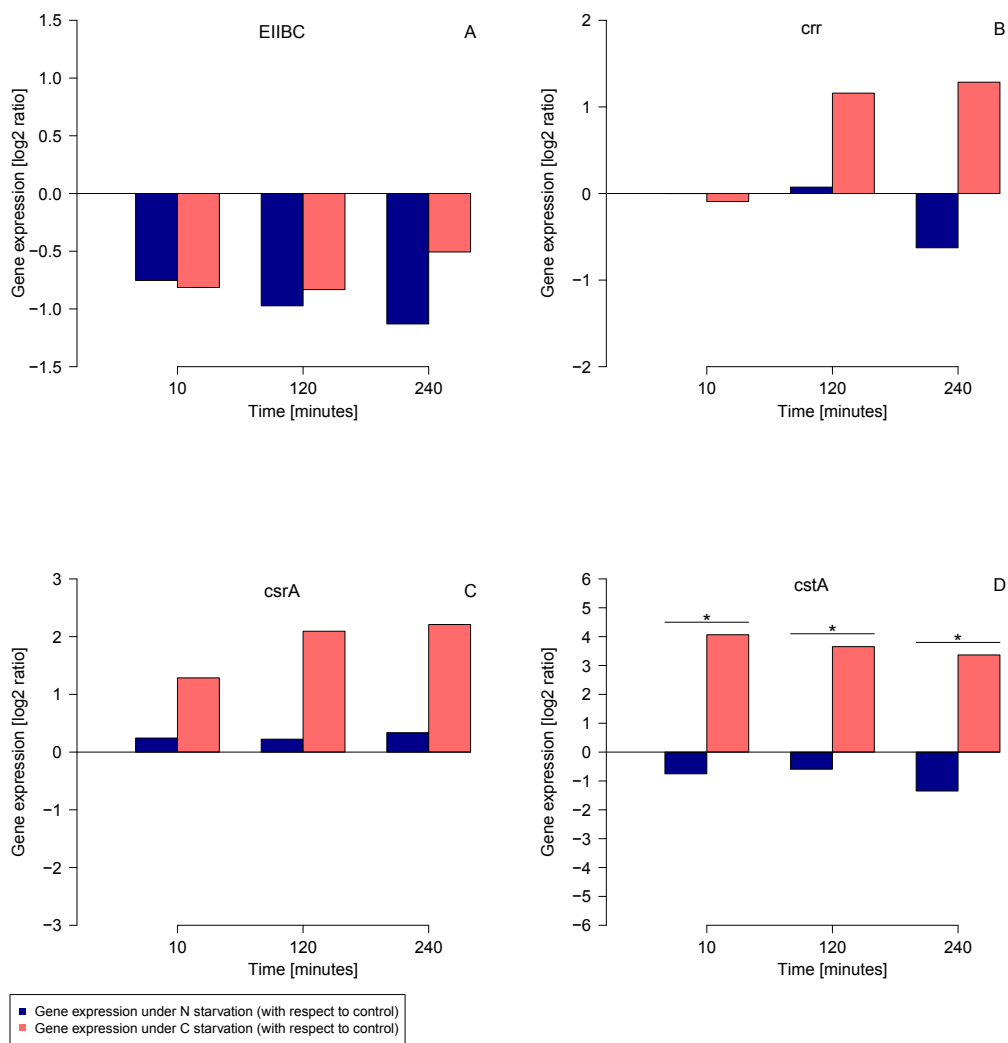
The expression of *mglB* was significantly different influenced by the two types of nu-

trient starvation (figure 4.5 E). Carbon starvation resulted in an enhanced expression level of *mglB* (log2 ratios to unstarved control: 4.49 (10 minutes), 2.59 (120 minutes) and 2.14 (240 minutes)) while during nitrogen starvation its expression level was lowered (log2 ratios to unstarved control: -1.26 (10 minutes), -2.49 (120 minutes) and -2.38 (240 minutes)) (figure 4.5 E).

After 10 minutes of carbon starvation, the expression level of *malE* had increased (log2 ratio to unstarved control: 1.61). At 120 minutes of carbon starvation, almost no difference in *malE* expression towards the unstarved control was found (log2 ratio: -0.22) and at the last sampling time point, the expression level of *malE* was slightly lowered in carbon starved cultures (log2 ratio to unstarved control: -0.62) (figure 4.5 F). Under nitrogen starvation, expression levels of *malE* were consistently low (log2 ratios to unstarved control: -0.79 (10 minutes), -0.56 (120 minutes) and -0.71 (240 minutes)) (figure 4.5 F).

The gene *araF* was found to have a constantly high expression level in response to carbon starvation. The differences in expression towards the unstarved control were more stringent in the later sampling time points (log2 ratios: 1.06 (10 minutes), 3.67 (120 minutes) and 3.04 (240 minutes)) (figure 4.5 G). Contrary, nitrogen starvation did not influence the expression of *araF* (figure 4.5 G). Differences in the expression level of *araF* between nitrogen and carbon starved cultures were found to be significant at 120 and 240 minutes (figure 4.5 G).

Even though statistically significant differences in expression could not be confirmed for most of the genes, the results indicate that carbon starvation caused a transcriptional response particularly towards carbon starvation, including elevated expression levels of genes involved in an improved scavenging of glucose and of genes involved in the uptake of other carbohydrates.





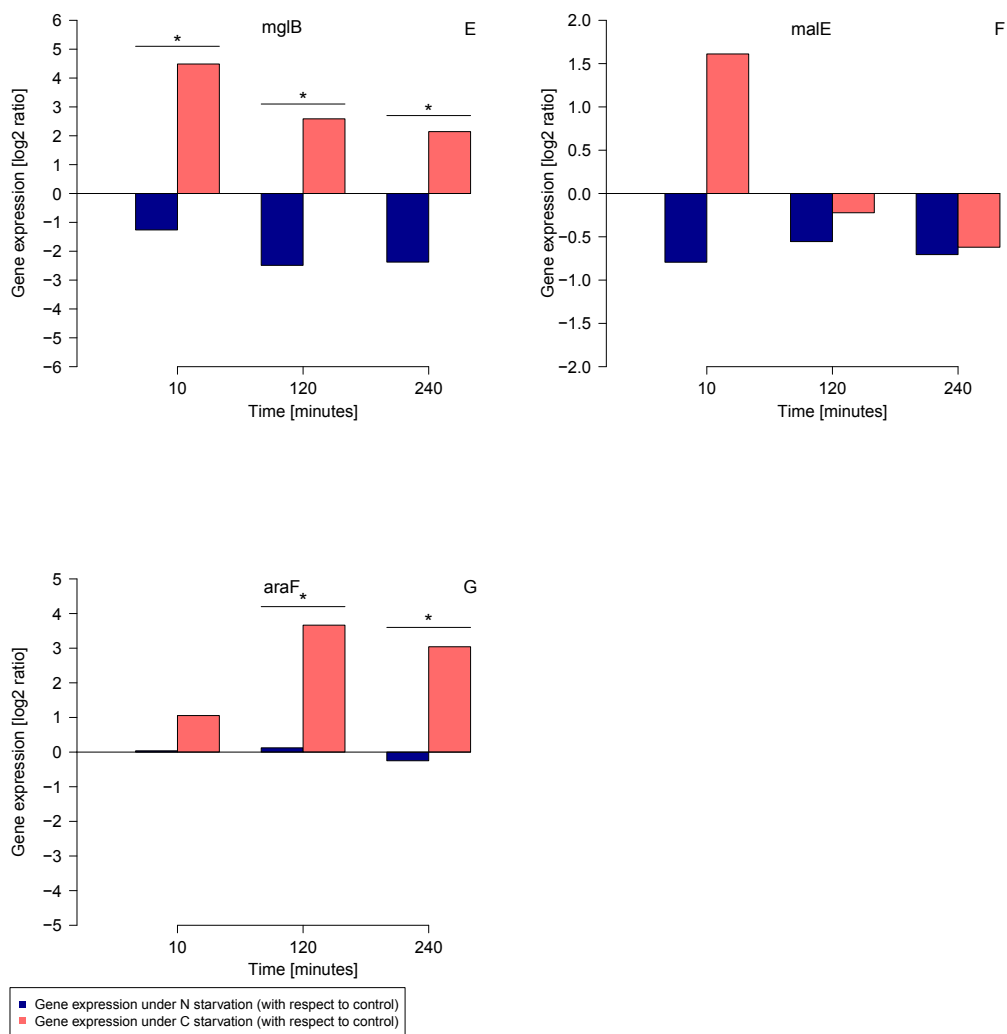


**Figure 4.5: Expression of carbon (glucose) key genes during nutrient starvation**

Log<sub>2</sub> ratios of *ElIBC* (A), *crr* (B), *csrA* (C), *cstA* (D), *mglB* (E), *malE* (F) and *araF* (G) expression in response to nutrient starvation with respect to the unstarved control at the sampling time points 10, 120 and 240 minutes after starvation onset. N = nitrogen, C= carbon; Statistical differences were estimated by the program DESeq (nbinom-test, \* p<0.05) for the comparison of gene expression levels in nitrogen and carbon starved cultures

### 4.1.2 Intracellular mobilization of deprived nutrients

The basic cellular starvation-survival response of nutrient depleted filter cultures included an elevated expression level of genes involved in the acquisition of external nitrogen and carbon. However, the nutrient starved cultures were not able to take up external nitrogen or carbon due to the complete removal of these nutrients from the growth medium. Hence, it was expected that the nutrient starved cultures mobilized internal nitrogen and carbon reservoirs to redistribute these nutrients obtained by autophagy processes. Concerning the nitrogen starved cultures, a special focus was put on the utilization of amino acids released by the degradation of proteins. Especially the nitrogen rich amino acids arginine, asparagine, glutamine, histidine, lysine and tryptophan were expected to be utilized since their degradation releases the ammonium groups from their side chains. Carbon starvation, as it was performed in this study by the complete removal of glucose from the growth medium, entailed a dual cost to the cultures since not only the supply of carbon atoms but also of energy was halted. Cellular lipids and polysaccharides have been found to act as efficient energy and carbon storage in microorganisms. Free fatty acids and sugars derived by autophagy of these compounds are proposed to be specialized and therefore more efficient carbon and energy sources than amino acids [Singh and Cuervo, 2012; Wilkinson, 1963]. Thereby, the expression level of genes involved in the degradation of lipids and fatty acids and of various polysaccharides and other carbohydrates was followed over time in carbon starved filter cultures. Additionally, the cellular abundance of eight fatty acids in carbon deprived filter cultures was compared to their abundance in the unstarved control. To complete this analysis, the abundance of free cellular amino acids in filter cultures starved for carbon was compared to their abundance in the unstarved control. Even though lipids and polysaccharides were proposed to represent primary internal carbon and energy sources, the utilization of cellular amino acids as additional carbon/energy reserves was possible since *E. coli* is able to utilize some external amino acids as sole carbon or energy sources [Yang *et al.*, 2015].

#### 4.1.2.1 Mobilization of nitrogen rich amino acids during nitrogen starvation

Table 4.1 shows the classification of the twenty amino acids with respect to their nitrogen allocation (number of nitrogen atoms in their side chain) and lists their one letter code. An amino acid was declared to have a high allocation for nitrogen when one or more nitrogen atoms are incorporated in its side chain. This is true for arginine, glutamine, asparagine, lysine, histidine and tryptophan (table 4.1). Henceforth, these amino acids were referred to as nitrogen rich in the following, whereas the remaining amino acids were referred to as nitrogen poor in the following since these only carry a

single nitrogen atom in their backbone (table 4.1).

**Table 4.1: Nitrogen allocation of amino acids**

<b>Amino acid</b>	<b>Nitrogen atoms in side chain</b>	<b>one letter code</b>
Alanine	0	A
Arginine	3	R
Asparagine	1	N
Aspartate	0	D
Cysteine	0	C
Glutamate	0	E
Glutamine	1	Q
Glycine	0	G
Histidine	2	H
Isoleucine	0	I
Leucine	0	L
Lysine	1	K
Methionine	0	M
Phenylalanine	0	F
Proline	0	P
Serine	0	S
Threonine	0	T
Tryptophan	1	W
Tyrosine	0	Y
Valine	0	V

Figure 4.6 shows the mean ratio  $\pm$  the standard error of the abundance of nitrogen rich amino acids in nutrient starved cultures compared to their abundance in the unstarved control over time (for detailed information on the analysis of free metabolites see chapter 3.6.1). Amino acid abundance was normalized to the free amino acid pool in the different cultures to make the data comparable. Next, the mean amino acid abundance (averaged over three biological replicates) in nutrient deficient cultures obtained at the three sampling time points was set each in relation to corresponding mean abundance levels in the unstarved control (averaged over three biological replicates) (see chapter 3.4.2).

In total, the abundance of asparagine, glutamine, lysine and tryptophan was lowered in response to nitrogen starvation at least at two out of the three sampling time points (when compared to the unstarved control). Glutamine and lysine were further less abundant in nitrogen starved cultures than in carbon starved cultures at each sampling time point. The remaining nitrogen rich amino acids (arginine, asparagine, histidine and tryptophan) were less abundant in nitrogen starved cultures than in carbon starved cultures at least at two out of the three sampling time points. At the remaining third

---

sampling time point these four amino acids showed a rather similar cellular abundance in nitrogen- and carbon starved cultures.

Arginine was about twice as abundant in nitrogen starved cultures than in the unstarved control at each sampling time point (ratio:  $2.63 \pm 0.39$  (10 minutes),  $2.17 \pm 0.18$  (120 minutes) and  $2.99 \pm 0.007$  (240 minutes)) (figure 4.6 A). In carbon starved cultures, arginine accumulated over time (ratio to unstarved control:  $1.55 \pm 0.26$  (10 minutes),  $9.15 \pm 1.09$  (120 minutes) and  $11.1 \pm 2.09$  (240 minutes)) (figure 4.6 A). At 120 and 240 minutes, arginine was significantly less abundant in nitrogen than in carbon starved cultures (figure 4.6 A).

Asparagine was found to be less abundant in nitrogen starved cultures than in the unstarved control at all sampling time points and the ratio of abundance was quiet similar over the time course ( $0.34 \pm 0.04$  (10 minutes),  $0.37 \pm 0.01$  (120 minutes) and  $0.37 \pm 0.001$  (240 minutes)) (figure 4.6 B). Asparagine was also less abundant in nitrogen starved cultures than in carbon starved cultures at 10 and 240 minutes after onset of starvation (ratio carbon starved cultures to unstarved control:  $0.97 \pm 0.1$  (10 minutes) and  $0.56 \pm 0.15$  (240 minutes)) (figure 4.6 B). At 10 minutes, the difference was proven to be statistically significant (figure 4.6 B). At 120 minutes, asparagine was almost comparable abundant in nitrogen and carbon starved cultures (figure 4.6 B).

The average abundance of cellular glutamine declined in response to nitrogen starvation (ratio to unstarved control:  $0.78 \pm 0.38$  (10 minutes),  $0.78 \pm 0.38$  (120 minutes) and  $0.82 \pm 0.003$  (240 minutes)) and increased upon carbon starvation (ratio to unstarved control group:  $1.59 \pm 0.16$  (10 minutes),  $1.14 \pm 0.10$  (120 minutes) and  $1.18 \pm 0.12$  (240 minutes)) (figure 4.6 C). Glutamine had a lower cellular frequency in nitrogen starved cultures than in carbon depleted ones at each sampling time point. At 120 and 240 minutes, the differences in glutamine abundance between the two nutrient depleted cultures were found to be statistically significant (figure 4.6 C).

Histidine was more or less twice as abundant in nitrogen starved cultures as in the unstarved control at each sampling time point (ratio:  $1.98 \pm 0.19$  (10 minutes),  $1.66 \pm 0.08$  (120 minutes) and  $2.21 \pm 0.01$  (240 minutes)) (figure 4.6 D). Under carbon starvation, free cellular histidine accumulated over time (compared to unstarved control) from a ratio of  $0.64 \pm 0.06$  (10 minutes) to a ratio of  $17.89 \pm 1.08$  (240 minutes) (figure 4.6 D). Further, the abundance of histidine was lower in nitrogen starved cultures than in carbon starved cultures at 120 and 240 minutes, for the time point 120 minutes the difference was found to be statistically significant (figure 4.6 D).

Lysine was less abundant in nitrogen starved cultures than in the unstarved control at 10 minutes (ratio:  $0.42 \pm 0.18$ ) and 120 minutes (ratio:  $0.69 \pm 0.57$ ) but accumulated afterwards and was about twice as abundant in nitrogen starved cultures at

---

240 minutes after the onset of starvation (ratio:  $1.93 \pm 0.008$ ) (figure 4.6 E). Cellular lysine was almost equally abundant in carbon starved cultures and the unstarved control at 10 minutes (ratio:  $0.89 \pm 0.32$ ) and accumulated over time, at 240 minutes it was about 2.5 times more abundant in carbon starved cultures than in the unstarved control (figure 4.6 E). At all time points, lysine was less abundant in nitrogen starved cultures than in the carbon starved cultures, for 10 and 120 minutes the differences were found to be statistically significant (figure 4.6 E).

At 10 and 120 minutes, tryptophan was less abundant in nitrogen starved cultures than in the unstarved control (ratio:  $0.62 \pm 0.07$  (10 minutes) and  $0.82 \pm 0.04$  (120 minutes)) and almost equally abundant in both cultures at 240 minutes (ratio:  $1.01 \pm 0.001$ ) (figure 4.6 F). In carbon starved cultures, tryptophan accumulated from a ratio of  $0.57 \pm 0.05$  (compared to unstarved control) at 10 minutes to a ratio of  $1.98 \pm 0.44$  (compared to unstarved control) at 240 minutes (figure 4.6 F). At 120 and 240 minutes, tryptophan was less abundant in nitrogen starved cultures than in carbon starved cultures, the differences were not found to be statistically different (figure 4.6 F).

Since the breakdown of ribosomes and proteins and the consequential release of amino acids is a well described process in *E. coli* cultures in response to several types of nutrient starvation [Davis *et al.*, 1986; Reeve *et al.*, 1984a; Zundel *et al.*, 2009], we expected a temporarily accumulation of the free cellular pool of amino acids in carbon- and nitrogen starved cultures of the present study. That is why the mobilization of nitrogen rich amino acids during nitrogen starvation was investigated not only by a comparison of their abundance between nitrogen starved cultures and the unstarved control. Here, we might had overlooked signals of amino acid utilization due to the starvation induced biased free amino acid pool in nitrogen starved cultures. The additional comparison of amino acid abundance between carbon- and nitrogen starved cultures provided a more reliable picture on amino acid utilization since the free amino acid pool was believed to be biased comparably due to autophagy processes under both types of starvation. With this in mind, the present analysis strongly suggests that the six nitrogen rich amino acids were utilized specifically during nitrogen starvation as they represent favorable nitrogen reserves.

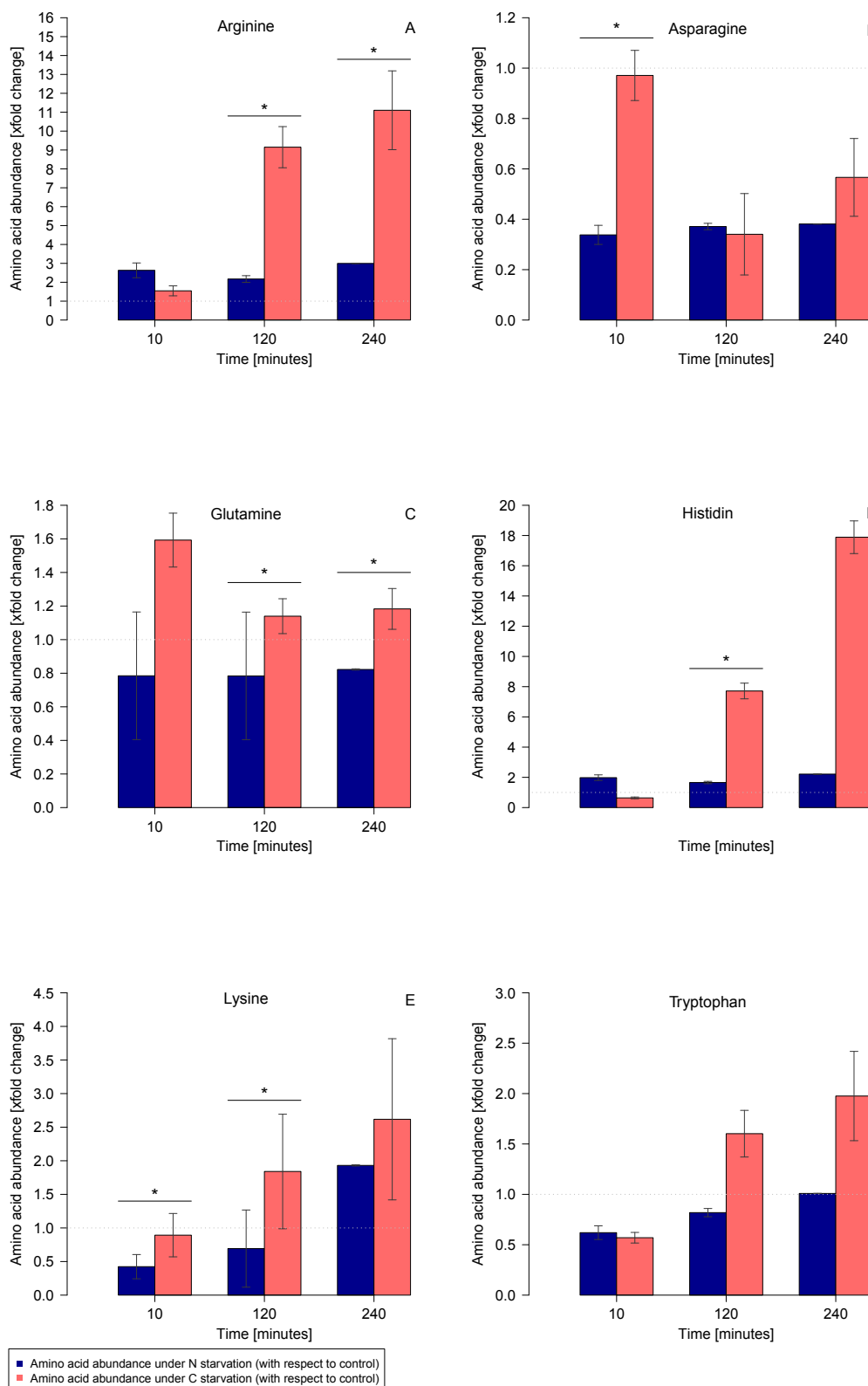


**Figure 4.6: Cellular abundance of nitrogen rich amino acids during nutrient starvation**  
 Mean ratio  $\pm$  standard error of arginine (A), asparagine (B), glutamine (C), histidine (D), lysine (E) and tryptophan (F) abundance in nutrient starved cultures compared to the unstarved control at the sampling time points 10, 120 and 240 minutes after starvation onset. N = nitrogen, C = carbon; Statistical differences were computed for the comparison of amino acid abundance in nitrogen- compared to carbon starved cultures by the Welch's test or the Student's-t test (one-tailed), \*  $p < 0.05$

#### 4.1.2.2 Mobilization of lipids during carbon starvation

Figure 4.7 shows the distribution of the log<sub>2</sub> ratio of lipid degradation related gene expression in nutrient starved cultures to lipid degradation related gene expression in the unstarved control group over time (for detailed information on gene expression analysis and the association of genes to metabolic pathways see chapter 3.8). The twenty-five genes integrated in this analysis and the information about the metabolic pathways in which they are involved can be found in chapter 6. Gene expression levels of the nutrient starved cultures were estimated for five sampling time points (see chapter 3.4.2). Figure 4.7 shows that the expression level of genes involved in lipid degradation was strongly enhanced in response to carbon starvation over the complete experimental time course. Nitrogen starvation did not influence the expression of lipid degradation related genes. Here, median log<sub>2</sub> ratios were always centered around zero, showing no difference in gene expression towards the unstarved control.

At ten minutes after the onset of starvation, the upper quantile of the boxplot displaying lipid degradation related gene expression in carbon starved cultures with reference to the unstarved control ended at a log<sub>2</sub> ratio of 0.07 (figure 4.7). Thus showing that at least 75 % of the analyzed genes had a higher expression level in the carbon deficient cultures. At the remaining sampling time points, the upper quantiles of the boxplots ended closely below zero (values between -0.08 at 60 minutes and -0.69 at 120 minutes) (figure 4.7) which means that still around 75 % of the genes had a higher expression level in response to carbon starvation. The upper whiskars of the corresponding boxplots decreased over the time course from a log<sub>2</sub> ratio of 6.14 at 10 minutes to a log<sub>2</sub> ratio of 3.84 at 240 minutes. In parallel, the upper quantiles declined from a log<sub>2</sub> ratio of 3.23 (10 minutes) to 2.21 (240 minutes) (figure 4.7). This decrease in length and extension showed that differences in gene expression between carbon starved cultures and the unstarved control were more pronounced right after the onset of carbon starvation and became slightly less stringent over the time course.

The length and the extension of all boxplots depicting the expression of lipid degradation related genes in nitrogen starved cultures with respect to their expression in the unstarved control were lower compared to the boxplots referring to the data of carbon starved cultures (figure 4.7). Median log<sub>2</sub> ratios of the boxplots displaying data of nitrogen deficient cultures were close to zero at all time points (figure 4.7) and were shown to be significantly lower than median log<sub>2</sub> ratios calculated for carbon starved cultures at 10, 60 and 240 minutes after onset of nutrient starvation (figure 4.7).

The analysis of lipid degradation related gene expression strongly suggest that lipophagy happened during the complete time course of carbon starvation. Further, lipid degra-

ation was a specific response towards carbon starvation, for nitrogen starved cultures no evidence of lipophagy was found.

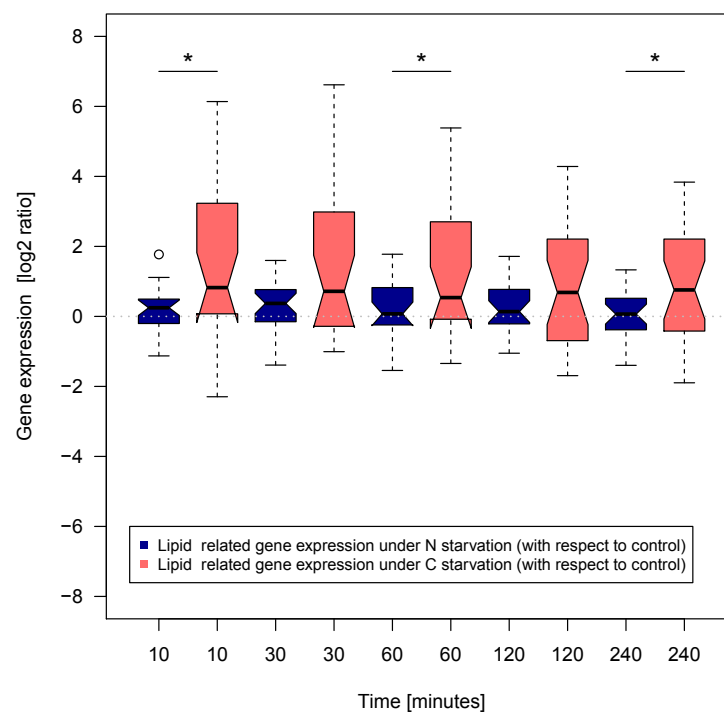


**Figure 4.7: Lipid degradation related gene expression in nutrient deficient cultures**

Distribution of the log<sub>2</sub> ratio of lipid degradation related gene expression in nutrient starved cultures compared to the unstarved control at the sampling time points 10, 30, 60, 120 and 240 minutes after starvation onset. N = nitrogen, C= carbon. Statistical differences were computed for the comparison of median log<sub>2</sub> ratios of nitrogen- and carbon starved cultures (with respect to control), Welch's test, one-tail, \*  $p < 0.05$



Figure 4.8 shows the mean ratio  $\pm$  the standard error of the abundance of eight fatty acids in nutrient starved cultures to their abundance in the unstarved control over time (for detailed information on the analysis of free metabolites see chapter 3.6.1). The complete names of the eight fatty acids analyzed are listed in chapter 6. In figure 4.8 the molecular formulas of the fatty acids are used as their identifiers. Mean fatty acid abundance (averaged over three biological replicates) in nutrient starved cultures obtained at three sampling time points were set each in relation to corresponding mean abundance levels in the unstarved control (averaged over three biological replicates) (see chapter 3.4.2).

Overall, the following results show that five out of the eight fatty acids were less abundant in carbon starved cultures than in nitrogen depleted ones at each sampling time point (figure 4.8).

The fatty acids  $C_{14}H_{28}O_2$ ,  $C_{16}H_{30}O_2$ ,  $C_{16}H_{32}O_2$  and  $C_{18}H_{34}O_2$  showed a lowered cellular abundance in response to carbon starvation at each sampling time point (mean ratios to unstarved control: all  $<1$ ) (figure 4.8 A-D). Nitrogen starvation lead to a markedly and continuous accumulation of these four fatty acids (when compared to unstarved control) (figure 4.8 A-D). Thus, each of the four fatty acids was less abundant in carbon starved cultures than in nitrogen depleted ones at each of the three sampling time points (figure 4.8 A-D). Some of these differences in cellular abundance were found to be statistically significant:  $C_{14}H_{28}O_2$  was significantly less abundant in response to carbon starvation at 240 minutes of nutrient starvation (figure 4.8 A). For the fatty acid  $C_{16}H_{30}O_2$ , a statistically significant lowered abundance in carbon depleted cultures could be shown for the later sampling time points (120 and 240 minutes) (figure 4.8 B). At 120 minutes of nutrient starvation,  $C_{16}H_{32}O_2$  was significantly lower abundant in carbon starved cultures than in nitrogen depleted ones (figure 4.8 C). Lastly, the fatty acid  $C_{18}H_{34}O_2$  was significantly less abundant in carbon starved cultures at each sampling time point (figure 4.8 D).

The abundance of the fatty acid  $C_{17}H_{26}O_3$  did not change in the beginning of nutrient starvation (ratios to unstarved control at 10 minutes:  $0.79 \pm 0.05$  (carbon starvation) and  $0.99 \pm 0.13$  (nitrogen starvation)) (figure 4.8 E). However,  $C_{17}H_{26}O_3$  accumulated under both types of nutrient starvation in the following time course (figure 4.8 E). The accumulation was faster and stronger in carbon starved cultures (ratios to unstarved control:  $1.5 \pm 0.07$  (120 minutes) and  $2.3 \pm 0.08$  (240 minutes)) than in nitrogen depleted ones (ratios to unstarved control:  $1.19 \pm 0.16$  (120 minutes) and  $1.52 \pm 0.05$  (240 minutes)) but statistical differences between the two nutrient starved cultures could not be confirmed (figure 4.8 E).

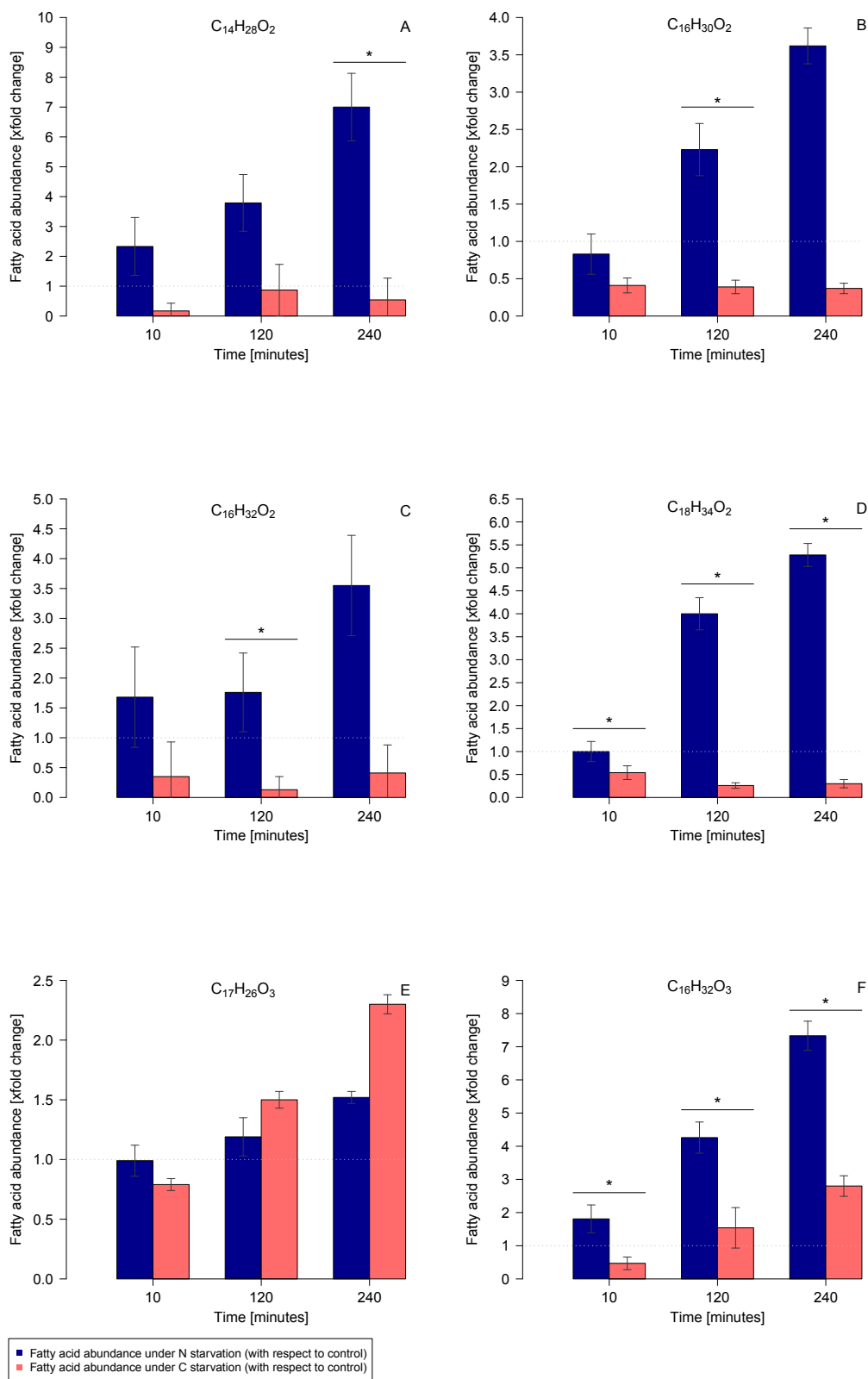
After 10 minutes of carbon starvation, the abundance of  $C_{16}H_{32}O_3$  was lowered (ratio

to unstarved control:  $0.47 \pm 0.19$ ) but the fatty acid accumulated in the remaining time course and was more abundant than in the unstarved control after 120 and 240 minutes of carbon starvation (ratios:  $1.54 \pm 0.61$  (120 minutes) and  $2.8 \pm 0.31$  (240 minutes)) (figure 4.8 F). Nitrogen starvation as well lead to an accumulation of  $C_{16}H_{32}O_3$  (ratio to unstarved control:  $1.81 \pm 0.42$  (10 minutes),  $4.26 \pm 0.47$  (120 minutes) and  $7.33 \pm 0.44$  (240 minutes)) (figure 4.8 F). The rise in cellular abundance of  $C_{16}H_{32}O_3$  was more pronounced in response to nitrogen starvation than in response to carbon starvation (figure 4.8 F). Differences in abundance of  $C_{16}H_{32}O_3$  between the two nutrient starved cultures were found to be statistically significant at each sampling time point (figure 4.8 F).

After 10 and 120 minutes of carbon starvation, the cellular  $C_{18}H_{34}O_3$  abundance was markedly reduced (ratios to unstarved control:  $0.04 \pm 0.24$  (10 minutes) and  $0.08 \pm 0.23$  (120 minutes)) but after 240 minutes it was about 4.5 times higher than in the unstarved control (figure 4.8 G).  $C_{18}H_{34}O_3$  accumulated constantly in response to nitrogen starvation (ratios to unstarved control:  $0.52 \pm 0.56$  (10 minutes),  $1.9 \pm 0.93$  (120 minutes) and  $2.65 \pm 1.06$  (240 minutes)) and was more abundant in nitrogen starved cultures than in carbon starved ones at 10 and 120 minutes (figure 4.8 G). At 120 minutes after the onset of nutrient starvation these differences in abundance were found to be statistically significant (figure 4.8 G).

The fatty acid  $C_{18}H_{28}O_5$  showed the highest accumulation of all detected fatty acids in response to carbon starvation (ratios to unstarved control:  $0.41 \pm 0.39$  (10 minutes),  $15.2 \pm 4.1$  (120 minutes) and  $13.17 \pm 2.18$  (240 minutes)) (figure 4.8 H). Over the experimental time course  $C_{18}H_{28}O_5$  accumulated as well in response to nitrogen starvation but not as stringent as in response to carbon starvation (ratios to unstarved control:  $4.74 \pm 1.55$  (10 minutes),  $4.39 \pm 0.9$  (120 minutes) and  $8.78 \pm 0.97$  (240 minutes)) (figure 4.8 H).

Given the findings on lipid degradation in response to carbon starvation (see figure 4.7), fatty acids, which are derived from lipids, were expected to be massively released into the free cellular pool of carbon starved cultures. The fact that the majority of the analyzed fatty acids tended to be less abundant in the free cellular pool of carbon starved cultures than in that of nitrogen starved ones suggests that fatty acids were used as carbon and/or energy source in response to carbon starvation. By targeting and investigating a higher number of fatty acids in more biological replicates of carbon starved cultures, the pattern of fatty acid utilization in response to carbon starvation might become stronger, leading to more statistical significant differences.



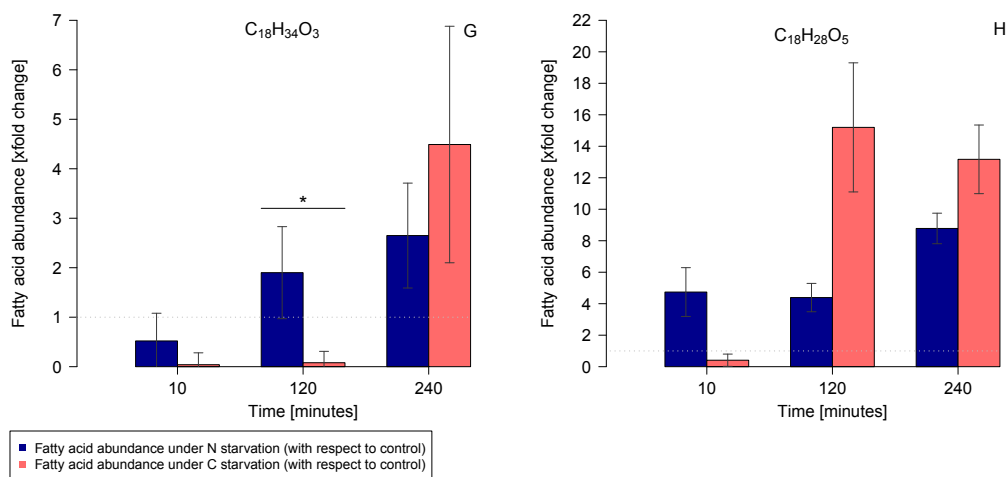


**Figure 4.8: Cellular abundance of fatty acids during nutrient starvation**

Mean ratio  $\pm$  standard error of C<sub>14</sub>H<sub>28</sub>O<sub>2</sub> (A), C<sub>16</sub>H<sub>30</sub>O<sub>2</sub> (B), C<sub>16</sub>H<sub>32</sub>O<sub>2</sub> (C), C<sub>18</sub>H<sub>34</sub>O<sub>2</sub> (D), C<sub>17</sub>H<sub>26</sub>O<sub>3</sub> (E), C<sub>16</sub>H<sub>32</sub>O<sub>3</sub> (F), C<sub>18</sub>H<sub>34</sub>O<sub>3</sub> (G) and C<sub>18</sub>H<sub>28</sub>O<sub>5</sub> (H) abundance in nutrient starved cultures compared to the unstarved control at the sampling time points 10, 120 and 240 minutes after starvation onset. N = nitrogen, C = carbon; Statistical differences were computed for the comparison of amino acid abundance in nitrogen- compared to carbon starved cultures by the Welch's test or the Student's-t test (one-tailed), \*  $p < 0.05$

### 4.1.2.3 Mobilization of carbohydrates during carbon starvation

Figure 4.9 shows the distribution of the log<sub>2</sub> ratio of carbohydrate degradation related gene expression in nutrient starved cultures to carbohydrate degradation related gene expression in the unstarved control over time (for detailed information on gene expression analysis and the association of genes to metabolic pathways see chapter 3.8). The one hundred and twenty-eight genes integrated in this analysis and the information about the metabolic pathways in which they are involved can be found in chapter 6. Gene expression levels of the nutrient starved cultures were estimated for five sampling time points (see chapter 3.4.2).

Figure 4.9 shows that carbohydrate degradation was more pronounced during carbon starvation than during nitrogen starvation. In response to carbon starvation about half of the genes involved in carbohydrate degradation showed higher expression levels than in the unstarved control. On the contrary, nitrogen starvation did not seem to influence the expression of carbohydrate degradation related genes at all.

Median log<sub>2</sub> ratios of the boxplots displaying carbohydrate degradation related gene expression in carbon starved cultures to the unstarved control were close to zero (on average 0.26) at all five sampling time points (figure 4.9). The upper whiskers of these boxplots ended at log<sub>2</sub> ratios between 2.49 (10 minutes) and 3.17 (120 minutes) and the lower whiskers ended at log<sub>2</sub> ratios between -2.45 (10 minutes) and -2.16 (240 minutes) (figure 4.9). Taken together, at each sampling time point about 50 % of the analyzed genes had a higher expression level in carbon starved cultures compared to the unstarved control group while the second half of genes had a lower expression level in the carbon deficient cultures. The average range of the expression levels did not change over the time course depicted by the similar length of the quantiles and whiskers of the five corresponding boxplots. Outliers depicting high differences in gene expression between carbon starved cultures and the unstarved control represented the data of genes involved in the degradation of galactose, glycol and glyoxylate.

Median log<sub>2</sub> ratios of the boxplots displaying carbohydrate degradation related gene expression in nitrogen deficient cultures to the unstarved control were as well close to zero at all five sampling time points (figure 4.9). Further, the upper and lower quantiles of these boxplots closely centered around zero and the lower and upper whiskers ended at a maximum log<sub>2</sub> ratio of about -1.8 (120 minutes) and about 1.5 (60 and 120 minutes), respectively (figure 4.9). The appearance of all described boxplots hinted on a higher similarity of gene expression between nitrogen starved cultures and the unstarved control as between carbon starved cultures and the unstarved control. At the sampling time points 10 and 120 minutes, the median log<sub>2</sub> ratios of gene expression were found to be significantly higher in carbon starved cultures than in nitrogen

deficient ones (figure 4.9).

The present analysis of the expression levels of genes involved in carbohydrate degradation suggests that carbon starved cultures utilized different internal carbohydrates. That only about half of the genes analyzed were found to have a higher expression level in response to carbon starvation might be explained by the fact that the analysis included various genes which are involved in the uptake and assimilation of different external carbon sources. Due to the lack of any kind of external carbon source, there was no need for the carbon starved cultures to express the corresponding genes over the complete time course.

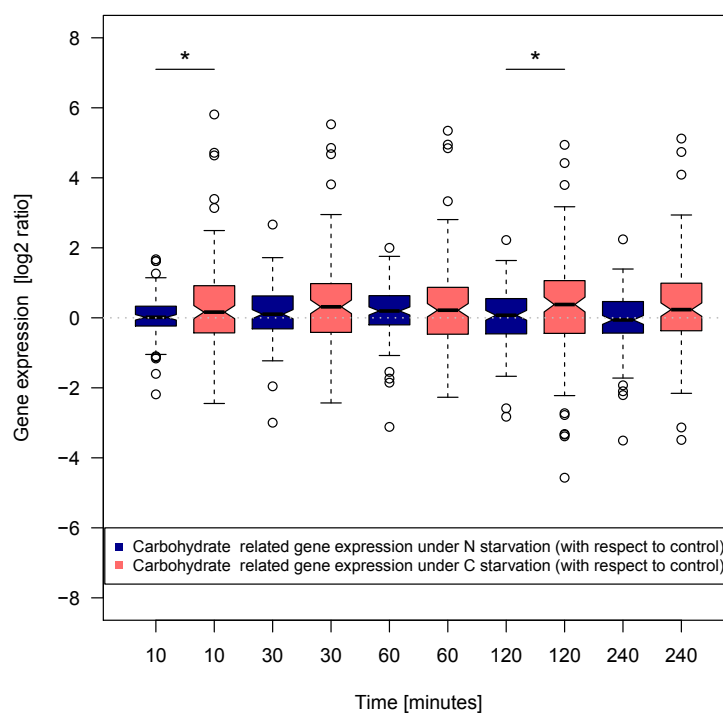


**Figure 4.9: Carbohydrate degradation related gene expression in nutrient deficient cultures**

Distribution of the log2 ratio of lipid degradation related gene expression in nutrient starved cultures compared to the unstarved control at the sampling time points 10, 30, 60, 120 and 240 minutes after starvation onset. N = nitrogen, C= carbon. Statistical differences were computed for the comparison of median log2 ratios of nitrogen- and carbon starved cultures (with respect to control), Wilcoxon's test, one-tail, \*  $p < 0.05$

#### 4.1.2.4 Mobilization of amino acids during carbon starvation

Figure 4.10 shows the mean ratio  $\pm$  the standard error of the cellular abundance of amino acids in nutrient starved cultures compared to their abundance in the unstarved control over time (for detailed information on the analysis of free metabolites see chapter 3.6.1). The amino acid abundance was normalized to the free amino acid pool in the different cultures to make the data comparable. Next, the mean amino acid abundance (averaged over three biological replicates) in nutrient deficient cultures obtained 10 minutes after start of starvation was set in relation to corresponding mean abundance levels in the unstarved control. The normalized amino acid abundance obtained at 120 and 240 minutes after start of nutrient starvation (in total six biological replicates) was pooled, averaged and as well set in relation to corresponding normalized and averaged abundance levels in the unstarved control.

Out of all amino acids, only glycine (G), proline (P) and serine (S) were significantly less abundant in carbon starved cultures than in nitrogen starved ones at both of the analyzed time points (10 and 120 & 240 minutes). The pattern of cellular abundance of the remaining amino acids was highly variable over time (figure 4.10).

The amino acids alanine (A), cysteine (C), glutamate (E), glycine (G), proline (P) and serine (S) were on average about half as abundant in carbon starved cultures than in the unstarved control at 10 and 120 & 240 minutes (ratios lay between 0.14 (C, 10 minutes) and 0.59 (A and E, 10 minutes) (figure 4.10 A, B). At 120 & 240 minutes, these amino acids were further significantly less abundant in response to carbon starvation than in response to nitrogen starvation (figure 4.10 B). For glycine, proline and serine a statistically significant lower abundance in carbon starved cultures (compared to nitrogen starved cultures) could also be confirmed for the sampling time point 10 minutes (figure 4.10 A). At 10 minutes after onset of carbon starvation, the mean abundance of asparagine (N) histidine (H) and tryptophan (W) was lowered (ratio to unstarved control: 0.93 (N), 0.64 (H) and 0.57 (W)). At this time point, histidine was shown to be significantly less abundant in response to carbon starvation than in response to nitrogen starvation (figure 4.10 A). At 120 & 240 minutes, the abundance of asparagine was still low but histidine and tryptophan had accumulated in response to carbon starvation (ratio to unstarved control: 12.8 (H) and 1.79 (W)) (figure 4.10 B).

For the amino acids arginine (R), aspartate (D), glutamine (Q), isoleucine/leucine (IL), lysine (K), methionine (M), phenylalanine (F), threonine (T) and tyrosine (Y) an elevated cellular abundance in response to carbon starvation (in comparison to the unstarved control) was found at at least one of the time points (figure 4.10 A, B). Out of these amino acids, arginine showed the highest difference in cellular abundance in

comparison to the unstarved control (ratio 120 & 240 minutes: 10.13) (figure 4.10 B). However, only arginine and phenylalanine were significantly less abundant in response to carbon starvation than in response to nitrogen starvation at 10 minutes (figure 4.10 A).

The cellular abundance of valine (V) was not affected in response to carbon starvation (ratio to unstarved control: 1.05 (10 minutes) and 0.99 (120 & 240 minutes) (figure 4.10 A, B) but its abundance in response to carbon starvation was significantly lower compared to its abundance in response to nitrogen starvation at 10 minutes (figure 4.10 A).

Since lipids and free fatty acids were strongly utilized over the complete time course of carbon starvation (see chapter 4.1.2.2 & 4.1.2.2) and are also known to be primary internal carbon and energy reserves, we suggested that amino acids would most likely represent only secondary, less favorable sources of carbon and energy. Due to the estimated release of amino acids in the free cellular pool of nutrient starved cultures, this analysis focused on the comparison of amino acid abundance in response to the two types of nutrient starvation (compare to chapter 4.1.2.1). Since out of all amino acids only glycine, proline and serine were found to be significantly less abundant in response to carbon starvation (in comparison to nitrogen starvation) at both time points, amino acids in general indeed seem to be less favorable internal sources of energy and carbon.



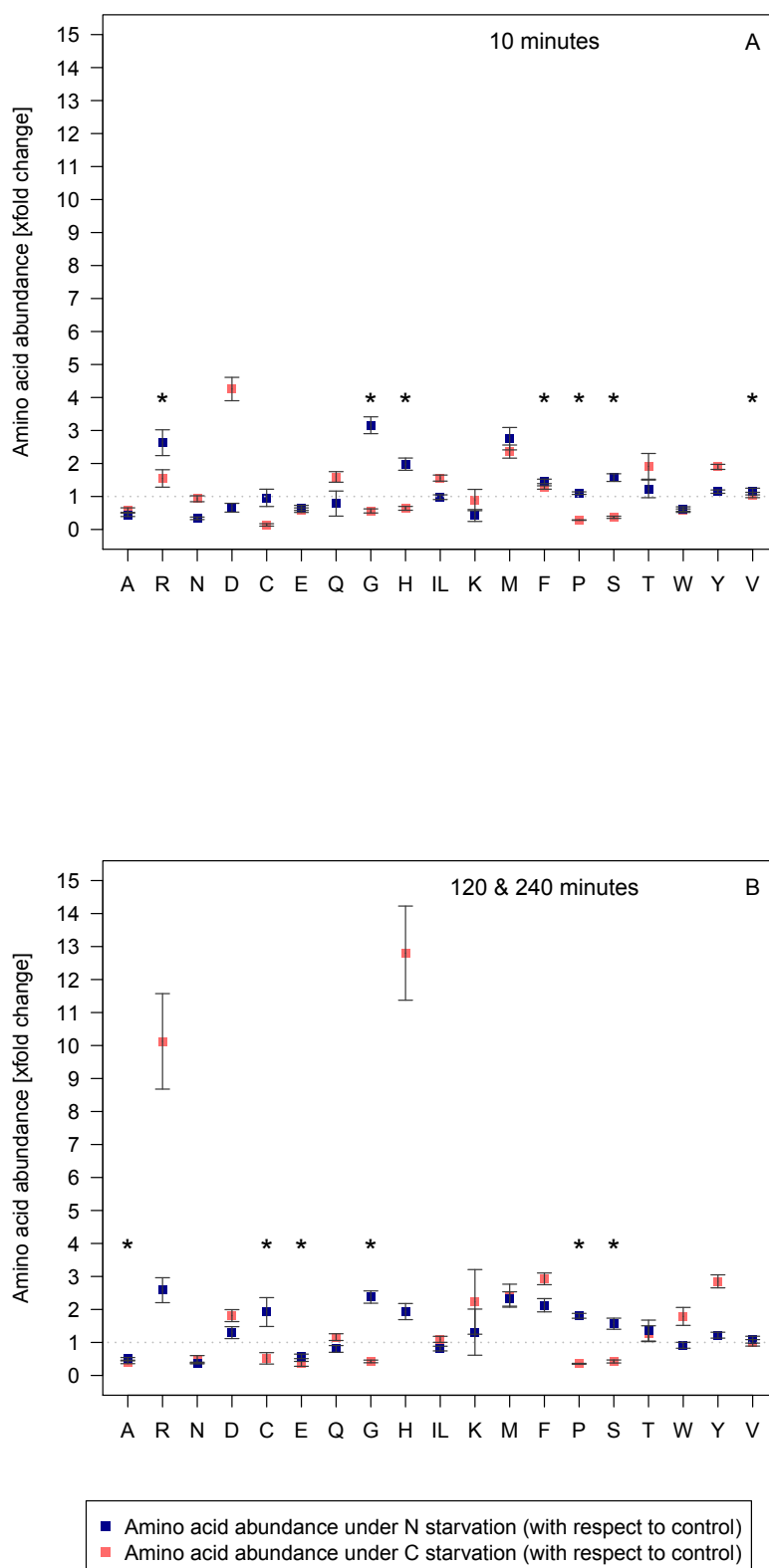


**Figure 4.10: Cellular abundance of amino acids during carbon starvation**

Mean ratio  $\pm$  standard error of amino acid abundance in nutrient starved cultures compared to the unstarved control at the sampling time points 10 minutes and 120 & 240 minutes after starvation onset. N = nitrogen, C= carbon; Statistical differences were computed for the comparison of amino acid abundance in nitrogen- compared to carbon starved cultures by the Welch's test or the Student's-t test (one-tailed), \*  $p < 0.05$

---

### 4.1.3 Nitrogen conservation in proteins and utilization of internal nitrogen reserves

Nitrogen starved filter cultures were expected to synthesize biomolecules which had been selected towards a lowered demand on nitrogen, thus reducing the cellular nitrogen budget during depletion of the external nitrogen source. Nitrogen conservation was thought to be particularly pronounced in proteins since they make up a high proportion of bacterial cellular mass (about 52% [Gottschalk, 1979]) and have therefore a high potential to reduce nutrient cost. Therefore, the nitrogen content of proteins significantly upregulated in response to nitrogen starvation was compared to the nitrogen content of proteins significantly upregulated in response to carbon starvation. Here, a general pattern of parsimonious nitrogen allocation was expected to be found in proteins upregulated in response to nitrogen starvation. We assumed that the effect of protein nitrogen conservation increased during the consistent starvation as the bacterial cells sensed that nitrogen starvation was persistent. In a subsequent analysis, the observed pattern of protein nitrogen allocation within the two protein sets was further disentangled by analyzing the amino acid composition of the proteins. Further, the amino acid abundance in the analyzed proteins was compared to the pool of free cellular amino acids in nitrogen- and carbon starved cultures to investigate how the amino acid composition of proteins was related to the amino acid availability in the cell. Special emphasis was put on the distribution of nitrogen rich amino acids (arginine, asparagine, glutamine, histidine, lysine and tryptophan) which had already been found to be less abundant in the free cellular pool of nitrogen starved cultures (in comparison to their abundance in the free pool of carbon starved cultures). The goal of this analysis was to relate the mobilization of those amino acids as internal nitrogen reservoirs to the conservation of nitrogen in upregulated proteins achieved through a lowered incorporation of the six nitrogen rich amino acids.

Since amino acids were not found to be primary reserves of carbon or energy (see chapter 4.1.2.4), the classification of amino acids exclusively according to their nitrogen demand was found to be legitimate in the present analysis.

#### 4.1.3.1 Protein nitrogen content

In figure 4.11, the nitrogen content of amino acid side chains of proteins significantly upregulated in response to nitrogen starvation (with respect to their level of regulation in response to carbon starvation) at a certain sampling time point was compared to the nitrogen content of amino acid side chains of proteins that were significantly upregulated in response to carbon starvation (with respect to their level of regulation in response to nitrogen starvation) at the given sampling time point (for detailed information on the analysis on protein regulation see chapter 3.8). The number of proteins

---

upregulated in response to nitrogen starvation or in response to carbon starvation is depicted for each sampling time point (see chapter 3.4.2). For each protein, the total amount of nitrogen atoms in their amino acid side chains was normalized by protein length. Next, this average number of nitrogen atoms per amino acid side chain was assigned to the given protein. Finally, the distribution of the average number of nitrogen atoms per amino acid side chain within the two protein sets (upregulated in response to nitrogen starvation and upregulated in response to carbon starvation) was depicted. Taken together, the average nitrogen content (measured as average number of nitrogen atoms per amino acid side chain) of proteins upregulated in response to nitrogen starvation was significantly lower (about 10 to 15 %) than that of proteins upregulated in response to carbon starvation at the sampling time points 60, 120 and 240 minutes (figure 4.11).

All five boxplots illustrating the distribution of nitrogen atoms per amino acid side chain in proteins upregulated in response to carbon starvation were comparatively taller than those boxplots illustrating the distribution of nitrogen atoms per amino acid side chain in proteins upregulated in response to nitrogen starvation (figure 4.11). These differences in size were mainly driven by the length of the upper whiskers, which ended above 0.5 nitrogen atoms per amino acid side chain for proteins upregulated in response to carbon starvation compared to maximal about 0.45 nitrogen atoms per amino acid side chain for proteins upregulated in response to nitrogen starvation (figure 4.11). In contrast, lower whiskers of all boxplots ended close to a value of 0.2 nitrogen atoms per amino acid side chain (figure 4.11). These observations revealed that the variation towards a higher average nitrogen content (depicted as the average number of nitrogen atoms per amino acid side chain) was more pronounced in proteins upregulated in response to carbon starvation than in proteins upregulated in response to nitrogen starvation. Further, the median number of nitrogen atoms per amino acid side chain was similar (around 0.35) between proteins upregulated in response to carbon starvation and proteins upregulated in response to nitrogen starvation at 10 minutes and at 30 minutes (figure 4.11). Nevertheless, proteins upregulated in response to carbon starvation at 10 minutes and at 30 minutes had on average 4.04 % and 5.73% respectively more nitrogen atoms per amino acid side chain than proteins upregulated in response to nitrogen starvation at the same time points. While the median of nitrogen atoms per amino acid side chain remained quite constant (around 0.35) in proteins upregulated in response to carbon starvation at the following sampling time points (60, 120 and 240 minutes), it decreased in proteins upregulated in response to nitrogen starvation (0.34 at 60 minutes, 0.32 at 120 minutes and 0.34 at 240 minutes) (figure 4.11). At these later sampling time points (60, 120 and 240 minutes), proteins upregulated in

response to nitrogen starvation were found to contain significantly less nitrogen atoms per amino acid side chain than proteins upregulated in response to carbon starvation. At 60 minutes, this difference in average nitrogen content (measured as average number of nitrogen atoms per amino acid side chain) was 9.76 %, at 120 minutes 15.5 % and at 240 minutes 10.44 %.

The present analysis highly suggests that proteins upregulated in response to nitrogen deprivation had been shaped by selection towards a lower nitrogen content. As we expected, this could be shown for the proteins that were significantly upregulated in response to nitrogen starvation in the later sampling time points (60, 120 and 240 minutes) when nitrogen starvation was sensed by the bacterial cells to be persistent.

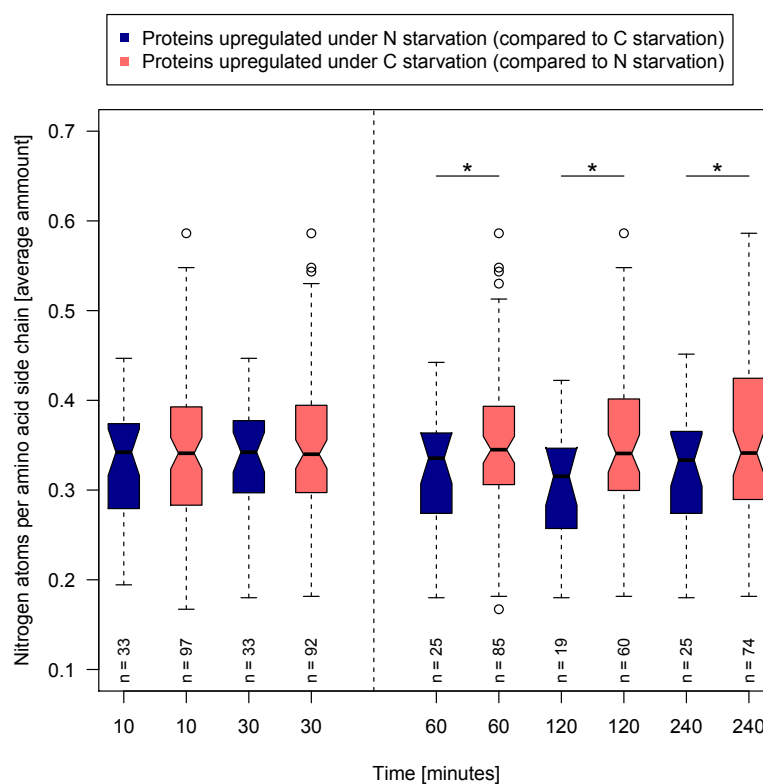


**Figure 4.11: Nitrogen content of proteins upregulated in response to nutrient starvation**

Distribution of the number of nitrogen atoms per amino acid side chain of proteins significantly upregulated in response to nitrogen (N) starvation (with respect to their level of regulation in response to carbon starvation,  $\log_2 > 2$ ) and of proteins significantly upregulated in response to carbon (C) starvation (with respect to their level of regulation in response to nitrogen starvation,  $\log_2 > 2$ ) at the sampling time points 10, 30, 60, 120 and 240 minutes after starvation onset. Levels of protein regulation were estimated by the program DESeq (nbinom-test, \*  $p < 0.05$ ). Statistical differences were computed for the comparison of protein nitrogen content of proteins upregulated in response to nitrogen starvation and of proteins upregulated in response to carbon starvation by the Welch's test (one-tail), \*  $p < 0.05$

#### 4.1.3.2 Nitrogen rich amino acids: avoided in proteins and utilized as nitrogen source

As we expected, the difference in nitrogen allocation between proteins significantly upregulated in response to nitrogen starvation (in comparison to carbon starvation) and proteins significantly upregulated in response to carbon starvation (in comparison to nitrogen starvation) was more pronounced and statistically significant at the later sampling time points (beginning at 60 minutes) of the starvation experiment (see figure 4.11). Therefore, proteins upregulated at these later time points were investigated in more detail to reveal their amino acid composition, focusing on differences in the abundance of nitrogen rich amino acids. Since our goal was to relate the distribution of nitrogen rich amino acids in proteins to their free cellular abundance, we focused on the sampling time points 120 and 240 minutes for which also metabolomic data were available. Data of the sampling time points 120 and 240 minutes were pooled together, in order to summarize all interesting data in a single figure. The combination of the two sampling time points reduced the number of proteins available for this analysis but enhanced the quality of the data sets. The remaining eighteen proteins that were significantly upregulated in response to nitrogen starvation at both time points (120 and 240 minutes) and forty-four proteins that were significantly upregulated in response to carbon starvation at both time points (120 and 240 minutes) were believed to be persistently upregulated in the later stage of nutrient starvation and thereby essential proteins of the corresponding starvation response (list of proteins in chapter 6). After this selection process, the abundance of each amino acid per protein upregulated in response to nitrogen starvation was calculated and normalized to the protein length. Equation 5 shows exemplary how this calculation for the abundance of the amino acid alanine (A) in one of the eighteen proteins upregulated in response to nitrogen starvation ( $N_{Protein}$ ) was performed.

$$A(N_{Protein1}) = \text{Abundance of A in } N_{Protein1} \div \text{Length of } N_{Protein1} \quad (5)$$

Next, the average abundance of each amino acid in the eighteen proteins upregulated in response to nitrogen starvation was calculated. Equation 6 shows this calculation exemplary for the amino acid alanine.

$$\emptyset A(N_{Protein}) = A(N_{Protein1}) + A(N_{Protein2}) + A(N_{Protein3}) \dots + A(N_{Protein18}) \div 18 \quad (6)$$

The same calculations were performed to obtain the average abundance of each amino acid in the forty-four proteins upregulated in response to carbon starvation ( $C_{Protein}$ ). Next, the ratio of the average abundance of a specific amino acid in proteins upregu-

lated in response to nitrogen starvation to the average abundance of this amino acid in proteins upregulated in response to carbon starvation was calculated. Equation 7 shows this calculation exemplary for the amino acid alanine.

$$A(N_{Protein}/C_{Protein}) = \varnothing A(N_{Protein}) \div \varnothing A(C_{Protein}) \quad (7)$$

This ratio (equation 7) was calculated for each amino acid and plotted on the y-axis of figure 4.12.

In order to relate the abundance of the amino acids in proteins to their availability in the free amino acid pool, metabolome data were prepared as following: the abundance of each amino acid in the free amino acid pool of one of the six nitrogen starved cultures (data of six nitrogen starved cultures were available in total: three biological replicates for the time point 120 minutes and three biological replicates for the time point 240 minutes) was normalized to the overall free amino acid pool of this culture. Equation 8 shows this calculation exemplary for the cellular abundance of alanine in the free amino acid pool of one of the six nitrogen starved cultures ( $N_{free}$ ).

$$A(N_{free1}) = \text{Abundance of A in } N_{free1} \div \text{Total free amino acid pool of } N_{free1} \quad (8)$$

Next, the average abundance of each amino acid in the free amino acid pool of the six nitrogen starved cultures was calculated. Equation 9 shows this calculation exemplary for the amino acid alanine.

$$\varnothing A(N_{free}) = A(N_{free1}) + A(N_{free2}) + A(N_{free3}) \dots + A(N_{free6}) \div 6 \quad (9)$$

The same calculations were performed to obtain the average abundance of each amino acid in the free amino acid pool of the six carbon starved cultures ( $C_{free}$ ). Next, the ratio of the average abundance of a specific amino acid in the free amino acid pool of nitrogen starved cultures to the average abundance of this amino acid in the free amino acid pool of carbon starved cultures was calculated. Equation 10 shows this calculation exemplary for the amino acid alanine.

$$A(N_{free}/C_{free}) = \varnothing A(N_{free}) \div \varnothing A(C_{free}) \quad (10)$$

This ratio (equation 10) was calculated for each amino acid and plotted on the x-axis of figure 4.12.

Figure 4.12 suggests that the conservation of nitrogen in proteins significantly upregulated in response to nitrogen starvation at 120 and 240 minutes was caused by a lowered incorporation of amino acids with a high nitrogen allocation (arginine, asparagine, glutamine and lysine). Even though these nitrogen rich amino acids were less abundant in the mentioned proteins, they did not accumulate in the free amino acid pool of nitrogen starved cultures but were rather less abundant than in the free amino acid pool of carbon starved cultures.

Proteins upregulated in response to nitrogen starvation incorporated amino acids with a high nitrogen allocation less often than proteins upregulated in response to carbon starvation (arginine  $R(N_{Protein}/C_{Protein})$ : 0.84, asparagine  $N(N_{Protein}/C_{Protein})$ : 0.83, glutamine  $Q(N_{Protein}/C_{Protein})$ : 0.61 and lysine  $K(N_{Protein}/C_{Protein})$ : 0.78) (figure 4.12). Out of these amino acids, only glutamine was found to be significantly less abundant in proteins upregulated in response to nitrogen starvation (figure 4.12). Histidine (H) and tryptophan (W), also nitrogen rich amino acids, were almost equally abundant in proteins upregulated in response to nitrogen starvation and in proteins upregulated in response to carbon starvation ( $H(N_{Protein}/C_{Protein})$ : 0.99 and  $W(N_{Protein}/C_{Protein})$ : 0.95) (figure 4.12). Despite their lowered abundance in proteins upregulated in response to nitrogen starvation, the abundance of the amino acids arginine (R), asparagine (N), glutamine (Q) and lysine (K) in the free amino acid pool of nitrogen starved cultures was lower than in the free amino acid pool of carbon starved cultures ( $R(N_{free}/C_{free})$ : 0.23,  $N(N_{free}/C_{free})$ : 0.77,  $Q(N_{free}/C_{free})$ : 0.69 and  $K(N_{free}/C_{free})$ : 0.59) (figure 4.12). The same was true for the abundance of histidine (H) and tryptophan (W) in the free amino acid pools ( $H(N_{free}/C_{free})$ : 0.15 and  $W(N_{free}/C_{free})$ : 0.51) (figure 4.12). Except for asparagine, these differences in abundance in the free amino acid pools were found to be significant (figure 4.12).

The nitrogen poor amino acids tyrosine (Y) and leucine (L) were significantly less abundant in the free amino acid pool of nitrogen starved cultures than in the free amino acid pool of carbon starved cultures ( $Y(N_{free}/C_{free})$ : 0.86 and  $L(N_{free}/C_{free})$ : 0.97) (figure 4.12). At this point it has to be stated that for leucine and isoleucine a common value of their abundance in the free amino acid pools was depicted in figure 4.12 since they were not distinguished during the analysis of free cellular metabolites (see chapter 3.6.1). Further, tyrosine and leucine were less abundant in proteins upregulated in response to nitrogen starvation than in proteins upregulated in response to carbon starvation ( $Y(N_{Protein}/C_{Protein})$ : 0.43 and  $L(N_{Protein}/C_{Protein})$ : 0.74) (figure 4.12). The nitrogen poor amino acid methionine (M) was less abundant in proteins upregulated in response to nitrogen starvation (in comparison to proteins upregulated in response to carbon starvation) ( $M(N_{Protein}/C_{Protein})$ : 0.80) but equally abundant

in the free amino acid pools of the two nutrient starved cultures ( $M(N_{free}/C_{free})$ : 0.96) (figure 4.12). Glutamate (E), also a nitrogen poor amino acid, was as well less abundant in proteins upregulated in response to nitrogen starvation than in proteins upregulated in response to carbon starvation ( $E(N_{Protein}/C_{Protein})$ : 0.79) and further significantly more abundant in the free amino acid pool of nitrogen starved cultures than in the free amino acid pool of carbon starved cultures ( $E(N_{free}/C_{free})$ : 1.64) (figure 4.12). The nitrogen poor amino acid valine (V) was found to be equally abundant in the two protein sets ( $V(N_{Protein}/C_{Protein})$ : 0.95) and also in the free amino acid pool of the two nutrient starved cultures ( $V(N_{free}/C_{free})$ : 1.10) (figure 4.12). The nitrogen poor amino acids phenylalanine (F) and isoleucine (I) were found to be more abundant in proteins upregulated in response to nitrogen starvation than in proteins upregulated in response to carbon starvation ( $F(N_{Protein}/C_{Protein})$ : 1.31 and  $I(N_{Protein}/C_{Protein})$ : 1.21) (figure 4.12). For phenylalanine (F), the difference in abundance between the two protein sets was found to be statistically significant (figure 4.12). Aspartate (D) (nitrogen poor) was almost equally abundant in proteins upregulated in response to nitrogen starvation and in proteins upregulated in response to carbon starvation ( $D(N_{Protein}/C_{Protein})$ : 1.02) (figure 4.12). Further, the two amino acids phenylalanine and aspartate were significantly less abundant in the free amino acid pool of nitrogen starved than in the free amino acid pool of carbon starved cultures ( $F(N_{free}/C_{free})$ : 0.73 and  $D(N_{free}/C_{free})$ : 0.72) (figure 4.12). The amino acid cysteine (C) (nitrogen poor) was about twice as abundant in proteins responding to nitrogen starvation than in proteins responding to carbon starvation ( $C(N_{Protein}/C_{Protein})$ : 2.14) (figure 4.12). The remaining nitrogen poor amino acids, namely threonine (T), alanine (A), serine (S), proline (P) and glycine (G), were found to be equally abundant in proteins upregulated in response to nitrogen starvation and in proteins upregulated in response to carbon starvation ( $N_{Protein}/C_{Protein}$  about 1.1) (figure 4.12). Further, alanine, serine, cysteine, proline and glycine were significantly more abundant in the free amino acid pool of nitrogen starved cultures than in the free amino acid pool of carbon starved cultures ( $A(N_{free}/C_{free})$ : 1.26,  $S(N_{free}/C_{free})$ : 3.70,  $C(N_{free}/C_{free})$ : 3.71,  $P(N_{free}/C_{free})$ : 5.12 and  $G(N_{free}/C_{free})$ : 5.59) (figure 4.12).

The observed trend of the abundance of the nitrogen rich amino acids arginine, asparagine, glutamine and lysine in proteins upregulated in response to nitrogen starvation suggests that selection owing to nitrogen deprivation had indeed shaped the amino acid composition of these proteins towards a lower nitrogen allocation. Statistical significance could only be confirmed for the abundance of glutamine and the two nitrogen rich amino acids histidine and tryptophan were, unless otherwise expected, not less abundant in proteins upregulated in response to nitrogen starvation (in comparison to



proteins upregulated in response to carbon starvation). Here, an analysis of protein regulation in response to nutrient starvation on more biological replicates than used in the present study might enhance the number of proteins available for the analysis on amino acid abundance and thereby help to clarify the present observations. However, the lowered abundance of most of the nitrogen rich amino acids in proteins upregulated in response to nitrogen starvation could be linked to an in total lowered abundance of nitrogen rich amino acids in the free amino acid pool of nitrogen starved cultures.

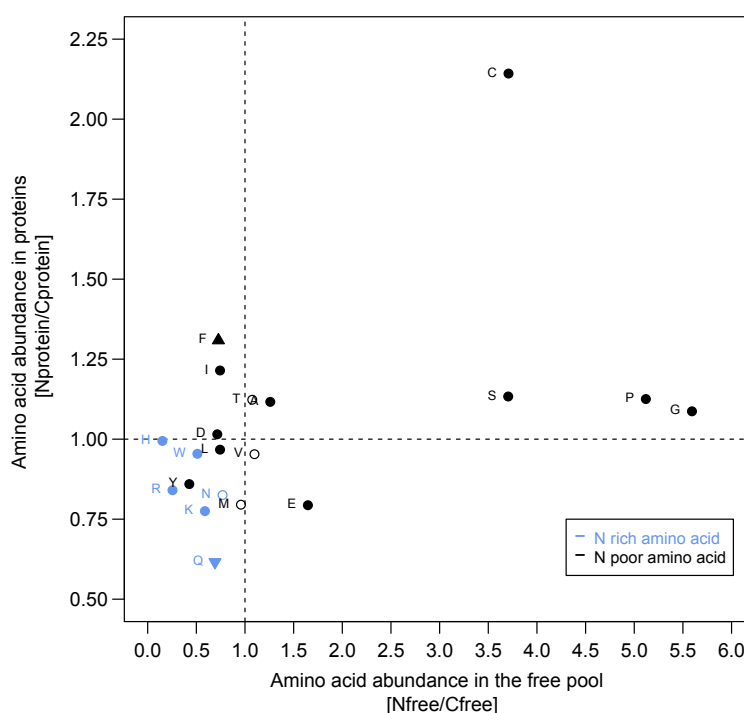


**Figure 4.12: Relation of protein amino acid composition and the availability of free amino acids during nutrient starvation**

Ratio of amino acid abundance in proteins significantly upregulated in response to nitrogen starvation (in comparison to carbon starvation,  $\log_2 > 2$ ) [=Nprotein] to amino acid abundance in proteins significantly upregulated in response to carbon starvation (in comparison to nitrogen starvation,  $\log_2 > 2$ ) [=Cprotein] on the y-axis. Levels of protein regulation were estimated by the program DESeq (nbinom-test, \*  $p < 0.05$ ). Ratio of amino acids abundance in the free amino acid pool of nitrogen starved cultures [=Nfree] to their abundance in the free amino acid pool of carbon starved cultures [=Cfree] on the x-axis. Averaged data of the sampling time points 120 and 240 minutes are shown.  $\Delta$  and  $\nabla$  mark statistical significances in protein amino acid abundance, filled symbols mark statistical significances in free amino acid abundance. Statistical differences were computed by the Welch's test, the Wilcoxon's test or the Student's-t test (one-tail), \*  $p < 0.05$

Among the eighteen proteins that were found to be significantly upregulated in response to nitrogen starvation (in comparison to carbon starvation) at 120 and 240 minutes, four were directly involved in nitrogen metabolism: the nitrogen regulatory protein Ntr, the AmtB transporter, the nitrogen assimilation control protein Nac and the glutamine synthetase. For a description of the function of these proteins see chapter 4.1.1.3. Six more proteins were encoded by genes of the Rut pathway (*rutA-F*) which was found to degrade pyrimidines and thereby releasing their nitrogen atoms [Loh *et al.*, 2006; Parales and Ingraham, 2010]. The eight remaining proteins were for example different transport and resistance proteins, for a complete list see chapter 6.

## 4.2 Persistent nitrogen limitation in continuous culture

Due to the extreme severity of the stress induced by the complete nitrogen depletion, there was no cell growth during the short-term starvation experiment. Therefore, in the setting of the short-term starvation experiment, it was explored whether selection owing to nitrogen deprivation had shaped the architecture of proteins upregulated in response to nitrogen starvation over millions of years of evolution. To extend the understanding of the dynamics of nitrogen allocation, cultures of *E. coli* Nissle 1917  $\Delta fliC$  were examined over longer and potentially evolutionary relevant time scales (1600 generations) in a continuous culture experiment. The continuous cultures were maintained under nitrogen limiting conditions that allowed them to grow and thereby to further evolve in a controlled environment (see chapter 3.5). Due to the different time frame and experimental setting, the continuously growing cultures, unlike the short-term nitrogen starved cultures, did not have the possibility to access cellular nitrogen reservoirs via massive autophagy. Thus, it was assured that continuous cultures directly depended on the external nitrogen source that was supplemented with the growth medium. For an optimal scavenging and processing of external nitrogen, continuous cultures were expected to primarily elevate the expression level of genes involved in assimilation and metabolism of nitrogen. Another cellular response towards nutrient availability is the adaptation of the cellular morphology. Next to these cellular responses, the continuous culture experiment aimed to reveal whether persistent nitrogen limitation causes a further reduction of the cellular nitrogen budget. Special emphasis was put on the dynamics of nitrogen allocation of proteins significantly upregulated in nitrogen limited continuous cultures over time. In a subsequent analysis, cultures that had evolved for 1600 generations under nitrogen limitation were competed against control cultures (nitrogen rich continuous cultures) and the ancestor. In the competition experiments, the cultures evolved in the nitrogen limited environment were expected to exhibit growth advantages in nitrogen limited medium.

### 4.2.1 Basic cellular response to nitrogen limitation

Persistent nitrogen limitation was expected to cause an elevation of the expression level of genes involved in the acquisition and metabolism of nitrogen. Genes of interest were common to those investigated in the short-term nitrogen starvation experiment since the cellular response to both types of nutrient stress (limitation and starvation) partly overlaps [Ferenci, 1999; Matin *et al.*, 1989]. Further, the ammonium uptake rate of continuous cultures was followed over time. To calculate the uptake rate, ammonium leftovers were detected in the depleted growth medium of the continuous cultures. Lastly, the morphology of continuous cultures on congo red screening agar was observed over time to detect changes in colony size and shape. The investigation

of these aspects of the response towards nitrogen availability aimed to validate the continuous culture experiment.

#### 4.2.1.1 Expression of key genes

Figure 4.13 shows the log<sub>2</sub> ratio of gene expression in nitrogen limited cultures versus the nitrogen rich control over 1600 generations (for detailed information on gene expression analysis and statistical differences see chapter 3.8). The average gene expression data (averaged over three biological replicates) of the nitrogen limited cultures obtained at six generations were tested against corresponding expression data of the nitrogen rich control cultures (averaged over three biological replicates) at these generations (see chapter 3.5.2). Log<sub>2</sub> ratios above zero indicated that the genes had a higher expression level in nitrogen limited cultures, whereas a log<sub>2</sub> ratio below zero testified a higher gene expression level in the nitrogen rich control.

All of the six analyzed genes had a higher expression level in nitrogen limited cultures than in nitrogen rich control cultures at each generation (figure 4.13). Moreover, these differences were, except for *glnG* at generation 200, found to be significant (figure 4.13). Also, log<sub>2</sub> ratios of all genes were higher in the generations 14/23, 1000 and 1600 than in the generations 100 to 500 (figure 4.13).

For the gene *glnA*, log<sub>2</sub> ratios around 5 were detected in the generations 14/23 and 1600. In the generations 100 to 1000, log<sub>2</sub> ratios lay between 1.29 and 2.80 (figure 4.13).

The expression level of the genes *glnG* and *glnL* were highly similar in all generations. In generation 14/23, log<sub>2</sub> ratios were about 3.2. In the following generations (100 to 500), log<sub>2</sub> ratios dropped to roughly 1 to 1.5 (*glnG*) and to about 1 to 2 (*glnL*), respectively. Finally, the log<sub>2</sub> ratios of both genes increased again to 2.59 (*glnG*) and 2.90 (*glnL*) in generation 1000 and further to 3.81 (*glnG*) and 4.60 (*glnL*) in generation 1600 (figure 4.13).

Also the genes *glnK*, *nac* and *amtB* were expressed in similar ways. These genes showed the highest log<sub>2</sub> ratios of all genes tested in generation 14/23 (8.87 (*glnK*), 7.03 (*nac*) and 7.65 (*amtB*)). Next, the log<sub>2</sub> ratios dropped to roughly 3.8 to 4.8 (generations 100 and 200) and further to 2 to 3 in generation 500. Then, log<sub>2</sub> ratios increased again to about 5 (generation 1000). At the end of the experiment (generation 1600), log<sub>2</sub> ratios lay at 6.32 (*glnK*), 5.93 (*nac*) and 5.13 (*amtB*) (figure 4.13).

The present findings confirm that the nitrogen limited minimal medium indeed caused a transcriptional response towards nitrogen limitation, including an increased expression level of genes involved in an improved scavenging of nitrogen.

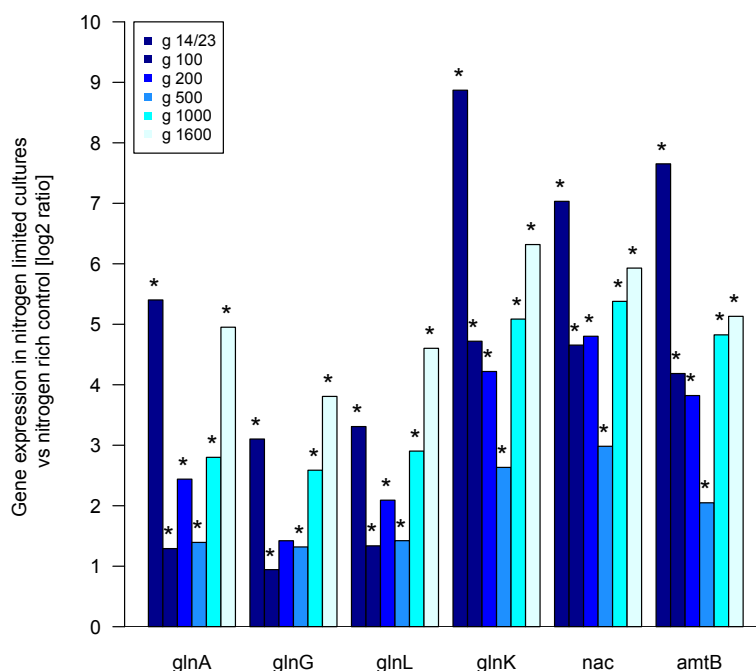


**Figure 4.13: Expression of nitrogen key genes during nitrogen limitation**

Log<sub>2</sub> ratios of *glnA*, *glnG*, *glnL*, *glnK*, *nac* and *amtB* expression in response to nitrogen limitation with respect to the nitrogen rich control cultures at the generations 14/23, 100, 200, 500, 1000 and 1600. For each generation, mean expression levels from biological triplicates of nitrogen limited cultures and nitrogen rich control cultures were determined by the program DESeq. Statistical differences were estimated by the program DESeq (nbinom-test, \* p<0.05) for the comparison of gene expression levels in nitrogen limited cultures and nitrogen rich control cultures.

#### 4.2.1.2 Enhancement of ammonium uptake

Figure 4.14 shows the amount of ammonium that was taken up from the growth medium by nitrogen limited cultures and by nitrogen rich control cultures over 1600 generations. Ammonium leftovers in the effluent of the cultures were measured via cation chromatography (for detailed information on cation chromatography see chapter 3.6.3) and the percentage of ammonium used up by the cultures was calculated. Mean values of ammonium usage  $\pm$  the standard deviation of two samples (see chapter 3.6.3) analyzed for each nutrient condition at eight generations (see chapter 3.5.2) are shown as percent values.

In total, the average ammonium uptake rate of nitrogen limited cultures at the generations 500 to 1500 (49.51 %) was 13.89 % higher than their average uptake rate at the generations 14 to 400 (35.62 %) (figure 4.14). This difference was found to be significant (Student's-t test, one-tailed, p<0.001).

For nitrogen limited cultures, an ammonium uptake rate of about 35 to 36 % was measured within the first 400 generations (figure 4.14). Then, an increase in the ammonium uptake rate of about 15 % was observed at generation 500 (figure 4.14). For

the generations 1000 and 1600, slightly lowered ammonium uptake rates compared to generation 500 were measured ( $51.85 \pm 0.16$  % at generation 500,  $46.67 \pm 0.16$  % at generation 1000 and  $50.00 \pm 0.14$  % at generation 1600). However, these uptake rates were still higher compared to the generations 14 to 400 (figure 4.14).

The amount of ammonium taken up by the nitrogen rich control cultures was relatively constant and low in all generations (values lay between  $3.08 \pm 1.63$  % (generation 400) and  $5.91 \pm 1.52$  % (generation 23)) (figure 4.14).

The analysis on the ammonium uptake rate suggests that some adaptive dynamics may have increased the ability of nitrogen limited cultures to take up ammonium over time, maybe via one or more mutations fixed in the populations.

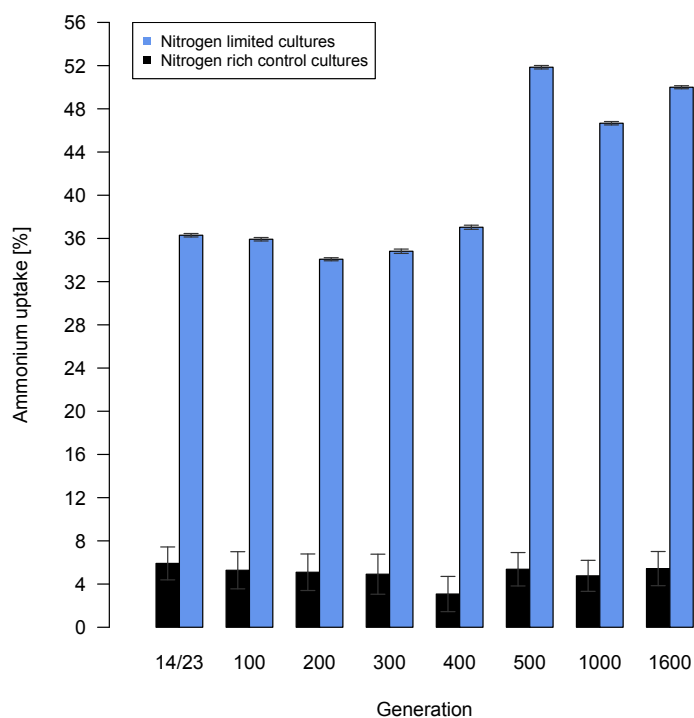


**Figure 4.14: Ammonium uptake during nitrogen limitation**

Ammonium uptake of nitrogen limited cultures and nitrogen rich control cultures at the generations 14/23, 100, 200, 300, 400, 500, 1000 and 1600. Mean uptake  $\pm$  standard deviation of two samples from nitrogen limited cultures or nitrogen rich control cultures are depicted as percent values

### 4.2.1.3 Morphological changes

After about 800 generations of cultivation in the nitrogen limited medium, colonies with morphotypes deviating from the *E. coli* Nissle 1917-specific rdar morphotype were detected during the weekly screening on congoed agar. All of these new arisen morphotypes appeared on congoed screening plates of each of the five nitrogen limited cultures. The new morphotypes were found at each subsequent congoed screening assay at almost equal frequency. Nevertheless, the colonies with the *E. coli* Nissle 1917-specific rdar morphotype remained in the nitrogen limited cultures. Figure 4.15 shows the distribution of the different morphotypes in a nitrogen limited culture at generation 1600. This phenomenon was specific to the nitrogen limited setting, in the nitrogen rich control cultures no morphotypes deviating from the rdar one were identified during the complete time course of the experiment (figure 4.16). The four



Figure 4.15: Morphotypes after 1600 generations under nitrogen limitation

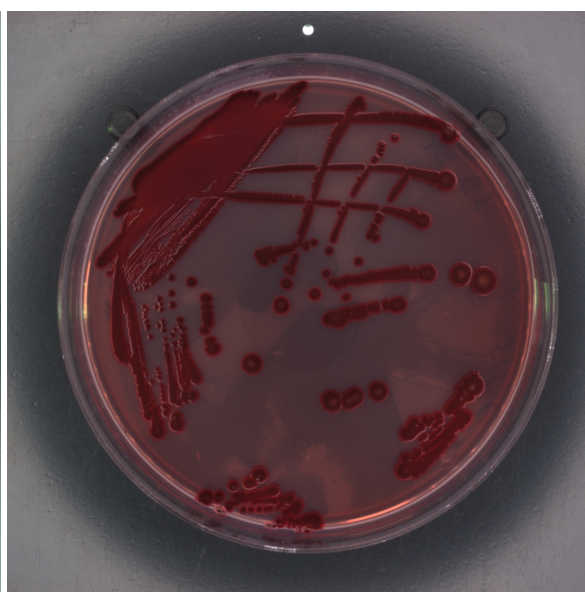


Figure 4.16: Morphotypes after 1600 generations under nitrogen rich control conditions

different morphotypes that were detected during the congoed screening of the nitrogen limited cultures are shown in the figures 4.17 to 4.20. Figure 4.17 shows the *E. coli* Nissle 1917-specific rdar morphotype whose colonies were red coloured and had a dry and rough surface. Figure 4.18 shows a colony which was found to be reddish and rough at its borders but else white/brownish and moist. Figure 4.19 shows one of the colonies that had the most deviating morphotype from the rdar one. It had a red and rough basis which was almost completely covered by a white and moist layer. Both of these new phenotypes were not as round shaped as the rdar one but roundish with small indentations (figure 4.18 and 4.19). The last morphotype detected in nitrogen limited cultures was red, dry and rough but the colonies were formed by many indentations (4.20).

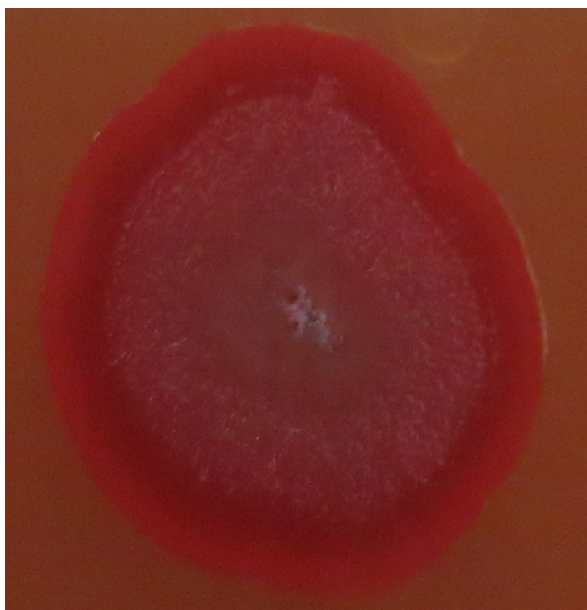


Figure 4.17: rdar morphotype

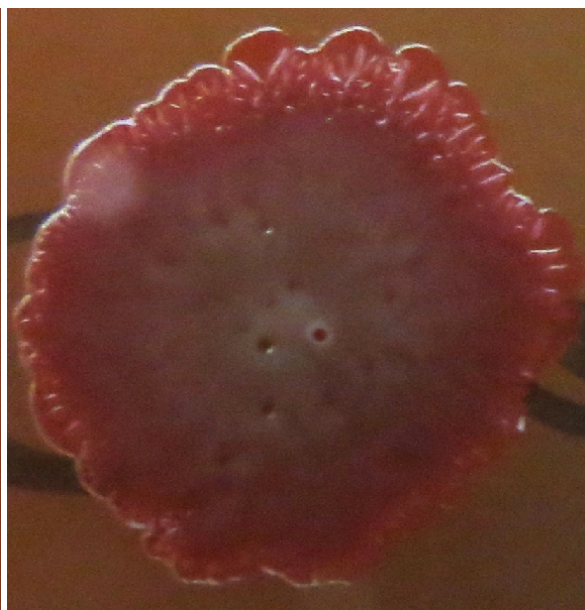


Figure 4.18: new morphotype 1

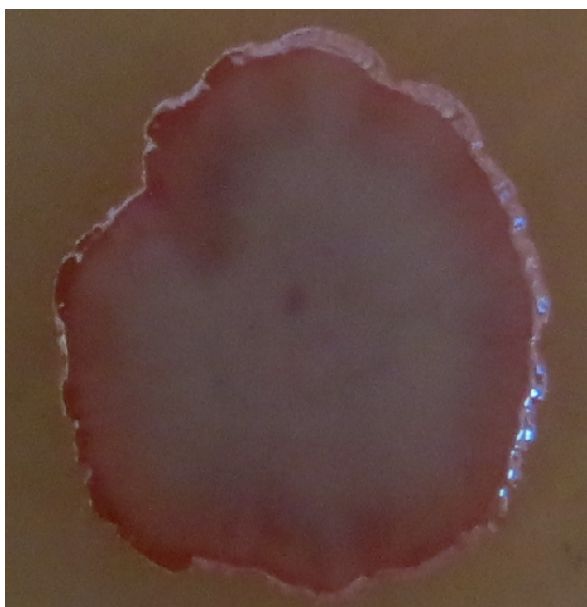


Figure 4.19: new morphotype 2

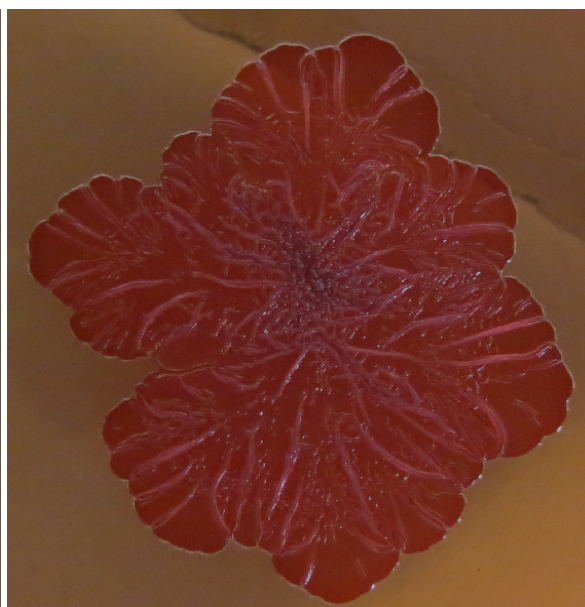
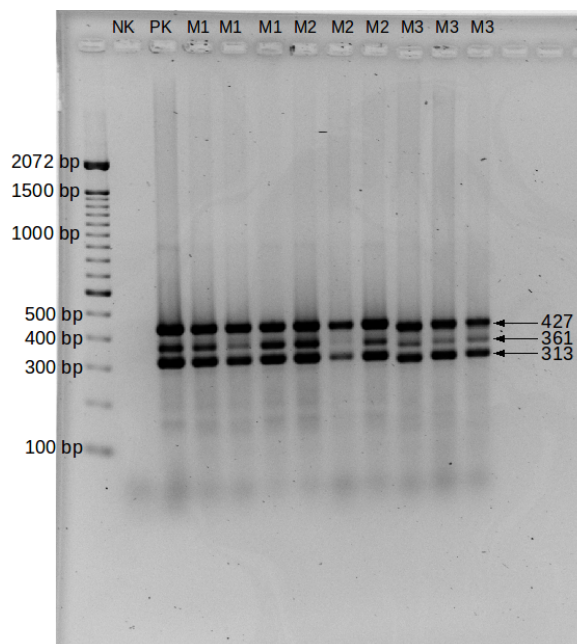


Figure 4.20: new morphotype 3

The colonies that expressed the rdar deviating morphotypes were analyzed in the *E. coli* Nissle 1917-specific multiplex PCR (see chapter 3.2.2.1) to verify that they represented the strain Nissle 1917 and not possible contaminations of other bacterial strains. The multiplex PCR amplifies fragments of the *E. coli* Nissle 1917-specific plasmids pMUT1 (product of 361 bp) and pMUT2 (products of 313 and 427 bp). The amplification products of all tested morphotypes (M1, M2 and M3) had specific products sizes on the agarose gel (figure 4.21), assuring that the new morphotypes indeed represented the strain Nissle 1917. The manifestation of the rdar deviating morphotypes might have entailed growth advantages for the continuous cultures that evolved in the nitrogen limited environment.





**Figure 4.21: Multiplex PCR assay of colonies from the nitrogen limited cultures**

The multiplex PCR was performed on colonies from the nitrogen limited cultures that showed morphotypes deviating from the *E. coli* Nissle 1917-specific rdar one on congeared agar. A negative control (water instead of DNA, NC) is shown in lane 1 and a positive control (DNA of strain Nissle 1917, PC) is shown in lane 2. Lane 3 to 11 show PCR products of colonies expressing the new morphotypes (M1, M2 and M3), three colonies per morphotype were tested. PCR product sizes are indicated

### 4.2.2 Signals of nitrogen conservation

Next to an improvement in nitrogen scavenging, nitrogen limited cultures were expected to decrease their cellular nitrogen budget over time to remain viable and competitive. In a first analysis, the overall cellular carbon to nitrogen ratio of the nitrogen limited cultures was compared to that of the nitrogen rich control cultures and to that of the ancestor. The carbon to nitrogen ratio was further disentangled by analyzing and comparing the overall cellular nitrogen and carbon content of the different cultures.

In a second analysis, special focus was on the dynamics of the protein nitrogen budget. It was expected that the global expression level of genes was linked to the nitrogen content of the encoded proteins, reflected in a reduced nitrogen allocation of proteins significantly upregulated in response to nitrogen limitation. Therefore, RNAseq data were produced and the nitrogen content of encoded proteins was analyzed over time. The effect of protein nitrogen conservation was further assumed to increase over generation time due to the persistent selection pressure exerted by nitrogen limitation. Consistent analyses were performed on RNAseq data that were produced for the nitrogen rich control cultures. Here, no signals of nitrogen conservation in upregulated proteins were expected since those cultures were not exposed to selection owing to nitrogen limitation.

#### 4.2.2.1 Cellular carbon and nitrogen content

Figure 4.22 shows the C/N ratio of nitrogen limited cultures and of nitrogen rich control cultures over 1600 generations. Cellular carbon and nitrogen content were measured via elemental analysis (for detailed information on elemental analysis see chapter 3.6.2). In figure 4.22, two values of the C/N ratio are depicted per nutrient condition (see chapter 3.6.2) at eight generations (see chapter 3.5.2). Further, the C/N ratio of the ancestor is depicted. Therefore, the C/N ratios of two biological replicates of the ancestor were determined (see chapter 3.6.2) and the mean of this two values was plotted.

In total, the C/N ratios of the nitrogen limited cultures were constantly higher compared to those of the nitrogen rich control and the ancestor. The differences were already pronounced after one day of continuous culturing. At generation 1600, the C/N ratio of the nitrogen limited cultures had increased by 24 % relative to the ancestor. Further, the average difference of the C/N ratio between nitrogen limited cultures and the nitrogen rich control cultures was 18.85 % which was found to be significant (Wilcoxon's, one-tail,  $p < 0.001$ ).

The mean C/N ratio of the ancestor was 3.40 (figure 4.22). Nitrogen rich control cultures had a slightly lower C/N ratio in the generations 23 to 200 (ratios between 3.36 (generation 23) and 3.17 (generation 100)) (figure 4.22). In the following gen-

erations (300-1600), the C/N ratios of the nitrogen rich control cultures lay between values of 3.32 (generation 300) and 3.71 (generation 400) (figure 4.22). At generation 500, an almost equal C/N ratio was determined for the two samples of the nitrogen rich control (3.39) which was comparable to the mean C/N ratio of the ancestor (figure 4.22).

Already after 14 generations of continuous culturing, the C/N ratios of cultures grown under nitrogen limitation had increased to 3.52 and 3.63, respectively (figure 4.22). After 100 generations, the C/N ratios had further increased to 3.80 and 3.96 and then remained relatively constant in the following generations (figure 4.22). At the end of the continuous culture experiment (1600 generations), one of the C/N ratios of the nitrogen limited cultures peaked at a value of 4.21 (figure 4.22).

The findings confirm that the element composition of the continuous cultures was affected by the element quantities of their surrounding. The different C/N ratios of the two growth media (full MM and N-lim NN) were reflected in a deviating C/N ratio of nitrogen rich control cultures and nitrogen limited cultures.

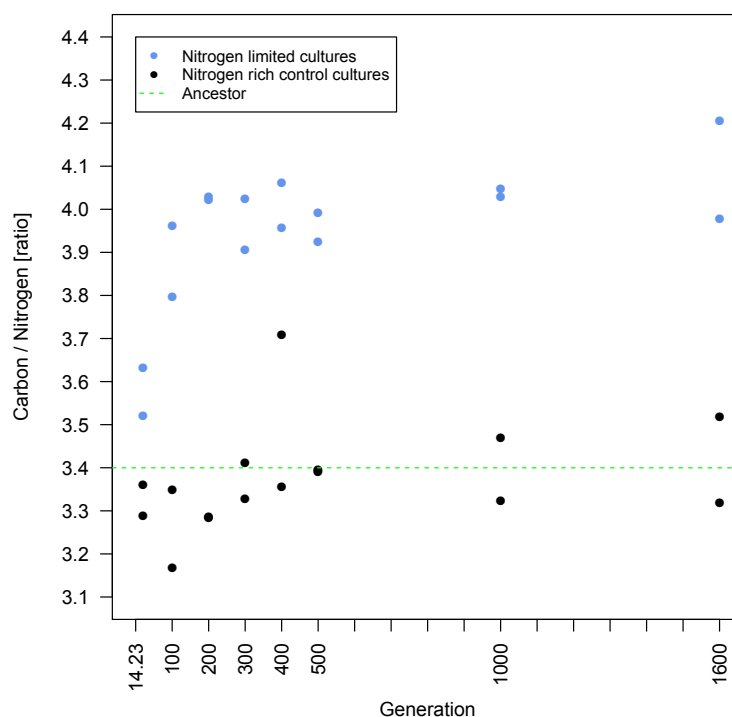


**Figure 4.22: Carbon to nitrogen ratio of the continuous cultures and their ancestor over time**  
Carbon to nitrogen (C/N) ratio of nitrogen limited cultures and nitrogen rich control cultures at the generations 14/23, 100, 200, 300, 400, 500, 1000 and 1600 and carbon to nitrogen ratio of the ancestor. C/N ratios of two samples from nitrogen limited or nitrogen rich control cultures and of two samples from the ancestor are depicted.

---

To gain further insights on the biological meaning of the variation observed in the C/N ratio, the trend of the carbon and nitrogen content of the continuous cultures and their ancestor was analyzed separately (figure 4.23). Nitrogen and carbon contents were obtained as single measures during the detection of the C/N ratio (see chapter 3.6.2).

In summary, the nitrogen content of the nitrogen limited cultures was lower than that of the nitrogen rich control cultures at the generations 100 to 1600 and consistently lower than the nitrogen content of the ancestor (figure 4.23 A). The average difference of the nitrogen content between nitrogen limited cultures and nitrogen rich control cultures was 14.87 % and found to be statistically significant (Wilcoxon's test, one-tailed,  $p < 0.001$ ). On the contrary, the carbon content of the nitrogen limited cultures, of the the nitrogen rich control and of the ancestor was rather similar over time, existing differences had no statistical significance (figure 4.23 B).

The mean nitrogen content of the ancestor was 12.46 % (figure 4.23 A). After 14 and 23 generations, respectively, the nitrogen limited cultures and the nitrogen rich control cultures showed a similar nitrogen content (nitrogen limited cultures:  $11.86 \pm 0.34$  % and nitrogen rich control cultures:  $12.16 \pm 0.45$  %) (figure 4.23 A). Further, the mean nitrogen content of nitrogen rich control cultures fluctuated slightly over time (values between  $13.41 \pm 1.26$  % (generation 100) and  $11.22 \pm 0.20$  % (generation 400)) (figure 4.23 A). On the contrary, the nitrogen content of the nitrogen limited cultures had decreased to  $10.52 \pm 0.83$  % at generation 100 and remained quiet constant until generation 500 ( $10.14 \pm 0.08$  % (generation 300)). At the generations 1000 and 1600, the cellular nitrogen content of the nitrogen limited cultures had further declined to about 9.8 % (figure 4.23 A).

The mean carbon content of the ancestor was 42.37 % (figure 4.23 B). At the generation 14 and 300, the carbon content of the nitrogen limited cultures was almost equal, namely  $42.41 \pm 0.30$  % and  $42.77 \pm 2.11$  %, respectively (figure 4.23 B). At the remaining generations, the carbon content of the nitrogen limited cultures was about 1 to 2.5 % lower than that of the ancestor (figure 4.23 B). The carbon content of the nitrogen rich control cultures was as well slightly lower than that of the ancestor, namely about 1.2 to 3 % (at generations 23, 200-500,1600) and about 4 % (at generation 1000) (figure 4.23 B). Only at generation 100, the carbon content of the nitrogen rich control was slightly higher (43.60 %) compared to that of the ancestor (figure 4.23, B). Further, for the nitrogen rich control, a 2 % lowered carbon content compared to that of the nitrogen limited cultures was detected at generation 14/23, else the carbon content of the two continuous cultures did not differ from each other (figure 4.23 B).

The observed differences in the C/N ratio between nitrogen limited cultures on the one hand and nitrogen rich control cultures and the ancestor on the other hand were found to be driven by a reduced cellular nitrogen content of the nitrogen limited cultures. This overall cellular nitrogen conservation is consistent with the underlying hypothesis that persistent nitrogen limitation is reflected in a reduced nitrogen demand.

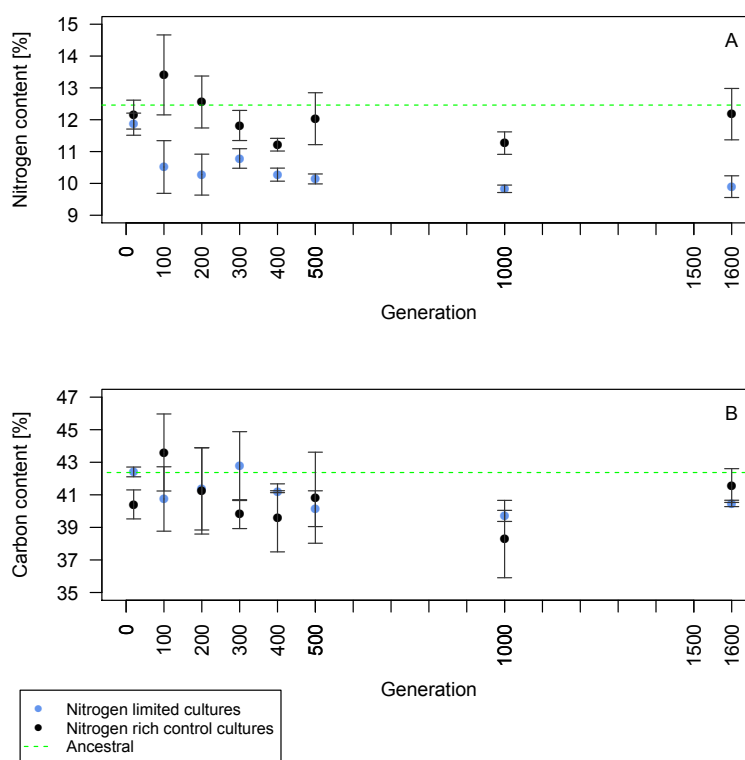


**Figure 4.23: Nitrogen and carbon content of continuous cultures and their ancestor over time**  
Cellular nitrogen content (A) and carbon content (B) of nitrogen limited cultures and nitrogen rich control cultures at the generations 14/23, 100, 200, 300, 400, 500, 1000 and 1600 and nitrogen (A) and carbon (B) content of the ancestor. Mean nitrogen and carbon content  $\pm$  standard deviation of two samples are depicted as percent values

#### 4.2.2.2 Protein nitrogen content

##### Protein nitrogen content in nitrogen limited cultures

In figure 4.24, the nitrogen content of amino acid side chains of proteins significantly upregulated in response to nitrogen limitation (with respect to their level of regulation in the ancestor) at a certain generation was compared to the nitrogen content of amino acid side chains of proteins that were significantly downregulated in response to nitrogen limitation (with respect to their level of regulation in the ancestor) at the given generation (for detailed information on the analysis on protein regulation see chapter 3.8). The number of proteins that were estimated to be up- or downregulated is depicted for each generation (see chapter 3.5.2). For each protein, the total amount of nitrogen atoms in their amino acid side chains was normalized by protein length. Next, this average number of nitrogen atoms per amino acid side chain was assigned to the given protein. Finally, the distribution of the average number of nitrogen atoms per amino acid side chain within the two protein sets (upregulated in response to nitrogen limitation and downregulated in response to nitrogen limitation) was depicted.

All in all, the mean nitrogen content (measured as average number of nitrogen atoms per amino acid side chain) of proteins significantly upregulated in response to nitrogen limitation was constantly lower than that of proteins significantly downregulated in response to nitrogen limitation. Differences were less pronounced in the generations 14 to 200 (4 %, 5.56 % and 1,7 %) than in the generations 500 to 1600 (10.78 %, 6.01 % and 7.07 %). In the later generations (500 to 1600), the differences in nitrogen content were statistically significant (figure 4.24). Further, proteins upregulated in response to nitrogen limitation after 1600 generations had on average a 4.5 % lower demand on nitrogen than those proteins that were upregulated at generation 14. For proteins that were estimated to be downregulated in response to nitrogen limitation, only a 1.6 % lowered nitrogen allocation was found at generation 1600 (compared to generation 14).

At each generation, the median number of nitrogen atoms per amino acid side chain was lower in proteins upregulated in response to nitrogen limitation compared to those proteins that were downregulated in response to this condition. Thereby, the median nitrogen content of proteins upregulated in response to nitrogen limitation was 0.35 at the generations 14 and 200 but lower (0.33 to 0.34, respectively) at the remaining generations (figure 4.24). In proteins downregulated in response to nitrogen limitation, the median nitrogen content was equal at the generations 14, 1000 and 1600 (0.37) and varied in the residual generations between 0.35 (generation 100 and 200) and 0.39 (generation 500) (figure 4.24). Moreover, the lower quantile and the lower whisker of boxplots displaying the distribution of the number of nitrogen atoms per amino acid side chain in proteins upregulated in response to nitrogen limitation were constantly

lower than those of the boxplots that showed the number of nitrogen atoms per amino acid side chain in proteins downregulated in response to nitrogen limitation. Hereby, the lower quantiles of the boxplots showing data of proteins upregulated in response to nitrogen limitation had values of 0.19 (generation 14 to 1000), 0.24 (generation 1600) and 0.3 (generation 200 to 1000) (figure 4.24). The lower quantiles of the corresponding boxplots had values between 0.31 (generation 14 and 1600), 0.29 (generation 100) and 0.3 (generation 200 to 1000) (figure 4.24). The lower whiskers of boxplots depicting data of proteins downregulated in response to nitrogen limitation varied between values of 0.2 and 0.31. The lower quantiles of these boxplots varied between 0.31 and 0.37 (figure 4.24). The upper whiskers of boxplots displaying the distribution of the number of nitrogen atoms per amino acid side chain in proteins upregulated in response to nitrogen limitation dropped from about 0.5 (generations 14 to 200) to 0.43 (generations 500 and 1600) and 0.47 (generation 1000), respectively (figure 4.24). Similarly, the upper quantiles of these boxplots dropped from a value of 0.4 at generation 14 to 0.39 (generation 100 to 1000) and further to 0.38 at generation 1600 (figure 4.24). Upper whiskers of boxplots showing the nitrogen content of proteins downregulated in response to nitrogen limitation were comparable in height (0.49 to 0.5) at the generations 200 to 1000 but lower at the generations 14 (0.45) and 1600 (0.46) (figure 4.24). The upper quantiles of these boxplots remained rather stable over time (0.39 to 0.4), except for generation 1600, where the value dropped to 0.39 (figure 4.24).

The analysis on protein nitrogen demand (measured as average number of nitrogen atoms per amino acid side chain) suggests that nitrogen conservation was indeed, as proposed, primarily found in proteins essential and thereby significantly upregulated in response to nitrogen limitation. Furthermore, parsimonious nitrogen allocation was even more pronounced in the later generations, most likely caused by the long-term selection pressure exerted by the persistent nitrogen limitation.

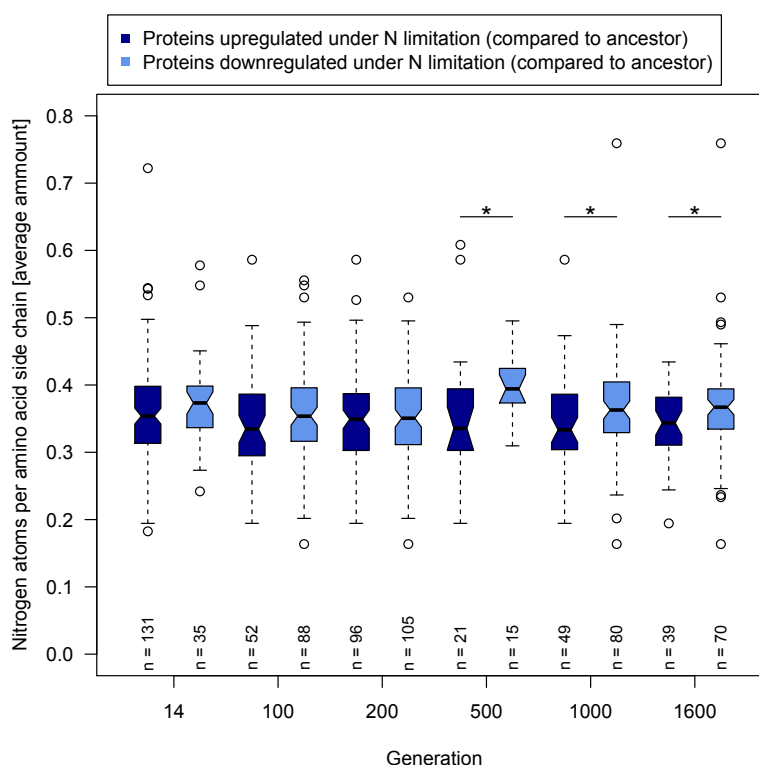


**Figure 4.24: Protein nitrogen content in response to nitrogen limitation**

Distribution of the number of nitrogen atoms per amino acid side chain of proteins significantly upregulated in response to nitrogen (N) limitation (with respect to their level of regulation in the ancestor,  $\log_2 > 2$ ) and of proteins significantly downregulated in response to nitrogen limitation (with respect to their level of regulation in the ancestor,  $\log_2 < 2$ ) at the generations 14, 100, 200, 500, 1000 and 1600. Levels of protein regulation were estimated by the program DESeq (nbinom-test, \*  $p < 0.05$ ). Statistical differences were computed for the comparison of protein nitrogen content of proteins upregulated in response to nitrogen limitation and proteins downregulated in response to nitrogen limitation by the Wilcoxon's test (one-tailed), \*  $p < 0.05$

### Protein nitrogen content in nitrogen rich control cultures

In figure 4.25, the nitrogen content of amino acid side chains of proteins significantly upregulated in nitrogen rich control cultures (with respect to their level of regulation in the ancestor) at a certain generation was compared to the nitrogen content of amino acid side chains of proteins that were significantly downregulated in nitrogen rich control cultures (with respect to their level of regulation in the ancestor) at the given generation (for detailed information on the analysis on protein regulation see chapter 3.8). The number of proteins that were estimated to be up- or downregulated is depicted for each generation (see chapter 3.5.2). The calculation of the average number of nitrogen atoms per amino acid side chain of each protein was done as described above for proteins of the nitrogen limited cultures.

In summary, the distribution of the nitrogen content (measured as average number of nitrogen atoms per amino acid side chain) above or below the median of a particular protein set (significantly upregulated or significantly downregulated) did not show obvious patterns of higher or lower nitrogen allocation towards the corresponding second protein set at any given generation (figure 4.25). However, the mean nitrogen content



was constantly higher in proteins upregulated in nitrogen rich control cultures. Differences were highest at generation 23 (10.11 %) and decreased and increased alternating afterwards (generation 100: 4.67 %, generation 200: 5.52 %, generation 500: 3.36 %, generation 1000: 6.91 % and generation 1600: 4.44 %). For the generations 23, 1000 and 1600, differences were found to be statistically significant (figure 4.25).

At each generation, the median number of nitrogen atoms per amino acid side chain was higher in proteins upregulated in nitrogen rich control cultures compared to those proteins that were downregulated in these cultures (figure 4.25). Thereby, the median number of nitrogen atoms per amino acid side chain of upregulated proteins was very similar at the beginning and at the end of the continuous culture experiment (generation 23: 0.38, generation 1600: 0.37). Between the generations 23 and 1600, the median increased and decreased alternating (figure 4.25). Similarly, the median number of nitrogen atoms per amino acid side chain of downregulated proteins was equal at the generations 23 and 1600 (0.35) and varied between values of 0.37 and 0.33 in the remaining generations (figure 4.25). Except for the median, no obvious difference in the distribution of the number of nitrogen atoms per amino acid side chain between the two different protein sets could be detected. The upper whiskers and quantiles of boxplots displaying the distribution of the number of nitrogen atoms per amino acid side chain in upregulated proteins increased and decreased alternating, values were between 0.46 and 0.63 and between 0.40 and 0.46, respectively (figure 4.25). The lower whiskers and quantiles of the corresponding boxplots showed a similar pattern, values varied between 0.15 and 0.30 and between 0.32 and 0.37, respectively (figure 4.25). For boxplots that display the number of nitrogen atoms per amino acid side chain of downregulated proteins, values of the upper whiskers were equal at generation 23, 500 and 1600 (0.51) and slightly higher (0.52) in the remaining generations. The upper quantiles were set at a value of 0.40 continuously, except for generation 100 (value: 0.43) (figure 4.25). The values of the lower quantiles and whiskers of the corresponding boxplots decreased and increased alternating over the generations, values were between 0.30 and 0.32 and between 0.11 and 0.21, respectively (figure 4.25).

As expected, no signals of nitrogen conservation were found in proteins significantly upregulated in the nitrogen rich control cultures. Actually, those proteins rather showed a higher average nitrogen demand (measured as number of nitrogen atoms per amino acid side chain) than proteins that were significantly downregulated. Due to the sufficient supply with nitrogen, upregulated proteins were most likely not targeted by selection since a reduced protein nitrogen budget would have entailed no growth advantage to the nitrogen rich control cultures.

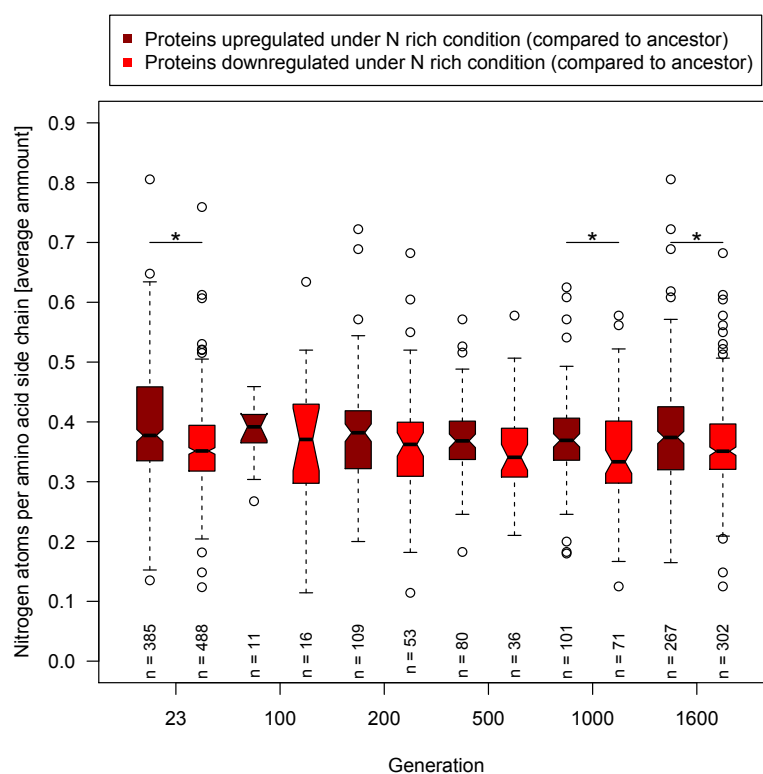


**Figure 4.25: Protein nitrogen content in nitrogen rich control cultures**

Distribution of the number of nitrogen atoms per amino acid side chain of proteins significantly upregulated in nitrogen (N) rich control cultures (with respect to their level of regulation in the ancestor,  $\log_2 > 2$ ) and of proteins significantly downregulated in nitrogen rich control cultures (with respect to their level of regulation in the ancestor,  $\log_2 < 2$ ) at the generations 23, 100, 200, 500, 1000 and 1600. Levels of protein regulation were estimated by the program DESeq (nbinom-test, \*  $p < 0.05$ ). Statistical differences were computed for the comparison of protein nitrogen content of proteins upregulated in nitrogen rich control cultures and proteins downregulated in nitrogen rich control cultures by the Wilcoxon's test (one-tailed), \*  $p < 0.05$

### Comparison of the protein nitrogen content in upregulated proteins of continuous cultures

Table 4.2 shows the mean nitrogen content (measured as average number of nitrogen atoms per amino acid side chain) of proteins significantly upregulated in response to nitrogen limitation (with respect to their level of regulation in the ancestor) at a certain generation and of proteins significantly upregulated in nitrogen rich control cultures (with respect to their level of regulation in the ancestor) at the given generation. Proteins whose data are depicted are the same that were analyzed in the figures 4.24 and 4.25.

The average number of nitrogen atoms per amino acid side chain of proteins significantly upregulated in response to nitrogen limitation was constantly lower than that of proteins significantly upregulated in nitrogen rich control cultures (table 4.2). The differences were highest at the generations 100 and 1600 (10.52 %) and lowest at generation 500 (2.7%) (table 4.2). In the remaining generations, the differences in the protein nitrogen content (measured as average number of nitrogen atoms per amino

acid side chain) of the two continuous cultures were rather similar (generation 14/23: 7.69 %, generation 200: 7.89 % and generation 1000: 8.11 %) (table 4.2). The described differences were found to be statistically significant (except for generation 500) at each generation.

The direct comparison of the mean protein nitrogen content confirmed that nitrogen conservation in upregulated proteins was restricted to the continuous cultures that had evolved under nitrogen limited conditions. This finding highly suggests that the protein nitrogen budget was shaped by selection owing to nitrogen limitation and not by dynamics of adaptational processes caused by the continuous culture experiment itself.

**Table 4.2: Nitrogen content of upregulated proteins in continuous cultures**

Mean nitrogen (N) content (measured as average number of nitrogen atoms per amino acid side chain) and its standard deviation (sd) of proteins significantly upregulated in response to nitrogen limitation (N limited) (with respect to their level of regulation in the ancestor,  $\log_2 > 2$ ) and of proteins significantly upregulated in nitrogen rich control cultures (N rich) (with respect to their level of regulation in the ancestor,  $\log_2 > 2$ ) at the generations 14/23, 100, 200, 500, 1000 and 1600. Levels of protein regulation were estimated by the program DESeq (nbinom-test, \*  $p < 0.05$ ). Differences in nitrogen content between the two protein sets are indicated in percent and statistical significance was computed for each generation by the Welch's test, the Student's-t test or the Wilcoxon's test (one-tailed), \*  $p < 0.05$

Generation	N content of N limited [mean $\pm$ sd]	N content of N rich [mean $\pm$ sd]	Difference [%]	Statistical significance one-tailed test, * $p < 0.05$
14/23	0.36 $\pm$ 0.08	0.39 $\pm$ 0.10	7.69	*
100	0.34 $\pm$ 0.07	0.38 $\pm$ 0.05	10.52	*
200	0.35 $\pm$ 0.07	0.38 $\pm$ 0.09	7.89	*
500	0.36 $\pm$ 0.1	0.37 $\pm$ 0.07	2.70	
1000	0.34 $\pm$ 0.07	0.37 $\pm$ 0.08	8.11	*
1600	0.34 $\pm$ 0.06	0.38 $\pm$ 0.09	10.52	*

### 4.2.3 Did adaptation to prolonged nitrogen limitation lead to growth advantages?

Persistent nitrogen limitation led to an improved nitrogen scavenging and caused a reduction of the cellular and protein nitrogen demand. It was assumed that these patterns of adaptation entailed growth advantages for the cultures evolved in nitrogen limited medium when grown under nutrient conditions identical to those to which they were exposed for 1600 generations. Growth of shaking cultures prepared from the two evolved continuous lines (nitrogen limited and nitrogen rich control) was directly compared to one another and also to growth patterns of their ancestor when cultivated in nitrogen limited minimal medium. In a second experiment, the two evolved continuous lines were directly competed against each other or against their ancestor in nitrogen limited medium. To distinguish cells of the different bacterial lines (evolved nitrogen limited- and nitrogen rich control line and ancestor) in the competing cultures, a kanamycin resistance was introduced into the genome of the ancestor and into the genome of bacteria obtained from the evolved nitrogen limited line. The same comparative and competitive growth experiments were performed in the full minimal medium, thus testing whether possible growth advantages in nitrogen limited medium came along with growth disadvantages in an environment in which ammonium was supplied in excess. In this context it was observed by Cooper and Lenski [2000] that the fitness gain which *E. coli* populations, that were serially propagated in glucose-supplemented minimal medium [Lenski *et al.*, 1991; Lenski and Travisano, 1994], had gained on glucose came along with a cost, namely reduced catabolic functions against a variety of other carbon sources, as D-ribose and fructose-6-phosphate.

#### 4.2.3.1 Fitness during comparative growth of evolved continuous cultures

Cultures of bacterial cells obtained from the generation 1600 of the two continuous lines (nitrogen limited and nitrogen rich control) as well as from the ancestor were cultivated separately in either the nitrogen limited minimal medium (figure 4.26 A) or in the full minimal medium (figure 4.26 B). Figure 4.26 shows the growth of the prepared cultures in a 96-well-plate of a microplate reader at 37 °C over 24 hours. All cultures were inoculated to an initial optical density (OD) of 0.005-0.008 (figure 4.26). Five biological replicates per bacterial line (evolved nitrogen limited, evolved nitrogen rich control or ancestor) were used, with technical duplicates per biological replicate. Mean OD values  $\pm$  standard deviation of the biological replicates were plotted to show the standard growth curves of the ancestor, the evolved nitrogen limited line and the evolved nitrogen rich control line.

In summary, all of the three bacterial lines tested showed similar patterns of growth

---

during incubation in nitrogen limited medium in the first two hours. The optical densities were comparable to each other in this time frame. Further, the slopes of the growth curves of the evolved nitrogen limited line and the evolved nitrogen rich control line were nearly equal between 1.5 and 4 hours of incubation. However, the evolved nitrogen limited line reached a markedly higher optical density than the two other bacterial lines (figure 4.26). In full minimal medium, the ancestor started to grow exponentially earlier than the evolved nitrogen limited and the evolved nitrogen rich control line but the slopes of all three growth curves in this growth phase were equal. Further, the ancestor entered stationary growth phase around one hour earlier than the two evolved continuous lines and its final stable optical density in this growth phase was lower compared to the maximal optical densities of the two evolved continuous lines. The highest optical density was reached by the evolved nitrogen limited line during stationary growth phase (figure 4.26).

In nitrogen limited medium, cultures of the evolved nitrogen limited line grew exponentially to a maximal OD of  $0.033 \pm 0007$  which was reached after 4 hours (figure 4.26 A). This maximal OD was found to be significantly higher than those of the evolved nitrogen rich control line and of the ancestor (figure 4.26 A). The given OD was stable for one hour and then dropped down continuously to  $0.024 \pm 0004$  at 8.5 hours. This final OD was maintained relatively constant in the remaining 15.5 hours (figure 4.26 A). The given optical density of the evolved nitrogen limited line remained significantly higher towards the ancestor until 19 hours of incubation and towards the evolved nitrogen rich control line until 12.5 hours of incubation (figure 4.26 A).

Cultures of the evolved nitrogen rich control line grew to a mean OD of  $0.008 \pm 0003$  (0.5 hours) in nitrogen limited medium and more or less kept this OD for another hour (figure 4.26 A). Then, growth continued exponentially until a maximal OD of  $0.020 \pm 0.002$  was reached at 3.5 hours (figure 4.26 A). Here, the evolved nitrogen rich control line entered stationary growth phase which was half an hour earlier compared to the evolved nitrogen limited line. Comparable to the evolved nitrogen limited line, the initial OD of the stationary growth phase decreased after one hour. However, this decrease to a mean OD of  $0.014 \pm 0.003$  at 6.5 hours was followed by another increase to an OD of  $0.017 \pm 0.002$  at 8.5 hours. For the remaining 15.5 hours, the OD remained rather stable at about 0.017 (figure 4.26 A).

The ancestor first grew to a mean OD of  $0.012 \pm 0.001$  within the first 2 hours of cultivation in nitrogen limited medium. In the next 10.5 hours, the growth curve appeared as jagged line, whereby decrease and increase of the OD alternated continuously. A stable stationary growth phase OD (about 0.015) was reached after 13 hours and maintained continuous for the rest of the observation (figure 4.26 A).

In full minimal medium, the evolved nitrogen rich control line grew to an OD of  $0.017 \pm 0.005$  in the first 30 minutes and then ceased growth for the next 1.5 hours (figure 4.26 B). After 2 hours, the evolved nitrogen rich control line started to grow exponentially to a maximal OD of  $0.355 \pm 0.019$  at 8 hours. Here, the evolved nitrogen rich control line entered stationary growth phase and the OD was maintained for the remaining 16 hours (figure 4.26 B).

The evolved nitrogen limited line did not grow in full minimal medium for 1.5 hours (figure 4.26 B). Then, it grew exponentially, whereby the slope of the growth curve equaled the slope of the nitrogen rich control's growth curve (figure 4.26 B). The exponential growth phase ended at 8.5 hours of incubation and the stationary growth phase was entered with an OD of  $0.399 \pm 0.04$  at this time point (figure 4.26 B). From 8.5 hours until 11.5 hours, the OD of the evolved nitrogen limited line remained constant (figure 4.26 B) and was significantly higher (figure 4.26 B) compared to the OD of the nitrogen rich control in this time range. Beginning at 12 hours, the mean OD of the evolved nitrogen limited line slightly decreased to about 0.38 and remained constant for the residual time course (figure 4.26 B).

The ancestor immediately started to grow exponentially in the full minimal medium. The slope of the growth curve during this growth phase was equal to the slopes of the growth curves of the evolved continuous lines (figure 4.26 B). After 7.5 hours, the ancestor reached its maximal OD ( $0.490 \pm 0.003$ ). For the next hour, this OD remained constant, then it dropped continuously until the final OD of  $0.289 \pm 0.0003$  was reached at 11.5 hours (figure 4.26 B). This OD did not change in the residual incubation period and was significantly lower than the ODs of the evolved nitrogen rich control line and the evolved nitrogen limited line in this time frame (figure 4.26 B) .

The fact that the evolved nitrogen limited line reached a significantly higher optical density than the other two bacterial lines (evolved nitrogen rich and ancestor) during the stationary growth phase in both media (nitrogen limited and nitrogen rich) suggests that the reduced cellular nitrogen budget of the bacteria that had evolved in the nitrogen limited medium for 1600 generations allowed the distribution of the nitrogen supplied in the comparative growth experiment to more single bacterial cells. Moreover, the long-term adaptation to the nitrogen limited medium did not seem to entail a cost to the evolved nitrogen limited line when grown without competition in the nitrogen rich medium.

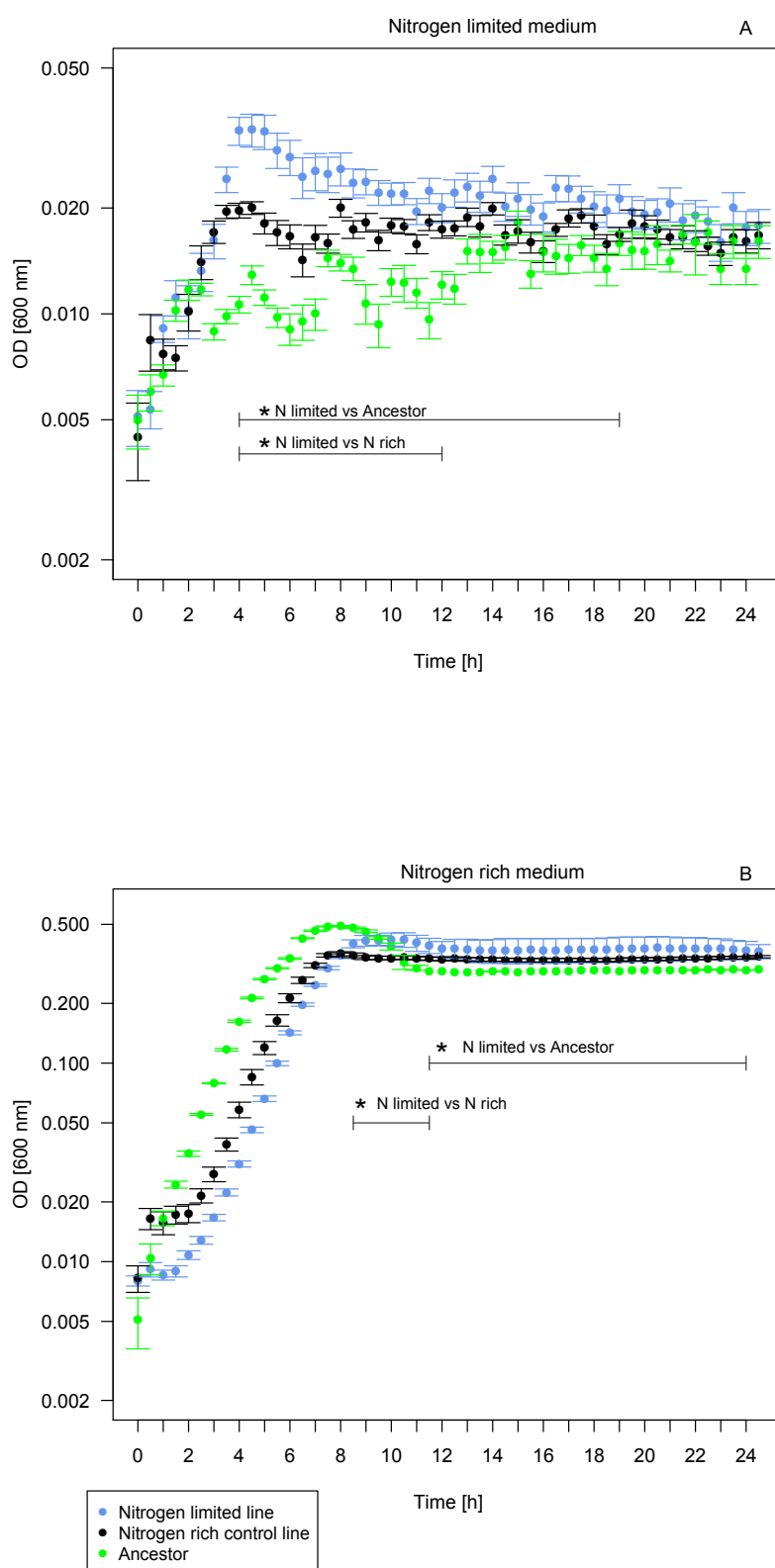


**Figure 4.26: Comparative growth of the evolved continuous lines and their ancestor**

Growth curves of cultures from the evolved nitrogen limited line, the evolved nitrogen rich control line and from the ancestor in nitrogen limited medium (A) and in full minimal medium (B) at 37 °C. Cell growth (optical density (OD) at 600 nm) over 24 hours is shown, ODs represent the mean values  $\pm$  the standard deviation of five biological replicates (with technical duplicates per biological replicate). Statistical differences in optical density between the evolved nitrogen limited line (N limited) and the ancestor and between the evolved nitrogen limited line and the evolved nitrogen rich line (Nrich) were calculated by the Wilcoxon's test (one-tailed), \*  $p < 0.05$

### 4.2.3.2 Fitness during competitive growth of evolved continuous cultures

#### Insertion of a kanamycin resistance

For the introduction of a kanamycin resistance gene into the genome of the ancestor and the evolved nitrogen limited line, the kanamycin resistance gene (*kanR*) was amplified by PCR from the plasmid pACYC177 (see chapter 3.2.2.2) and subsequently separated by gel electrophoresis (figure 4.27 1). The amplified fragments, obtained from in total six equal PCR reactions, had a length of 1240 bp and were extracted from the agarose gel and next concentrated by DNA precipitation (figure 4.27 2). In a third step, the purified *kanR* gene, as well as the cloning vector pUC18 (2.686 kb), were digested with the enzymes KpNI and PstI. Restriction sites for KpNI and PstI were located in the multiple cloning site (MCS) of pUC18 (figure 4.27 3). The digestion mixtures were separated on an agarose gel, digested *kanR* was 1232 bp long and digested pUC18 had a size of 2.659 kb (figure 4.27 3). The corresponding bands were extracted from the agarose gel and DNA from various digestion mixtures was unified and concentrated via DNA precipitation (figure 4.27 4). Next, the digested *kanR* gene was ligated into the multiple cloning site of pUC18, resulting in the vector pUC-kanR with a length of 3.891 kb (figure 4.27 5). In a further step, pUC-kanR was linearized by a single cut of the restriction enzyme NdeI and the *kanR* gene again was amplified by PCR from the vector (see chapter 3.2.2.3). Additional to the amplification, an overhang was added to *kanR* whose sequence was homologue to the chromosomal region downstream of the arabinose operon of *E. coli*. Resulting DNA fragments of various PCR approaches were again unified and concentrated by DNA precipitation (figure 4.27 6). Finally, the 1515 bp long *kanR* gene was separated by gel electrophoresis, extracted from the agarose gel (figure 4.27 7) and then transformed into electrocompetent bacteria of the 1600th generation of the nitrogen limited line as well as into electrocompetent bacteria of the ancestor (figure 4.27 8, N limited kanR and Ancestor kanR). Beforehand, transformation of the plasmid pkD46 into the corresponding bacterial cells had been performed (figure 4.27 7) which helped to insert *kanR* into the bacterial chromosomes (downstream of the arabinose operon) by its  $\lambda$  Red recombinase system. Colonies that were able to grow on LB-kan-agar after this procedure had successfully integrated *kanR* into their genome (figure 4.27 8).

When grown together, kanamycin resistant bacteria were distinguished from not genetically modified ones by diluting and spreading a sample of the common culture on kanamycin containing LB-agar (LB-kan-agar). Here, only kanamycin resistant bacteria were able to grow and form colonies. Additionally, part of the same diluted sample was spread on original LB-agar on which kanamycin resistant as well as not resistant bacteria were able to grow. Cell density of the two competing bacterial lines in the common



culture was determined by the number of colony forming units on the two solid media. Hereby, the number of colony forming units on LB-kan-agar directly revealed the proportion of kanamycin resistant bacteria in the common culture. The proportion of unmodified bacteria in the common culture was determined by subtracting the number of colony forming units on LB-kan-agar from the number of colony forming units on LB-agar.

In a preliminary competition experiment no differences in growth and biomass between the evolved N limited kanR and the unmodified evolved nitrogen limited line were detected, neither when competed in nitrogen limited nor when competed in full minimal medium (see chapter 6), thus revealing that the engineered kanamycin resistance behaved selectively neutral.

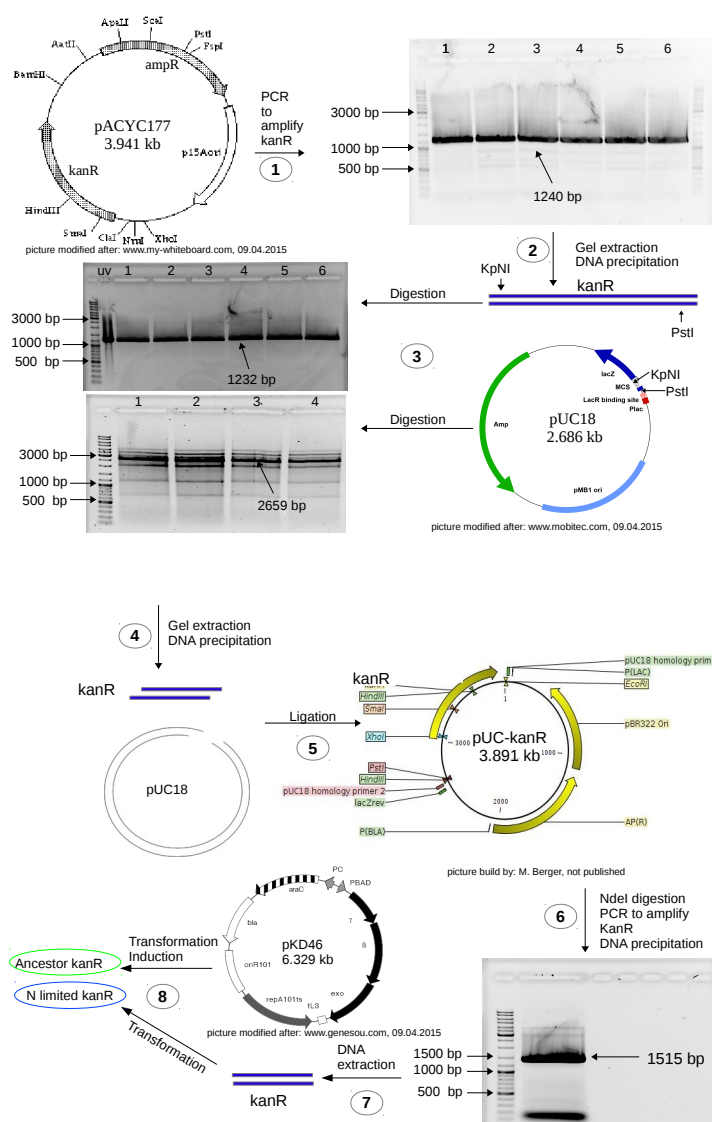


**Figure 4.27: Insertion of a kanamycin resistance into the ancestor and the evolved nitrogen limited line**

Cloning strategy for the insertion of a kanamycin resistance into the chromosome of the ancestor and of bacteria of the 1600th generation of the nitrogen limited continuous line. Overhangs were attached to *kanR* for its insertion downstream of the arabinose operon

### Competition in nitrogen limited medium

Competition experiments in nitrogen limited minimal medium were performed between the evolved nitrogen limited line and the ancestor (figure 4.28 A), between the evolved nitrogen rich control line and the ancestor (figure 4.28 B) and between the evolved nitrogen limited- and nitrogen rich control line (figure 4.28 C). Triplicates of the competing bacterial lines were grown as shaking cultures in a shaking incubator (37 °C, 180 rpm) for 24 hours. The ratio of the two bacterial lines was initially set to 1:1 and the growth medium was inoculated to a culture density of about  $2 \times 10^6$  CFU/ml. Growth was observed by determining the number of colony forming units. Figure 4.28 shows the growth of the competing cultures as mean number of colony forming units per milliliter  $\pm$  the standard deviation over time. To differentiate between bacteria of the different lines, one of the two bacterial lines that were competed against each other carried a kanamycin resistance (for detailed information on the insertion of the antibiotic resistance see figure 4.27).

In total, the evolved nitrogen limited line showed a faster increase of biomass than the evolved nitrogen rich control line and than the ancestor within the first six hours of competition in nitrogen limited medium. After 24 hours of competition, the evolved nitrogen limited line still had a higher maximal cell density than the ancestor. Contrary, during competition of the two evolved continuous lines, no difference in the maximal cell density after 24 hours was observed. No difference in growth at all was observed when the evolved nitrogen rich line and the ancestor were competed against each other in nitrogen limited medium.

After the initial inoculation (0 hours) of nitrogen limited medium with the evolved nitrogen limited line and the ancestor (ancestor:  $2.09 \times 10^6 \pm 6.54 \times 10^4$  CFU/ml, nitrogen limited:  $2.00 \times 10^6 \pm 4.50 \times 10^4$  CFU/ml), bacteria of the ancestor barely increased their cell density ( $3.02 \times 10^6 \pm 7.42 \times 10^4$  CFU/ml at 4 hours and  $2.90 \times 10^6 \pm 6.57 \times 10^5$  CFU/ml at 6 hours) (figure 4.28 A). At 4 hours, the evolved nitrogen limited line was about two times more present ( $6.71 \times 10^6 \pm 7.45 \times 10^4$  CFU/ml) than the ancestor. The amount of CFU/ml of the evolved nitrogen limited line decreased to  $5.20 \times 10^6 \pm 8.12 \times 10^5$  at 6 hours. Nevertheless, a significantly higher density of the evolved nitrogen limited line in the common culture could be verified for both time points (figure 4.28 A). After 24 hours, the evolved nitrogen limited line was still significantly more present in the competing culture ( $6.08 \times 10^7 \pm 3.30 \times 10^6$  CFU/ml) but the cell density of the ancestor had increased as well, namely to  $3.93 \times 10^7 \pm 5.28 \times 10^6$  CFU/ml (figure 4.28 A).

When grown as a common culture in nitrogen limited medium, the cell densities of

the evolved nitrogen rich control line and the ancestor were similar to each other at all sampling time points (figure 4.28 B). Initially (0 hours), both formed about  $2.1 \times 10^6$  CFU/ml (figure 4.28 B). After 4 hours, the evolved nitrogen rich control line had increased its cell density to  $3.17 \times 10^6 \pm 7.50 \times 10^4$  CFU/ml and from the ancestor  $3.46 \times 10^6 \pm 9.82 \times 10^4$  CFU/ml were detected (figure 4.28 B). At 6 hours, the number of CFU/ml of bacteria of the ancestor ( $3.43 \times 10^6 \pm 6.49 \times 10^5$  CFU/ml) was almost equal to the number obtained after 4 hours, whereas the evolved nitrogen rich control line showed a decreased number of  $1.96 \times 10^6 \pm 1.09 \times 10^6$  CFU/ml compared to the sampling time point 4 hours (figure 4.28 B). Further, the number of bacteria of both bacterial lines increased to  $4.13 \times 10^7 \pm 5.84 \times 10^6$  CFU/ml (ancestor) and to  $5.13 \times 10^7 \pm 5.64 \times 10^6$  CFU/ml (nitrogen rich control) at 24 hours (figure 4.28 B).

When competing the two evolved continuous lines with each other, bacteria of both lines were evenly distributed in the common shaking culture directly after inoculation of the nitrogen limited medium (nitrogen rich control:  $1.90 \times 10^6 \pm 7.65 \times 10^4$  CFU/ml, nitrogen limited:  $1.80 \times 10^6 \pm 8.84 \times 10^4$  CFU/ml) (figure 4.28 C). After 4 hours, the evolved nitrogen limited line had increased their cell density to  $7.18 \times 10^6 \pm 7.42 \times 10^4$  CFU/ml, while the evolved nitrogen rich control line only grew to  $2.76 \times 10^6 \pm 6.32 \times 10^4$  CFU/ml (figure 4.28 C). For both competing evolved lines, a drop in the number of CFU/ml was detected after 6 hours (compared to 4 hours), however, the evolved nitrogen limited line was about 3.5 times more present in the competing cultures ( $5.20 \times 10^6 \pm 7.52 \times 10^5$  CFU/ml) than the nitrogen rich control one ( $1.52 \times 10^6 \pm 5.90 \times 10^5$  CFU/ml) (figure 4.28 C). At 4 and 6 hours, differences in the number of CFU/ml between the two continuous lines were found to be significant (figure 4.28 C). After 24 hours, the density of the shaking culture had increased again and the number of CFU/ml of bacteria of both evolved lines was almost equal to each other (nitrogen rich control:  $5.10 \times 10^7 \pm 5.21 \times 10^6$ , nitrogen limited:  $6.12 \times 10^7 \pm 6.25 \times 10^6$ ) (figure 4.28 C).

The present data suggest that the documented improvement of nitrogen scavenging and reduction of the cellular nitrogen budget entailed growth advantages to the evolved nitrogen limited line when cultivated under nitrogen limitation in competition with bacteria that did not evolve in a nitrogen limited environment. Since the competition experiment between the evolved nitrogen limited line and the ancestor did not show any differences in their growth, the observed growth advantage of the evolved nitrogen limited line can be related to their long-term adaptation to a nitrogen limited environment and was not caused by the previous long-term continuous cultivation in a minimal medium itself.

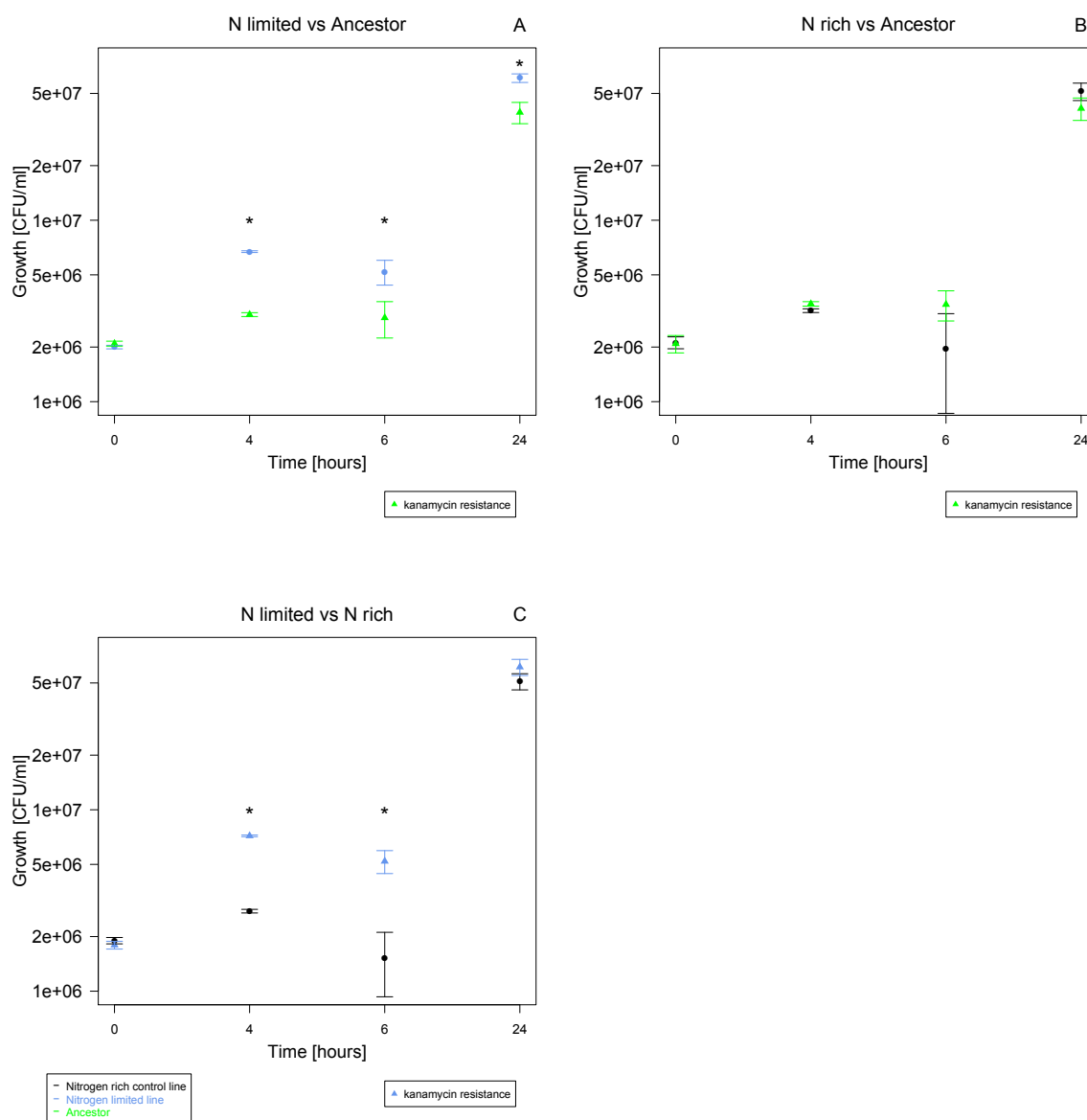


**Figure 4.28: Competitive growth of the evolved continuous lines and their ancestor in nitrogen limited medium**

Growth curves of competing shaking cultures in nitrogen limited minimal medium. Competitive growth of the evolved nitrogen limited line (N limited) and the ancestor in A, of the evolved nitrogen rich control line (N rich) and the ancestor in B and of the evolved nitrogen limited line and the evolved nitrogen rich control line in C is shown by the number of colony forming units at 0, 4, 6 and 24 hours. Data are depicted as the mean value  $\pm$  the standard deviation obtained from biological triplicates. Statistical differences in the number of CFU/ml between the bacterial lines were calculated by the Student's t-test test (one-tailed), \*  $p < 0.05$

### Competition in full minimal medium

Competition experiments in full minimal medium were performed between the evolved nitrogen limited line and the ancestor (figure 4.29 A), between the evolved nitrogen rich control line and the ancestor (figure 4.29 B) and between the two evolved continuous lines (figure 4.29 C). Cultures were prepared and competed as described for the competition experiments in nitrogen limited medium.

In summary, no difference in growth was observed when the two evolved continuous lines were competed against each other in full minimal medium. Similarly, the nitrogen rich control and the ancestor showed nearly identical cell densities and growth patterns when grown in competition with each other. When the evolved nitrogen limited line was competed against the ancestor, the ancestor showed a higher number of CFU/ml directly after inoculation and at 4 hours. However, after 6 and 24 hours both cultures were almost equally present in the common culture.

When the evolved nitrogen limited line was competed against the ancestor in full minimal medium, bacteria of the ancestor had a higher initial density ( $2.47 \times 10^6 \pm 5.30 \times 10^5$  CFU/ml) than the nitrogen limited ones ( $7.75 \times 10^5 \pm 2.22 \times 10^5$  CFU/ml) (figure 4.29 A). Further, their increase in cell density was more intense in the first hours compared to the increase in cell density of bacteria of the evolved nitrogen limited line. At 4 hours, the ancestor showed a significantly higher cell density ( $1.37 \times 10^8 \pm 5.28 \times 10^7$  CFU/ml) than the evolved nitrogen limited line ( $4.69 \times 10^7 \pm 2.44 \times 10^7$  CFU/ml) (figure 4.29 A). However, at 6 hours, both bacterial lines had reached their maximal cell density which was similar to each other (ancestor:  $4.84 \times 10^8 \pm 1.13 \times 10^8$  CFU/ml, nitrogen limited:  $6.32 \times 10^8 \pm 9.22 \times 10^7$  CFU/ml) (figure 4.29 A). After 24 hours of incubation, measured cell densities were similar to those obtained at 6 hours, the ancestor formed  $4.12 \times 10^8 \pm 1.22 \times 10^8$  CFU/ml and the evolved nitrogen limited line formed  $4.68 \times 10^8 \pm 9.22 \times 10^7$  CFU/ml (figure 4.29 A).

When competed in full MM, cell densities of the evolved nitrogen rich control line and the ancestor were highly similar to each other at any sampling time point. The initial number of CFU/ml was about  $1.7 \times 10^6$  for both competing bacterial lines (figure 4.29 B). After 4 hours, the evolved nitrogen rich control line had increased to  $2.87 \times 10^7 \pm 1.42 \times 10^7$  CFU/ml and the ancestor had reached  $4.83 \times 10^7 \pm 1.09 \times 10^6$  CFU/ml (figure 4.29 B). A further rise in cell density was detected after 6 hours of incubation, here, the evolved nitrogen rich control line formed  $6.72 \times 10^8 \pm 8.53 \times 10^7$  CFU/ml while the ancestor formed  $5.19 \times 10^8 \pm 8.85 \times 10^7$  CFU/ml (figure 4.29 B). After 24 hours, the number of CFU/ml of both competing lines was with about  $4.3 \times 10^8$  CFU/ml almost equal to each other (figure 4.29 B).

During competition of the two evolved continuous lines in full minimal medium, the initial (0 hours) cell density was  $7.43 \times 10^5 \pm 3.45 \times 10^5$  CFU/ml for the evolved nitrogen rich control line and  $2.01 \times 10^6 \pm 2.08 \times 10^5$  CFU/ml for the evolved nitrogen limited line (figure 4.29 C). At the remaining time points, the amount of CFU/ml of both evolved continuous lines was similar to each other. First, an increase in cell density to  $3.49 \times 10^7 \pm 1.13 \times 10^7$  CFU/ml (nitrogen rich control) and to  $4.60 \times 10^7 \pm 2.00 \times 10^7$  CFU/ml (nitrogen limited) was detected after 4 hours (figure 4.29 C). This was followed by a further increase of both evolved continuous lines to  $6.41 \times 10^8 \pm 9.06 \times 10^7$  CFU/ml (nitrogen rich control) and to  $5.33 \times 10^8 \pm 3.58 \times 10^7$  CFU/ml (nitrogen limited) at 6 hours (figure 4.29 C). At 24 hours, cell numbers of both evolved continuous lines were similar to those obtained after 6 hours, namely  $4.68 \times 10^8 \pm 4.46 \times 10^7$  CFU/ml (nitrogen rich control) and  $3.63 \times 10^6 \pm 5.67 \times 10^7$  CFU/ml (nitrogen limited) (figure 4.29 C).

While the bacteria that had evolved in nitrogen limited medium were found to have growth advantages during competition with the ancestor and the evolved nitrogen rich control line in nitrogen limited medium, no difference in growth could be observed between the two evolved continuous lines in full minimal. When competed against the ancestor, the evolved nitrogen limited line showed a significantly lower amount of colony forming units within the first 4 hours of competition. This observation might hint on a cost which the bacteria that had evolved under nitrogen limited conditions had to pay during the adaptation to an environment in which nitrogen is available in excess.

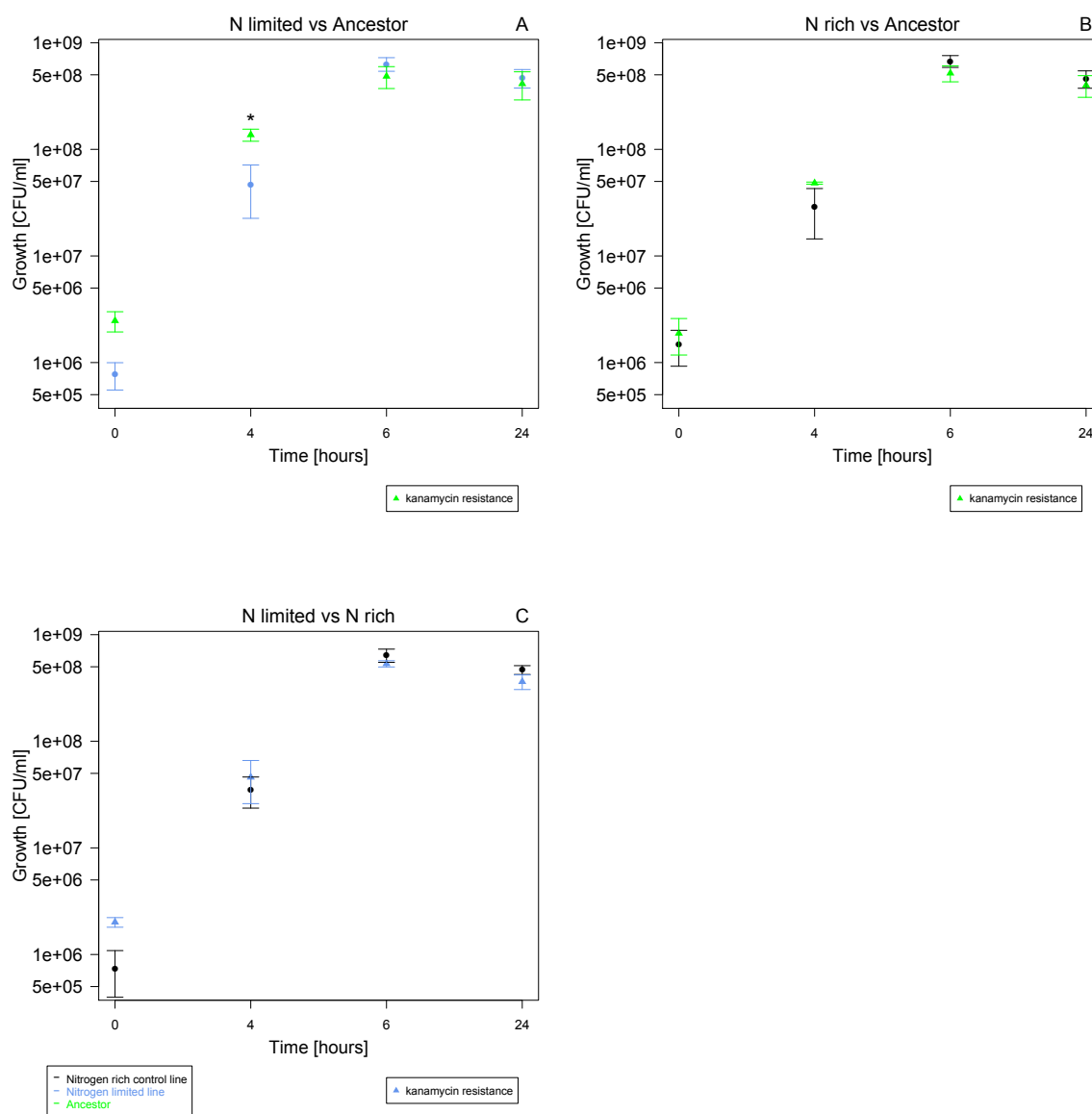


**Figure 4.29: Competitive growth of the evolved continuous lines and their ancestor in full minimal medium**

Growth curves of competing shaking cultures in full minimal medium. Competitive growth of the evolved nitrogen limited line (N limited) and the ancestor in A, of the evolved nitrogen rich control line (N rich) and the ancestor in B and of the evolved nitrogen limited line and the evolved nitrogen rich control line in C is shown by the number of colony forming units at 0, 4, 6 and 24 hours. Data are depicted as the mean value  $\pm$  the standard deviation obtained from biological triplicates. Statistical differences in the number of CFU/ml between the bacterial lines were calculated by the Student's t-test test (one-tailed), \*  $p < 0.05$

## 5 Discussion

### 5.1 Transient nutrient starvation of filter cultures

In the short-term starvation experiment, cultures of *E. coli* Nissle 1917  $\Delta fliC$  were starved for either nitrogen or carbon. This experiment enabled a change of the nutrient environment, from a growth medium with all necessities to a growth medium of the same composition except that either ammonium (nitrogen source) or glucose (carbon source) was missing, within a few seconds. The filter culture experiment further allowed a quick harvest and quench of metabolism of the bacterial cultures (see chapter 3.6.1). This was essential in order to obtain valid snapshots of the metabolic composition which can change within seconds [Visser *et al.*, 2002]. In summary, both types of nutrient starvation triggered a common cellular starvation-survival response, including a reduction of bulk-protein synthesis, elevated expression level of genes involved in the acquisition and metabolism of the nutrient concerned as well as dynamics of nutrient specific key metabolites (figure 5.1). Next to this primary response, the nutrient starved cultures utilized internal reservoirs of nitrogen and carbon. Here, carbon starved cultures were found to primarily degrade lipids, fatty acids and carbohydrates (in comparison to nitrogen starved cultures) while nitrogen starved cultures were found to mobilize nitrogen rich amino acids and pyrimidines (in comparison to carbon starved cultures) (figure 5.1). On the molecular level we could show that the nitrogen content of proteins upregulated in response to nitrogen starvation (in comparison to carbon starvation) was reduced in the later stage of nitrogen starvation. This was due to a lowered incorporation of the nitrogen rich amino acids arginine, asparagine, glutamine and lysine while the nitrogen rich amino acids were found to be equally abundant in proteins upregulated in response to nitrogen starvation and in proteins upregulated in response to carbon starvation (figure 5.1).



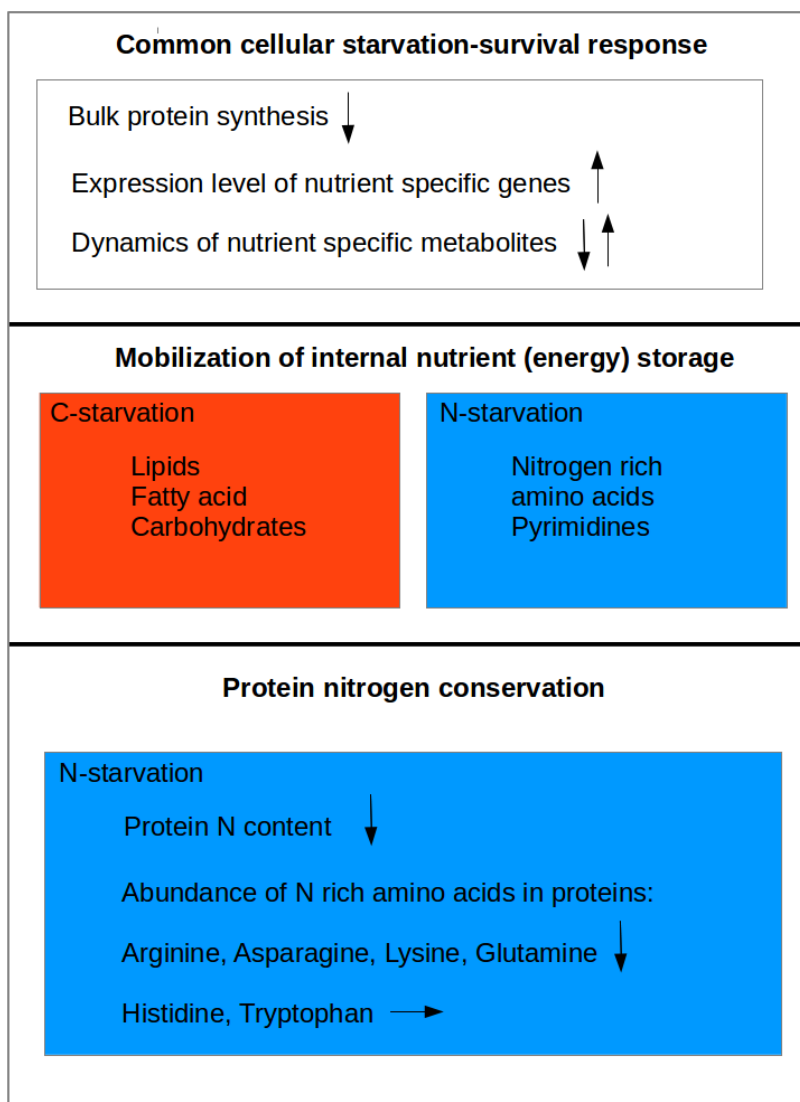


**Figure 5.1: Impact of nutrient starvation on *E. coli***  
N = nitrogen, C= carbon

### 5.1.1 Basic cellular starvation-survival response

#### 5.1.1.1 Decrease of protein synthesis

An important part of the starvation-survival response is the decrease of bulk protein synthesis [Hengge-Aronis, 2000; Reeve *et al.*, 1984b]. In this study the level of protein synthesis was measured by the expression level of ribosomal genes during carbon or nitrogen starvation. For nitrogen and carbon starved cultures, a decrease of ribosomal gene expression levels (in comparison to the unstarved control) was already observed 10 minutes after the onset of nutrient starvation and became more pronounced over the time course (4 hours) in both types of nutrient starvation. Even though there was no constant measurement of gene expression over the four hours of the experiment, it was assumed that ribosomal genes had a continuously lower expression level over this time course, depicted by the data obtained at the five sampling time points. The decreased expression level of ribosomal genes in the nutrient deficient cultures hinted on a decrease of protein synthesis as a part of the stress response towards nutrient starvation. The reduction of protein synthesis under nutrient starvation was observed in different bacteria and is associated to the lowered expression level of genes related to exponential growth [Nyström *et al.*, 1990; Reeve *et al.*, 1984a]. This obviously goes along with an arrest of growth which was shown to be true for the cultures of *E. coli* Nissle 1917  $\Delta$ *fliC* immediately after they were transferred to the nutrient deficient media. The arrest of growth or at least its reduction is a common response in bacteria towards basically all types of stress conditions and is a crucial step in the process of adaptation of the cellular physiology to the unfavorable condition [Jozefczuk *et al.*, 2010].

#### 5.1.1.2 Metabolic cascades

Microorganisms possess several mechanisms to sense the availability of nutrients and translate the monitored signals into nutrient specific intracellular responses [López-Maury *et al.*, 2008; Postma *et al.*, 1993]. Many of the molecules involved in the nutrient signaling pathways have been identified and the ability to recapitulate published data about the dynamics of these nutrient specific compounds allowed to validate the filter culture starvation experiment performed in this study.

As described for enteric bacteria, external nitrogen limitation goes along with a decrease of the cellular glutamine level [Brauer *et al.*, 2006; Ikeda *et al.*, 1996; Schmitz, 2000]. Present data of the nitrogen starved cultures confirmed these previous findings. Glutamine levels of filter cultures deprived of ammonium were lower compared to the unstarved control at 240 minutes after the onset of nitrogen starvation. Ammonium, the preferred nitrogen source of *E. coli*, is assimilated directly into glutamine

and glutamate via two different assimilation pathways [van Heeswijk *et al.*, 2013]. The GS/GOGAT pathway has a high affinity towards ammonium and is thereby primarily used for ammonium assimilation when the availability of external nitrogen is low [Reitzer, 2003]. The elevated synthesis of proteins belonging to the GS/GOGAT pathway is triggered by the nitrogen regulatory (Ntr) system. The nitrogen sensors of the Ntr system of enteric bacteria seem to respond to changes of cellular glutamine levels rather than to the external nitrogen status [Schmitz, 2000; van Heeswijk *et al.*, 2013]. Thus, glutamine is not only a marker for the external nitrogen quantity but also directly involved in the intracellular response towards nitrogen availability.

2-oxoglutarate is integral to ammonium assimilation since it provides the carboxylic acid skeleton to glutamine and glutamate. This metabolite was found to increase in response to nitrogen starvation [Brauer *et al.*, 2006; Ninfa and Jiang, 2005]. In accordance with these literature findings, nitrogen starved cultures of the present study showed an increased level of 2-oxoglutarate compared to the unstarved control during the four hours of starvation. The peak of the 2-oxoglutarate level of nitrogen starved cultures was detected ten minutes upon nitrogen removal. When external nitrogen is depleted, as in the filter cultures starved for ammonium, the assimilation of ammonium and thereby the synthesis of glutamine and glutamate ceases. Thus, premade 2-oxoglutarate is not longer utilized and most likely accumulates in the cells. Further, 2-oxoglutarate might be released during the degradation of the amino acids that were mobilized as internal nitrogen reserve in nitrogen starved filter cultures (see chapter 5.1.2.2).

Both, the decrease of glutamine as well as the increase of 2-oxoglutarate were clearly nitrogen specific responses. In carbon starved cultures the opposite trend of nutrient levels was detected, 2-oxoglutarate abundance was lower and glutamine abundance was higher compared to the unstarved control. The elevated glutamine level in carbon starved cultures might have been caused by the release of amino acids during the starvation induced degradation of ribosomes and proteins [Davis *et al.*, 1986; Reeve *et al.*, 1984a; Zundel *et al.*, 2009]. Since glutamine was not found to be utilized by carbon starved filter cultures (see chapter 5.1.2.1), it most likely accumulated in the free amino acid pool. On the contrary, 2-oxoglutarate might have been one of the carbon containing compounds that were utilized by carbon starved cultures (see chapter 5.1.2.1). Thus, its cellular abundance decreased upon carbon starvation.

As expected, glucose levels dropped immediately after glucose removal from the carbon starved cultures. At two and four hours after the onset of starvation, the ratio of glucose abundance between carbon starved cultures and the unstarved control was close to zero, showing that carbon starved cultures had almost completely converted

available glucose. In contrast, glucose levels in nitrogen starved cultures were higher than in the unstarved control. These cultures ceased growth upon nitrogen removal and most likely lowered glucose import due to a reduced need in the context of the growth arrest.

The abundance of PEP and cAMP increased markedly in carbon starved cultures with a peak ten minutes after glucose removal. Thereafter, PEP and cAMP levels fell off but remained higher than in the unstarved control. Brauer *et al.* [2006] as well observed a rise in PEP levels in glucose starved cultures of *E. coli*, using the filter culture experiment that was adapted for this study. In *E. coli*, PEP functions as the phosphate donor for the phosphotransferase system (PTS) that transports sugars as glucose through the cell membrane and in parallel phosphorylates them via a phosphorylation cascade [Deutscher *et al.*, 2006]. When glucose or other sugars transported via PTS are not available, the cellular abundance of PEP rises, probably due to its lacking consumption [Brauer *et al.*, 2006]. The increase of cAMP upon glucose removal is as well a known occurrence in glucose starved *E. coli* [Brauer *et al.*, 2006; Notley-mcrobbs *et al.*, 1997]. In the presence of glucose cellular cAMP levels remain low. When glucose is depleted, cAMP is synthesized by the enzyme adenylate cyclase [Matin *et al.*, 1989]. cAMP binds to and thereby activates the catabolite regulation protein (CRP) [Deutscher *et al.*, 2006]. The cAMP-CRP complex plays a central role in the carbon starvation response of *E. coli* and has been shown to control at least 195 target promoters on its genome [Shimada *et al.*, 2011]. Most of the corresponding genes that are under regulation of the cAMP-CRP complex are involved in the catabolism of alternate carbon sources [Kolb *et al.*, 1993].

The level of PEP was similar in nitrogen starved cultures and in the unstarved control, showing that the rise of PEP level is (in the framework of this study) a response particularly towards glucose starvation. Interestingly, the cAMP level was elevated in the nitrogen starved cultures at two and four hours after the onset of starvation although not as strong as in the carbon starved cultures. Literature findings on this matter revealed that cAMP-CRP is also involved in nitrogen assimilation and further might play a role in the regulation of nitrogen metabolism [van Heeswijk *et al.*, 2013]. The elevated level of cAMP in nitrogen starved cultures is thereby consistent with the described literature findings.

### 5.1.1.3 Improved nutrient scavenging

The described metabolic cascades in the framework of nutrient starvation trigger an adaption of gene expression levels. This leads to an improved scavenging of the desired nutrient and/or to the utilization of the concerned nutrient from a variety of different sources [Matin *et al.*, 1989].

*E. coli* possesses two pathways for ammonium assimilation and which of them is used strongly depends on nitrogen availability. The GS/GOGAT cycle is used for ammonium assimilation in nitrogen poor environments [Reitzer, 2003]. The involved enzyme glutamine synthetase is encoded by the gene *glnA* [Colombo and Villafranca, 1986] whose transcription is affected by the nitrogen state of the cell [Leigh and Dodsworth, 2007]. In the present study, nitrogen starved cultures showed a markedly higher expression level of the gene *glnA* (compared to the unstarved control), pointing out to the usage of the GS/GOGAT cycle for ammonium assimilation. Unstarved control cultures most likely assimilated ammonium via the alternative GDH pathway. This energy cheap route of ammonium assimilation is used when nitrogen is available in excess [Helling, 1994] as it was the case for the unstarved control.

Similar to *glnA*, the expression level of the gene *glnK* is elevated during the absence of ammonium [van Heeswijk *et al.*, 2013]. Under conditions of nitrogen deprivation GlnK, the product of *glnK*, regulates many facets of nitrogen metabolism. It has been shown to be involved in adenylation of GS [van Heeswijk *et al.*, 2013] and thereby enhancing its metabolic activity [Foor *et al.*, 1975]. Further, GlnK affects viability during periods of nitrogen depletion [Blauwkamp and Ninfa, 2002] and is involved in the regulation of ammonium transport activity via the AmtB ammonia transporter [Javelle *et al.*, 2004]. In the present study, *glnK* was found to have the highest log<sub>2</sub> ratio of gene expression (nitrogen starved cultures versus unstarved control) among all genes tested in the context of a nitrogen starvation related response. This observation is consistent with the pivotal role of *glnK* under conditions of nitrogen starvation.

The two genes *glnL* and *glnG* also were found to have higher expression levels in nitrogen starved cultures than in the unstarved control. The products of these genes, NtrC and NtrB, compose a two component system which is involved in the transcriptional control of about 100 genes belonging to the nitrogen regulatory (Ntr) response of *E. coli*. The Ntr response is pivotal for survival under nitrogen depleted conditions and the genes of the Ntr regulon are for example involved in the assimilation of ammonium and the scavenge of other nitrogen containing sources [Reitzer, 2003].

Finally, the genes *nac* and *amtB* had a higher expression level in nitrogen starved cultures compared to the unstarved control. The gene *nac* codes for the nitrogen assimilation control protein Nac that is under nitrogen deprived conditions involved in the regulation of genes belonging to the Ntr system [Muse and Bender, 1998]. The

ammonia channel protein AmtB is encoded by *amtB* and participates in the uptake of ammonium in *E. coli* [Soupene *et al.*, 1998]. The elevated expression level of *amtB* is consistent with the finding of Hua *et al.* [2004] who showed a markedly increase of *amtB* transcript levels in *E. coli* when grown under nitrogen limited conditions. Soupene *et al.* [1998] proposed that the function of AmtB rather lies in the increase of the diffusion rate of ammonia (NH<sub>3</sub>) across the cytoplasmatic membrane than in the active transport of ammonium or ammonia.

Cultures that were deprived for carbon did not show statistical differences in the expression of the described genes when compared to the unstarved control.

As a first finding, the expression level of the gene with the identifier ECABU\_c13150 (referred to as EIIBC) was decreased in carbon starved cultures at all sampling time points (compared to the unstarved control). This gene codes for the domains B and C of the glucose specific EII complex of the phosphotransferase system (PTS). EIIBC is the membrane associated protein of the PTS and transports sugars into the cytoplasm and in parallel transfers its phosphoryl group to them [Deutscher *et al.*, 2006]. It is likely that the attempts of carbon starved cultures to import glucose via the EIIBC membrane protein were stopped or at least decreased quite soon after the onset of starvation due to a quick establishment of pathways signaling that external glucose was exhausted. This might have been mirrored in the decreased expression level of the EIIBC encoding gene in carbon starved cultures. On the contrary, carbon starved cultures increased the expression level of the gene *crr* (compared to the unstarved control) at 120 and 240 minutes after the onset of starvation. The gene *crr* encodes the domain A of the glucose specific EII complex of the PTS. In enteric bacteria, the glucose specific EIIA protein is not only involved in the phosphorylation cascade of the PTS but also executes regulatory functions. Among other things, EIIA regulates the utilization of a variety of carbon sources when glucose is not available [Deutscher *et al.*, 2006]. The elevated expression level of *crr* in glucose starved culture suggests that the cultures adapted their metabolism for the usage of alternate carbohydrates. This is consistent with the finding that the expression level of the genes *mglB*, *malE* and *araF* increased during carbon starvation (when compared to the unstarved control). These genes encode periplasmatic binding proteins for the sugars galactose [Scholle *et al.*, 1987], maltose [Duplay *et al.*, 1984] and arabinose [Duplay *et al.*, 1984].

The polypeptide CstA which is encoded by the gene *cstA* was found to be involved in the transport of peptides [Schultz and Matin, 1991]. The *cst* genes are carbon starvation response genes that depend on the abundance of cAMP and assist the cell in escaping carbon starvation through nutrient scavenging [Matin, 1991; Schultz *et al.*, 1988]. Indeed, *cstA* was found to have a higher expression level in carbon starved cultures than in the unstarved control.

The last gene investigated in the basic cellular starvation-survival response is designated *csrA*, the carbon storage regulator [Romeo *et al.*, 1993]. The protein encoded by *csrA*, CsrA, is involved in the regulation of many aspects concerning carbohydrate metabolism [Sabnis *et al.*, 1995; Yang *et al.*, 1996]. In accordance with its global role in carbohydrate metabolism, the expression level of *csrA* was elevated in carbon starved cultures (with respect to the unstarved control) at each sampling time point.

Most of the genes investigated in the framework of a response towards carbon (glucose) starvation had a lower expression level in nitrogen starved cultures than in the unstarved control, statistically significant differences could not be shown for any of the genes.

### 5.1.2 Intracellular mobilization of deprived nutrients

#### 5.1.2.1 Mobilization of carbon and energy reserves during carbon starvation

Nutrient starvation does not only cause a basic cellular response in bacteria, thus enhancing the scavenging of the desired nutrient and developing a more stress resistant phenotype, but also triggers the breakdown of biomolecules and the utilization of the released nutrient reserves. Carbon starvation, as it was performed in the filter culture experiment by the complete removal of glucose, entailed a dual cost to the cultures since not only the supply with carbon atoms but also with energy was halted. Cellular lipids and polysaccharides have been found to act as energy and carbon storage in microorganisms. Free fatty acids and sugars derived by autophagy of these storage compounds are proposed to be specialized and therefore highly efficient carbon and energy sources [Singh and Cuervo, 2012; Wilkinson, 1963]. Thus, literature research on metabolic pathways involved in the breakdown of lipids and polysaccharides under carbon starvation was done and combined with an analysis of the expression level of genes involved in these pathways (see chapter 3.8).

Indeed, genes involved in the breakdown of lipids had markedly higher expression levels in carbon starved cultures (compared to the unstarved control). The major constituents of lipids are fatty acids, glycerol and choline [Gottschalk, 1979]. In the metabolome analysis performed on the filter cultures, eight fatty acids were detected. Four of the fatty acids were consistently less abundant in carbon starved cultures than in the unstarved control and two more were less abundant in carbon starved cultures right after the onset of starvation. Studies in yeast support that lipid degradation contributes to the energetic balance of the cell by the release of free fatty acids and sugars [Albers *et al.*, 2007; Singh and Cuervo, 2012]. Contrary to eukaryotes, bacteria do not accumulate lipids as storage compound [Gottschalk, 1979; Singh and Cuervo, 2012] but they contain high amounts of lipids in their membranes. Phospholipids, a

major constituent of bacterial membranes, make up about ten percent of the cellular dry weight [Gottschalk, 1979; Heath *et al.*, 2002]. Further, fatty acids, lipids and lipid-derived components are present freely within *E. coli* cells [DiRusso and Nyström, 1998], thereby being a target for degradation which is easy to access. Moreover, long chain fatty acids were identified to support growth of *E. coli* when provided as sole carbon source and also represent an essential source of energy in their natural habitats, the intestine of vertebrates [Clark and Cronan, 2005]. The potential of long chain fatty acids to serve as carbon and energy source is most likely due to the fact that their degradation yields acetyl-CoA [DiRusso and Nyström, 1998] which is further metabolized by the tricarboxylic acid (TCA) cycle [Gottschalk, 1979]. Hence, the enhanced expression level of genes involved in lipid degradation goes along with the dynamics of several fatty acids identified in the metabolome of carbon starved filter cultures, confirming lipids and fatty acids, respectively as integral reserves of carbon and energy for *E. coli*.

Further emphasis was put on genes involved in the degradation of carbohydrates, as for example different sugars (e.g. galactose and sucrose), polysaccharides (e.g. glycogen, starch), sugar acids, sugar alcohols and sugar derivatives. The pattern of expression of these genes revealed that at each time point about half of them had a higher expression level in carbon starved cultures than in the unstarved control, suggesting that at least some of the described compounds acted as carbon and energy storage and were utilized during carbon starvation. Especially polyglucoses are described as efficient carbon and energy reserves in literature. During growth under glucose sufficient conditions, *E. coli* stores some of the glucose which it takes up as glycogen [Gottschalk, 1979]. Glycogen can be broken down rapidly during carbon starvation [Wilkinson, 1963] and has been considered for several decades as primary endogenous energy reserve of *E. coli* [Ribbons and Dawes, 1963]. Regarding these findings it is most likely that glycogen belonged to the carbohydrates that were degraded in carbon starved filter cultures.

For nitrogen starved cultures neither lipid nor carbohydrate degradation could be shown, clearly proofing a nutrient specific cellular response.

Even though lipids and polysaccharides were shown to represent primary internal carbon and energy sources for the carbon starved cultures, the utilization of cellular amino acids as additional carbon/energy reserves was possible since *E. coli* is able to utilize some external amino acids as sole carbon or energy source [McFall and Newman, 1996; Yang *et al.*, 2015]. Hence, amino acids released by autophagy of proteins and ribosomes due to the carbon stress response [Davis *et al.*, 1986; Reeve *et al.*, 1984a; Zundel *et al.*, 2009] might had been not only incorporated in newly synthesized proteins but also served as secondary carbon and/or energy sources in carbon starved cultures. To test this hypothesis, amino acid abundance in carbon starved cultures was analyzed



with respect to their abundance in the unstarved control and to their abundance in nitrogen starved cultures, without putting emphasis on particular amino acids as it was done during the analysis on nitrogen storage compounds in cultures starved for nitrogen (see chapter 5.1.2.2). During nitrogen starvation, we considered nitrogen rich amino acids as nitrogen reserves since their degradation releases the ammonium from their side chains. On the contrary, the classification of an amino acid as a potential carbon or energy source is not straight forward since all carbon skeletons obtained by the degradation of amino acids are oxidized by the TCA cycle, thus yielding usable energy and carbohydrates [Berg *et al.*, 2002; Gottschalk, 1979]. Considering that each of the twenty amino acids is a potential source of carbon and/or energy that can be utilized during carbon starvation, the abundance of all amino acids in carbon starved cultures was analyzed. Due to the estimated release of amino acids in the free cellular pool of both nutrient starved cultures (by the starvation-induced breakdown of proteins and ribosomes), we expected a temporarily and similar accumulation of the free amino acid pool in carbon- and nitrogen starved cultures. Thus, the analysis on amino acid utilization in carbon starved cultures focused on the comparison of amino acid abundance in response to the two types of nutrient starvation. If we had only compared the amino acid abundance in the free pool of carbon starved cultures to the unstarved control, we might have overlooked signals of amino acid utilization due to the starvation induced biased amino acid pool of carbon starved cultures. In summary, only three amino acids, namely serine, proline and glycine were significantly less abundant in carbon starved cultures than in nitrogen starved cultures at both analyzed time points. The carbon skeletons of serine and glycine are required for the synthesis of several cellular metabolites [Reitzer, 2003], suggesting a recycling of those amino acids in carbon starved cultures to redistribute the obtained carbon atoms. Moreover, serine and proline were found to serve as sole carbon and energy source for *E. coli* when supplemented to the growth medium [Chen and Maloy, 1991; Franklin and Venables, 1976; McFall and Newman, 1996]. Regarding these literature findings it is likely that the carbon starved cultures degraded their internal reservoirs of these amino acids since they represent additional sources of carbon and energy. The role of glycine as carbon or energy source is not discussed satisfyingly in literature. Nevertheless, glycine was utilized by cultures of *E. coli* MG1655 that were grown in a defined minimal medium without any other carbon or nitrogen sources than an equal molar mixture of all twenty amino acids [Yang *et al.*, 2015]. This leads to the possibility that glycine can only be utilized by *E. coli* in the presence of other amino acids as it was the case in the free amino acid pool of carbon starved cultures. All remaining amino acids were either found to be consistently more abundant in carbon starved cultures than in nitrogen starved ones or showed different patterns of abundance, some accumulating, others de-

creasing (in comparison to nitrogen starved cultures) over time. This strongly implies that these amino acids were not or only temporarily utilized under carbon starvation.

Taken together, internal lipids and carbohydrates seemed to be preferably utilized by carbon starved cultures of the present study, confirming their suggested role as primary and efficient carbon and energy storage. Amino acids rather seemed to be utilized ancillary which might be explained by the persistent breakdown of the primary carbon and energy storage molecules (lipids and carbohydrates) during the four hours of carbon starvation.

#### **5.1.2.2 Mobilization of nitrogen reserves during nitrogen starvation**

The present data showed that carbon starved cultures primarily utilized free lipids and carbohydrates as energy and carbon source. Nitrogen starved cultures were rather proposed to mobilize free cellular amino acids as nitrogen reserves. Especially the six nitrogen rich amino acids arginine, asparagine, glutamine, histidine, lysine and tryptophan were considered as potential nitrogen storage since their degradation releases the additional ammonium molecules of their side chains [Keseler *et al.*, 2013]. Hence, the abundance of the nitrogen rich amino acids in the free amino acid pool of nitrogen starved cultures was analyzed. Consistent with the analysis of amino acid utilization during carbon starvation, special focus was on the abundance of amino acids in the free amino acid pool of nitrogen starved cultures in comparison to carbon starved cultures (due to the estimated biased free amino acid pool of nutrient starved cultures, see chapter 5.1.2.1).

Indeed, each of the six nitrogen rich amino acids was at least at two out of the three sampling time points about half as abundant in nitrogen starved cultures than in carbon starved cultures. For most of these differences a statistically significant difference could be shown. The amino acid glutamine plays a particular role in nitrogen metabolism since it provides ammonium in the synthesis of different cellular metabolites, such as nucleotides and several amino acids [Reitzer, 2003]. Hence, it is highly likely that free cellular glutamine is primarily targeted under nitrogen starvation to redistribute its ammonium molecules. Arginine and asparagine belong to the organic compounds which can be utilized by *E. coli* as sole exogenous nitrogen source [Reitzer, 2003]. Thus, the biomolecules involved in transport and metabolism of these two amino acids might be induced as a part of the nitrogen starvation response, allowing a quick utilization of them as internal nitrogen source. Further, 11 % of a cell's nitrogen is present in arginine and still 6% in lysine [Reitzer, 2003] which makes both amino acids a quantitative nitrogen reserve. Histidine can not be used as sole exogenous nitrogen source by *E. coli* [Schaechter, 2009] but its transport is regulated by the global nitrogen regulatory (ntr) system which is involved in scavenging of nitrogen-containing

compounds [Reitzer, 2003]. It is therefore possible that histidine can be utilized as nitrogen source in the presence of other amino acids as it was the case in the free amino acids pool of nitrogen starved cultures. When glucose is present in the medium, the enzyme tryptophanase is repressed and thereby tryptophan can not be degraded by *E. coli* [Keseler *et al.*, 2013]. Nevertheless, tryptophan was less abundant in nitrogen starved cultures than in carbon starved cultures at 120 and 240 minutes after onset of starvation. Even though tryptophan might not had been degraded completely, the ammonium group of its side chain could had been removed and redistributed during nitrogen starvation. The described literature findings for arginine, asparagine, glutamine, histidine and lysine strongly suggest that these amino acids play a major role in nitrogen metabolism and are consistent with the present data, showing the decrease of their cellular abundance in nitrogen starved filter cultures. Hence, it is most likely that the nitrogen rich amino acids were utilized by nitrogen starved filter cultures to regain and redistribute the nitrogen atoms of their amino acid side chains.

In addition to the mobilization of nitrogen rich amino acids, we observed that six proteins that were significantly upregulated in response to nitrogen starvation (in comparison to carbon starved cultures) were encoded by the genes *rutA-F* of the ‘Rut Pathway’. During nitrogen limitation the Rut pathway enables *E. coli* to degrade pyrimidines, thus releasing their nitrogen atoms [Loh *et al.*, 2006]. The Rut pathway was also found to be required for the usage of pyrimidines as sole external nitrogen source but only at room temperature [Loh *et al.*, 2006]. The seventh protein of the Rut Pathway is the uracil transporter needed for the uptake of pyrimidines from the environment [Parales and Ingraham, 2010]. In the present study, this protein was not found to be differently regulated in response to the two types of nutrient starvation. The discussed findings suggest that nitrogen starved filter cultures did not only utilize nitrogen rich amino acids but also free cellular pyrimidines as nitrogen reserve.

### **5.1.3 Nitrogen conservation in proteins is linked to a biased free amino acid pool**

Since the nitrogen starved filter cultures were completely deprived of their exogenous nitrogen source, only intracellular nitrogen sources (such as nitrogen rich amino acids) were utilizable for the distribution of nitrogen atoms into biomolecules synthesized in response to nitrogen starvation. However, internal nitrogen sources clearly do not have the potential to assure a long lasting nitrogen supply. In order to decrease the needed nitrogen budget during nitrogen starvation, biomolecules involved in the nitrogen starvation response were expected to be biased towards a lowered nitrogen allocation. Previous studies support that natural selection owing to recurring nitrogen deprivation over evolutionary relevant time scales had shaped the architecture of biomolecules to-

wards a lowered demand on nitrogen atoms [Acquisti *et al.*, 2009a; Elser *et al.*, 2006, 2011]. Hereby, special attention has to be given to patterns of nitrogen conservation in proteins since these biomolecules contribute a high fraction to cellular biomass (up to 50 % in prokaryotes) [Giese, 1979] so that their biochemical composition has a major influence on the nitrogen budget of *E. coli*. Especially those proteins that are crucial in the response towards nitrogen starvation were suggested to be favorable targets of the cumulative effects of the selection pressure exerted by nitrogen starvation. Hence, the nitrogen content of proteins significantly upregulated in response to nitrogen starvation (in comparison to carbon starvation) was analyzed, targeting the amount of nitrogen atoms in the amino acid side chains. As a comparison, the amount of nitrogen atoms in the amino acid side chains of proteins significantly upregulated in response to carbon starvation (in comparison to nitrogen starvation) was analyzed. After 10 and 30 minutes of nutrient starvation, only minor and not statistically significant differences in the overall nitrogen content of proteins upregulated in response to nitrogen starvation and proteins upregulated in response to carbon starvation could be identified. At the later time points (60, 120 and 240 minutes), a strongly reduced demand on nitrogen could be confirmed for proteins upregulated in response to nitrogen starvation and the difference towards the nitrogen demand of proteins upregulated in response to carbon starvation was statistically significant. Most of the proteins that were found to be significantly upregulated in response to nitrogen starvation at these later sampling time points were involved in nitrogen metabolism and assimilation (see chapter 6). Baudouin-Cornu *et al.* [2001] observed similar patterns of element conservation in assimilatory proteins of *E. coli* and of *S. cerevisiae*. They compared the budget on carbon and sulfur atoms of proteins that are involved in the assimilation of these elements to the demand on these elements in the overall proteome. For both species their analyses revealed that carbon and sulphur are less often incorporated in proteins that are involved in the assimilation of the particular element when compared to the carbon and sulfur cost of the complete proteome. Moreover, proteins of *S. cerevisiae* which are involved in the assimilation of nitrogen were found to be low in nitrogen when compared to the nitrogen content of sulphur assimilatory proteins. All proteins of microorganisms that are involved in nutrient scavenging, including metabolic and assimilatory ones, are indeed crucial components of the response towards nutrient deprivation. Thus, it is highly likely that natural selection owing to nutrient deprivation had operated on the described proteins to lower their demand on the nutrient they are linked to. In periods of nutrient deprivation, the lowered allocation of the depleted element to its assimilatory and metabolic proteins results in an overall reduced cellular nutrient budget. This helps the organism to outlast the unfavorable condition. Eight other proteins that were significantly upregulated in response to nitrogen starvation and biased towards a

lowered nitrogen allocation were different transport and also resistance proteins (see chapter 6). This shows that nitrogen conservation is not restricted to proteins directly involved in nitrogen metabolism and -assimilation. The nitrogen content of proteins of the plant species *A. thaliana* and *Oryza sativa* was found to be negatively correlated with the expression level of the encoding genes [Elser *et al.*, 2006]. Li *et al.* [2009] as well showed that proteins upregulated in *E. coli*, *S. cerevisiae* and *S. pombe* entailed a lowered carbon and nitrogen content. A study by [Bragg and Wagner, 2009] revealed that mutations that cause even small increases in gene expression level, thus enhancing the material cost of the corresponding biomolecules, would be visible to natural selection during conditions of nitrogen- or carbon limitation in *S. cerevisiae*. Thus, natural selection was found to act on all highly abundant biomolecules against mutations that increase their element cost since a high demand on an element would hamper growth during its depletion.

The lowered demand on nitrogen (measured as nitrogen atoms per amino acid side chain) of proteins significantly upregulated in response to nitrogen starvation at 120 and 240 minutes after the onset of starvation was caused by a lowered incorporation of the amino acids arginine, asparagine, glutamine and lysine. These amino acids possess additional nitrogen atoms in their side chains. However, the lowered incorporation was only statistically significant for glutamine and further, the amino acids histidine and tryptophan which also possess additional nitrogen atoms were found to be equally abundant in proteins upregulated in response to nitrogen starvation and in proteins upregulated in response to carbon starvation. To clarify this matter it would be of paramount importance to analyze a higher number of proteins with respect to their nitrogen demand. This could be achieved by RNA sequencing of more biological replicates of nitrogen- and carbon starved filter cultures which would most likely provide a higher number of proteins significantly upregulated in the response to the two types of nutrient starvation. Nevertheless, the nitrogen based amino acid usage bias in proteins upregulated in response to nitrogen starvation could directly be linked to the fact that amino acids differ in their number of nitrogen atoms. A reduction of nitrogen rich amino acids in proteins through natural selection owing to prolonged or recurring nitrogen deficiency during the evolutionary history of a species has been described to reduce the overall protein nitrogen demand [Elser *et al.*, 2011]. A comparison of nitrogen distribution in plant and animal proteomes revealed that nitrogen allocation was on average 7.1 % lower in the analyzed plant species compared to the animal species [Elser *et al.*, 2006]. However, domesticated plants and plants that live in symbiosis with nitrogen-fixing bacteria did not show patterns of nitrogen conservation in their proteins [Acquisti *et al.*, 2009a]. Taken together, signatures of element based amino acid usage bias in proteins, aiming to conserve nitrogen, are restricted to organisms that directly

depend on the nutrient availability in their environments since they synthesize their biomolecules, such as amino acids, from scratch, using the elements they take up from their surrounding. For these organisms, a reduced demand on nitrogen rich amino acids is considered to be advantageous for growth and reproduction during periods of low nitrogen availability since it allows the allocation of nitrogen to other cellular components [Sterner and Elser, 2002]. Further, a study by [Bragg and Wagner, 2009] confirmed that mutations that cause single amino acid replacements which enhance the element demand of proteins would be visible to natural selection during conditions of nitrogen- or carbon limitation in *S. cerevisiae*. The fact that no signatures of nitrogen conservation were found in proteomes of animals [Elser *et al.*, 2006] can be explained by their lifestyle and their diet. Animals are to some extent able to vary their food source and feeding ground and moreover take up preformed, nitrogen containing biomolecules with their diet. Hence, animals less likely have been exposed to strong or prolonged nitrogen constraints during their evolutionary history. The same is true for plants that cooperate with nitrogen fixing bacteria and for domesticated plants that grow under nitrogen enriched conditions due to fertilization.

The different studies described before have in common that their outcome was based on computational analyses of published proteomic and genomic data but laboratory evidence for signatures of nitrogen conservation was missing. The short-term starvation experiment of this study was useful to explore whether selection exerted by nitrogen deprivation over millions of years of evolution indeed had shaped the architecture of proteins upregulated in response to nitrogen starvation. The present results highly suggest that selection owing to nitrogen deprivation had operated on the proteome of *E. coli*, leading to a biased usage of amino acids in proteins that are upregulated in response to nitrogen starvation. Further, nothing was known on the cellular processes that enable selection to shape protein amino acid composition for parsimonious nutrient allocation. In the present study, the lowered incorporation of nitrogen rich amino acids in proteins upregulated in response to nitrogen starvation could directly be linked to the lowered abundance of these amino acids in the free amino acid pool. This observation highly suggests that environmental availability of nitrogen has driven the efficiency of translation via biased abundance of free amino acids. When a particular amino acid needed for protein synthesis is not or hardly available in the cell, translation most likely decelerates which entails growth disadvantages to an organisms. The data of the present study suggest that nitrogen rich amino acids had a low abundance in the free amino acid pool of nitrogen starved cultures (compared to carbon starved cultures) due to their utilization as nitrogen source. Thus, purifying selection owing to nitrogen deprivation had most likely acted against mutations that caused a higher abundance of nitrogen rich amino acids in proteins during the evolutionary history of

*E. coli*. On the contrary, mutations leading to amino acid substitutions towards amino acids which are less nitrogen demanding most likely had undergone positive selection since they enabled the organism concerned to synthesize its proteins and thereby to grow and leave descendants faster. Hence, these kind of substitutions were likely to be fixed in *E. coli* populations. Even though this kind of selective pressure is expected to be low [Elser *et al.*, 2011], it entails cumulative effects during recurrent nitrogen limitation over evolutionary relevant time scales which were reflected in the lowered nitrogen demand of proteins that were analyzed in the present nitrogen starved cultures.

## 5.2 Persistent nitrogen limitation in continuous culture

In the long-term continuous culture experiment, cultures of *E. coli* Nissle 1917  $\Delta fliC$  were maintained in exponential growth phase for 1600 generations under nitrogen limitation or under nitrogen sufficient conditions. This experiment enabled us to observe evolution in action since the impact of nitrogen availability on the cellular nitrogen demand of *E. coli* could be monitored over long and potentially evolutionary relevant time scales. In summary, nitrogen limitation triggered a cellular response, including an elevated expression level of genes involved in the acquisition and metabolism of nitrogen, an enhancement of ammonium uptake and a change of the cellular morphology on congo red agar (figure 5.2). Next to these primary cellular responses, the overall cellular nitrogen demand and the nitrogen content of upregulated proteins were reduced in cultures that were grown under prolonged nitrogen limitation (figure 5.2). The lowered nitrogen content of proteins upregulated in response to nitrogen limitation was suggested to be caused by global changes of the expression level of the encoding genes. Lastly, it could be shown that the adaptation to prolonged nitrogen limitation entailed growth advantages during recurring nitrogen limitation. Further, the adaptation to prolonged nitrogen limitation seemed to entailed growth disadvantages during the early phase of competitive growth with the ancestor under nitrogen sufficient conditions (figure 5.2).



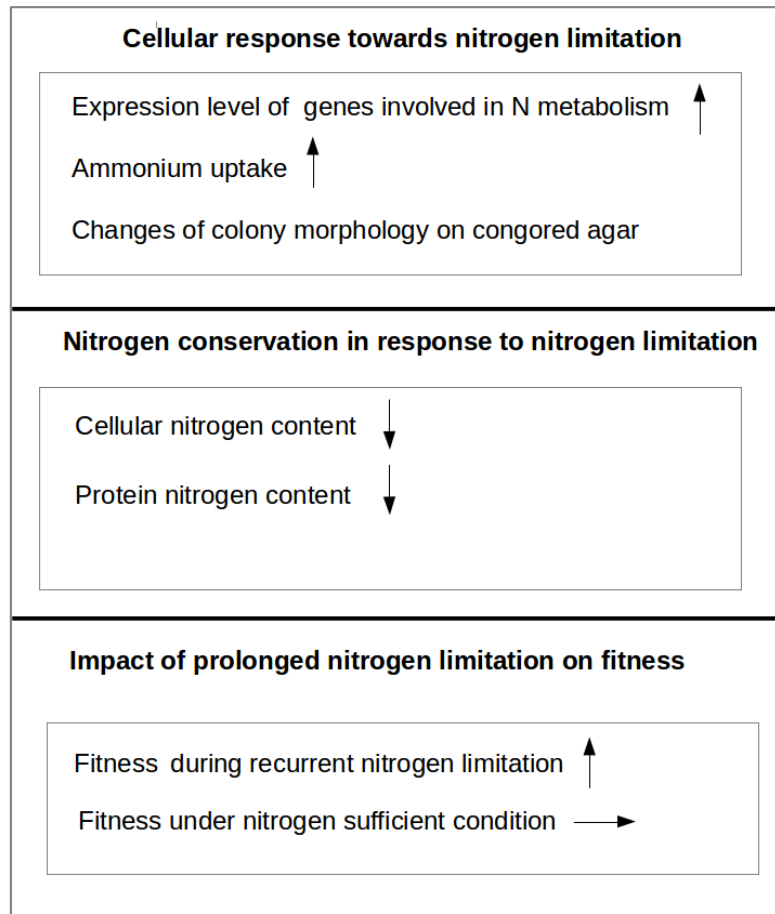


**Figure 5.2: Impact of nitrogen limitation on *E. coli***  
N = nitrogen, C= carbon

### 5.2.1 Basic cellular response to nitrogen limitation

#### 5.2.1.1 Improved nitrogen acquisition

Microorganisms possess several mechanisms to sense the availability of nutrients [López-Maury *et al.*, 2008; Postma *et al.*, 1993] and to trigger a nutrient specific response in case of nutrient limitation. The response towards nutrient limitation includes an adaptation of gene expression, leading to an improved scavenging of the desired nutrient [Matin *et al.*, 1989].

All of the in total six genes analyzed, which are involved in nitrogen metabolism and assimilation, were found to have a significantly higher expression level in nitrogen limited cultures than in nitrogen rich control cultures at each sampled generation. The elevated expression level of the gene *amtB* in nitrogen limited cultures hinted on an increased abundance of the encoded ammonia channel protein AmtB. AmtB participates in the uptake of ammonium in *E. coli* [Soupene *et al.*, 1998]. An enhanced expression level of *amtB* in *E. coli* grown under nitrogen limited conditions was also confirmed by Hua *et al.* [2004]. For ammonium assimilation nitrogen limited cultures used the GS/GOGAT cycle. This could be shown by the elevated expression level of the gene *glnA*. The gene *glnA* encodes the enzyme glutamine synthetase of the GS/GOGAT cycle [Colombo and Villafranca, 1986]. GS has a high affinity towards ammonium and thus the GS/GOGAT cycle is the preferred route of ammonium assimilation under nitrogen limited conditions [Reitzer, 2003]. The gene *glnK* is involved in the regulation of the metabolic activity of GS [Foor *et al.*, 1975] and in the regulation of the ammonium transport activity via AmtB [Javelle *et al.*, 2004]. The high expression level of the gene *glnK* in nitrogen limited cultures further confirmed that the cultures tried to enhance their ammonium uptake rate and used the GS/GOGAT cycle for ammonium assimilation. The genes *nac*, *glnL* and *glnG* are involved in the transcriptional control of the Ntr (nitrogen regulatory) system [Muse and Bender, 1998; Reitzer, 2003]. The Ntr system is a crucial part of the response towards nitrogen deprivation. Genes that belong to this system contribute for example to the scavenge of various nitrogen containing sources [Reitzer, 2003]. The finding that the genes *nac*, *glnL* and *glnG* had a higher expression level in nitrogen limited cultures verified that the supplied ammonium quantities indeed supported only suboptimal growth and thus triggered a nutrient stress response, aiming for example for the utilization of nitrogen sources next to ammonium.

#### 5.2.1.2 Enhancement of ammonium uptake

The analysis of gene expression patterns in nitrogen limited cultures revealed that the cultures enhanced the expression level of the gene *amtB* which encodes the ammonia channel protein AmtB. Moreover, the genes involved in the regulation of ammonium

transport (*glnK*, *glnG*, *glnL* and *nac*) were found to have a higher expression level in response to nitrogen limitation as well. Actually, the ammonium uptake rate of the nitrogen limited cultures increased by 14 % over time which indeed suggests that the abundance of the ammonia channel protein AmtB was enhanced due to the observed gene expression patterns. However, all genes analyzed had the highest expression levels directly after the start of the continuous cultures (generation 14) and at the generations 1000 and 1600. On the contrary, the ammonium uptake rate of nitrogen limited cultures was similar (about 36 %) from the beginning of the continuous culture experiment until generation 400. From generation 500 on, the ammonium uptake rate was about 14 % higher than before (on average 50 %). Thus, a higher number of AmtB could not be the only explanation of the improved ammonium scavenging observed in the later generations. One might speculate that mutations affecting the efficiency of the ammonia channel protein AmtB or the induction of secondary transport systems were involved in the improvement of ammonium scavenging. In this context, Notley-McRobb and Ferenci [1999] detected regulatory mutations at the *mgl* locus in glucose limited continuous cultures of *E. coli*. The transcription unit *mglBAC* encodes the galactose ABC transporter [Keseler *et al.*, 2013]. This transporter is known to be an additional transport system for glucose and was found to be active under conditions of glucose limitation [Ferenci, 1996]. Notley-McRobb and Ferenci [1999] showed that isolates that carried regulatory mutations in the short *mgl* operator sequence (*mglO*) exhibited improved rates of glucose transport.

Despite the enhanced ammonium uptake rate of the nitrogen limited cultures of the present study, still about half of the ammonium which was supplied with the growth medium remained unused. Senn *et al.* [1994] observed that residual glucose levels varied with the dilution rate in glucose limited continuous cultures of *E. coli*. The higher the dilution rate, the higher was the amount of residual glucose. In the present continuous culture experiment, the dilution rate was restricted by the sensitivity of the medium pump. The slowest possible flow rate of incoming fresh culture medium and effluent culture broth was used and thus setting the lowest possible dilution rate. A more sensitive medium pump would have allowed an even slower flow rate and thus a lower dilution rate. Hence, the time range for nutrient scavenging from the growth medium would have been prolonged, possibly resulting in an even higher ammonium uptake rate of nitrogen limited cultures.

In nitrogen rich control cultures, the ammonium uptake rate remained constant over 1600 generations (about 6 %). The growth medium of these cultures was supplemented with each nutrient in excess, so it was expected that high amounts of ammonium remained unused.

### 5.2.1.3 Morphological changes

The laboratory of Richard Lenski has serially propagated cultures of *E. coli* in a glucose-supplemented minimal medium for ten thousands of generations [Lenski *et al.*, 1991; Lenski and Travisano, 1994]. For the evolving cultures it was observed that larger individual cell sizes correlate with a higher fitness in the given environment [Lenski and Travisano, 1994; Philippe *et al.*, 2009]. Stanek *et al.* [2009] proposed that the larger cells have a reduced demand for cell wall components due to their lowered ratio of surface area to volume. A reduced synthesis of cell wall components as peptidoglycan and lipopolysaccharides decreases the energy and carbon demand of the cell and thus makes it more competitive in the given environment in which glucose is the nutrient depleted first. The individual cell size and -shape of bacteria grown under persistent nitrogen limitation in the present study were not documented. However, the continuous cultures were plated weekly on a congoled screening agar on which *E. coli* Nissle 1917 forms round colonies which appear red, dry and rough. This rdar morphotype is formed by the binding of cellulose and curli fimbriae, both components of the extracellular matrix of several enterobacteria, to the congoled dye [Gophna *et al.*, 2001; Zogaj *et al.*, 2001]. Further, the rdar morphotype is an important determinant of multicellular behavior, as cell aggregation, biofilm formation and adherence to liquid and solid abiotic surfaces [Römling *et al.*, 1998; Zogaj *et al.*, 2003]. After about 800 generations of continuous cultivation under nitrogen limitation, in total three additional morphotypes, deviating in colour, shape and/or surface from the rdar one, were detected on congoled screening agar. These morphotypes arose in each of the five independent nitrogen limited cultures and remained at a stable frequency until the end of the experiment. It is possible that the observed differences of the morphotype on congoled agar were associated to changes of components of the extracellular matrix of individual cells. Curli fimbriae are surface proteins [Olsen *et al.*, 1989] and their distribution might had been decreased in response to nitrogen limitation in order to reduce the overall nitrogen budget. Further, two of the new morphotypes formed a moisty and slimy layer on the colony surface. Bacterial slime layers were found to have different functions, like fimbriae they are involved in the adherence of cells to surfaces [Todar, 2016]. Thus, the part of the cells from a nitrogen limited culture that formed the slimy upper layer when grown on congoled agar might had enhanced its ability to attach to components of the continuous culture experiment, such as tubing or the culture vessels. A more sessile lifestyle might had been advantageous for the uptake of the supplied nutrients, especially the limiting ammonium. Actually, bacterial biofilm had to be removed from the tubing system of the continuous culture experiment but markedly more often in the nitrogen rich control cultures than in the nitrogen limited cultures. However, for nitrogen rich control cultures no changes in the rdar morphotype were detected over the 1600 generations.

Lastly, all of the three newly formed colony morphotypes were not completely roundish shaped as the rdar one but appeared with smaller or bigger indentations. For individual cells, the ratio of surface area to volume is an important factor for nutrient uptake and metabolism. A smaller individual cell size allows for example a larger ratio of surface area to volume and this correlates with a fast uptake and intracellular distribution of nutrients [Koch, 1996]. Further, the cell shape affects nutrient acquisition and the ability to attach to surfaces [Young, 2007]. In this context, it is possible that the observed changes of the shape of colonies grown on congored were associated with an adaptive change of individual cell size or -shape during growth under nitrogen limited conditions.

### **5.2.2 Signals of nitrogen conservation**

#### **5.2.2.1 Increase of the carbon to nitrogen ratio**

Nitrogen limited cultures were found to optimize their utilization of nitrogen. This is essential for bacteria growing under nutrient limitation since they need their cellular biomolecules for growth and reproduction. A mobilization of own internal nutrient reserves obtained by autophagy, as it was shown in the short-term starvation experiment, is thereby not likely and bacteria exclusively depend on the nutrient quantities which they take up from their surrounding. Moreover, we assumed that persistent nutrient limitation is a force that further reduces the nitrogen demand to maintain bacteria grown under this unfavorable condition viable and competitive. Indeed, the C/N ratio of nitrogen limited cultures had already increased (with respect to the C/N ratio of the ancestor) after 14 generations. At generation 200, the C/N ratio of nitrogen limited cultures peaked and remained constant in the following generations. For nitrogen rich control cultures no difference in the C/N ratio with respect to that of the ancestor was detected over the complete time course of the experiment. All in all, the statistically significant difference of the C/N ratio between nitrogen limited cultures and nitrogen rich control cultures was 18.85 %. When the overall carbon and nitrogen content of the different cultures was disentangled, it could be shown that the increased C/N ratio in nitrogen limited cultures was exclusively driven by a decrease of the cellular nitrogen content while the cellular carbon content remained constant over time and comparable to that of the nitrogen rich control and the ancestor. In total, nitrogen limited cultures had an about 15 % lowered nitrogen content than nitrogen rich control cultures and the ancestor. This finding is consistent with the composition of the culture media that were supplemented to the continuous cultures. The full minimal medium in which nitrogen rich control cultures were grown provided each nutrient, including ammonium sulphate as nitrogen source and glucose as carbon source, in excess. The nitrogen limited minimal medium that was used for the cultivation of nitrogen limited cultures

---

provided 400 times less ammonium sulphate while the concentrations of the residual nutrients, including glucose, were maintained unchanged. Thus, the adaptation of the C/N ratio in nitrogen limited cultures could directly be linked to a decreased cellular nitrogen content caused by a lowered nitrogen supplementation. The adaptation of the cellular element composition to that of the surrounding environment was also observed in various prokaryotes, fungi algae and plants [Danger and Chauvet, 2013; Rhee, 1978; Scott *et al.*, 2012; Shaver and Melillo, 1984]. Lacking homeostasis of elements is associated to the lifestyle. All of the mentioned organisms take up individual elements and use them for the de novo synthesis of their biomolecules. Thus, these organisms directly depend on the nutrient availability in their surrounding environment. In contrast, heterotrophic organism are capable of 'stoichiometric homeostasis'. These organisms maintain a constant element composition (within some biologically limited bounds) independent of their surrounding [Kooijman, 1995; Sterner and Elser, 2002] by the ingestion of bounded nutrient constituents and by the modification of their ingestion rate, food selectivity and food sources [Frost *et al.*, 2005].

#### 5.2.2.2 Nitrogen conservation in upregulated proteins

Nitrogen limited cultures were found to increase their C/N ratio by a decrease of the overall cellular nitrogen content. Here, it was assumed that a reduced protein nitrogen demand contributed to this overall decline of the nitrogen budget. Different studies on various microorganisms and plants already suggested that upregulated proteins exhibit a lower demand on sulfur and nitrogen atoms compared to downregulated proteins [Elser *et al.*, 2006; Li *et al.*, 2009; Mazel and Marlière, 1989]. By examining continuous cultures over longer and potentially evolutionary relevant time scales (1600 generations) in a nitrogen limited environment, this study aimed to reveal whether the global expression level of genes is indeed linked to the nitrogen content of the encoded proteins. Therefore, the nitrogen content (measured as average number of nitrogen atoms per amino acid side chain) of proteins encoded by genes with a given expression level threshold of 2 ( $\log_2$  ratio  $> 2$  with respect to the ancestor) was analyzed over the 1600 generations of continuous cultivation in the nitrogen limited medium. Actually, it could be shown that the mean nitrogen content of these significantly upregulated proteins was consistently lower than that of significantly downregulated proteins which were encoded by genes with a given expression level threshold of -2 ( $\log_2$  ratio  $< 2$  with respect to the ancestor). Moreover, the differences in nitrogen allocation between the up- and downregulated proteins became even more pronounced and significant in the later generations (500 to 1600). This was due to a decrease in the mean nitrogen content of upregulated proteins over time, which was 0.36 at generation 14 and 0.34 at the generations 1000 and 1600. In downregulated proteins, the mean nitrogen content was similar in the early and later generations (0.37 at generation 14, 1000 and 1600).

During nutrient deprivation, upregulated proteins are likely to be under the strongest selection pressure [Elser *et al.*, 2006] since they represent a vigorous nutrient saving potential. The continuous culture experiment did not aim to identify possible de novo mutations that could have affected the protein nitrogen demand by amino acid usage bias. Thus, the decline of the mean nitrogen content of the upregulated proteins over time might be explained by changes on global patterns of gene regulation. It is possible that expression levels of genes encoding nitrogen demanding proteins were lowered over time to decrease the overall protein nitrogen content during the persistent nitrogen limitation. Possible mechanisms that can affect gene expression are for example mutations in regulatory regions of genes or mutations in genes that encode repressors or activators of transcription [Seyffert, 2003]. A study of [Herring *et al.*, 2006] showed that regulatory mutations can entail growth advantages during prolonged growth in a constant environment. In three out of five *E. coli* populations that had evolved in glycerol minimal medium for 44 days, Herring *et al.* [2006] identified regulatory mutations in genes encoding the two major subunits of RNA polymerase. Even though it was not clear why these mutations were beneficial to the cultures, it could be shown that they were the main reason for an increase of growth rate in the given environment [Herring *et al.*, 2006].

In nitrogen rich control cultures, the mean nitrogen content of significantly upregulated proteins ( $\log_2$  ratio  $> 2$  with respect to the ancestor) was higher (significantly higher in the generations 23, 1000 and 1600) than that of significantly downregulated proteins ( $\log_2$  ratio  $< -2$  with respect to the ancestor) in each generation. Due to the excess nitrogen amount that was supplied with the growth medium, clearly no selection pressure owing to nitrogen deprivation acted on these continuous cultures. Thus, upregulated proteins were not likely to be targeted in order to decrease their nitrogen budget. Moreover, next to the mean nitrogen content, no obvious difference in the overall distribution of nitrogen atoms per amino acid side chain between the two protein sets of the nitrogen rich control cultures was found.

Lastly it could be shown that the proteins estimated as significantly upregulated in the nitrogen limited cultures had a significantly (except for generation 500) lower nitrogen allocation than the proteins estimated as significantly upregulated in the nitrogen rich control cultures. This is an important fact since it validates that the observed conservation of nitrogen in proteins upregulated in response to nitrogen limitation can be directly linked to the lowered availability of ammonium in the growth medium and is not an artifact of the continuous culture experiment itself.

### 5.2.3 Improved fitness under nitrogen limited conditions

Prolonged cultivation in nitrogen limited minimal medium was shown to increase the ammonium uptake rate of the continuous cultures and further resulted in a reduction of the cellular- and protein nitrogen content. To quantify these adaptational processes, fitness of the evolved nitrogen limited cultures under the experimental nutritional conditions was measured and compared to fitness of the ancestor and to that of the evolved nitrogen rich control cultures under identical nutritional conditions. Fitness was reflected by the propensity to leave descendants [Elena and Lenski, 2003] and was measured in comparative growth experiments and in head-to-head competition between two of the described bacterial lines (1600th generation of nitrogen limited cultures, 1600th generation of nitrogen rich control cultures and ancestor). For competitive growth experiments, a kanamycin resistance was introduced into the genomes of bacterial cells derived from the ancestor and from the evolved nitrogen limited cultures. The antibiotic resistance allowed to discriminate bacteria of two competing lines from one another by their ability to grow on kanamycin containing LB-agar. The kanamycin resistance marker was shown to be selectively neutral (see chapter 6) so that the competitive growth experiments directly revealed the fitness of the analyzed bacterial lines in the given nutritional environment.

When the three different bacterial lines were grown separately in nitrogen limited minimal medium, growth curves equaled each other especially in the exponentially phase of growth. However, the evolved nitrogen limited line reached a significantly higher maximal cell density than the two other bacterial lines. These results suggest, that the evolved nitrogen limited line was more efficient than the two other bacterial lines in the late exponential growth phase, when the limited nitrogen source was close to exhaustion. Most likely, the improved efficiency of nitrogen scavenging and -metabolism enabled the evolved nitrogen limited line to capture and process the supplied nitrogen even when it was almost depleted in the growth medium. Further, the documented lower cellular- and protein nitrogen content of the evolved nitrogen limited line might have allowed more single cells to grow on the given nitrogen quantities. During head-to-head competitive growth in a common culture, the growth differences of the different bacterial lines were even more pronounced. Here, the evolved nitrogen limited line showed a significantly faster increase of biomass when grown in competition with the evolved nitrogen rich control line and also when grown in competition with the ancestor. After 24 hours of competition, the evolved nitrogen limited line still had a significantly higher maximal cell density than the ancestor. When grown in competition with the evolved nitrogen rich control line, cell densities of both evolved continuous lines were equal after 24 hours. The described findings further underline that the acquired adaptations in the uptake of nitrogen and its cellular distribution



entailed growth advantages to the cultures that had evolved under prolonged nitrogen limitation when grown together with cultures that did not adapt to prolonged nitrogen limitation. Most likely, the nitrogen limited line was able to take up and process the supplied nitrogen faster and more efficient than the evolved nitrogen rich control line and the ancestor, respectively. Additionally to the improved nitrogen processing, the lowered overall nitrogen content might have allowed the evolved nitrogen limited line to budget with the supplied nitrogen more efficiently and thereby to increase their cellular biomass faster in comparison to the other bacterial lines. The growth advantage of the evolved nitrogen limited line in nitrogen limited medium was clearly associated to their long-term cultivation in a nitrogen limited environment. This became obvious since no difference in growth at all was observed when the nitrogen rich control line, which had evolved in the same minimal medium but with a higher ammonium quantity, and the ancestor were competed against each other in nitrogen limited medium. R. Lenski serially propagated cultures of *E. coli* in a glucose-supplemented minimal medium for ten thousands of generations [Lenski *et al.*, 1991; Lenski and Travisano, 1994]. After 10000 generations, head-to-head competition experiments with marked evolved strains and the ancestor in the given minimal medium revealed that the evolved strains had increased their fitness by 50 % (relative to the ancestor) [Lenski *et al.*, 1998]. It was further observed that the higher fitness in the given environment correlated with larger individual cell sizes of the evolved bacteria [Lenski and Travisano, 1994; Philippe *et al.*, 2009]. Stanek *et al.* [2009] proposed that the larger cells had a reduced demand for cell wall components due to their lowered ratio of surface area to volume. A reduced synthesis of cell wall components, such as peptidoglycan and lipopolysaccharides, decreases the energy and carbon demand of the cell and thus makes it more competitive in the given environment in which glucose was the nutrient depleted first. The previously described findings of the competition experiments in nitrogen limited medium confirm the idea that a reduced cellular element demand entails growth advantages to *E. coli* when the element concerned is limited in its surrounding environment.

In the context of the competition experiments, the question arose whether the adaptation to nitrogen limiting conditions entailed a cost to the evolved nitrogen limited line during growth under distinct nutritional conditions. Such a trade off in fitness can be caused by different mechanisms. First, it is possible that a single mutation entails a benefit for growth in one environment but is harmful under deviating conditions. Similarly, mutation accumulation in genes can be useful in one environment but harmful in another one. Lastly, a particular mutation might provide better fitness in one environment but behaves neutral in the other environment, thus having no effect on fitness during growth in this particular environment [Elena and Lenski, 2003]. So far, genomes of the evolved continuous lines have not been analyzed with respect to

de novo mutations. However, even without considering each single mutation, general dynamics of fitness of the evolved continuous lines and their ancestor were analyzed in nitrogen rich full minimal medium.

When grown separately in full minimal medium, the growth curves of the ancestor, of the evolved nitrogen limited line and of the evolved nitrogen rich control line equaled each other. However, the cell densities of the evolved nitrogen limited line were significantly higher than those of the ancestor in the stationary phase of growth. The cell densities of the evolved nitrogen limited line were also significantly higher than those of the evolved nitrogen rich control line between 8.5 hours and 11.5 hours of growth (this time range corresponded as well to the stationary phase of growth of both bacterial lines). As already discussed for the comparative growth experiment in nitrogen limited medium, the evolved nitrogen limited line seemed to benefit from their lowered cellular- and protein nitrogen content in the late exponential growth phase, when the nutrient concentration (including nitrogen) in the growth medium became low. During head-to-head competition, no differences in cell density were detected when the evolved nitrogen limited line was competed against the evolved nitrogen rich control line and also not when the evolved nitrogen rich control line was competed against the ancestor. However, during head-to-head competition between the evolved nitrogen limited line and the ancestor, the ancestor had significantly higher cell densities right after inoculation of the growth medium and at 4 hours. At 6 hours and 24 hours, no differences in cell density between the two bacterial lines were observed anymore. This observation might hint on a cost which the bacteria that had evolved under nitrogen limited conditions had to pay during the adaptation to an environment in which nitrogen is available in excess. It is possible that the evolved nitrogen limited line had to adapt their route of ammonium assimilation and -metabolism to the nitrogen rich conditions, thus showing a delayed start of exponential growth compared to the ancestor which was already grown in full minimal medium right before the competition experiment and thereby used to the nitrogen quantity of this medium. However, competition experiments in a medium with a different nitrogen source than ammonium might reveal more pronounced growth disadvantages of the evolved nitrogen limited line since they would need to adapt their metabolism and gene expression towards the utilization of a varying ammonium source. Consistently with this proposal, [Cooper and Lenski, 2000] observed that the fitness gain on glucose of *E. coli* populations that were serially propagated in glucose-supplemented minimal medium [Lenski *et al.*, 1991; Lenski and Travisano, 1994] came along with reduced catabolic functions against a variety of other substrates, as D-ribose and fructose.

---

## 6 Conclusion & Outlook

In the present study, we investigated the strength of natural selection exerted by nitrogen deprivation on molecular evolution of *Escherichia coli*. A special emphasis was put on the cellular processes that enable selection to shape the composition and abundance of biomolecules for parsimonious nitrogen allocation. All in all, our results highly indicate that natural selection owing to nitrogen deprivation is able to lower the protein nitrogen content by amino acid usage bias and by changes in the regulation of gene expression levels. By observing evolution in action in continuously growing cultures, there is now laboratory based evidence for parsimonious nitrogen allocation in response to nitrogen deprivation. The present findings further show that even after shaping the architecture of biomolecules over millions of years of evolution, natural selection exerted by nitrogen deprivation still has the potential to reduce the protein nitrogen content even more. Further, the long-term adaptation to nitrogen limitation results in a growth advantage under this nutrient condition.

The short-term starvation experiment revealed that selection owing to nitrogen deprivation had shaped the architecture of proteins upregulated in response to nitrogen starvation over the evolutionary history of *E. coli*. These proteins exhibit a markedly lowered nitrogen content which is caused by a decreased incorporation of the nitrogen rich amino acids arginine, asparagine, glutamine and lysine. Further, the avoidance of nitrogen rich amino acids in the described proteins could be directly linked to their lowered abundance in the free amino acid pool of nitrogen starved *E. coli*. Depletion of free cellular nitrogen rich amino acids was shown to have resulted from the utilization of those as nitrogen sources. These findings highly suggest that environmental availability of nitrogen has driven the efficiency of translation via biased concentration of free amino acids. In order to clarify this assumption, an integration of ribosome profiling in the described starvation experiment could be a very useful next step. Ribosome profiling is a sequencing technique which targets exclusively mRNA sequences that are bound to ribosomes [Ingolia, 2014]. Thus, it produces a snapshot of all the ribosomes that are translating mRNA at a particular time point. The obtained data provide information on the speed of the translating ribosomes and could thereby confirm the assumption that the biased abundance of free cellular amino acids during nitrogen starvation affects the speed of translation of the proteins involved in the nitrogen starvation response. Additionally to the documented amino acids usage bias in proteins upregulated in response to nitrogen starvation, a reduced protein length could contribute to the reduction of the protein nitrogen content. Here, it will be interesting to compare the length of proteins upregulated in response to nitrogen starvation to those that are downregulated in response to nitrogen starvation.

The continuous culture experiment performed in this study enabled us to observe the

impact of nitrogen availability on the cellular budget of this element over evolutionary relevant time scales. The first finding was that nitrogen limited continuous cultures enhanced their ammonium uptake rate over time. This increase could partly be explained by an elevated expression level of the gene *amtB* which encodes the ammonia channel protein AmtB. Nevertheless, it will be interesting to search for the additional adaptive processes that were involved in the improved nitrogen scavenging. For this, one might analyze the nucleotide sequence of *amtB* to screen for possible de novo mutations which might have caused an enhanced efficiency of AmtB. However, since ammonium is the preferred nitrogen source of *E. coli*, AmtB is believed to function properly and it would be astonishing if its efficiency had indeed been further optimized in the framework of the present continuous culture experiment. Such a finding would contribute to the quantification of the selection pressure exerted by nitrogen limitation. Next to the improved nitrogen scavenging, nitrogen limited continuous cultures increased their cellular carbon to nitrogen ratio by a global decrease of the overall nitrogen content. Consistently, we could show that the nitrogen allocation of proteins upregulated in nitrogen limited cultures decreased over time. Here, the global expression level of genes was shown to be the driving force for the reduced nitrogen content of the encoded proteins. It will be interesting to have a closer look on the mechanisms that affected gene expression levels during the continuous culture experiment. DNA sequencing of the cultures might reveal some regulatory mutations that lowered the expression level of particular genes and thus reducing the nitrogen budget through a lowered protein synthesis. Obviously, genes with an in general higher expression level under nitrogen limitation are the most interesting ones that should be screened for mutations since these exhibit the highest potential for protein nitrogen conservation. Analysis of single point mutations that arose during the continuous culture experiment will further contribute to the identification of possible nucleotide substitutions in the coding sequences of genes with a high expression level under nitrogen limitation. If one compared DNA sequences of the ancestor with those of bacteria that had evolved under nitrogen limitation, one might detect mutations that caused an exchange of a nitrogen rich amino acid into a less nitrogen demanding one in proteins upregulated in response to nitrogen limitation. Such a finding would obviously lead to a further reduction of the protein nitrogen budget. However, the number of single base mutations which affect the protein amino acid composition is predicted to be very low. The rate of single base mutations is indicated with an order of  $10^{-10}$  to  $10^{-9}$  per base pair per replication [Barrick and Lenski, 2013]. *Escherichia coli* Nissle 1917 has a genome size of 5.1 Mb. Hence, the given rate corresponds to one point mutation in every 200 to 2000 generations. Thus, if one assumes a stable mutation rate during the continuous culture experiment, only a small amount of single base substitutions might have been

fixed in the *E. coli* cultures that evolved for 1600 generations under nitrogen limitation. The last observation of the continuous culture experiment was that bacteria that had evolved in the nitrogen limited environment for 1600 generations exhibited growth advantages when competed against the nitrogen rich control and their ancestor under nitrogen limited conditions. The growth advantages were assumed to be caused by the adaptation (improved nitrogen scavenging, reduced overall nitrogen content) to the long-termed cultivation under nitrogen limiting conditions. Nevertheless, the competition experiments that had been performed only provided a small insight into the fitness of the different bacterial lines. Here, one could repeat the experiments with bacteria that had evolved for different generations under nitrogen limitation to see at which generation fitness had improved first and/or the strongest. Moreover, it will be interesting to link the acquired growth advantages to particular mutations. The competition experiments were also performed in nitrogen rich medium. In this environment, differences in growth between the nitrogen limited line and the ancestor were observed in the early phase of competitive growth. It is further possible that the adaptations that were beneficial for growth with quantitatively low ammonium exhibit a more pronounced cost during growth in a more distinct nutrient environment. It will therefore be interesting to compete the different bacterial lines in an environment with for instance a different nitrogen source.

Lastly, data of the five nitrogen limited continuous cultures were considered as biological replicates in each of the analyses performed for this study. As a next step, it is of great interest to analyze whether the five independent nitrogen limited continuous cultures had acquired different or parallel molecular changes during the 1600 generations. If different mutations got fixed in the replicate cultures, one might investigate their individual impact on growth and reproduction under nitrogen limiting conditions. In this context it will also be necessary to take a closer look on those bacteria that showed changes in their morphotype when incubated on congo red agar. Bacteria with from the Nissle 1917-specific red, dry and rough deviating morphotypes were found in each of the five independent nitrogen limited continuous cultures which suggests that the observed changes were somehow beneficial under nitrogen limiting conditions.

As a technical suggestion, the present data can be optimized by an integration of protein sequencing. In this study, protein abundance was correlated to the expression level of the encoding gene which was shown to be a valid assumption for *E. coli* by Ishihama *et al.* [2008]. Nevertheless, analyses of the proteome of short-term nitrogen starved cultures and long-term nitrogen limited continuous cultures could confirm our method of correlation. At this stage, the required amount of biomass for this technique was not realizable in the experimental setup of both experiments but this might change in the future.

## Appendix

### Full minimal medium

1) For 1 liter full minimal medium add to 500 ml dH<sub>2</sub>O

5 g	Glucose C <sub>6</sub> H <sub>12</sub> O <sub>6</sub> · H <sub>2</sub> O	f.c. 0.5 %
0.2 g	Magnesiumsulfate MgSO <sub>4</sub> · 7 H <sub>2</sub> O	f.c. 0.02%
0.5 g	Sodiumchloride (NaCl)	f.c. 0.05 %
0.5 g	Sodiumcitrate (C <sub>6</sub> H <sub>5</sub> Na <sub>3</sub> O <sub>7</sub> ·2H <sub>2</sub> O)	f.c. 0.05 %

Dissolve everything by shaking and fill up with dH<sub>2</sub>O to 889 ml.

Sterile filtrate the solution via a disposable bottle top filter

(pore size 0.22 µm) in a sterile 1 l glass bottle.

2) Add aseptically the following sterile stock solutions in the order below

60 ml	500 mM Dipotassiumhydrogenphosphate (K <sub>2</sub> HPO <sub>4</sub> )	f.c. 50 mM
40 ml	500 mM Potassiumdihydrogenphosphate (KH <sub>2</sub> PO <sub>4</sub> )	f.c. 50 mM
10 ml	40 % Ammoniumsulfate ((NH <sub>4</sub> ) <sub>2</sub> SO <sub>4</sub> )	f.c. 0.4 %
100 µl	2 M Calcium chloride (CaCl <sub>2</sub> ·2H <sub>2</sub> O)	f.c. 0.2 mM
1 ml	1000 X trace element solution	f.c. 1 X

### Stock solutions

#### 500 mM Dipotassiumhydrogenphosphate (87,1 g/l)

For 500 ml stock solution add 43.55 g Dipotassiumhydrogenphosphate to 400 ml dH<sub>2</sub>O.

Dissolve everything by shaking and fill up with dH<sub>2</sub>O to 500 ml.

Autoclave for 15 min at 121 °C.

**500 mM Potassiumdihydrogenphosphate (68 g/l)**

For 500 ml stock solution add 34 g Potassiumdihydrogenphosphate to 400 ml dH<sub>2</sub>O. Dissolve everything by shaking and fill up with dH<sub>2</sub>O to 500 ml. Autoclave for 15 min at 121 °C.

**40 % Ammoniumsulfate (400 g/l)**

For 100 ml stock solution add 40 g Ammoniumsulfate to 80 ml dH<sub>2</sub>O. Dissolve everything by shaking and fill up with dH<sub>2</sub>O to 100 ml. Autoclave for 15 min at 121 °C.

**2 M Calcium chloride (294 g/l)**

For 10 ml stock solution add 2,94 g Calcium chloride to 8 ml dH<sub>2</sub>O. Dissolve everything by shaking and fill up with dH<sub>2</sub>O to 10 ml. Sterile filtrate with a syringe filter (pore size 0.22 µm) in a sterile bottle.

**1000 X trace element solution**

For 10 ml stock solution add the following nutrients to 8 ml dH<sub>2</sub>O. First, place the glass bottle with 8 ml dH<sub>2</sub>O on a magnetic stirrer. Add the nutrients one after another in the order below. Before adding the next nutrient, make sure that everything is dissolved.

500 mg Mangesesulfate (MnSO <sub>4</sub> H <sub>2</sub> O)	f.c. 0.005 %
50 mg Zincsulfate (ZnSO <sub>4</sub> 7 H <sub>2</sub> O)	f.c. 0.0005 %
5 mg Ironsulfate (FeSO <sub>4</sub> 7 H <sub>2</sub> O)	f.c. 0.00005 %
50 mg Coppersulfate (CuSO <sub>4</sub> 5 H <sub>2</sub> O)	f.c. 0.0005 %

Fill up with dH<sub>2</sub>O to 10 ml.

Wrap the bottle in foil and leave it on the magnetic stirrer over night. Next day, sterile filtrate (bottle top filter, pore size 0.22 µm) the solution in a sterile glass bottle.

Notes

f.c. = final concentration

**N-Lim minimal medium**

Stick to the protocol for the full minimal medium with the following changes:

- 1) Glucose, Magnesiumsulfate, Sodiumchloride and Sodiumcitrate are dissolved in a final volume of 898 ml dH<sub>2</sub>O.
  
- 2) Use the following stock solution of Ammoniumsulfate  
1 ml 1 % Ammoniumsulfate ((NH<sub>4</sub>)<sub>2</sub>SO<sub>4</sub>) f.c. 0.001 %

Stock solution**1 % Ammoniumsulfate (10 g/l)**

For 10 ml stock solution add 100 mg Ammoniumsulfate to 8 ml dH<sub>2</sub>O.

Dissolve everything by shaking and fill up with dH<sub>2</sub>O to 10 ml.

Autoclave for 15 min at 121 °C.

Notes

f.c. = final concentration



**Figure 4.1**

List of the fifty ribosomal genes integrated in the analysis of protein synthesis. The genes were obtained from:

GO:0003735 ('structural constituent of ribosome').

<b>Gene identifier</b>	<b>Gene identifier</b>	<b>Gene identifier</b>	<b>Gene identifier</b>
ECABU_c40760	ECABU_c40750	ECABU_c13020	ECABU_c25180
ECABU_c37640	ECABU_c37630	ECABU_c37420	ECABU_c37410
ECABU_c37400	ECABU_c37390	ECABU_c37380	ECABU_c37350
ECABU_c37340	ECABU_c37330	ECABU_c37320	ECABU_c37310
ECABU_c37300	ECABU_c37290	ECABU_c37280	ECABU_c37270
ECABU_c37260	ECABU_c37250	ECABU_c37240	ECABU_c37220
ECABU_c37190	ECABU_c37170	ECABU_c37160	ECABU_c37150
ECABU_c37140	ECABU_c37120	ECABU_c36400	ECABU_c36390
ECABU_c36000	ECABU_c35770	ECABU_c09490	ECABU_c47630
ECABU_c47620	ECABU_c47590	ECABU_c34840	ECABU_c19720
ECABU_c19700	ECABU_c45000	ECABU_c44980	ECABU_c44970
ECABU_c44420	ECABU_c17190	ECABU_c03830	ECABU_c03820
ECABU_c29100	ECABU_c29070		

**Figure 4.7**

List of the genes that were analyzed in the framework of lipid degradation in carbon starved filter cultures and the metabolic pathways to which the genes are associated.

<b>Gene identifier</b>	<b>Metabolic pathway</b>
ECABU_c03260	fatty acid-oxidation I
ECABU_c05350	acyl-CoA hydrolysis oleate $\beta$ -oxidation
ECABU_c05590	sophorolipid degradation
ECABU_c05810	acyl-CoA hydrolysis oleate $\beta$ -oxidation
ECABU_c12610	phospholipases
ECABU_c19490	fatty acid $\beta$ -oxidation I
ECABU_c19980	fatty acid $\beta$ -oxidation I
ECABU_c20630	fatty acid $\beta$ -oxidation I fatty acid activation
ECABU_c22760	fatty acid $\beta$ -oxidation I
ECABU_c25730	glycerophosphodiester degradation glycerol and glycerophosphodiester degradation
ECABU_c25760	glycerol degradation I glycerophosphodiester degradation glycerol and glycerophosphodiester degradation
ECABU_c25770	glycerol degradation I glycerophosphodiester degradation glycerol and glycerophosphodiester degradation
ECABU_c26730	pyruvate fermentation to butanoate fatty acid $\beta$ -oxidation I isoleucine degradation I phenylacetate degradation I (aerobic) valine degradation I
ECABU_c26740	fatty acid $\beta$ -oxidation I
ECABU_c38460	glycerol degradation I glycerophosphodiester degradation glycerol and glycerophosphodiester degradation

<b>Gene identifier</b>	<b>Metabolic pathway</b>
ECABU_c38790	glycerophosphodiester degradation glycerol and glycerophosphodiester degradation
ECABU_c43030	phospholipases
ECABU_c43070	phosphatidylcholine resynthesis via glycerophosphocholine
ECABU_c43470	fatty acid $\beta$ -oxidation I
ECABU_c43480	pyruvate fermentation to butanoate fatty acid $\beta$ -oxidation I androstenedione degradation phenylacetate degradation I (aerobic)
ECABU_c44320	glycerol degradation I glycerol and glycerophosphodiester degradation
ECABU_c44570	glycerol degradation V glycerol degradation II glycerol degradation to butanol
ECABU_c45770	pyruvate fermentation to butanoate fatty acid $\beta$ -oxidation I isoleucine degradation I phenylacetate degradation I (aerobic) valine degradation I
ECABU_c47450	fatty acid $\beta$ -oxidation I
ECABU_c47720	pyruvate fermentation to butanoate fatty acid $\beta$ -oxidation I isoleucine degradation I acetyl-CoA fermentation to butyrate II oleate $\beta$ -oxidation phenylacetate degradation I (aerobic) valine degradation I

**Figure 4.8**

List of the fatty acids that were analyzed in the framework of lipid degradation in carbon starved filter cultures.

<b>Molecular formular</b>	<b>Fatty acid</b>	<b>Classification</b>
C14H28O2	4,8-dimethyl-dodecanoic acid	branched fatty acid
C16H30O2	7-palmitoleic acid	unsaturated fatty acid
C16H32O2	2-propyl-tridecanoic acid	branched fatty acid
C16H32O3	4-hydroxy palmitic acid	hydroxy fatty acid
C17H26O3	7-hydroxy-10E,16-heptadecadien-8-ynoic acid	hydroxy fatty acid
C18H34O2	5-octadecylenic acid	unsaturated fatty acid
C18H34O3	8R-hydroxy-9Z-octadecenoic acid	octadecanoid
C18H28O5	12-oxo-14,18-dihydroxy-9Z,13E,15Z-octadecatrienoic acid	octadecanoid

**Figure 4.9**

List of the genes that were analyzed in the framework of carbohydrate degradation in carbon starved filter cultures and the metabolic pathways to which the genes are associated.

Gene identifier	Metabolic pathway
ECABU_c00670	L-arabinose degradation I L-ascorbate degradation I & II (bacterial, aerobic)
ECABU_c00680	L-arabinose degradation I
ECABU_c00690	L-arabinose degradation I
ECABU_c01150	anhydromuropeptides recycling
ECABU_c01370	glucose and glucose-1-phosphate degradation
ECABU_c02160	ADP-L-glycero- $\beta$ -D-manno-heptose biosynthesis
ECABU_c02200	ketogluconate metabolism
ECABU_c02820	L-idonate degradation ketogluconate metabolism
ECABU_c03270	ADP-L-glycero- $\beta$ -D-manno-heptose biosynthesis
ECABU_c03920	ketogluconate metabolism
ECABU_c04340	lactose degradation II & III
ECABU_c04810	glycogen degradation I
ECABU_c05890	D-galactarate degradation I D-glucarate degradation I glycolate and glyoxylate degradation I
ECABU_c07220	N-acetylglucosamine degradation I & II D-galactosamine and N-acetyl-D-galactosamine degradation anhydromuropeptides recycling
ECABU_c07230	N-acetylglucosamine degradation I & II
ECABU_c07420	glucose and glucose-1-phosphate degradation glycogen degradation I & II glycogen biosynthesis I (from ADP-D-Glucose) sucrose degradation II (sucrose synthase) GDP-glucose biosynthesis II L-ascorbate biosynthesis V starch degradation V UDP-glucose biosynthesis L-ascorbate biosynthesis IV D-galactose degradation V (Leloir pathway) sucrose biosynthesis I (from photosynthesis)
ECABU_c07950	galactose degradation I (Leloir pathway) starch degradation V trehalose degradation II & VI D-galactose degradation V (Leloir pathway)
ECABU_c07960	galactose degradation I & III D-galactose degradation V (Leloir pathway)
ECABU_c07970	galactose degradation I & III D-galactose degradation V (Leloir pathway)
ECABU_c07980	galactose degradation I & III UDP-D-galactose biosynthesis D-galactose degradation V (Leloir pathway)
ECABU_c08630	glucose and glucose-1-phosphate degradation
ECABU_c09080	anhydromuropeptides recycling
ECABU_c09570	CMP-KDO biosynthesis I & II
ECABU_c10290	glucose and glucose-1-phosphate degradation
ECABU_c10660	galactitol degradation D-galactosamine and N-acetyl-D-galactosamine degradation
ECABU_c13210	chitin degradation II anhydromuropeptides recycling
ECABU_c13330	N-acetylglucosamine degradation II
ECABU_c14580	anhydromuropeptides recycling
ECABU_c14680	trehalose degradation II & VI
ECABU_c14860	superpathway of lipopolysaccharide biosynthesis CMP-KDO biosynthesis I & II
ECABU_c15180	sucrose degradation II (sucrose synthase) L-ascorbate biosynthesis IV & V UDP-glucose biosynthesis sucrose biosynthesis I (from photosynthesis)
ECABU_c15920	trehalose biosynthesis V starch degradation V
ECABU_c16000	galactose degradation I (Leloir pathway)
ECABU_c17480	D-galacturonate degradation I
ECABU_c17590	chitobiose degradation
ECABU_c18650	D-mannose degradation GDP-mannose biosynthesis
ECABU_c18690	$\beta$ -D-glucuronide and D-glucuronate degradation
ECABU_c18930	anhydromuropeptides recycling
ECABU_c19900	chitobiose degradation
ECABU_c23810	GDP-mannose biosynthesis
ECABU_c24210	galactitol degradation

Gene identifier	Metabolic pathway
ECABU_c24990	fructose degradation
ECABU_c26250	glucose and glucose-1-phosphate degradation
ECABU_c21110	Entner-Doudoroff pathway I superpathway of $\beta$ -D-glucuronide and D-glucuronate degradation superpathway of glycolysis and Entner-Doudoroff 5-dehydro-4-deoxy-D-glucuronate degradation D-fructuronate degradation D-glucosaminatate degradation
ECABU_c21120	Entner-Doudoroff pathway I superpathway of glycolysis and Entner-Doudoroff
ECABU_c23560	L-ascorbate biosynthesis IV & V UDP- $\alpha$ -D-glucuronate biosynthesis (from UDP-glucose)
ECABU_c23750	sucrose degradation II (sucrose synthase) L-ascorbate biosynthesis IV & V UDP-glucose biosynthesis sucrose biosynthesis I (from photosynthesis)
ECABU_c24260	galactitol degradation D-galactosamine and N-acetyl-D-galactosamine degradation
ECABU_c27080	homolactic fermentation glycolysis III glucose and glucose-1-phosphate degradation glycogen degradation I GDP-glucose biosynthesis II trehalose degradation I & II
ECABU_c27470	anhydromuropeptides recycling
ECABU_c27540	anhydromuropeptides recycling
ECABU_c28450	galactose degradation I (Leloir pathway) starch degradation V trehalose degradation II & VI D-galactose degradation V (Leloir pathway)
ECABU_c29750	L-sorbose degradation D-sorbitol degradation II
ECABU_c30560	D-glucarate degradation I superpathway of D-glucarate and D-galactarate degradation
ECABU_c30570	D-glucarate degradation I superpathway of D-glucarate and D-galactarate degradation
ECABU_c30700	superpathway of fucose and rhamnose degradation fucose degradation
ECABU_c30720	superpathway of fucose and rhamnose degradation fucose degradation
ECABU_c30730	superpathway of fucose and rhamnose degradation fucose degradation
ECABU_c30740	superpathway of fucose and rhamnose degradation fucose degradation
ECABU_c31130	anhydromuropeptides recycling
ECABU_c31420	5-dehydro-4-deoxy-D-glucuronate degradation
ECABU_c31830	chitobiose degradation
ECABU_c32160	L-sorbose degradation
ECABU_c33100	superpathway of N-acetylglucosamine, N-acetylmannosamine and N-acetylneuraminatate degradation
ECABU_c33460	superpathway of (KDO)2-lipid A biosynthesis superpathway of lipopolysaccharide biosynthesis CMP-KDO biosynthesis I & II
ECABU_c33490	L-ascorbate biosynthesis IV & V UDP- $\alpha$ -D-glucuronate biosynthesis (from UDP-glucose)
ECABU_c34150	ketogluconate metabolism
ECABU_c34960	lactose degradation II & III
ECABU_c34970	lactose degradation II & III
ECABU_c35100	D-galacturonate degradation I
ECABU_c35110	D-galacturonate degradation I $\beta$ -D-glucuronide and D-glucuronate degradation
ECABU_c35380	D-galactarate degradation I D-glucarate degradation I glycolate and glyoxylate degradation I
ECABU_c35390	D-galactarate degradation I D-glucarate degradation I
ECABU_c35410	D-galactarate degradation I superpathway of D-glucarate and D-galactarate degradation
ECABU_c35500	N-acetylglucosamine degradation I & II D-galactosamine and N-acetyl-D-galactosamine degradation anhydromuropeptides recycling
ECABU_c35530	galactitol degradation D-galactosamine and N-acetyl-D-galactosamine degradation
ECABU_c35880	O-antigen building blocks biosynthesis anhydromuropeptides recycling UDP-N-acetyl-D-glucosamine biosynthesis I
ECABU_c36120	superpathway of (KDO)2-lipid A biosynthesis superpathway of lipopolysaccharide biosynthesis CMP-KDO biosynthesis I
ECABU_c36130	superpathway of (KDO)2-lipid A biosynthesis superpathway of lipopolysaccharide biosynthesis CMP-KDO biosynthesis I & II
ECABU_c36300	N-acetylneuraminatate and N-acetylmannosamine degradation
ECABU_c36330	N-acetylneuraminatate and N-acetylmannosamine degradation
ECABU_c37590	chitin degradation II

Gene identifier	Metabolic pathway
ECABU_c38370	glycogen degradation I & II starch degradation V
ECABU_c38380	glycogen degradation I & II starch degradation V
ECABU_c38570	glycogen degradation I & II starch degradation V
ECABU_c38600	glycogen degradation I
ECABU_c38680	D-gluconate degradation L-idonate degradation ketogluconate metabolism
ECABU_c39580	trehalose degradation II & VI
ECABU_c39650	D-galacturonate degradation I superpathway of $\beta$ -D-glucuronide and D-glucuronate degradation 5-dehydro-4-deoxy-D-glucuronate degradation D-fructuronate degradation
ECABU_c39960	ketogluconate metabolism
ECABU_c40070	xylose degradation I
ECABU_c40080	xylose degradation I
ECABU_c40270	L-arabinose degradation I L-ascorbate degradation I & II
ECABU_c40280	arginine degradation II (AST pathway) ethanol degradation I mixed acid fermentation superpathway of fucose and rhamnose degradation threonine degradation IV pyruvate fermentation to ethanol I & III 2-deoxy- $\alpha$ -D-ribose 1-phosphate degradation superpathway of purine deoxyribonucleosides degradation superpathway of pyrimidine deoxyribonucleosides degradation L-lactaldehyde degradation (aerobic) ethanol degradation II & IV
ECABU_c40370	mannitol degradation I
ECABU_c40600	ADP-L-glycero- $\beta$ -D-manno-heptose biosynthesis
ECABU_c41740	D-galactonate degradation
ECABU_c41750	Entner-Doudoroff pathway I superpathway of $\beta$ -D-glucuronide and D-glucuronate degradation superpathway of glycolysis and Entner-Doudoroff 5-dehydro-4-deoxy-D-glucuronate degradation D-fructuronate degradation D-glucosaminatate degradation
ECABU_c41760	D-galactonate degradation
ECABU_c42010	cellulose and hemicellulose degradation
ECABU_c42130	O-antigen building blocks biosynthesis anhydromuropeptides recycling UDP-N-acetyl-D-glucosamine biosynthesis I
ECABU_c42650	enterobacterial common antigen biosynthesis UDP-N-acetyl- $\alpha$ -D-mannosaminouronate biosynthesis
ECABU_c42660	enterobacterial common antigen biosynthesis UDP-N-acetyl- $\beta$ -D-mannosaminouronate biosynthesis
ECABU_c42670	dTDP-L-rhamnose biosynthesis I enterobacterial common antigen biosynthesis O-antigen building blocks biosynthesis dTDP-N-acetylthomosamine biosynthesis
ECABU_c42680	dTDP-L-rhamnose biosynthesis I enterobacterial common antigen biosynthesis O-antigen building blocks biosynthesis dTDP-N-acetylthomosamine biosynthesis
ECABU_c42700	enterobacterial common antigen biosynthesis dTDP-N-acetylthomosamine biosynthesis
ECABU_c43330	Entner-Doudoroff pathway I superpathway of $\beta$ -D-glucuronide and D-glucuronate degradation superpathway of glycolysis and Entner-Doudoroff 5-dehydro-4-deoxy-D-glucuronate degradation D-fructuronate degradation D-glucosaminatate degradation
ECABU_c43340	D-galactonate degradation
ECABU_c43860	galactose degradation I (Leloir pathway) starch degradation V trehalose degradation II & VI D-galactose degradation V (Leloir pathway)
ECABU_c44060	superpathway of fucose and rhamnose degradation L-rhamnose degradation I
ECABU_c44070	superpathway of fucose and rhamnose degradation L-rhamnose degradation I
ECABU_c44080	superpathway of fucose and rhamnose degradation L-rhamnose degradation I
ECABU_c44090	superpathway of fucose and rhamnose degradation L-rhamnose degradation I
ECABU_c45380	L-sorbose degradation
ECABU_c45430	L-sorbose degradation D-sorbitol degradation II

Gene identifier	Metabolic pathway
ECABU_c45480	homolactic fermentation glycolysis I & III (from glucose) gluconeogenesis I superpathway of glycolysis and Entner-Doudoroff superpathway of glycolysis, pyruvate dehydrogenase, TCA, and glyoxylate bypass O-antigen building blocks biosynthesis sucrose degradation II (sucrose synthase) GDP-mannose biosynthesis sucrose biosynthesis I (from photosynthesis) UDP-N-acetyl-D-glucosamine biosynthesis I
ECABU_c46380	D-allose degradation
ECABU_c46390	D-allose degradation
ECABU_c46720	melibiose degradation
ECABU_c47270	anhydromuropeptides recycling
ECABU_c47570	L-arabinose degradation I L-ascorbate degradation I & II (bacterial, aerobic)
ECABU_c47990	anhydromuropeptides recycling
ECABU_c48050	trehalose degradation I (low osmolarity)
ECABU_c49590	superpathway of $\beta$ -D-glucuronide and D-glucuronate degradation D-fructuronate degradation
ECABU_c49600	superpathway of $\beta$ -D-glucuronide and D-glucuronate degradation D-fructuronate degradation
ECABU_c50160	2-deoxy- $\alpha$ -D-ribose 1-phosphate degradation superpathway of purine deoxyribonucleosides degradation superpathway of pyrimidine deoxyribonucleosides degradation
ECABU_c50180	2-deoxy- $\alpha$ -D-ribose 1-phosphate degradation purine ribonucleosides degradation superpathway of purine deoxyribonucleosides degradation superpathway of pyrimidine deoxyribonucleosides degradation
ECABU_c24250	galactitol degradation D-galactosamine and N-acetyl-D-galactosamine degradation



**Figure 4.12**

Genes with significantly higher expression level in nitrogen starved cultures at 120 and 240 minutes and the corresponding encoded proteins

<b>Gene identifier</b>	<b>Protein</b>
ECABU_c05330	nitrogen regulatory protein
ECABU_c05340	amtB transporter
ECABU_c07030	hypothetical protein
ECABU_c10330	putative transport protein
ECABU_c10340	flavin:NADH reductase (Rut Pathway)
ECABU_c10350	NADH dehydrogenase/NAD(P)H nitroreductase (Rut Pathway)
ECABU_c10360	pyrimidine utilization protein D (Rut Pathway)
ECABU_c10370	pyrimidine utilization protein C (Rut Pathway)
ECABU_c10380	isochorismatase family protein (Rut Pathway)
ECABU_c10390	monooxygenase (Rut Pathway)
ECABU_c17920	inner membrane transport protein YnfM
ECABU_c21610	hypothetical protein
ECABU_c22560	nitrogen assimilation control protein Nac
ECABU_c22570	transcriptional regulator Cbl
ECABU_c39890	putative resistance protein
ECABU_c43740	glutamine synthetase
ECABU_c45100	thiamine biosynthesis protein ThiC
ECABU_c45540	hypothetical protein

**Figure 4.12**

Genes with significantly higher expression level in carbon starved cultures at 120 and 240 minutes and the corresponding encoded proteins.

<b>Gene identifier</b>	<b>Protein</b>
ECABU_c04230	putative cytochrome subunit of dehydrogenase
ECABU_c04570	putative membrane protein YaiY
ECABU_c05900	allantoin permease
ECABU_c06210	cation efflux system protein CusC
ECABU_c06220	cation efflux system protein CusF
ECABU_c06230	cation efflux system protein CusB
ECABU_c06480	carbon starvation protein A
ECABU_c06970	putative alpha helical protein
ECABU_c08770	biofilm regulator BssR
ECABU_c14760	putative membrane protein YchH
ECABU_c16500	aldehyde dehydrogenase A
ECABU_c16560	putative cytoplasmic protein
ECABU_c16580	hypothetical protein
ECABU_c17820	hypothetical protein
ECABU_c20630	long chain fatty acid CoA-ligase
ECABU_c21580	L-arabinose-binding periplasmic protein
ECABU_c24800	D-galactose-binding periplasmic protein
ECABU_c24940	putative transcriptional regulator
ECABU_c28410	stationary phase inducible protein CsiE
ECABU_c28980	putative sigma 54 modulator
ECABU_c29220	hypothetical protein
ECABU_c29300	hypothetical protein
ECABU_c31430	putative acetyl-CoA acetyltransferase with thiolase domain
ECABU_c32680	major pilus subunit operon regulatory protein PapI
ECABU_c33770	glycolate oxidase subunit GlcE
ECABU_c33780	glycolate oxidase subunit GlcD
ECABU_c36850	hypothetical protein

---

<b>Gene</b>	<b>Protein</b>
ECABU_c40270	L-ribulose-5-phosphate 4-epimerase
ECABU_c40280	aldehyde dehydrogenase B
ECABU_c42330	high affinity ribose transport protein RbsD
ECABU_c42340	high affinity ribose transport ATP-binding protein RbsA
ECABU_c42360	D-ribose-binding periplasmic protein precursor
ECABU_c44190	periplasmic protein CpxP precursor
ECABU_c46120	cation/acetate symporter ActP
ECABU_c46140	acetyl-Coenzyme A synthetase
ECABU_c46710	MelR regulator of melibiose operon
ECABU_c47460	hypothetical protein
ECABU_c47470	lipoprotein YjfO precursor
ECABU_c47850	hypothetical protein
ECABU_c47860	hypothetical protein
ECABU_c47940	ABC transporter substrate-binding protein YtfQ
ECABU_c47950	ATPase
ECABU_c47960	ABC transporter permease protein YtfT
ECABU_c47970	ABC transporter permease protein YjfF

**Figure 4.27**

Nucleotide sequence of the pUC-kanR (3891 bp) vector build in this study to generate a kanamycin resistance marker for the head-to-head competition experiments (see chapter 4.2.3.2).

```

CGAGCTCGAATTTCGTAATCATGGTCATAGCTGTTTCCTGTGTGAAATTGTTATCCGCTCACAAATCCAC
ACAACATAACGAGCCGGAAGCATAAAGTGTAAGCCTGGGGTGCCTAATGAGTGAGCTAACTCACATTAA
TTGCGTTGCGCTCACTGCCCGCTTCCAGTCGGGAAACCTGTCGTGCCAGCTGCATTAATGAATCGGCC
AACGCGCGGGGAGAGGCGGTTTGCATTTGGCGCTTCCCGCTTCCCTCGCTCACTGACTCGCTGCGCT
CGGTGCTTCCGCTGCGGCGAGCGGTATCAGCTCACTCAAAGGCGGTAATACGGTTATCCACAGAATCAG
GGGATAACGCAGGAAAGAACATGTGAGCAAAAGGCCAGCAAAGGCCAGGAACCGTAAAAAGGCCGCT
TGCTGGCGTTTTTCCATAGGCTCCGCCCCCTGACGAGCATCACAAAAATCGACGCTCAAGTCAGAGGT
GGGAAACCCGACAGGACTATAAAGATACCGAGCGTTTCCCCTGGAAGCTCCCTCGTGCCTCTCCCT
TTCCGACCCTGCCGCTTACCGGATACCTGTCGCGCTTCTCCCTTCGGGAAGCGTGGCGTTTTCTCATA
GCTCACGCTGTAGGTATCTCAGTTCCGGTGTAGGTCGTTCCGCTCCAAGCTGGGCTGTGTGCACGAACCC
CCGTTCCAGCCGACCGCTGCGCCTTATCCGTAACCTATCGTCTTGAGTCCAACCCGGTAAGACACGACT
TATCCGCACTGGCAGCAGCCACTGGTAACAGGATTAGCAGAGCGAGGTATGTAGGCGGTGCTACAGAGT
TCTTGAAGTGGTGGCTAACCTACGGCTACACTAGAAGGACAGTATTTGGTATCTGCGCTCTGCTGAAGC
CAGTTACCTTCGGAAAAAGAGTTGGTAGCTCTTGATCCGGCAAAACAAACCACCGCTGGTAGCGGTGGTT
TTTTTGTGTTGCAAGCAGCAGATTACGCGCAGAAAAAAGGATCTCAAGAAGATCCTTTGATCTTTTCTA
CGGGTCTGACGCTCAGTGGAACGAAAACCTCACGTTAAGGATTTTGGTCAATGAGATTATCAAAAAAGGA
TCTTCACCTAGATCCTTTTAAATTAATAAATGAAGTTTTAAATCAATCTAAAGTATATATGAGTAAACTT
GGTCTGACAGTTACCAATGCTTAATCAGTGAGGCACCTATCTCAGCGATCTGTCTATTTTCGTTCCATCA
TAGTTGCCCTGACTCCCGCTCGTGTAGATAACTACGATACGGGAGGGCTTACCATCTGGCCCAGTGCTG
CAATGATACCGCGAGACCCACGCTCACCGGCTCCAGATTTATCAGCAATAAACCAGCCAGCCGGAAGGG
CCGAGCGCAGAAGTGGTCTCGCAACTTTATCCCGCTCCACTCCAGTCTATTAATTGTTGCCGGGAAGCTA
GAGTAAGTAGTTCCGCAAGTTAATAGTTTGGCACAAGTTGTTGCCATTGCTACAGGCATCGTGGTGTCA
GCTCGTCTGTTTTGGTATGGCTTCATTCAGCTCCGGTTCCCAACGATCAAGGCGAGTTACATGATCCCCCA
TGTTGTGCAAAAAAGCGGTTAGCTCCTTCGGTCTCCGATCGTTGTCAGAAGTAAGTTGGCCGCAAGTGT
TATCACTCATGGTTATGGCAGCACTGCATAATTCTCTTACTGTATGCCATCCGTAAGATGCTTTTCTG
TGACTGGTGAAGTCAACCAAGTCAATCTGAGAATAGTGTATGCGGCGACCGAGTTGCTCTTGGCCGG
CGTCAATACGGGATAATACCGCGCCACATAGCAGAACTTTAAAGTGCCTCATCTTGGAAAAACGTTCTT
CGGGGCGAAAACTCTCAAGGATCTTACCCTGTTGAGATCCAGTTCGATGTAACCCACTCGTGCACCCA
ACTGATCTTACGATCTTTTACTTTTACCAGCGTTTCTGGGTGAGCAAAAACAGGAAGGCAAAATGCCG
CAAAAAAGGGAATAAGGGCGACACGGAATGTTGAATACTCATACTTTCCTTTTCAATATATTGAA
GCATTTATCAGGTTATTGTCTCATGAGCGGATACATATTTGAATGTATTTAGAAAAATAAACAAATAG
GGTTCCGCGCACATTTCCCGAAAAAGTGCCACCTGACGTCTAAGAAACCATTATATCATGACATTA
CCTATAAAAAATAGGCGTATCACGAGGCCCTTTCGCTCTCGCGGCTTTCGGTGTATGACGGTGAAAACCTCT
GACACATGCAGCTCCCGGAGACGGTACAGCTTGTCTGTAAGCGGATGCCGGGAGCAGACAAGCCCGTC
AGGGCGCGTCAGCGGGTGTGGCGGGTGTGCGGGCTGGCTTAACTATGCGGCATCAGAGCAGATTGTAC
TGAGAGTGCACCATATGCGGTGTGAAATACCGCACAGATGCCGTAAGGAGAAAAATACCGCATCAGGCGCC
ATTCGCTTCCGCGCACATTTCCCGAAAAAGTGCCACCTGACGTCTAAGAAACCATTATATCATGACATTA
TGCGGAAAGGGGATGTGCTGCAAGGCGATTAAGTTGGGTAACGCCAGGGTTTTCCAGTACGACGTT
GTAAAACGACGGCCAGTGCCAAGCTTGCATGCCTGCAGTAAGCCAGTATACACTCCGCTAGCGCTGAGG
TCTGCTCGTGAAGAAGGTGTTGCTGACTCATAACAGGCTGAATCGCCCATCATCCAGCCAGAAAGT
GAGGGAGCCACGGTTGATGAGAGCTTTGTTGTAGGTGGACCAGTTGGTGATTTTGAACTTTTGCTTTTGC
CACGGAACGGTCTGCGTTGTCGGGAAGATGCGTGATCTGATCCTTCAACTCAGCAAAAAGTTGATTTAT
TCAACAAAGCCACGTTGTGTCTCAAAATCTCTGATGTTACATTGCACAAGATAAAAAATATATCATCATG
AACAATAAAACTGTCTGCTTACATAAACAGTAATACAAGGGGTGTTATGAGCCATATTCACGGGAAAC
GTCTTGTCTGAGGCCGCGATTAATTTCAACATGGATGCTGATTTATATGGGTATAAATGGGCTCGCGA
TAATGTGCGGCAATCAGGTGCGACAATCTATCGATTGTATGGGAAGCCCGATGCGCCAGAGTTGTTTCT
GAAACATGGCAAAGGTAGCGTTGCCAATGATGTTACAGATGAGATGGTCAGACTAAACTGGCTGACGGA
ATTTATGCCCTCTCCGACCATCAAGCATTATCCGTACTCCTGATGATGCATGGTTACTCACCCTGC
GATCCCGGGAAAAACAGCATTCCAGGTATTAGAAGAAATATCCTGATTCAGGTGAAAAATATTGTTGATGC
GCTGGCAGTGTTCCTGCGCCGGTTGCATTCCGATTCCTGTTTGAATGTCTTTTAAACAGCGATCGCGT
ATTTGCTCTGCTCAGGCGCAATCACGAATGAATAACGGTTTGGTTGATGCGAGTGATTTTGTATGACGA
GCGTAATGGCTGGCCTGTTGAACAAGTCTGGAAAGAAATGCATAAGCTTTTGCCATTCTCACCGGATTC
AGTCGTCACCTCATGGTGATTTCTCACTTGATAACCTTATTTTACGAGGGGAAATTAATAGGTTGTAT
TGATGTTGGACGAGTCCGAATCGCAGACCGATACAGGATCTTGCCATCCTATGGAACCTGCCCTCGGTGA
GTTTTCTCCTTATTACAGAAACGGCTTTTTCATAAATCAGAATTTGGTTAATTGGTTGTAACACTGAAATG
GCAGTTTTCATTTGATGCTCGATGAGTTTTTCTAATCAGAATTTGGTTAATTGGTTGTAACACTGAAAG
CATTACGCTGACTTGACGGGACGGTAC

```

### Chapter 4.2.3.2

Figure 6.1 shows the growth of nitrogen limited cultures (N limited) and kanamycin resistant nitrogen limited cultures (N limited kanR) during head-to-head competition. The picture shows no differences in growth between the two cultures, neither in nitrogen limited minimal medium nor in full minimal medium, thus confirming that the kanamycin resistance, used as a culture marker, was selectively neutral.

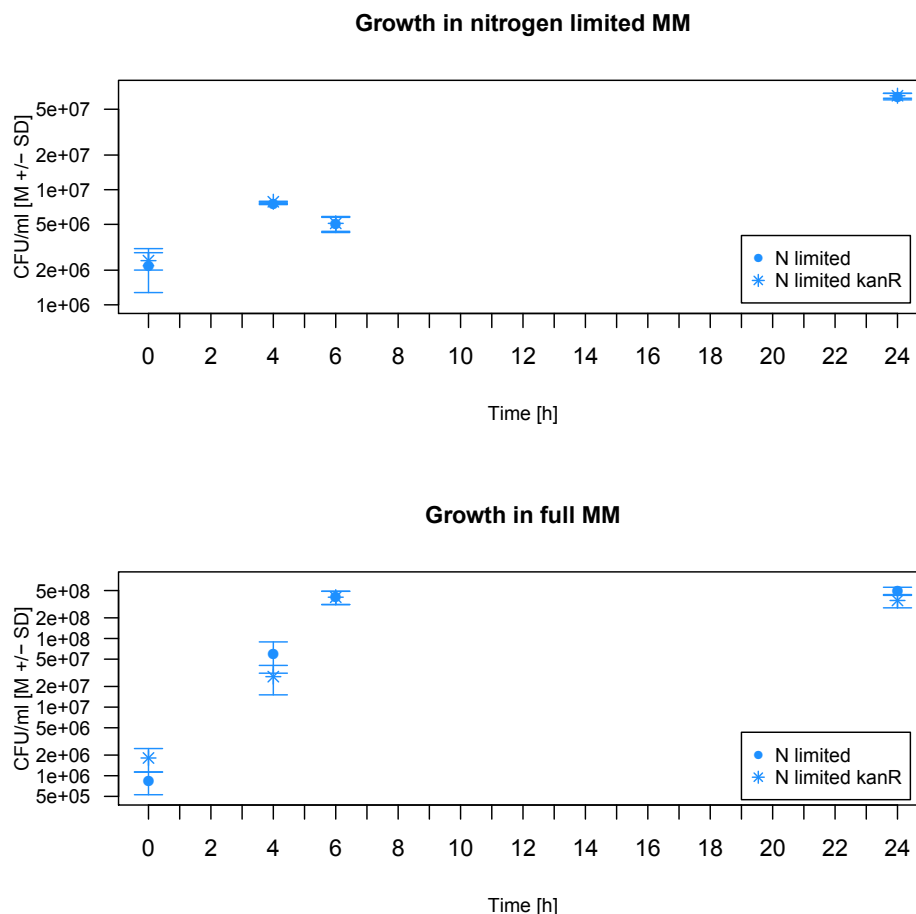


**Figure 6.1: Testing neutrality of the kanamycin resistance marker**

Growth curves of competing shaking cultures in nitrogen limited minimal medium (upper graph) and in full minimal medium (lower graph). Competitive growth of the nitrogen limited continuous line (N limited) and of the kanamycin resistant nitrogen limited (N limited kanR) is shown by the number of colony forming units (CFU/ml) at 0, 4, 6 and 24 hours. Data are depicted as the mean value  $\pm$  the standard deviation obtained from biological triplicates.

---

## References

- Acquisti, C., Elser, J. J., and Kumar, S. (2009a). Ecological nitrogen limitation shapes the DNA composition of plant genomes. *Molecular biology and evolution*, 26(5):953–956.
- Acquisti, C., Kumar, S., and Elser, J. J. (2009b). Signatures of nitrogen limitation in the elemental composition of the proteins involved in the metabolic apparatus. *Proceedings. Biological sciences / The Royal Society*, 276:2605–2610.
- Albers, E., Larsson, C., Andlid, T., Walsh, M. C., and Gustafsson, L. (2007). Effect of nutrient starvation on the cellular composition and metabolic capacity of *Saccharomyces cerevisiae*. *Applied and environmental microbiology*, 73(15):4839–4848.
- Anders, S. and Huber, W. (2010). Differential expression analysis for sequence count data. *Genome biology*, 11(10):R106.
- Barrick, J. E. and Lenski, R. E. (2013). Genome dynamics during experimental evolution. *Nature reviews. Genetics*, 14(12):827–39.
- Baudouin-Cornu, P., Surdin-Kerjan, Y., Marlière, P., and Thomas, D. (2001). Molecular evolution of protein atomic composition. *Science*, 293(5528):297–300.
- Ben-Hamida, F. and Schlessinger, D. (1966). Synthesis and breakdown of ribonucleic acid in *Escherichia coli* starving for nitrogen. *Biochimica et Biophysica Acta*, 119:183–191.
- Berg, J., Tymoczko, J., and Stryer, L. (2002). Carbon Atoms of Degraded Amino Acids Emerge as Major Metabolic Intermediates. In *Biochemistry*, chapter 23.5. W.H. Freeman and Company, New York, 5 edition.
- Blauwkamp, T. a. and Ninfa, A. J. (2002). Physiological role of the GlnK signal transduction protein of *Escherichia coli*: Survival of nitrogen starvation. *Molecular Microbiology*, 46(1):203–214.

- Blum-Oehler, G., Oswald, S., Eiteljörge, K., Sonnenborn, U., Schulze, J., Kruis, W., and Hacker, J. (2003). Development of strain-specific PCR reactions for the detection of the probiotic *Escherichia coli* strain Nissle 1917 in fecal samples. *Research in microbiology*, 154(1):59–66.
- Bragg, J. G. and Wagner, A. (2009). Protein material costs: single atoms can make an evolutionary difference. *Trends in genetics*, 25(1):5–8.
- Brauer, M. J., Yuan, J., Bennett, B. D., Lu, W., Kimball, E., Botstein, D., and Rabinowitz, J. D. (2006). Conservation of the metabolomic response to starvation across two divergent microbes. *Proceedings of the National Academy of Sciences of the United States of America*, 103(51):19302–19307.
- Campbell, N. A. and Reece, J. B. (2003). *Biologie*. Spektrum Verlag, Heidelberg, 6th edition.
- Canfield, D. E., Glazer, A. N., and Falkowski, P. G. (2010). The evolution and future of Earth’s nitrogen cycle. *Science*, 330(6001):192–196.
- Chang, A. and Cohen, S. (1978). Construction and characterization of amplifiable multicopy DNA cloning vehicles derived from the P15A cryptic miniplasmid. *Journal of bacteriology*, 134:1141–1156.
- Chen, L. M. and Maloy, S. (1991). Regulation of proline utilization in enteric bacteria: cloning and characterization of the *Klebsiella put* control region. *Journal of bacteriology*, 173(2):783–790.
- Clark, D. and Cronan, J. (2005). Two-Carbon Compounds and Fatty Acids as Carbon Sources. *EcoSal Plus*, 1(2).
- Colombo, G. and Villafranca, J. J. (1986). Amino-acid sequence of *escherichia-coli* glutamine synthetase deduced from the DNA nucleotide sequence. *Journal of biological chemistry*, 261(23):10587–10591.

- Cooper, V. S. and Lenski, R. E. (2000). The population genetics of ecological specialization in evolving *Escherichia coli* populations. *Nature*, 407(6805):736–739.
- Danger, M. and Chauvet, E. (2013). Elemental composition and degree of homeostasis of fungi: Are aquatic hyphomycetes more like metazoans, bacteria or plants? *Fungal Ecology*, 6(5):453–457.
- Danger, M., Daufresne, T., Lucas, F., Pissard, S., and Lacroix, G. (2008). Does Liebig’s law of the minimum scale up from species to communities? *Oikos*, 117(11):1741–1751.
- Datsenko, K. a. and Wanner, B. L. (2000). One-step inactivation of chromosomal genes in *Escherichia coli* K-12 using PCR products. *Proceedings of the National Academy of Sciences of the United States of America*, 97(12):6640–6645.
- Davis, B. D., Luger, S. M., and Tai, P. C. (1986). Role of ribosome degradation in the death of starved *Escherichia coli* cells. *Journal of bacteriology*, 166(2):439–45.
- Deutscher, J., Francke, C., and Postma, P. W. (2006). How phosphotransferase system-related protein phosphorylation regulates carbohydrate metabolism in bacteria. *Microbiology and molecular biology reviews*, 70(4):939–1031.
- DiRusso, C. C. and Nyström, T. (1998). The fats of *Escherichia coli* during infancy and old age: Regulation by global regulators, alarmones and lipid intermediates. *Molecular Microbiology*, 27:1–8.
- Discoveries, M. (2013). Report MD1125 Metabolomic Profiling of *Escherichia coli*. pages 1–11.
- Drake, D. R. and Brogden, K. A. (2002). Continuous-Culture Chemostat Systems and Flowcells as Methods to Investigate Microbial Interactions.



- 
- In *Polymicrobial Diseases*, number 49, chapter 2. ASM Press, Washington, D.C.
- Duplay, P., Bedouelle, H., Fowler, A., Zabin, I., Saurin, W., and Hofnung, M. (1984). Sequences of the malE Gene and of Its Product, the Protein of Escherichia coli K12. *The Journal of Biological Chemistry*, 259(16):10606–10613.
- Dykhuizen, D. E. and Hartl, D. L. (1983). Selection in chemostats. *Microbiological reviews*, 47(2):150–168.
- Elena, S. F. and Lenski, R. E. (2003). Evolution experiments with microorganisms: the dynamics and genetic bases of adaptation. *Nature reviews. Genetics*, 4(6):457–469.
- Elser, J. J., Acquisti, C., and Kumar, S. (2011). Stoichiogenomics: the evolutionary ecology of macromolecular elemental composition. *Trends in ecology & evolution*, 26(1):38–44.
- Elser, J. J., Fagan, W. F., Subramanian, S., and Kumar, S. (2006). Signatures of ecological resource availability in the animal and plant proteomes. *Molecular Biology and Evolution*, 23(10):1946–1951.
- Ferenci, T. (1996). Adaptation to life at micromolar nutrient levels: the regulation of Escherichia coli glucose transport by endoinduction and cAMP. *FEMS microbiology reviews*, 18(4):301–317.
- Ferenci, T. (1999). Regulation by nutrient limitation. *Current opinion in Microbiology*, 2:208–213.
- Foor, F., Janssen, K. a., and Magasanik, B. (1975). Regulation of synthesis of glutamine synthetase by adenylylated glutamine synthetase. *Proceedings of the National Academy of Sciences of the United States of America*, 72(12):4844–4848.
-

- 
- Franklin, F. and Venables, W. (1976). Biochemical, genetic, and regulatory studies of alanine catabolism in *Escherichia coli* K12. *Molecular and General Genetics*, 149(2):229–237.
- Frost, P. C., Evans-White, M. a., Finkel, Z. V., Jensen, T. C., and Matzek, V. (2005). Are you what you eat? Physiological constraints on organismal stoichiometry in an elementally imbalanced world. *Oikos*, 109:18–28.
- Giese, A. (1979). *Cell Physiology*. W.B. Saunders Company, Philadelphia, 5th edition.
- Gophna, U., Barlev, M., Seijffers, R., Oelschlager, T. A., and Hacker, J. (2001). Curli Fibers Mediate Internalization of *Escherichia coli* by Eukaryotic Cells. *Infection and Immunity*, 69(4):2659–2665.
- Gottschalk, G. (1979). *Bacterial metabolism*. Springer Verlag, New York, 1st edition.
- Hancock, V., Vejborg, R. M., and Klemm, P. (2010). Functional genomics of probiotic *Escherichia coli* Nissle 1917 and 83972, and UPEC strain CFT073: comparison of transcriptomes, growth and biofilm formation. *Molecular genetics and genomics : MGG*, 284(6):437–54.
- Harder, W. and Dijkhuizen, L. (1983). Physiological response to nutrient limitation. *Annual review of microbiology*, 37:1–23.
- Hardie, D. G. (2011). Cell biology. Why starving cells eat themselves. *Science*, 331(6016):410–411.
- Heath, R., Jackowski, S., and Rock, C. (2002). Fatty acid and phospholipid metabolism in prokaryotes. In *Biochemistry of Lipids, Lipoproteins and Membranes*, chapter 3. Elsevier Science B.V., 4th edition.
- Helling, R. B. (1994). Why does *Escherichia coli* have two primary pathways for synthesis of glutamate? *Journal of Bacteriology*, 176(15):4664–4668.

- 
- Helling, R. B. (1998). Pathway choice in glutamate synthesis in *Escherichia coli*. *Journal of Bacteriology*, 180(17):4571–4575.
- Hengge-Aronis, R. (2000). The general stress response in *Escherichia coli*. In *Bacterial Stress Responses*, pages 249–260. ASM Press, Washington, DC.
- Herbert, D., Elsworth, R., and Telling, R. C. (1956). The continuous culture of bacteria; a theoretical and experimental study. *Journal of general microbiology*, 14(3):601–622.
- Herring, C. D., Raghunathan, A., Honisch, C., Patel, T., Applebee, M. K., Joyce, A. R., Albert, T. J., Blattner, F. R., van den Boom, D., Cantor, C. R., and Palsson, B. O. (2006). Comparative genome sequencing of *Escherichia coli* allows observation of bacterial evolution on a laboratory timescale. *Nature genetics*, 38(12):1406–1412.
- Hua, Q., Yang, C., Oshima, T., Mori, H., and Shimizu, K. (2004). Analysis of Gene Expression in *Escherichia coli* in Response to Changes of Growth-Limiting Nutrient in Chemostat Cultures. *Society*, 70(4):2354–2366.
- Ikeda, T., Shauger, A., and Kustu, S. (1996). *Salmonella typhimurium* Apparently Perceives External Nitrogen Limitation as Internal Glutamine Limitation. *Journal of molecular biology*, 259(4):589–607.
- Ingolia, N. T. (2014). Ribosome profiling: new views of translation, from single codons to genome scale. *Nature Reviews Genetics*, 15(3):205–213.
- Ishihama, Y., Schmidt, T., Rappsilber, J., Mann, M., Hartl, F. U., Kerner, M. J., and Frishman, D. (2008). Protein abundance profiling of the *Escherichia coli* cytosol. *BMC genomics*, 9(102).
- J. Koolman, K. R. (2003). *Taschenatlas der Biochemie*. Georg Thieme Verlag, Stuttgart, 3. edition.

- 
- Javelle, A., Severi, E., Thornton, J., and Merrick, M. (2004). Ammonium sensing in *Escherichia coli*. Role of the ammonium transporter AmtB and AmtB-GlnK complex formation. *The Journal of biological chemistry*, 279(10):8530–8538.
- Jozefczuk, S., Klie, S., Catchpole, G., Szymanski, J., Cuadros-Inostroza, A., Steinhauser, D., Selbig, J., and Willmitzer, L. (2010). Metabolomic and transcriptomic stress response of *Escherichia coli*. *Molecular systems biology*, 6(364):1–16.
- Kaplan, R. and Apirion, D. (1975a). Decay of ribosomal acid in *Escherichia coli* cells starved for various nutrients. *Journal of biological chemistry*, 250(8):3174–3177.
- Kaplan, R. and Apirion, D. (1975b). The fate of ribosomes in *Escherichia coli* cells starved for a carbon source. *Journal of biological chemistry*, 250(5):1854–1863.
- Keseler, I. M., Mackie, A., Peralta-Gil, M., Santos-Zavaleta, A., Gama-Castro, S., Bonavides-Martinez, C., Fulcher, C., Huerta, a. M., Kothari, A., Krummenacker, M., Latendresse, M., Muniz-Rascado, L., Ong, Q., Paley, S., Schroder, I., Shearer, a. G., Subhraveti, P., Travers, M., Weerasinghe, D., Weiss, V., Collado-Vides, J., Gunsalus, R. P., Paulsen, I., and Karp, P. D. (2013). EcoCyc: fusing model organism databases with systems biology. *Nucleic Acids Research*, 41:D605–D612.
- Koch, A. (1996). What size should a bacterium be? A question of scale. *Annual review of microbiology*, 50:317–348.
- Kolb, A., Busby, S., Buc, H., Garges, S., and Adhya, S. (1993). Transcriptional Regulation by cAMP and Its Receptor Protein. *Annual Review of Biochemistry*, 62:749–797.
- Kooijman, S. (1995). The stoichiometry of animal energetics. *Journal of Theoretical Biology*, 177(2):139–149.

- 
- Kraft, C., Deplazes, A., Sohrmann, M., and Peter, M. (2008). Mature ribosomes are selectively degraded upon starvation by an autophagy pathway requiring the Ubp3p/Bre5p ubiquitin protease. *Nature Cell Biology*, 10(5):602–610.
- Langmead, B., Trapnell, C., Pop, M., and Salzberg, S. L. (2009). Ultrafast and memory-efficient alignment of short DNA sequences to the human genome. *Genome biology*, 10(3):R25.
- Leigh, J. A. and Dodsworth, J. A. (2007). Nitrogen regulation in bacteria and archaea. *Annual review of microbiology*, 61:349–377.
- Lenski, R. (2015). <http://myxo.css.msu.edu/ecoli/dm25liquid.html>; 02.02.2015.
- Lenski, R. E., Mongold, J. a., Sniegowski, P. D., Travisano, M., Vasi, F., Gerrish, P. J., and Schmidt, T. M. (1998). Evolution of competitive fitness in experimental populations of *E. coli*: what makes one genotype a better competitor than another? *Antonie van Leeuwenhoek*, 73(1):35–47.
- Lenski, R. E., Rose, M., Simpson, S., and Tadler, S. (1991). Long-Term Experimental Evolution in *Escherichia coli*. I. Adaptation and Divergence During 2,000 Generations. *The American naturalist*, 138(6):1315–1341.
- Lenski, R. E. and Travisano, M. (1994). Dynamics of adaptation and diversification: a 10,000-generation experiment with bacterial populations. *Proceedings of the National Academy of Sciences of the United States of America*, 91(15):6808–6814.
- Li, N., Lv, J., and Niu, D.-K. (2009). Low contents of carbon and nitrogen in highly abundant proteins: evidence of selection for the economy of atomic composition. *Journal of molecular evolution*, 68(3):248–255.
- Loh, K. D., Gyaneshwar, P., Markenscoff Papadimitriou, E., Fong, R., Kim, K.-S., Parales, R., Zhou, Z., Inwood, W., and Kustu, S. (2006). A

- 
- previously undescribed pathway for pyrimidine catabolism. *Proceedings of the National Academy of Sciences of the United States of America*, 103(13):5114–5119.
- López-Maury, L., Marguerat, S., and Bähler, J. (2008). Tuning gene expression to changing environments: from rapid responses to evolutionary adaptation. *Nature reviews. Genetics*, 9(8):583–593.
- Maaloe, O. and Kjeldgaard, N. (1966). *Control of Macromolecular Synthesis: A Study of DNA, RNA, and Protein Synthesis in Bacteria*. Benjamin, W.A., New York.
- Magasanik, B. and Neidhardt, F. (1987). Regulation of carbon and nitrogen utilization. In *Escherichia coli and Salmonella typhimurium: Cellular and Molecular Biology*, chapter 2, pages 1318–1325. American Society for Microbiology, Washington, D.C.
- Magoc, T., Wood, D., and Salzberg, S. L. (2013). EDGE-pro: Estimated Degree of Gene Expression in Prokaryotic Genomes. *Evolutionary bioinformatics online*, 9:127–136.
- Maier, T., Güell, M., and Serrano, L. (2009). Correlation of mRNA and protein in complex biological samples. *FEBS Letters*, 583(24):3966–3973.
- Mandelstam, I. (1963). Protein turnover and its function in the economy of the cell. *Annals of the New York Academy of Sciences*, 102:621–636.
- Martínez-Gómez, K., Flores, N., Castañeda, H. M., Martínez-Batallar, G., Hernández-Chávez, G., Ramírez, O. T., Gosset, G., Encarnación, S., and Bolivar, F. (2012). New insights into *Escherichia coli* metabolism: carbon scavenging, acetate metabolism and carbon recycling responses during growth on glycerol. *Microbial Cell Factories*, 11(46).
- Matin, A. (1991). MicroReview The molecular basis of carbon-starvation-induced general resistance in *Escherichia coli*. *Molecular Microbiology*, 5(1):3–10.
-

- 
- Matin, A., Auger, E. A., Blum, P. H., and Schultz, E. (1989). Genetic basis of starvation survival in nondifferentiating bacteria. *Annual review of microbiology*, 43:293–316.
- Mazel, D. and Marlière, P. (1989). Adaptive eradication of methionine and cysteine from cyanobacterial light-harvesting proteins. *Nature*, 341(6239):245–248.
- McFall, E. and Newman, E. (1996). *Amino acids as carbon sources. In Escherichia coli and Salmonella: Cellular and Molecular Biology*. ASM Press, Washington, D.C.
- Muse, W. B. and Bender, R. a. (1998). The nac (nitrogen assimilation control) gene from Escherichia coli. *Journal of bacteriology*, 180(5):1166–1173.
- Nelson, D. L. and Cox, M. M. (2000). *Lehninger Principles of Biochemistry*. Worth Publishers, New York, 3rd edition.
- Ninfa, A. and Jiang, P. (2005). PII signal transduction proteins: sensors of  $\alpha$ -ketoglutarate that regulate nitrogen metabolism. *Current opinion in Microbiology*, 8(2):168–173.
- Notley-mcrob, L., Death, A., and Ferenci, T. (1997). The relationship between external glucose concentration and cAMP levels inside Escherichia coli: implications for models of phosphotransferase-mediated regulation of adenylate cyclase. *Microbiology*, 143:1909–1918.
- Notley-McRobb, L. and Ferenci, T. (1999). Adaptive mgl-regulatory mutations and genetic diversity evolving in glucose-limited Escherichia coli populations. *Environmental microbiology*, 1(1):33–43.
- Nyström, T., Flärdh, K., and Kjelleberg, S. (1990). Responses to multiple-nutrient starvation in marine Vibrio sp. strain CCUG 15956. *Journal of bacteriology*, 172(12):7085–7097.

- 
- Olsen, A., Jonsson, A., and Normak, S. (1989). Fibronectin binding mediated by a novel class of surface organelles on *Escherichia coli*. *Nature*, 338:652–655.
- Overbeeke, N. and Lugtenberg, B. (1982). Recognition site for phosphorus-containing compounds and other negatively charged solutes on the PhoE protein of the outer membrane of *Escherichia coli* K12. *European Journal of Biochemistry*, 126:113–118.
- Paliy, O. and Gunasekera, T. S. (2007). Growth of *E. coli* BL21 in minimal media with different gluconeogenic carbon sources and salt contents. *Applied microbiology and biotechnology*, 73(5):1169–1172.
- Parales, R. E. and Ingraham, J. L. (2010). The surprising Rut pathway: an unexpected way to derive nitrogen from pyrimidines. *Journal of bacteriology*, 192(16):4086–4088.
- Peterson, C. N., Mandel, M. J., and Silhavy, T. J. (2005). *Escherichia coli* starvation diets: Essential nutrients weigh in distinctly. *Journal of Bacteriology*, 187(22):7549–7553.
- Philippe, N., Pelosi, L., Lenski, R. E., and Schneider, D. (2009). Evolution of penicillin-binding protein 2 concentration and cell shape during a long-term experiment with *Escherichia coli*. *Journal of Bacteriology*, 191(3):909–921.
- Pine, M. (1965). Heterogeneity of protein turnover in *E. coli*. *Biochimica et biophysica acta*, 104:439–456.
- Postma, P. W., Lengeler, J. W., and Jacobson, G. R. (1993). Phosphoenolpyruvate:carbohydrate phosphotransferase systems of bacteria. *Microbiological reviews*, 57(3):543–594.
- Purves, W. K., Sadava, D., Orians, G. H., and Heller, H. C. (2006). *Biology*. Elsevier GmbH, München.



- 
- Reeve, C. a., Amy, P. S., and Matin, A. (1984a). Role of protein synthesis in the survival of carbon-starved *Escherichia coli* K-12. *Journal of bacteriology*, 160(3):1041–1046.
- Reeve, C. A., Bockman, A. T., and Matin, A. (1984b). Role of protein degradation in the survival of carbon-starved *Escherichia coli* and *Salmonella typhimurium*. *Journal of bacteriology*, 157:758–763.
- Reitzer, L. (2003). Nitrogen assimilation and global regulation in *Escherichia coli*. *Annual review of microbiology*, 57:155–176.
- Reitzer, L. (2004). Biosynthesis of Glutamate, Aspartate, Asparagine, L-Alanine, and D-Alanine. *EcoSal Plus*, Domain3:Me.
- Rhee, G. Y. (1978). Effects of N : P Atomic Ratios and Nitrate Limitation on Algal Growth , Cell Composition , and Nitrate Uptake. *Limnology and Oceanography*, 23(1):10–25.
- Ribbons, D. and Dawes, E. (1963). Environmental and growth conditions affecting the endogenous metabolism of bacteria. *Annals of the New York Academy of Sciences*, 102:564–586.
- Romeo, T., Gong, M., Liu, M. Y., and Brun-Zinkernagel, a. M. (1993). Identification and molecular characterization of *csrA*, a pleiotropic gene from *Escherichia coli* that affects glycogen biosynthesis, gluconeogenesis, cell size, and surface properties. *Journal of bacteriology*, 175(15):4744–4755.
- Römling, U., Sierralta, W., Eriksson, K., and Normark, S. (1998). Multicellular and aggregative behaviour of *Salmonella typhimurium* strains is controlled by mutations in the *agfD* promoter. *Molecular Microbiology*, 28(2):249–264.
- Ropers, D., de Jong, H., Page, M., Schneider, D., and Geiselman, J. (2006). Qualitative simulation of the carbon starvation response in *Escherichia coli*. *Bio Systems*, 84(2):124–152.

- Sabnis, N. a., Yang, H., and Romeo, T. (1995). Pleiotropic regulation of central carbohydrate metabolism in *Escherichia coli* via the gene *csrA*. *Journal of Biological Chemistry*, 270(49):29096–29104.
- Sambrook, J. and Russell, D. (2001). *Molecular cloning: a laboratory manual*. Cold Spring Harbour Laboratory Press, Cold Spring Harbor, New York, 3rd. edition.
- Schaechter, M. (2009). *Encyclopedia of Microbiology*. Academic Press, San Diego, 3rd edition.
- Schmitz, R. (2000). Internal Glutamine and Glutamate Pools in *Klebsiella pneumoniae* Grown Under Different Conditions of Nitrogen Availability. *Current Microbiology*, 41(5):357–362.
- Scholle, A., Vreemann, J., Blank, V., Nold, A., Boos, W., and M.D., M. (1987). Sequence of the *mglB* gene from *Escherichia coli* K12: comparison of wild-type and mutant galactose chemoreceptors. *Molecular and General Genetics*, 208(1-2):247–253.
- Schultz, J. E., Latter, G. I., and Matin, A. (1988). Differential regulation by cyclic AMP of starvation protein synthesis in *Escherichia coli*. *Journal of bacteriology*, 170(9):3903–3909.
- Schultz, J. E. and Matin, A. (1991). Molecular and functional characterization of a carbon starvation gene of *Escherichia coli*. *Journal of molecular biology*, 218(1):129–140.
- Scott, J. T., Cotner, J. B., and LaPara, T. M. (2012). Variable stoichiometry and homeostatic regulation of bacterial biomass elemental composition. *Frontiers in Microbiology*, 3(42).
- Senn, H., Lendenmann, U., Snozzi, M., Hamer, G., and Egli, T. (1994). The growth of *Escherichia coli* in glucose-limited chemostat cultures: a re-examination of the kinetics. *Biochimica et Biophysica Acta*, 1201(3):424–436.

- 
- Seyffert, W. (2003). Genregulation bei Eubakterien. In *Lehrbuch der Genetik*, chapter 8. Spektrum Akademischer Verlag, Heidelberg, 2nd edition.
- Shaver, G. and Melillo, J. (1984). Nutrient Budgets of Marsh Plants : Efficiency Concepts and Relation to Availability. *Ecology*, 65(5):1491–1510.
- Shimada, T., Fujita, N., Yamamoto, K., and Ishihama, A. (2011). Novel Roles of cAMP Receptor Protein (CRP) in Regulation of Transport and Metabolism of Carbon Sources. *PLoS ONE*, 6(6).
- Singh, R. and Cuervo, A. M. (2012). Lipophagy: Connecting Autophagy and Lipid Metabolism. *International Journal of Cell Biology*, 2012:1–12.
- Soupene, E., He, L., Yan, D., and Kustu, S. (1998). Ammonia acquisition in enteric bacteria: physiological role of the ammonium/methylammonium transport B (AmtB) protein. *Proceedings of the National Academy of Sciences of the United States of America*, 95(12):7030–7034.
- Stanek, M. T., Cooper, T. F., and Lenski, R. E. (2009). Identification and dynamics of a beneficial mutation in a long-term evolution experiment with *Escherichia coli*. *BMC evolutionary biology*, 9:302.
- Sterner, R. and Elser, J. (2002). *Ecological Stoichiometry - The biology of elements from molecules to the biosphere*. Princeton University Press, New Jersey, 1st edition.
- Todar, K. (2016). *Todar's Online Textbook of Bacteriology*.
- Troge, A. (2012). *Studien am Flagellensystem des Escherichia coli Stammes Nissle 1917 ( EcN ) im Hinblick auf seine Funktion als Probiotikum Studies on the flagellar system of Escherichia coli Nissle 1917 ( EcN ) with regard to its function as a probiotic*. Wuerzburg.

- 
- van Heeswijk, W. C., Westerhoff, H. V., and Boogerd, F. C. (2013). Nitrogen assimilation in *Escherichia coli*: putting molecular data into a systems perspective. *Microbiology and molecular biology reviews*, 77(4):628–695.
- Vejborg, R. M., Friis, C., Hancock, V., Schembri, M. a., and Klemm, P. (2010). A virulent parent with probiotic progeny: comparative genomics of *Escherichia coli* strains CFT073, Nissle 1917 and ABU 83972. *Molecular genetics and genomics*, 283(5):469–484.
- Visser, D., van Zuylen, G., van Dam, J., Oudshoorn, A., Eman, M., and Ras, C. (2002). Rapid sampling for analysis of in vivo kinetics using the BioScope: A system for continuous-pulse experiments. *Biotechnol Bioengineering*, 79(6):674–681.
- Wang, L., Feng, Z., Wang, X., Wang, X., and Zhang, X. (2010). DEGseq: an R package for identifying differentially expressed genes from RNA-seq data. *Bioinformatics (Oxford, England)*, 26(1):136–138.
- Wilkinson, J. F. (1963). Carbon and Energy Storage in Bacteria. *Journal of general microbiology*, 32:171–176.
- Yang, H., Liu, M. Y., and Romeo, T. (1996). Coordinate genetic regulation of glycogen catabolism and biosynthesis in *Escherichia coli* via the CsrA gene product. *Journal of bacteriology*, 178(4):1012–1017.
- Yang, Y., Pollard, A., Höfler, C., Poschet, G., Wirtz, M., Hell, R., and Sourjik, V. (2015). Relation between chemotaxis and consumption of amino acids in bacteria. *Molecular Microbiology*, 96(6):1272–1282.
- Yanisch-Perron, C., Vieira, J., and Messing, J. (1985). Improved M13 phage cloning vectors and host strains: nucleotide sequence of the M13mpl8 and pUC19 vectors. *Gene*, 33:103–119.
- Young, K. D. (2007). Bacterial morphology: why have different shapes? *Current Opinion in Microbiology*, 10(6):596–600.

Zogaj, X., Bokranz, W., Nimtz, M., and Ro, U. (2003). Production of Cellulose and Curli Fimbriae by Members of the Family Enterobacteriaceae Isolated from the Human Gastrointestinal Tract. *Infection and Immunity*, 71(7):4151–4158.

Zogaj, X., Nimtz, M., Rohde, M., Bokranz, W., and Romling, U. (2001). The multicellular morphotypes of *Salmonella typhimurium* and *Escherichia coli* produce cellulose as the second component of the extracellular matrix. *Molecular Microbiology*, 39(6):1452–1463.

Zundel, M. A., Basturea, G. N., and Deutscher, M. P. (2009). Initiation of ribosome degradation during starvation in *Escherichia coli*. *RNA Society*, 15:977–983.

**Versicherung nach § 6 Abs. 3, Nr. 6**  
**Oath pursuant to § 6 Abs. 3, No. 6**

Hiermit versichere ich, dass ich die vorgelegte Dissertation selbst und ohne unerlaubte Hilfe angefertigt, alle in Anspruch genommenen Quellen und Hilfsmittel in der Dissertation angegeben habe und die Dissertation nicht bereits anderweitig als Prüfungsarbeit vorgelegen hat.

I hereby declare that I have produced the presented thesis by myself and without unpermitted help, that all sources and aids used are indicated, and that this dissertation has not been presented elsewhere as an examination paper.

---

Ort, Datum

---

Name

## Presentations

**Henze, S.**, Kurtz, J., Dobrindt, U., Acquisti, C. (2011): An experimental evolution approach to quantify the selection pressure exerted by Nitrogen availability on genome evolution. Symposium der VW-Stiftung, Sylt. Poster presentation

**Henze, S.**, Kurtz, J., Dobrindt, U., Acquisti, C. (2012): Is environmental N availability affecting evolutionary change? A direct answer from experimental evolution: N starvation of *Escherichia coli* in chemostats. Symposium der Münster Graduate School of Evolution, Münster. Poster presentation

**Henze, S.**, Kurtz, J., Dobrindt, U., Acquisti, C. (2013): An experimental approach to directly quantify the impact of Nitrogen availability on genome evolution in *Escherichia coli*. Symposium der Münster Graduate School of Evolution, Münster. Oral presentation

**Henze, S.**, Kurtz, J., Dobrindt, U., Acquisti, C. (2014): Combining metabolomics and transcriptomics to track the dynamics of nutrient allocation in *Escherichia coli*. Symposium der Münster Graduate School of Evolution, Münster. Oral presentation

## Lebenslauf